Investigation of the mechanism of L-asparaginase-induced acute pancreatitis

Thesis submitted in accordance with the requirements of

Cardiff University

for the degree of Doctor of Philosophy

Shuang Peng

July, 2017

This thesis is dedicated to my parents and my wife for their support and encouragement

Abstract

Intracellular Ca^{2+} and adenosine triphosphate (ATP) are the key elements needed for stimulant-evoked exocytotic enzyme secretion from pancreatic acinar cells. Physiological Ca^{2+} signals consist of repetitive spikes confined to the secretory granule region, which stimulate ATP production; whereas sustained global cytosolic Ca^{2+} elevations - toxic Ca^{2+} signals decrease ATP levels and cause necrosis leading to the inflammation of the pancreas - acute pancreatitis (AP), a life-threatening disease currently without specific therapy. The work presented in this thesis focuses on the mechanisms underlying the development of pancreatitis evoked by L-asparaginase and the potential ways to intervene asparaginase-associated pancreatitis (AAP). Asparaginase is an essential element of the chemotherapy regimen in the successful treatment of acute lymphoblastic leukaemia (ALL), the most common childhood cancer. But asparaginase treatment can lead to AAP, which is a side-effect of ALL treatment occurring in about 5–10% of cases. Following AP, further treatment with asparaginase is withheld to prevent recurrence of AP; however, withholding scheduled asparaginase is associated with a potential increase in ALL relapse. Understanding the pathogenesis of AAP could lead to effective therapies for this complication, potentially reducing toxicity and allowing re-exposure to continue treatment with asparaginase.

The data presented within this thesis show that asparaginase induces pathological intracellular (cytosolic and mitochondrial) Ca^{2+} responses in pancreatic acinar cells. We have found that asparaginase caused enlarged Ca^{2+} entry and substantially reduced Ca^{2+} extrusion in pancreatic acinar cells due to decrease in intracellular ATP levels. Asparaginase-induced pathology highly depends on proteinase activated receptor 2 (PAR2) and its inhibition largely prevents both toxic Ca^{2+} signals and necrosis. We tested the effects of

pharmacological blockade of Ca^{2+} release activated Ca^{2+} (CRAC) entry by the specific Ca^{2+} channel inhibitor GSK-7975A and found that GSK-7975A markedly reduced asparaginase-induced cytosolic Ca^{2+} overload and also protected effectively against the development of necrosis. Interestingly, energy supplements such as adding pyruvate, fructose or galactose to pancreatic acinar cells had profound protective effects on asparaginase-induced Ca^{2+} overload, ATP loss and necrosis *in vitro* while removal of glucose did not have a significant effect. Galactose feeding had a dramatic protective effect in an asparaginase-induced *in vivo* model of AP.

This study provides fresh evidence for the pathogenic mechanisms of AAP and the results presented in this thesis demonstrate both Ca^{2+} and ATP are pivotal for the pathophysiological process by which asparaginase treatment of ALL may cause AAP. We can therefore conclude that combining inhibition of Ca^{2+} overload with energy supplements could be a potential therapeutic approach to protect against AAP. This would prevent AP development and allow continuous of the successful asparaginase treatment during ALL childhood cancer treatments.

Acknowledgements

First and foremost, I would like to express my deepest appreciation to my supervisors Dr Oleg Gerasimenko, Dr Julia Gerasimenko and Prof Ole Petersen for their constant support, encouragement and invaluable guidance throughout my PhD study. Without their tireless support, brilliant advice and regular feedback, this project would not be shaped. Oleg's work provided a good foundation from which many of the ideas included in this thesis were derived from. They showed so much kindness and patience in taking their time to share knowledge and build me up more scientifically. Their passion, hardworking and critical views for science have influenced me profoundly. I will always be indebted to their teachings, advice and support throughout my PhD programme. Further, I am deeply grateful eternally and sincerely to supervisors Prof Liwei Wang and Prof Lixin Chen from Jinan University, who supported and encouraged me to study in the United Kingdom.

I also owe a great deal of gratitude to a number of friends and colleagues. Those especially deserving of a mention include Dr Pawel Ferdek, Dr Monika Jakubowska, Dr Tetyana Tsugorka, Dr Oleksiy Gryschenko, Dr Eloise Stapleton, Dr Richard Charlesworth. I have learned a great deal from all of them.

I would also like to thank Dr Kerrie Thomas, Mrs Swapna Khandavalli, Mrs Nathalie Rees, Ms Beverley Plummer, Mr Barry Rodd, who helped my postgraduate study registration in Cardiff University trouble free.

I wish to thank Mr Derek Scarborough for histology services and demonstration of histological sample processing and slide preparation and Mr Marc Isaacs for assistance with conventional widefield microscopy.

Many thanks to everyone in JBIOS for looking after the mice. Special thanks to Mrs Veronica Walker, Mr Michael Underwood, Mr Patrick Mason, Miss Helen Read and Mr Rhys Perry for your help, demonstration and advice.

Thanks very much to my parents for their endless support and encouragement. I would not be the person I am today and complete my study without you both, thanks for always believing in me from the very beginning and supporting me every step of the way. I would also like to thank my wife for your encouragement and accompany. I will always be eternally grateful to all of you and my family for your support and love.

Finally, I would like to thank China Scholarship Council (CSC) and Jinan University kindly supported and funded my study. Also many thanks to the Medical Research Council (MRC) and Children with Cancer UK for funding this research project and sponsoring me to attend various conferences.

Table of Contents

List of Tables

List of Figures

Abbreviations

$[Ca^{2+}]$	Calcium concentration
$[Ca^{2+}]_{ER}$	$[Ca^{2+}]$ in the endoplasmic reticulum
$[Ca^{2+}]_i$	Cytosolic calcium concentration
$[Ca^{2+}]_m$	mitochondrial $[Ca^{2+}]$
AAP	Asparaginase Associated Pancreatitis
ACh	Acetylcholine
ADH	Alcohol dehydrogenase
ADP	Adenosine diphosphate
ALL	Acute lymphoblastic leukemia
AP	Acute pancreatitis
Asn	Asparagine
ASNase	L-Asparaginase
ATP	Adenosine triphosphate
Ca^{2+}	Calcium ions
CAD	CRAC activation domain
cADPR	Cyclic adenosine diphosphate ribose
CALP	Ca^{2+}-like peptides
CaM	Calmodulin
cAMP	Cyclic adenosine monophosphate
CaSR	Calcium-sensing receptor
CC	Coiled-coil
CCCP	Carbonyl cyanide 3-chlorophenylhydrazone
CCK	Cholecystokinin
CECT	contrast-enhanced computed tomography
CER-AP	Cerulein-induced Acute Pancreatitis
CFTR	Cystic fibrosis transmembrane conductance regulator

CICR	Calcium induced calcium release
CP	Chronic pancreatitis
CPA	Cyclopiasonic acid
CRAC	Ca^{2+} Release-Activated Ca^{2+} Channel
DAG	Diacylglycerol
DFS	Disease-free survival
DMSO	Dimethyl sulfoxide
E. coli	*Escherichia coli*
EDTA	Ethylene diamine tetraacetic acid
EF-hand	Calcium binding helix-loop-helix structural domain
EGTA	Ethylene glycol tetraacetic acid
ER	Endoplasmic reticulum
ERCP	endoscopic retrograde cholangiopancreatography
ERK1/2	Extracellar signal-regulated kiase
EtOH	Ethanol
FAEE	Fatty acid ethyl esters
G protein	Guanine nucleotide binding protein
GI	Gastrointestinal
GPCR	G protein-coupled receptor
H&E	Hematoxylin-eosin
HEPES	4-(2-hydroxyethyl)-1-piperazineethanesulfonic acid
I_{CRAC}	CRAC current
IP_3	Inositol 1,4,5-trisphosphate
IP_3R	Inositol 1,4,5-trisphosphate receptor
JNK	c-jun N-terminal kinase
MCU	Mitochondrial Ca^{2+} uniporter

MgGreen	Magnesium Green
MODS	Multiple organ dysfunction syndrome
MPTP	Mitochondrial permeability transition pore
NAADP	Nicotinic acid adenine dinucleotide phosphate
NAD	Nicotinamide adenine dinucleotide
NCX	Na^{+}/Ca^{2+} exchanger
P/S	Proline-serine-rich domain
PAR2	Protease activated receptor 2
PARS	Protease activated receptors
PI	Propidium Iodide
PIP_2	Phosphatidylinositol bisphosphate
PLC	Phospholipase C
PMCA	Plasma membrane calcium-activated ATPase
POAEE	Palmitoleic acid ethyl ester
PRSS1	Mutations of human cationic trypsinogen
PTP	Permeability transition pore
PZ	Pancreozymin
RNS	Reactive nitrogen species
ROS	Reactive oxygen species
RyR	Ryanodine receptor
SCID	Severe combined immune deficiency
SERCA	Sarcoplasmic/endoplasmic reticulum calcium ATPase
SIRS	Systemic immune response syndrome
SOAR	STIM-Orai activation region
SOCE	Store operated calcium entry
SPINK1	Serine protease inhibitor Kazal type 1
STIM1	Stromal interaction molecule 1
Tg	Thapsigargin

TIRF	Total internal reflection fluorescence
TLC-S	Taurolithocholic acid 3-sulfate
TPCs	Two-pore channels
VIP	Vasoactive intestinal peptide
WT	Wild type
ZGs	Zymogen granules
$\Delta\psi_m$	Mitochondrial membrane potential

Publications

Peng, S., Gerasimenko, J.V., Tsugorka, T., Gryshchenko, O., Samarasinghe, S., Petersen, O.H. and Gerasimenko, O.V. (2016) Calcium and adenosine triphosphate control of cellular pathology: asparaginase-induced pancreatitis elicited via protease-activated receptor 2. *Philosophical Transactions of the Royal Society B: Biological Sciences* 371(1700), article number: 20150423. doi: 10.1098/rstb.2015.0423.

Gerasimenko, J.V., **Peng, S**, Tsugorka, T. and Gerasimenko, O.V. (2017) Ca^{2+} signalling underlying pancreatitis. *Cell Calcium* 10.1016/j.ceca.2017.05.010

Chapter 1

Introduction

The Pancreas

Anatomy and histology

The pancreas both as an organ and a seat of disease was generally ignored in ancient times. This may be due to the location of the gland hidden in the retroperitoneum. A Greek anatomist and surgeon Herophilus (335–280 BC) who is considered the Father of Scientific Anatomy firstly identified the pancreas in about 300 BC (1). However, this organ was named by an eminent Greek physician and anatomist Rufus of Ephesus in about 100 AD (2). Etymologically, the term 'pancreas' is a Latin adaptation of Greek παγκρέας (παγ = all or whole, and κρέας = flesh, or meat), which is most probably because the pancreas contains no bones or cartilage and has a relatively uniform composition and consistency (3). Andreas Vesalius (1514 - 1564) gave a fair description of the pancreas. According to his work, the *Fabric of the Human Body*, the pancreas seems to be a gland impressed with the vessels running through it. However, he had no knowledge about the ductal system of the pancreas and considered it as a protective organ for the stomach (4). In 1642, Johann George Wirsung (1589 - 1643), a German anatomist and the prosector to Veslingus in Padua, described the main duct of the human pancreas (5).

The pancreas (Figure 1.1) is the crucial digestive and endocrine glandular organ in humans. The pancreas is a lobulated and retroperitoneal gland about 15 cm long and 5 cm wide with its weight ranging from 82 to 117 g. It lies transversely behind the stomach and across the lumbar spine (L1 - L2) within the left upper abdominal cavity. The pancreas is partitioned into four parts: the head, the neck, the body and the tail. The head of the pancreas is embedded in the duodenal loop. The neck is located anterior to the superior mesenteric artery. The body of the pancreas, the largest part of the pancreas lying behind

the base of the stomach, is located between the neck and the tail and its posterior edge is close to the lumbar region. The tail of the pancreas is a thin and narrow part to the left of the pancreas and ends abutting the spleen. The tail of pancreas is surrounded by serosa whereas the other parts are found in the retroperitoneal space. Therefore the lesions of the pancreas are often deep and hidden. The pancreas has two main ducts: the main pancreatic duct (duct of Wirsung) and the accessory pancreatic duct (duct of Santorini). Pancreatic juice passes from the pancreatic duct through the ampulla of Vater into the duodenum.

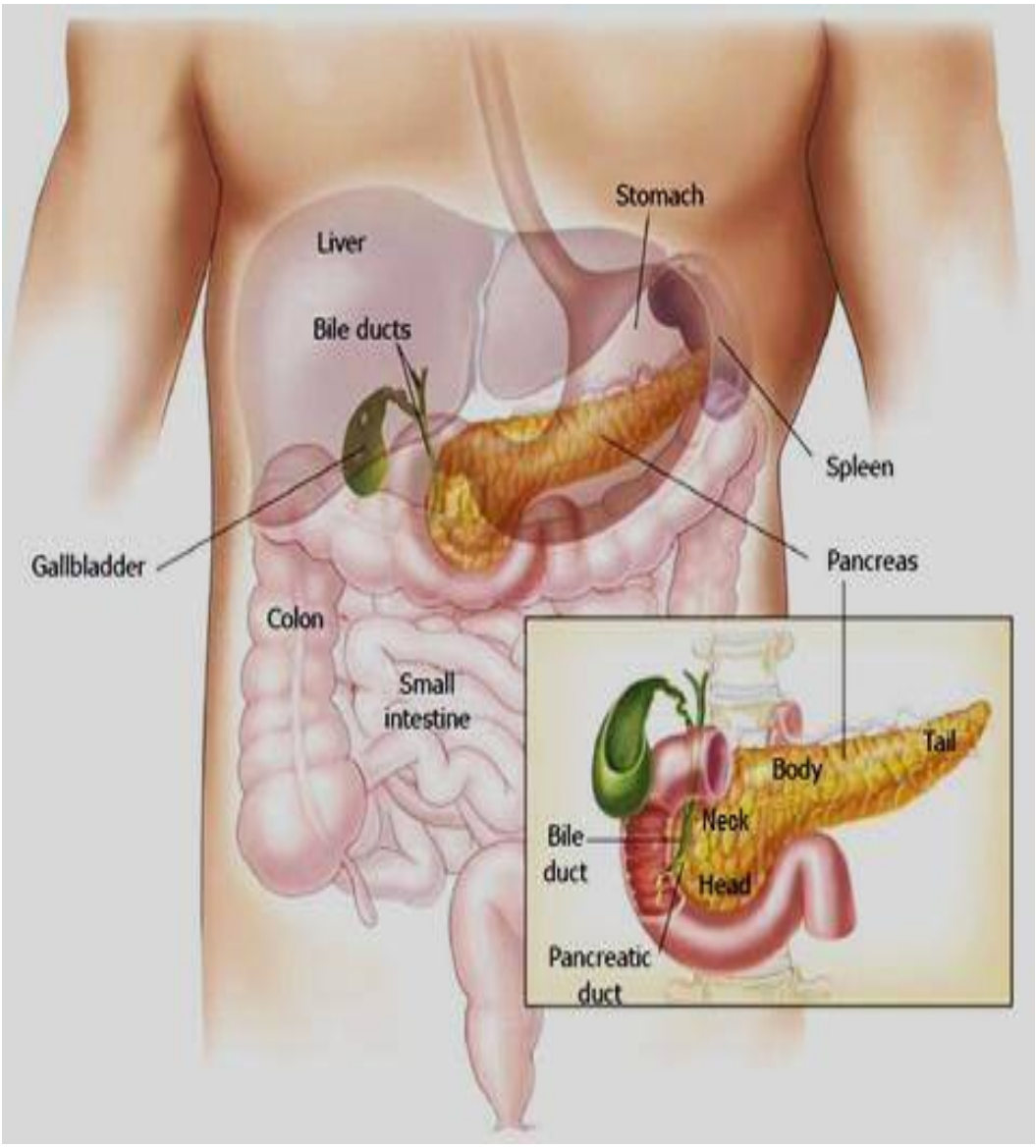

Figure 1.1 Anatomy of the pancreas in the human body.

In humans, the pancreas is located in the abdominal cavity. It lies transversely behind the stomach and is close to the duodenum. The pancreas consists of four parts: the head, the neck, the body and the tail. (Modified from *Cid-Arregui A and Juarez V, World J Gastroenterol, 2015*) (6)

The pancreas is a dual-function gland which has both exocrine and endocrine functions (Figure 1.2). The endocrine functions are performed by the islets of Langerhans, formed by the clustered endocrine cells, which are small, island-like structures within the exocrine pancreatic tissue that account for only 1–2% of the entire organ (7). There are approximately one million islets in the pancreas and a larger number of smaller islets distributed in the head and a smaller number of larger islets distributed in the tail of the pancreas (8). Although these cell clusters distributed among the pancreatic acinar cells vary in size and shape, they still can be classified by their secretory functions: β cells, accounting for 65–80% of the total islet cells, secrete insulin while the less common glucagon-secreting α cells are also involved in blood glucose homeostasis (9). The other cells include δ cells which secrete somatostatin (regulates/stops α and β cells) (10) and PP cells which secrete pancreatic polypeptide (regulates pancreatic secretion) (11,12). Recently, it has been reported that ghrelin is expressed in human fetal pancreas and pancreatic ghrelin cells may therefore constitute a new islet cell type (13). Although there is similarity of islets cellular composition among different species, their cytoarchitecture differs greatly (Figure 1.3). Generally, islets are primarily composed of β-cells located in the center surrounded by other cell types in the periphery in rodents (14). However, it is indicated that human islets show close interconnection between α- and β-cells (15). In contrast, the exocrine functions are performed by the pancreatic acini and the duct. The pancreatic duct cells, mainly centroacinar cells, secrete pancreatic juice which contains water (up to 97%) and bicarbonate ions. Bicarbonate ions, which are alkaline, can neutralize the acidic chime and gastric acid in the duodenum in order to provide the most suitable pH conditions for digestive enzymes working in the small intestine. The pancreatic acinar cells filled with secretory granules secrete the digestive enzymes (trypsinogen, chymotrypsinogen, lipase, amylase and other digestive enzymes). Pancreatic secretions drain to the main pancreatic duct via intralobular ducts and then pass directly into the

duodenum. Once this pancreatic fluid is released in the intestine, the enzyme enterokinase activates trypsinogen to trypsin. Subsequently, trypsin cleaves the rest of the trypsinogen, chymotrypsinogen as well as other precursor digestive enzymes to their active forms. The exocrine functions of pancreas are controlled by humoral regulation (via the hormones gastrin, cholecystokinin (CCK) and secretin) and, to a lesser extent, the parasympathetic nerves.

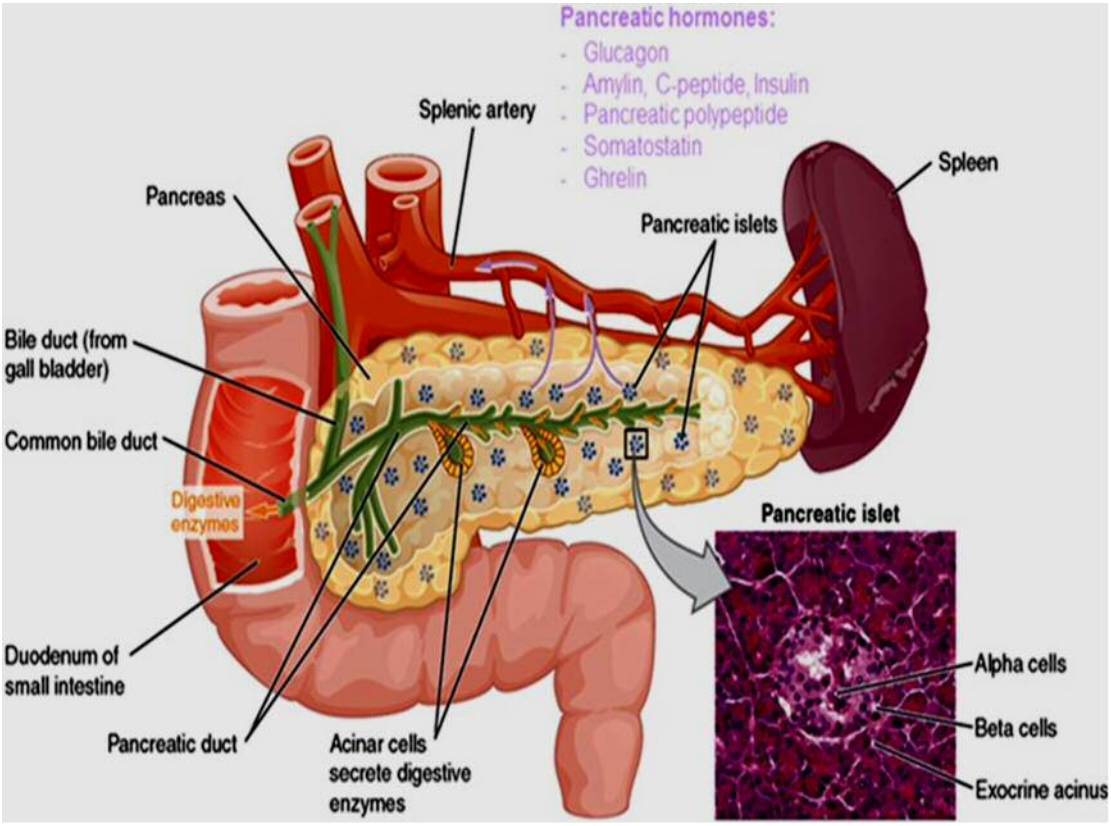

Figure 1.2 Anatomical organization and histology of the pancreas.

The endocrine function of the pancreas is regulated by the pancreatic islets of Langerhans involving the secretion of various hormones to the blood stream from different cell types. The exocrine function is mediated by acinar cells that secrete digestive enzymes into the duodenum via the pancreatic duct. The micrograph shows the histology of pancreatic tissue. (Adapted from *Röder PV et al, Exp Mol Med, 2016*) (9)

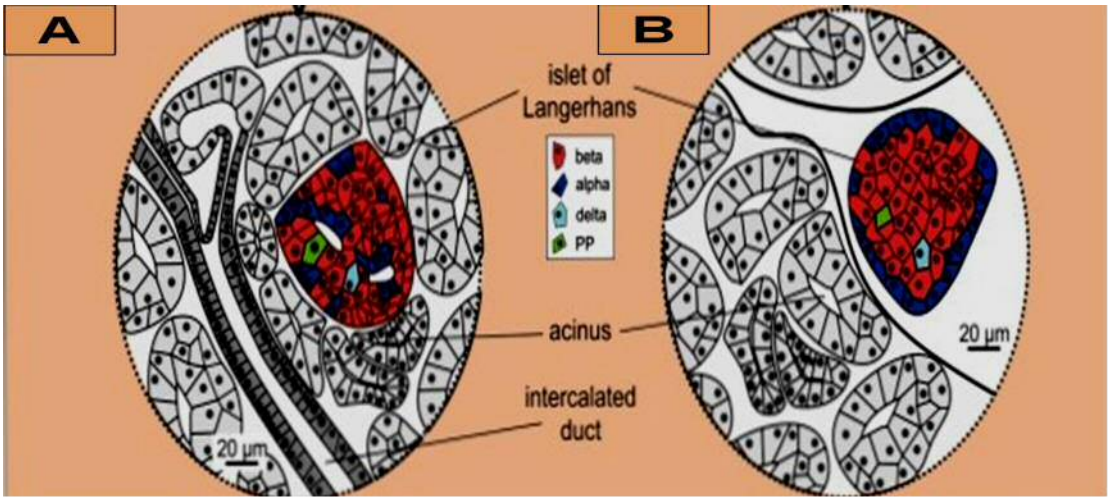

Figure 1.3 Microanatomy of the pancreas of the human and the mouse.

Microscopic anatomical structure of the pancreas reveals cell cytoarchitecture of the islets of Langerhans within the pancreas are markedly different between the human (A) and the mouse (B). (Modified from *Dolenšek J et al, Islets, 2015*) (16)

Endocrine function

The endocrine function of the pancreas is well known for its association with diabetes mellitus. The first written record of diabetes was in the Egyptian manuscript around 1500 BC. The term diabetes mellitus, reflecting the fact that the urine of those affected had a sweet taste, was first used by the Greek physician Aretaeus of Cappadocia (fl. 1st century AD). In 1889, Joseph von Mering and Oskar Minkowski found that removing the pancreas from dogs caused diabetes (17–19). This provided the first clue that diabetes is associated with the pancreas and the pancreas plays a key role in maintaining glucose homeostasis. In 1893, Laguesse suggested that the islet cells (described by Langerhans in 1869) of the pancreas were the histologic components involved in the pancreas of the patient with diabetes (20). All these studies had a breakthrough in 1921. Frederick Grant Banting and Charles Herbert Best discovered insulin when they recovered dogs that was nearly moribund in diabetic coma by injecting an extract from the pancreatic islet cells of healthy dogs (21). Together with James Collip and John Macleod, they purified the hormone insulin from bovine pancreases so that it could be used clinically for the first time to treat a patient with diabetes (22). Many scientists have received the Nobel Prize for diabetes-related investigations since 1923 because of their outstanding achievement in the study of diabetes and related aspects of glucose metabolism (Table 1.1).

The endocrine functions of the pancreas are diverse and involve various different hormonal regulations. These functions are largely dissociated with those of exocrine pancreas and will not be discussed further here.

Table 1.1 Nobel Prizes for Diabetes-Related Research. (Modified from *Polonsky KS, N Engl J Med, 2012)* (22)

Recipient	Year	Category	Contribution
F.G. Banting and J.J.R. Macleod	1923	Medicine	Discovery of insulin
C.F. Cori and G.T. Cori	1947	Medicine	Discovery of the course of the catalytic conversion of glycogen
B.A. Houssay	1947	Medicine	Discovery of the role of hormones released by the anterior pituitary lobe in the metabolism of sugar
F. Sanger	1958	Chemistry	Work on the structure of proteins, especially insulin
E.W. Sutherland	1971	Medicine	Discoveries concerning the mechanisms of action of hormones
R. Yalow	1977	Medicine	Development of radioimmunoassays for peptide hormones
E.H. Fischer and E.G. Krebs	1992	Medicine	Discoveries concerning reversible protein phosphorylation as a biologic regulatory mechanism

Exocrine function

In the mid-17th century, Regnier de Graaf (1641 - 1673) collected and investigated the pancreatic juice by way of using a hollow quill of a goose feather to cannulate the pancreatic duct of a dog (23). This was the initial study on discovering the role of the pancreas in digestive processes. However, the groundbreaking discovery of the digestive function of the pancreas was made by the great French physiologist Claude Bernard (1813 - 1878), who is called ‘‘one of the greatest of all men of science’’. He showed the pancreatic juice could emulsify fatty foods as well as contribute to the absorption of fats (24,25). He also demonstrated the digestive action of the pancreas to convert starch into sugar (25). This was the first evidence that confirmed the digestive function of the pancreas and what had been believed was that digestion did not take place entirely within the stomach. During the 19th century, Ivan Petrovich Pavlov (1849 - 1936), a Russian physiologist known primarily for his work in classical conditioning, indicated that pancreatic secretion was mediated by neural reflexes via a special pancreatic fistula in the dog (26). However, Ernest Starling and his brother-in-law William Bayliss demonstrated the hormone secretin was involved in pancreatic secretion (27–29). This proved the existence of a hormonal mechanism in regulating secretory function of the pancreas (30). In 1943, Harper and Raper reported the second hormone named pancreozymin (PZ) was able to stimulate the secretion of pancreatic enzymes (31). Subsequently, Jorpes and Mutt found that cholecystokinin (CCK) and PZ possessed the same biological properties of stimulating pancreatic enzyme secretion (32). The actions from PZ (the release of enzymes from the pancreas) and CCK (the contraction of the gallbladder, which forces bile into duodenum) were recognized as coming from one protein. Nowadays, it is generally solely known and used as CCK. It is now clear that pancreatic secretion is controlled by both neural and hormonal regulation (7,33,34).

An acinus and its draining ductule are the fundamental functional unit of the exocrine pancreas (Figure 1.4). As mentioned above, the small ductal cells-centroacinar cells secrete a HCO_3^- rich fluid, when stimulated by the hormone secretin (Table 1.2). An acinus is defined as any cluster of cells is assembled by many-lobed sacs, that is, pancreatic acinus is organized by several hundred acinar cells. These cells are linked by multiple gap junctions which regulates both direct chemical and electrical intercellular communication between cells (35–37). The main function of the pancreas which is the exocrine function consisting of synthesis and secretion of digestive enzymes (Table 1.2). The exocrine secretory process is composed of six successive steps: synthesis, segregation, intracellular transport, concentration, intracellular storage, and discharge (38). Cellular organelles e.g. ribosomes, endoplasmic reticulum (ER), Golgi apparatus and zymogen granules etc. are involved in this process within pancreatic acinar cell from the initiation of digestive enzymes production to the destination of triggering exocytosis. Generally, the secretory process of exocytosis is regulated by cytosolic Ca^{2+} concentration ($[Ca^{2+}]_i$) and this process is known as “stimulus-secretion coupling” (39–43), whereby only a low level of initial stimulus could be enormously amplified via multiple messengers in this chain reaction and resulted in cellular stimulation. In human, CCK is one of the most important hormone stimulating pancreatic acinar cells for secretion.

Table 1.2 The exocrine functions of pancreas.

Secretory component	Cell type	Primary stimuli
Water and bicarbonate ions	Centroacinar cells	Secretin
Digestive enzymes	Acinar cells	CCK

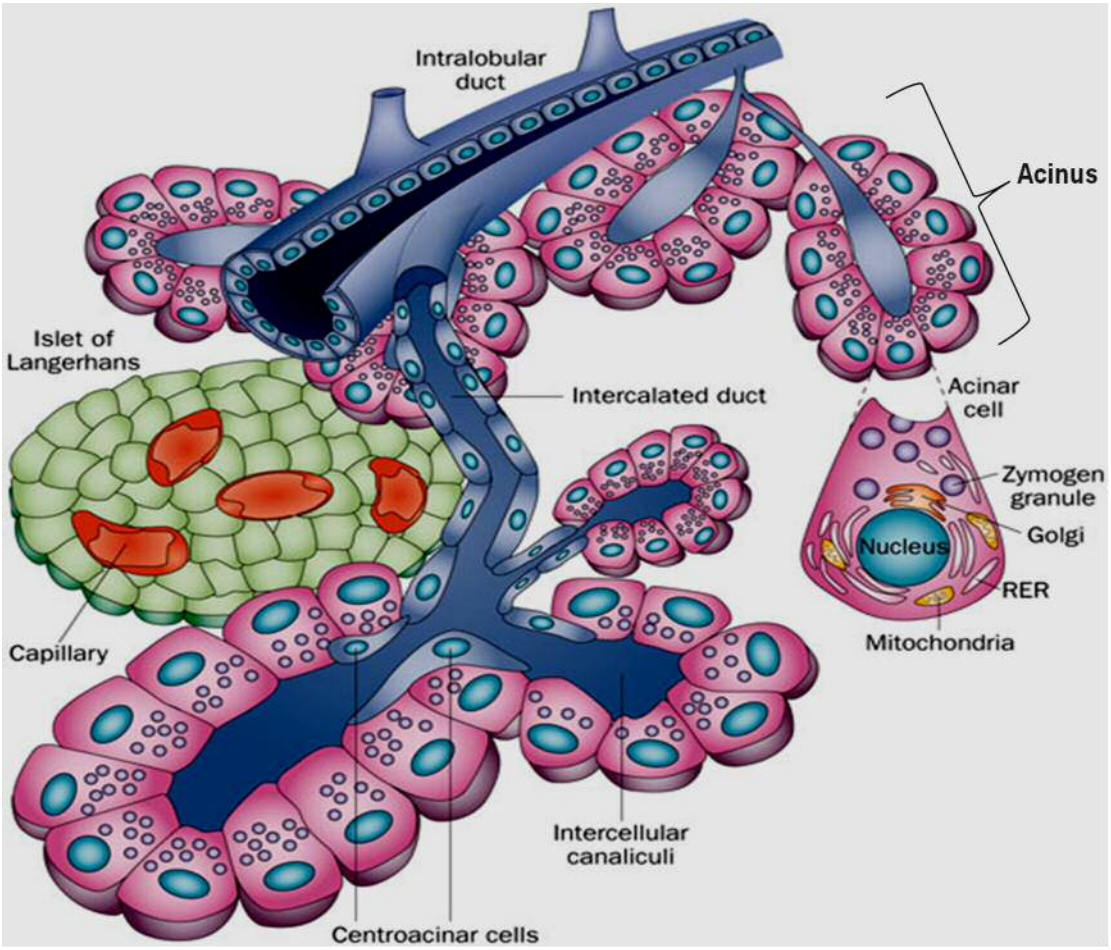

Figure 1.4 The exocrine pancreas.

The functional unit of the exocrine pancreas is composed of an acinus and its draining ductule. An acinus surrounding a central lumen open to the duct system is formed by pancreatic acinar cells. Pancreatic acinar cells synthesize, store and secrete digestive enzymes for the digestion and absorption of food in the small intestine. Digestive enzymes are secreted through the apical membrane of the acinar cell into small intercalated ducts that are directly connected to increasingly larger intralobular ducts that join the main pancreatic duct. (Modified from *Logsdon CD & Ji B, Nat Rev Gastroenterol Hepatol. 2013*) (44)

Pancreatic acinar cells

Pancreatic acinar cell is the dominant (up to 80%) cell type in the pancreas (45). Each pancreatic acinar cell is polarized with two visible areas: basolateral pole and apical pole (Figure 1.5). They are separated by the mitochondrial belt which can buffer the calcium from the apical pole to the basolateral pole. The basolateral pole is larger (even up to 90% of the cell volume) than the apical pole, and the majority of the endoplasmic reticulum (ER) is located in basolateral area. However, the endoplasmic reticulum can penetrate the mitochondria belt into the apical pole (46). The apical pole contains zymogen granules (ZGs) where digestive proenzymes are stored.

The main function of acinar cells is to secrete digestive enzymes in response to eating food. This secretion is mediated by acetylcholine (ACh), which is released from the endings of the vagus nerve, and the circulating hormone cholecystokinin (CCK). The secretion process itself takes place by exocytosis. The granule membrane fuses with the apical (luminal) cell membrane and subsequently the opening pole of the granule allows zymogens to move into the acinar lumen. The acinar cells and the small ducts each secrete a neutral Cl^- rich and a HCO_3^- rich fluid respectively so that the zymogens can move from the duct system into the gut.

As was previously mentioned, ACh or CCK activates pancreatic acinar cells to secrete an isotonic NaCl-rich pancreatic acinar juice containing a majority of enzymes and precursor enzymes. Enzymes contained in the acinar fluid are active α-amylase, lipases and colipase as well as various other enzymes (e.g. collagenase, elastase, phospholipase A and ribonuclease), whereas the precursor enzymes are trypsinogen, chymotrypsinogen and procarboxypeptidases. These protease precursors are activated in the small intestine, initiated by intestinal enzyme enterokinase converts trypsinogen to

trypsin. Subsequently, trypsin activates trypsinogen auto-catalytically and also activates the other precursors. The neutral pancreatic acinar juice, containing these enzymes and enzyme precursors, is delivered to intercellular cananiculus where it is mixed with the HCO_3^- rich fluid secreted by the centroacinar cells in response to stimulation with the hormone secretin (47–49).

The physiological functions of pancreatic acinar cells are controlled by calcium (50). Different patterns of cytosolic calcium responses differentiate between physiology and pathology. Physiological concentration of ACh and CCK evoke either small cytosolic $[Ca^{2+}]_i$ oscillations, which are often confined only to apical area of the cell or global calcium waves that originate in the apical area and spread toward the basolatoral area (51,52). The ACh or CCK receptors at the basolateral plasma membrane receive stimuli for secretion (such as ACh or CCK) leading to the generation of a second messenger response, which in turn liberates calcium from the intracellular stores (53–55).

A

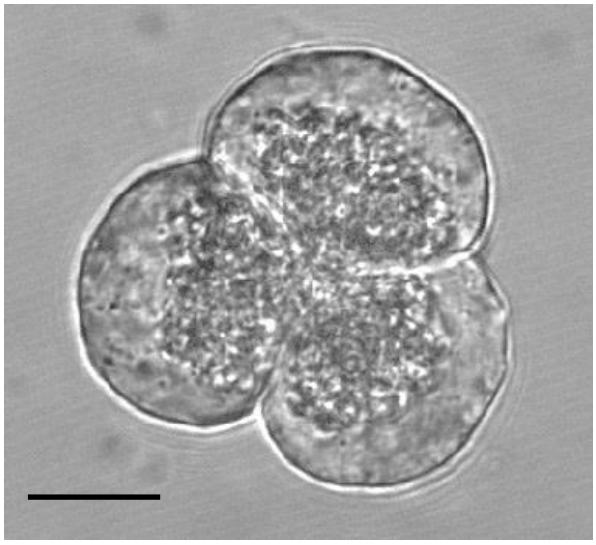

B

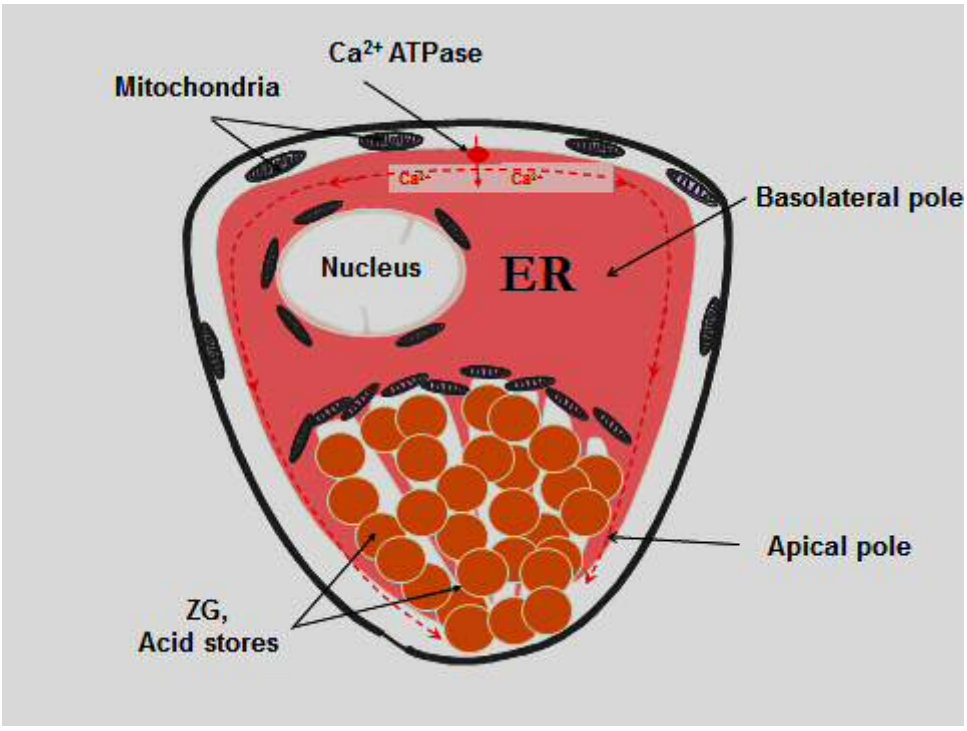

Figure 1.5 Structure of pancreatic acinar cell.

(A) Transmitted light image from the confocal microscope shows typical triplet pancreatic acinar cells isolated from mouse pancreas. Scale bar is 10 μm. (B) Schematic illustration of the pyramid-shaped structure of a pancreatic acinar cell. The basolateral pole contains most of the ER; zymogen granules are stored in the apical pole. (Adapted from *Gerasimenko JV et al, J Cell Sci, 2006*) (55)

Early studies indicated that the ER was the principal intracellular calcium store and the neurotransmitters ACh as well as the circulating hormone CCK elicited Ca^{2+} release from the ER (56–58). Intracellular water soluble messenger inositol 1,4,5-trisphosphate (IP_3) was discovered and shown releasing Ca^{2+} from the ER in permeabilized pancreatic acinar cells (59,60). Although the original discovery of IP_3-evoked Ca^{2+} release was found on pancreatic acinar cells, it is still difficult to understand why physiological Ca^{2+} signals occur specifically in the apical granular pole, which contains mostly ZGs and little ER (52,61–64). Ca^{2+} tunnel experiments answered this question and demonstrated that Ca^{2+} taken up at the base of the cell into the ER could diffuse easily in the ER lumen and reach the apex via thin ER extensions penetrating deeply into the granular area between the ZGs (65,66). Moreover, the highest concentration or the most sensitive IP_3 receptors (IP_3Rs) are concentrated in the apical region of the pancreatic acinar cells (67,68). Ca^{2+} release in mouse pancreatic acinar cells is dependent on IP_3 receptor (IP_3R) subtypes 2 and 3, which can replace by each other (69). Knockout both subtypes resulted in no IP_3-mediated Ca^{2+} release(69). Physiologically Ca^{2+} signals occurring in the apical pole are essential for activating exclusive Cl^- channels present in the apical membrane-Ca^{2+}-activated Cl^- channels, which are important for acinar fluid and the exocytotic enzyme secretion (70). The mitochondria distributed in a very specific manner in the acinar cells. Due to their ability to soak up Ca^{2+}, the localization of mitochondria could preventing the spread of cytosolic Ca^{2+} signals from the apical pole into the basal part of the cell containing the nucleus (71,72).

Intracellular calcium signalling in the pancreas

Calcium as an intracellular messenger

In 1959, Nobel laureate Otto Loewy described the role of calcium ions in the organism by a witty remark: “Ja Kalzium, das ist alles!” (73). It is undeniable that calcium ion (Ca^{2+}) is one of the most important signaling molecules in the organism and impact nearly every aspect of cellular life (74,75). External stimuli can be transduced by calcium signalling into cells, which participate in the regulation of heartbeat, muscle contraction, neuronal signal coding, gene expression, fertilisation, cell growth and proliferation, cell migration, cell cycle, apoptosis, cancer, neurogenesis, learning and memory as with synaptic plasticity and other physiological and pathological processes (76–85). Studies on calcium signalling cover the understanding of the different levels of calcium signalling dynamics from cellular organelles to whole organs. The regulatory mechanism of calcium signalling is complex and it can interact with other signal networks in the cell. As calcium signalling integrates a wide range of cellular functions, the transduction of calcium signalling mediated by Ca^{2+} is under strict control, that is, Ca^{2+} acts on different types of cells under tight spatiotemporal coordination with different intensities to regulate their specific physiological functions.

Ca^{2+} plays an important role in cell signal transduction, this is because protein and enzyme conformations and their interactions are regulated by $[Ca^{2+}]_i$. $[Ca^{2+}]_i$ change can trigger the alteration of shape and charge in proteins and enzymes, which can affect function. There are two primary calcium signalling transduction pathways in eukaryotic cells. The first pathway is that Ca^{2+} enters into cells directly through the activated ion channels and transporters. The other one is that Ca^{2+} acts as a second messenger indirectly involved in signal

transduction. For example, extracellular stimulus or signals can activate calcium signalling by G protein-coupled receptor (GPCR) (86). G protein coupled receptors (GPCRs), also known as seven-transmembrane domain receptors, are expressed in all eukaryotic cells (87), and more than 2,000 genes in the human genome that encode GPCRs, which are the largest receptor molecule superfamily on the cell membrane (88). Structurally, G proteins are heterotrimeric complexes which made up of alpha (α), beta (β) and gamma (γ) subunits (89). There are a large number of diseases associated with GPCRs, and about 40% of modern drugs target GPCRs (90).

Normally, resting cytoplasmic [Ca^{2+}] is maintained at about 100 nM in eukaryotic cells, which is 20,000-fold lower than extracellular [Ca^{2+}] (74). To maintain this low concentration, various membrane calcium pumps, channels and exchangers are involved in coordinating this very tight control process. ATPase pumps are responsible for cytosolic Ca^{2+} clearance, that is, sarco/endoplasmic reticulum Ca^{2+} ATPase (SERCA) pumps Ca^{2+} into the endoplasmic reticulum (ER) or plasma membrane Ca^{2+} ATPase (PMCA) pumps push Ca^{2+} out of the cell (Figure 1.6). Both SERCA and PMCA are P type ATPases which remove two or one Ca^{2+} per ATP hydrolyzed, respectively (91). In many cell types, the Na^{+}/Ca^{2+} exchanger (NCX) is an antiporter membrane protein that removes calcium from cells, which exchanges one Ca^{2+} for the import of three Na^{+} (92). Interestingly, the high-affinity, low-capacity PMCA pumps are effective at maintaining low $[Ca^{2+}]_i$ over long durations, whereas the low-affinity, high-capacity NCX make the rapid adjustments needed during generation of action potentials in excitable cells (92–95). Hence, they complement each other for internal [Ca^{2+}] homeostasis. However, NCX only plays a minor role in pancreatic acinar cells (96,97). Notably, calmodulin can substantially increase both Ca^{2+} binding affinity and pump rate of PMCA (98,99).

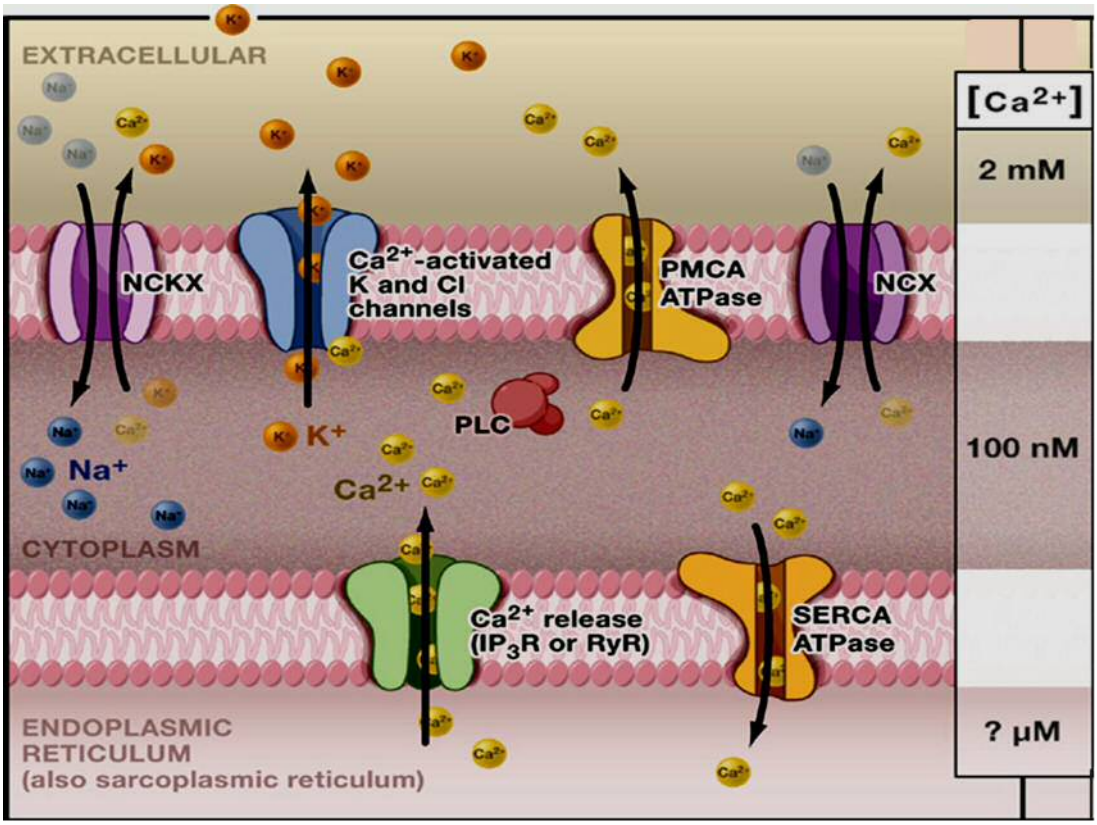

Figure 1.6 Maintaining Ca^{2+} homeostasis and using Ca^{2+} gradients for signalling.

Cytoplasmic [Ca^{2+}] is maintained at about 100 nM in pancreatic acinar cells by extrusion mainly via two transporters: sarco/endoplasmic reticular Ca^{2+} ATPase (SERCA) and plasma membrane Ca^{2+} ATPase (PMCA). The Na^{+}/Ca^{2+} exchanger (NCX), a major secondary regulator of $[Ca^{2+}]_i$ imports three Na^{+} in exchange for the export of one Ca^{2+}. However, NCX plays a very minor role in cytosolic Ca^{2+} clearance in pancreatic acinar cells. Intracellular Ca^{2+} depolarizes pancreatic acinar cells by activating Cl^{-} channels in the apical pole. (Modified from *Clapham DE, Cell. 2007*) (74)

Generally, exocytosis is activated by a rise in the $[Ca^{2+}]_i$ (100–102). In excitable cells e.g. nerve and endocrine cells; exocytosis is normally trigged by Ca^{2+} entry via special voltage-activated Ca^{2+} channels in the plasma membrane. Membrane depolarization leads to voltage-gated channels open, which is caused by action potentials (103). However, pancreatic acinar cell is electrically non-excitable cell and not able to fire action potentials. Therefore, stimulus-secretion coupling is dependent on Ca^{2+} release from intracellular stores to the cytosol (104). It has been established that the initial secretory response of pancreatic acinar cell to ACh or CCK stimulation is independent of extracellular Ca^{2+}, whereas external Ca^{2+} is indispensable for sustained secretion (43). Ca^{2+} release from the intracellular Ca^{2+} stores into the cytosol inevitably activates Ca^{2+} pumps in the plasma membrane, which causes intracellular Ca^{2+} from the internal stores to be extruded to the extracellular fluid (105). In this situation, a well-known process known as store-operated Ca^{2+} entry is activated by the reduction of $[Ca^{2+}]$ in the intracellular stores (106). Such Ca^{2+} signalling is transmitted from the stores to the plasma membrane activating store-operated channels (SOCs) that allow Ca^{2+} entry (107). Due to this store-operated Ca^{2+} entry (SOCE) the sustained secretory response is maintained in pancreatic acinar cells during prolonged stimulation.

Calcium release

Pancreatic acinar cell is the typical polarized mammalian exocrine gland cell, which is particularly attractive and generally accepted model for studying Ca^{2+} transport processes. This is because characteristic subcellular distributions of cellular organelles including the ER, the mitochondria and the ZGs, etc. which are crucial to Ca^{2+} signalling, facilitated the description of intracellular Ca^{2+} signalling events (46,55,71,108,109). It has been well established that a rise in $[Ca^{2+}]_i$ of pancreatic acinar cells is stimulated by either ACh or CCK. Physiological concentration of the neurotransmitter ACh or the hormone CCK evokes small $[Ca^{2+}]_i$ oscillations, which are the typical Ca^{2+} signal pattern consists of repetitive $[Ca^{2+}]_i$ spikes often confined only to apical (granular) area of the cell. Whereas increasing the stimulating agonist concentration causes global calcium waves that originate in apical area and spread toward the basolatoral area.

There are two major signal transduction pathways (Figure 1.7) that induce Ca^{2+} release in pancreatic acinar cells: 1) nervous (ACh) stimulation mediated Ca^{2+} release; 2) hormonal (CCK) stimulation initiated Ca^{2+} release. Both the physiological stimulants act on the outside of the acinar plasma membrane (53,54). ACh binds to muscarinic M3 receptors (110) activating phospholipase C (PLC) via G protein pathway leading to the breakdown of phosphatidylinositol 4,5-bisphosphate (PIP_2). The subsequent generation of inositol 1,4,5-trisphosphate (IP_3), an intracellular messenger, regulates the release of Ca^{2+} from the ER (59). CCK acts on high affinity CCK1 receptors in the basolateral plasma membrane (111,112). Subsequently, the enzyme ADP-ribosyl cyclase is activated by a yet unknown mechanism to form two separate messengers: nicotinic acid adenine dinucleotide phosphate (NAADP) and cyclic ADP-ribose (cADPR) (113). The three messengers, IP_3, cADPR, and NAADP, can liberate Ca^{2+} from the ER by activating IP_3Rs (69) and RyRs

(114,115), respectively.

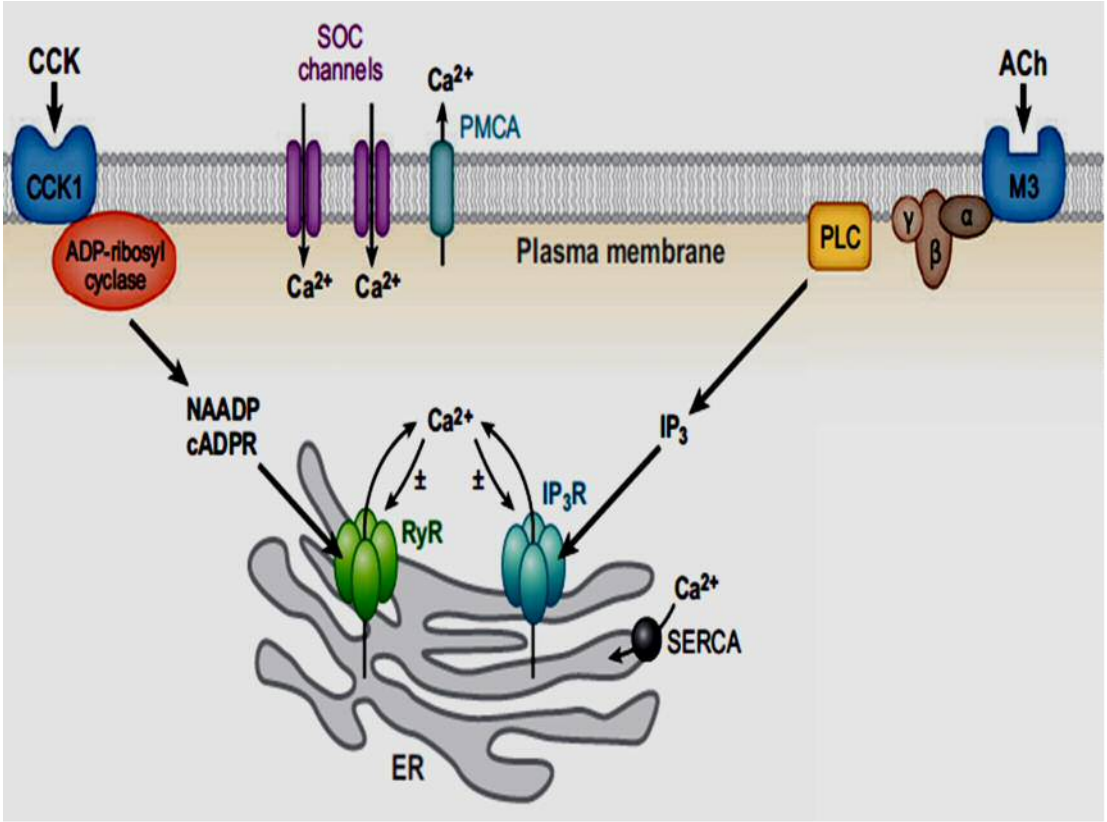

Figure 1.7 Local Ca^{2+} signalling in a pancreatic acinar cell.

Calcium signalling events occur at the plasma membrane. Two receptor pathways are shown. CCK interaction with CCK1 receptors results in activation of the cytosolic enzyme ADP-ribosyl cyclase, which generates cADPR and NAADP. ACh binding to muscarinic M3 receptors activates, via interaction with a classical trimeric G protein, phospholipase C (PLC) generating the messenger IP_3. cADPR and NAADP activate RyRs, whereas IP_3 activates IP_3Rs in intracellular stores to release Ca^{2+} from ER. (Adapted from *Petersen OH & Tepikin AV, Annu Rev Physiol. 2008*) (50)

In fact, physiological Ca^{2+} signals occurring in the apical granular area are not only due to Ca^{2+} release from ER, but also Ca^{2+} could be released from ZGs and other acid pools in the apical pole (Figure 1.8) (55,116,117). It was shown that both IP_3 and cADPR - derived from nicotinamide adenine dinucleotide (NAD) can release Ca^{2+} on isolated ZGs (118). Subsequently, in a study of permeabilized pancreatic acinar cells it was shown that IP_3, cADPR and NAADP - derived from Nicotinamide adenine dinucleotide phosphate (NADP) can all liberate Ca^{2+} from both the ER and ZGs dominated acid pools in the apical granular area (55,119). It also has been demonstrated that IP_3 activates IP_3Rs, whereas cADPR or NAADP activates RyRs to release Ca^{2+} on isolated nuclei surrounded by several layers of ER (120). Recently, it has been reported that NAADP-evoked Ca^{2+} release from endosomes/lysosomes is completely dependent on functional two-pore channels (TPCs) (121,122), and particularly on TPC2 (123). This triggers Ca^{2+}-induced Ca^{2+} release (CICR) by RyR subtypes 1 and 3 occurring from the zymogen granules and the ER (123).

Cytosolic Ca^{2+} signals elicited by physiological agonists – ACh or CCK or directly by one of the intracellular messengers - IP_3, cADPR or NAADP are always initiated in the apical pole of pancreatic acinar cells. This is because of the concentration of critical Ca^{2+} release channels in the apical pole rather than the concentration of agonist receptors in the apical membrane (51,124). Mapping of intracellular CICR sites by local Ca^{2+} uncaging specifically in the apical pole demonstrated this point of view. CICR elicited in the apical pole produce a Ca^{2+} wave progressing toward the basolatoral area. However, local Ca^{2+} uncaging failed to trigger CICR at the base (51). As shown in Figure 1.8, CICR depends on both functional Ca^{2+} release channels - IP_3Rs and RyRs. The RyRs seem uniformly distributed throughout the cell (125), which differs from the distribution of IP_3Rs (67,68). CICR is central to all types of Ca^{2+} signal generation in the acinar cells. Therefore, either IP_3R or RyR antagonists can abrogate Ca^{2+} spiking regardless of the primary stimulus (126).

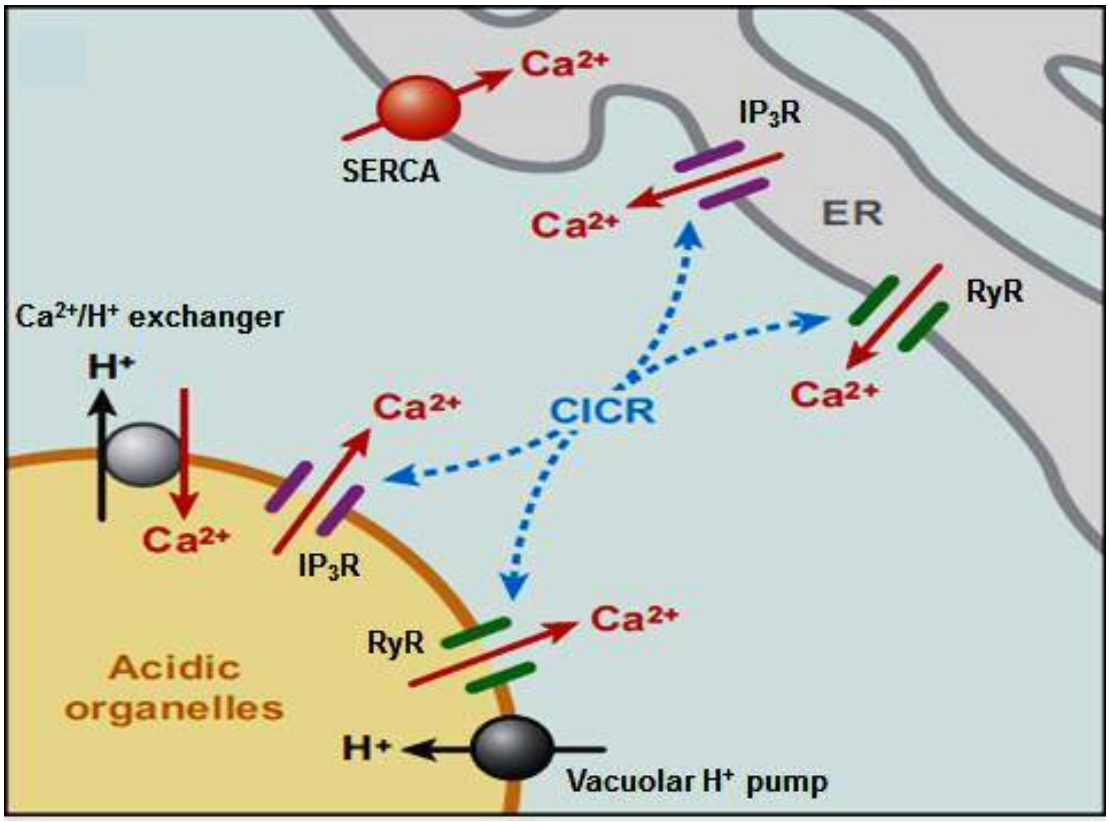

Figure 1.8 Ca^{2+} release from two types of intracellular stores in the apical pole.

Two principal stores are located in the apical pole : 1) ER with SERCA (red) and both IP_3Rs as well as RyRs; 2) acidic organelles with a vacuolar H^+ pump (black), also with both IP_3Rs and RyRs. Ca^{2+} release from both the ER and the acidic Ca^{2+} store can be induced by Ca^{2+}-releasing messengers: IP_3, cADPR, or NAADP. Ca^{2+}-induced Ca^{2+} release (CICR) is the physiological cytosolic Ca^{2+} signal generated by interaction between the two stores as well as interaction between RyRs and IP_3Rs. (Adapted from *Petersen OH & Tepikin AV, Annu Rev Physiol. 2008*) (50)

The reason for Ca^{2+} signalling events in intact acinar cells are complex is that repetitive Ca^{2+} spiking requires co-operation between functionally active IP_3Rs and RyRs (80). In other words, Ca^{2+}-mediated positive and negative interactions between IP_3Rs and RyRs are functionally important for physiological Ca^{2+} signalling events generation. For example, intracellular Ca^{2+} release induced by an increase of IP_3 concentration will subsequently activate RyRs inducing further Ca^{2+} release. The rising phase of the cytosolic Ca^{2+} signal is initiated by this positive feed-forward effect. However, when $[Ca^{2+}]_i$ reaches at a certain higher level, a further $[Ca^{2+}]_i$ rise suppress opening of both IP_3Rs and RyRs, which explains the falling phase of the spike by this negative feedback effect (127).

The termination of Ca^{2+} signals has the same importance as their initiation. During sustained stimulation with ACh, plateau of elevated $[Ca^{2+}]_i$ represents a delicate balance of Ca^{2+} entry through store-operated Ca^{2+} channels (SOCs) in the basal membrane (128,129) and Ca^{2+} extrusion mainly through Ca^{2+} pumps located in the apical plasma membrane (PMCA) (96,130). Discontinuation of supramaximal ACh stimulation immediately causes Ca^{2+} pump (SERCA)-mediated Ca^{2+} reuptake into the ER and a rapid reduction of $[Ca^{2+}]_i$ back to the resting level (66). $[Ca^{2+}]$ in the ER ($[Ca^{2+}]_{ER}$) takes much longer to recover fully than $[Ca^{2+}]_i$ (128). However, physiological concentrations of ACh or CCK cause small amounts of Ca^{2+} release from ER, which evoke the smallest and shortest cytosolic Ca^{2+} spikes, has proven to be impossible to decrease $[Ca^{2+}]_{ER}$ during each spike (131).

Calcium entry and extrusion

Although intracellular Ca^{2+} release from ER induced by physiological concentration of ACh or CCK for secretion is the primary event, Ca^{2+} entry and extrusion can simultaneously regulate the overall cellular Ca^{2+} homeostasis, which is essential for both physiology and pathology of pancreatic acinar cells. If any regulatory process of Ca^{2+} transport is out of control that would lead to cellular Ca^{2+} overload causing cell death (132–134). Therefore the plasma membrane must be relatively impermeable to Ca^{2+} and Ca^{2+} movement across the plasma membrane provides a clear example of the steady state $[Ca^{2+}]_i$ in pancreatic acinar cells with extreme structural and functional polarization. In other words, PMCA is not only maintain a low $[Ca^{2+}]_i$, but also restore the low $[Ca^{2+}]_i$ after a challenge-elicited $[Ca^{2+}]_i$ increase. Upon $[Ca^{2+}]_i$ of above 100 nM, Ca^{2+} extrusion is activated to adjust $[Ca^{2+}]_i$ back to the resting level. Whereas, Ca^{2+} entry occurred predominantly across the basolateral membrane is responsible for refilling the ER (135). The process and transport mechanisms of Ca^{2+} entry and extrusion across the plasma membrane of pancreatic acinar cells is regulated by specific Ca^{2+} channels and pumps (Figure 1.9).

As mentioned previously, unlike many electrically excitable cells, pancreatic acinar cells do not possess functional NCX. The process of Na^+/Ca^{2+} exchange plays an important role in restoring a low $[Ca^{2+}]_i$ following an action potential (92). However, the rate of Ca^{2+} extrusion following stimulation induced $[Ca^{2+}]_i$ elevation in pancreatic acinar cells is not influenced by the removal of extracellular Na^+ (96,105). Hence, the only mechanism for Ca^{2+} exit across the plasma membrane is via the PMCA (96,136). Interestingly, this pump is specifically concentrated in the apical plasma membrane rather than evenly distributed over the plasma membrane, and therefore physiological concentration of agonist-elicited $[Ca^{2+}]_i$ above the basal level of 100 nM can activate PMCA-mediated Ca^{2+} extrusion in the apical pole and Ca^{2+} is mainly

extruded into the acinar lumen (137). The concentration of PMCA in the apical membrane is functionally important due to the initiation of intracellular Ca^{2+} release sites are in the apical pole. However, inappropriate Ca^{2+} entry across the basal membrane causes Ca^{2+} overload when pancreatic acinar cells are challenged by pathological stimulus, which PMCA cannot deal with this adequately because of its limited capacity (138). The half-maximal rate of calcium extrusion depends on $[Ca^{2+}]_i$ of approximately 200 nM, but calcium extrusion mechanism was almost completely saturated when $[Ca^{2+}]_i$ is above 400 nM (139). Overall, pancreatic acinar cells solely depend on the PMCA to extrude excess intracellular Ca^{2+} in order to maintain and restore $[Ca^{2+}]_i$ within the physiological range, but substantial cytosolic Ca^{2+} overload leads to malfunctioning of this well-functioning extrusion mechanism.

It has been known that pancreatic acinar sustained secretory response and exocytosis is dependent on the presence of external Ca^{2+} (43,140). Physiological concentration of agonist-elicited Ca^{2+} spiking is primarily generated by internal Ca^{2+} release from intracellular stores, principally the ER (50,59). This does not increase Ca^{2+} permeability in the plasma membrane. Upon $[Ca^{2+}]_i$ increases, plasma membrane Ca^{2+} ATPases (PMCAs) are activated to extrude more cytosolic Ca^{2+} in order to maintain resting level of $[Ca^{2+}]_i$ (130). Due to the rate of Ca^{2+} extrusion of PMCA is faster than the rate of Ca^{2+} taken up into the ER by SERCA, $[Ca^{2+}]_{ER}$ would be depleted gradually if there were not a mechanism of compensatory Ca^{2+} uptake from the external solution (141). It has been well established that Ca^{2+} release-activated Ca^{2+} (CRAC) channels, which are the one of the best known store-operated Ca^{2+} channels (SOCs), in the baso-lateral plasma membrane regulate this uptake mechanism (Figure 1.9) and CRAC channels have generally been well characterized (106,142–144).

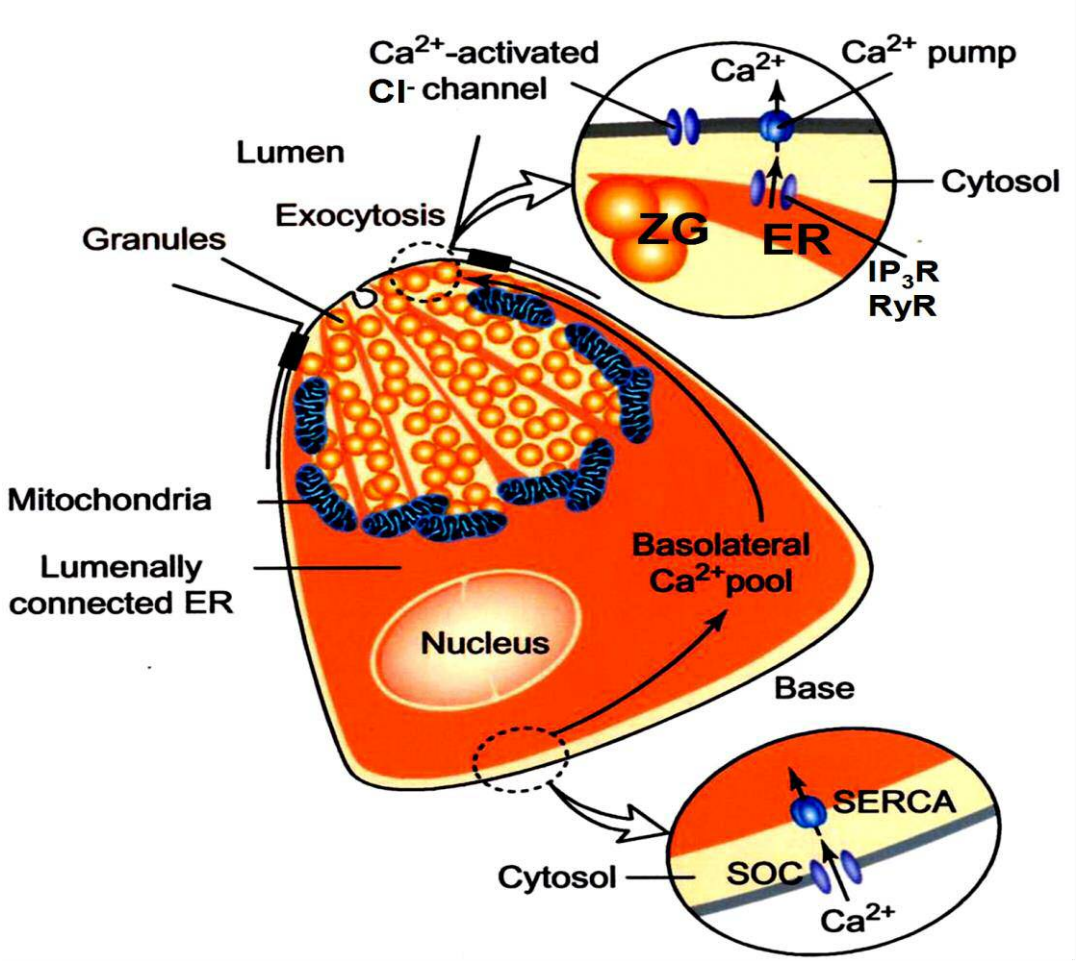

Figure 1.9 Ca^{2+} transport-entry and extrusion in pancreatic acinar cell.

Agonist stimulation liberate Ca^{2+} from endoplasmic reticulum (ER) store in the apical pole of the cell via the Ca^{2+} release channels-IP_3 receptors (IP_3Rs) and ryanodine receptors (RyRs). Ca^{2+} pumps (PMCAs) concentrated in the apical membrane extrude Ca^{2+} released from the apical part of the ER into the acinar lumen. Ca^{2+} enters through a store-operated channel (SOC) in the basal membrane and then is pumped into the ER by the Ca^{2+} pump (SERCA). Thereafter, Ca^{2+} flow through the lumenally continuous ER from the basal to the apical pole. (Adapted from *Petersen OH et al, Trends Neurosci. 2001*) (65)

Endowed with several particular biophysical features including high Ca^{2+} selectivity and a low unitary conductance (106), functional CRAC channels are assembled from two protein families: the Orai proteins and the stromal interaction molecule (STIM) proteins (145). Orai proteins form the ion channel pore and in particular Orai1 is the molecule responsible for Ca^{2+}-selective CRAC channel currents, which is essential for CRAC channel activity (146,147). STIM proteins are functionally as the ER calcium sensors and activators of CRAC channels. Identification of stromal interaction molecule 1 (STIM1) as the mammalian ER Ca^{2+} sensor (148,149) and Orai1/CRACM1 or Orai1/STIM1 as a component of the CRAC channel illuminate key steps in the molecular mechanism of SOCE (146,150–152). Following identification of Orai1 and STIM1 as two essential components of the CRAC channel, many works were turned to understand the pore architecture of the CRAC channel and the basis of Ca^{2+} influx.

Orai1, as an essential component of the CRAC current (I_{CRAC}) (153), was firstly identified by studies of T-lymphocytes using linkage analysis and positional cloning from patients with a severe combined immune deficiency (SCID) syndrome (146). Orai1 consists of four transmembrane domains (TM1-TM4) with cytosolic N- and C-termini, which contain STIM1 binding sites (Figure 1.10). It has been demonstrated that Orai1 is an essential pore subunit and encodes the pore-forming subunit of the CRAC channel (154). The mutation of several acidic residues of Orai1 identified in TM1 (E106), TM3 (E190), and the TM1–TM2 (D110, D112, and D114) loop transforms ion selectivity or permeation (154–158). Subsequent study of the crystal structure of the *Drosophila* Orai channel revealed that this calcium influx channel is composed of a hexameric assembly of Orai subunits arranged in concentric layers around a central ion pore, which traverses the membrane and extends into the cytosol (159). It has been suggested that anion binding may play an important role in Orai gating mechanism that keeps the pore closed in the resting state (159).

However, this gating mechanism is still elusive and remains to be determined.

STIM1 is a 77 kDa type I single-pass membrane protein with a luminal NH_2 terminus and a cytoplasmic COOH terminus localized predominantly in the ER membrane with multiple predicted protein interaction or signalling domains (Figure 1.10) (148,151,160). The ER luminal N-terminal region of STIM1 contains two residing domains: an EF-hand (EF) calcium binding motif and a sterile α-motif (SAM). EF functionally acts as the protein with ER Ca^{2+} sensing (148,151) and SAM regulates STIM oligomerization (161). Although the cytosolic C-terminus is composed of several distinct coiled-coil (CC) domains and modules, the most critical region is a roughly 100 amino acid CRAC activation domain (CAD), which is also known as STIM-Orai activation region (SOAR) (155,162–166). CAD/SOAR binds to Orai, and a polybasic domain at the extreme COOH terminus interacts with the plasma membrane (PM) at ER-PM junctions, that is necessary and sufficient to activate I_{CRAC} (163,167).

In most cells, 75–85% of endogenous STIM1 is distributed in the ER membrane (168,169). Total internal reflection fluorescence (TIRF) and confocal microscopy showed that STIM1 is primarily localized throughout the ER when Ca^{2+} stores are full. Upon store depletion, STIM1 redistributes into discrete puncta near the plasma membrane (148,151,160,161,170–172). Electron microscopy revealed the most precise localization of STIM1, that is, the clustered STIM1 aggregates into puncta and accumulates within ER-PM junctions which are the junctional ER structures located 10-25nm from the plasma membrane (147,160).

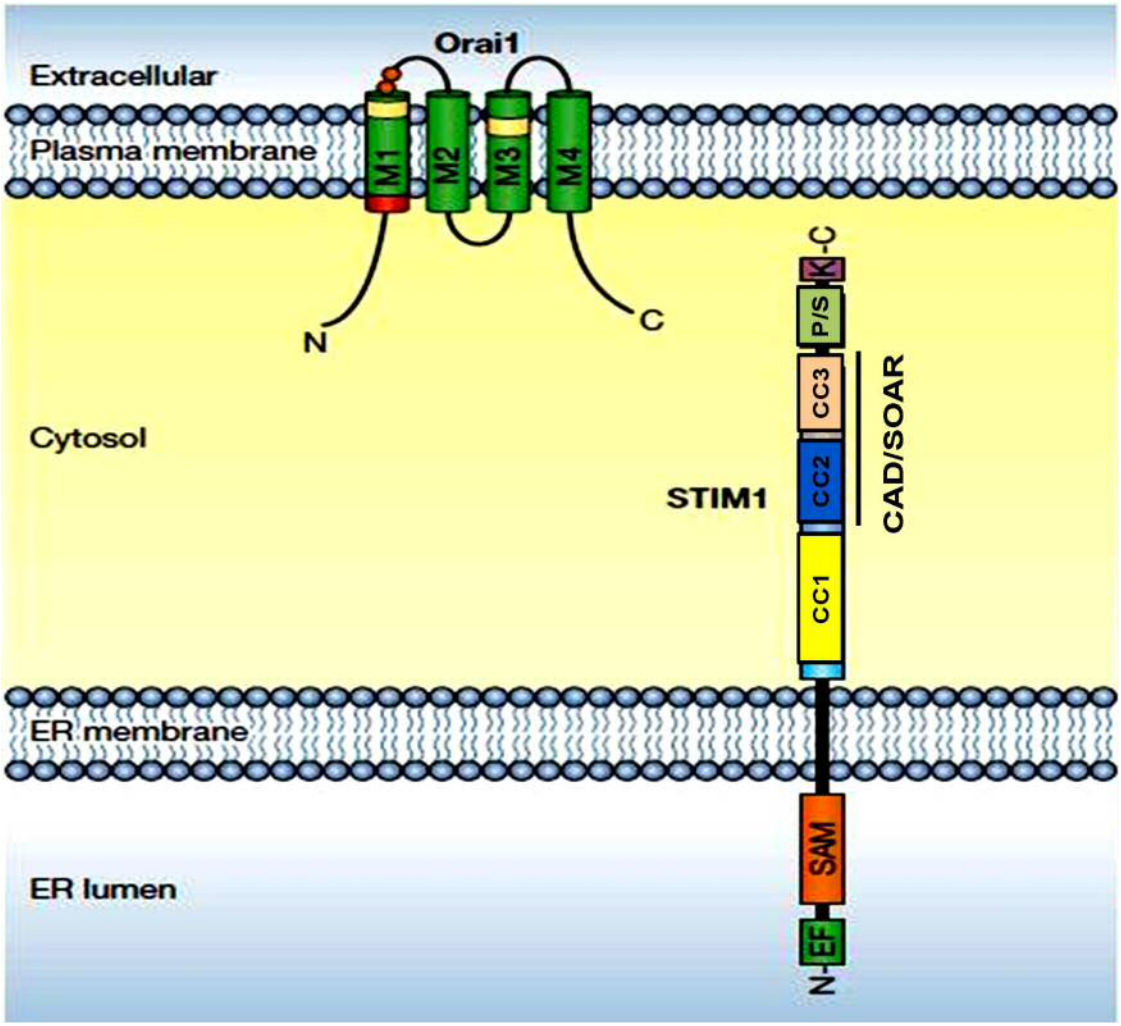

Figure 1.10 Structure and functional domains of Orai1 and STIM1.

Orai1 is a four times membrane-spanning Ca^{2+}-selective channel with four transmembrane domains (TM1-TM4) and C and N termini directed to the cytoplasm. STIM1 is a single-transmembrane protein localized primarily in the ER membrane. The organization of the major predicted domains include EF-hand followed by a sterile α-motif (SAM) in the N terminus directed to the luminal side, and coiled-coil domains 1-3 (CC1-3), which harbor CAD/SOAR, proline-serine-rich domain (P/S), and lysine-rich domain (K-rich) on the cytosolic side in the C terminus. (Modified from *Lewis RS, Nature. 2007*) (145)

Based on identification of structural functional domain organization of STIM and Orai, the mechanism of the molecular choreography of SOCE has been well established (142,173,174). The activation process of SOCE by store depletion is highly dynamic and dependent on the redistribution of STIM and Orai in the cell (Figure 1.11). Under the physiological condition of the resting state of the cells, STIM1 and Orai1 diffuse and mobilize throughout the ER and plasma membrane, respectively (148,151,161,163,175–177). In resting cells with replete Ca^{2+} stores, Ca^{2+} is bound to EF-hand domain forming a stable complex with the SAM domain on the luminal side. After ER store depletion, Ca^{2+} dissociates from the EF-hand and lead to the homogeneous distribution of clustered STIM1 accumulate in the ER-PM junctions and aggregates into puncta (50,142,145,148,160,176). The sites of Orai/STIM interaction are ER-PM junctions where STIM1 binding to Orai1 enhance the local concentration of STIM1 near Orai1, leading to rapid and efficient CRAC channel opening to trigger Ca^{2+} entry. This process is reversible only if Ca^{2+} is refilled in the ER store. In this scenario, EF-hand domain binds Ca^{2+} and facilitates the complex formation with SAM domain again, which results in deactivation of Orai (176,178,179).

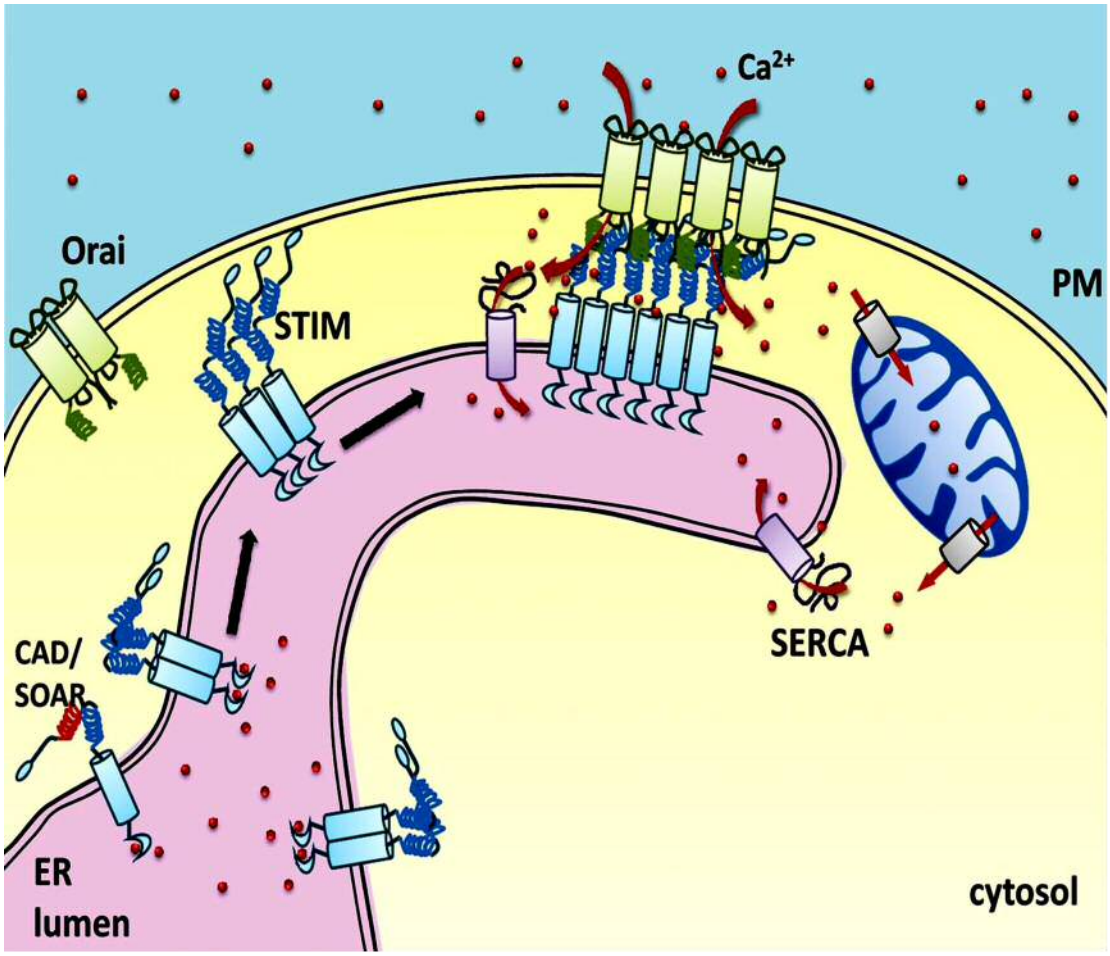

Figure 1.11 Molecular mechanism of store-operated Ca^{2+} entry.

The diagram depicts the process of store-operated Ca^{2+} entry. At resting level of $[Ca^{2+}]_{ER}$, Ca^{2+} is binding EF-hand on the luminal side which maintain STIM in inactive state. Upon store depletion, Ca^{2+} dissociate from EF-hand domain, which triggers a conformational change of STIM and then STIM translocate and accumulate to ER-PM junctions by diffusion in the ER membrane. At the junctions, CAD/SOAR of STIM interacts and activates channels composed of Orai subunits via electrostatic interaction, thereby lead to opening of Orai1 Channels and Ca^{2+} entry. (Modified from *Shen WW & Demaurex N, Biochem Soc Trans. 2012*) (166)

Calcium signalling and mitochondrial functions

It has been well established that the critical importance of intracellular Ca^{2+} and ATP for the regulation of exocytotic secretion in pancreatic acinar cells. Also, It is clear that exocytosis initiation is triggered by a rise in the $[Ca^{2+}]_i$ in a various of cell types, but this would not happens if intracellular ATP is absence (180). Pancreatic acinar cells place special demands on the mitochondria to regulate Ca^{2+} homeostasis and energy requirements, in other words, mitochondria have evolved mechanisms for modifying energy production according to the change of $[Ca^{2+}]_i$. Therefore, mitochondria are extremely essential for physiological function of the acinar cells. In pancreatic acinar cells, mitochondria take up very specific positions and comprise three distinct groups: peri-granular, perinuclear, and sub-plasmalemmal (71,109,181,182). Quantification of mitochondrial density in different parts of the acinar cells of pancreatic tissue segments shows that the highest density of mitochondria are distributed in the peri-granular region, where mitochondria occupied 22.9 ± 1.95 % of the area (Figure 1.12). The perinuclear area has a lower density of mitochondria, which occupied 9.07 ± 0.97% of the total area of the region, than the peri-granular (22.9 ± 1.95%) or peripheral areas (12.45 ± 0.78%), but nevertheless is significantly higher than in the non-specific regions (Figure 1.12).

Exocytosis requires ATP and ACh- or CCK-elicited Ca^{2+} signals activate the secretion process will therefore increase ATP consumption. Mitochondrial ATP production occurs by oxidative phosphorylation and the change of nicotinamide adenine dinucleotide (NADH) auto-fluorescence, which can serve as a valuable indicator of mitochondrial metabolism, in intact living cells can reflect this process (183,184). Cytosolic Ca^{2+} oscillations trigger repetitive rises in the NADH concentration, whereas a sustained elevation of $[Ca^{2+}]_i$ only produce just one large NADH transient (185). This indicate that oscillating

$[Ca^{2+}]_i$ responses induced by physiological agonist concentrations are more efficient than a sustained $[Ca^{2+}]_i$ elevation caused by supramaximal agonist concentrations to stimulate mitochondrial energy production. It is remarkable that stimulation with physiological concentration of ACh or CCK, in spite of the increased ATP breakdown, does not decrease the cytosolic ATP concentration, but actually increase a modest ATP concentration, which occurs primarily in the mitochondria and depends on mitochondrial oxidative phosphorylation (186). When mitochondrial oxidative phosphorylation is inhibited, neurotransmitter/hormone stimulation cause a decrease in the cellular ATP level (186). Due to Ca^{2+} is taken up into the mitochondria via the mitochondrial calcium uniporter (MCU) (187–189), a rise in local $[Ca^{2+}]$ in the apical pole is quickly followed by a rise in the mitochondrial $[Ca^{2+}]$ ($[Ca^{2+}]_m$). Consequently, this stimulates three dehydrogenases in the Krebs cycle (190,191). Ca^{2+} release from the mitochondria is the relatively slow process, which ensures stimulation of mitochondrial ATP production. Therefore, stimulation of $[Ca^{2+}]_m$ generates energy not only for fueling the secretion process but also for the processes responsible for extrusion of Ca^{2+} by PMCA through the apical membrane (137) and reuptake of Ca^{2+} via SERCA into the ER (Figure 1.13).

The peri-granular mitochondria play a central role in stimulus-secretion and stimulus-metabolism coupling (182). They focus the cytosolic Ca^{2+} signals in the crucial apical region and optimize the opportunity for local ATP delivery aimed at securing the sustained exocytotic secretion. At the same time, the perigranular mitochondrial belt prevents invasion of Ca^{2+} signals initiated in the apical pole into the basal region as well as the nucleus.

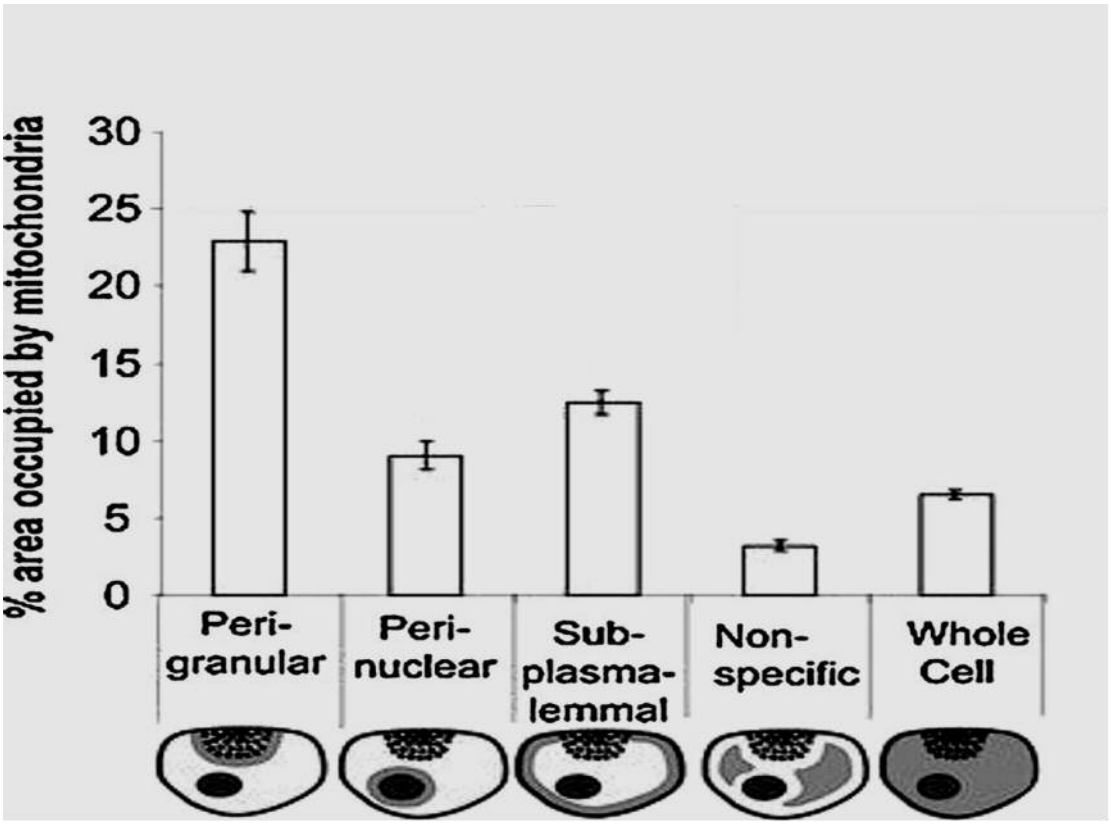

Figure 1.12 The quantitative distribution of mitochondria in intact acinar cells of the pancreas.

The bar charts illustrate the mean percentage area of specific region occupied by mitochondria in pancreatic acinar cells. Perigranular region (22.9 ± 1.95%), subplasmalemmal region (12.45 ± 0.78%) and perinuclear region (9.07 ± 0.97%) are the dominant areas for mitochondria located in the acinar cells. (Modified from *Johnson PR et al, Cell Tissue Res. 2003*) (181)

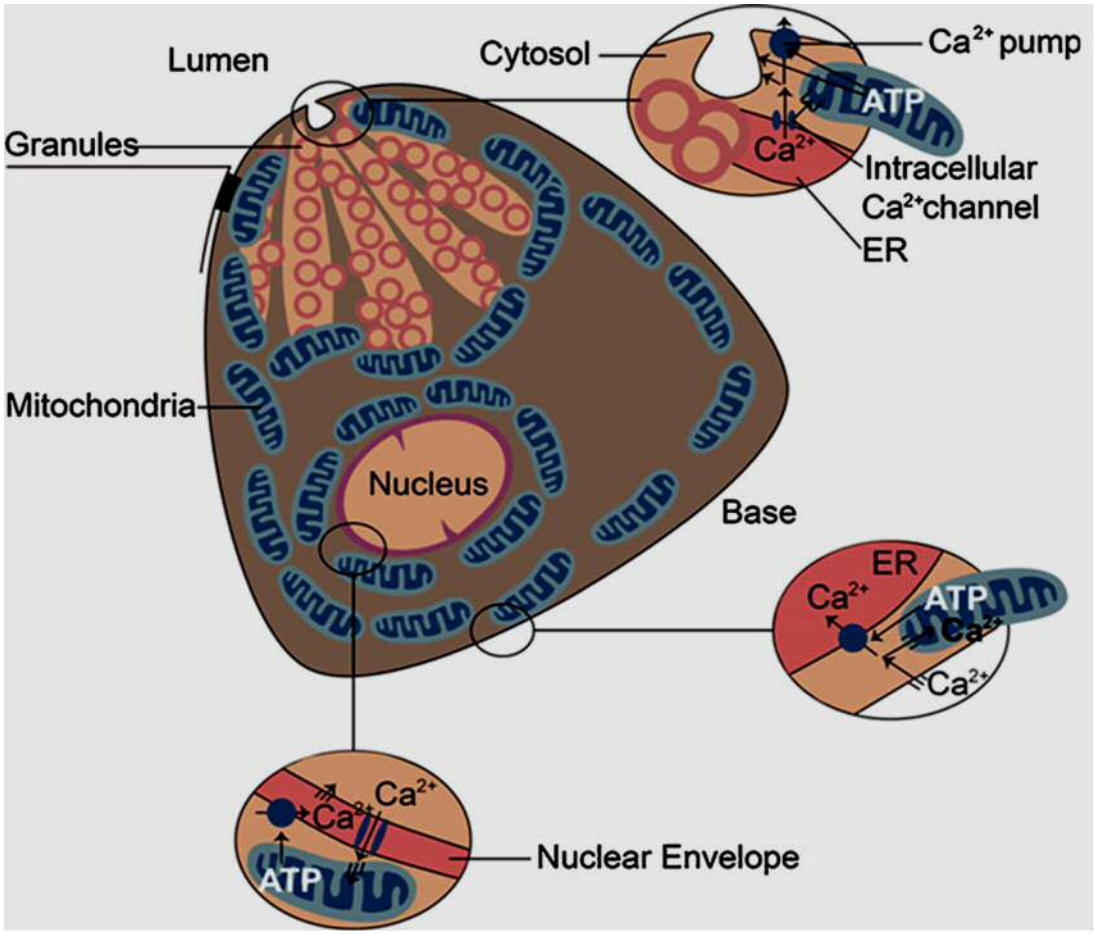

Figure 1.13 Primary functions of the three mitochondrial groups in pancreatic acinar cell.

The diagram depicts the three different mitochondrial groups and their primary functions in pancreatic acinar cell. The peri-granular mitochondria are as a Ca^{2+} buffer barrier and supply ATP for secretory function in the apical region. The peripheral mitochondria provide ATP locally for the Ca^{2+} pump-mediated ER Ca^{2+} uptake. The perinuclear mitochondrial ring is likely to act as a barrier protected against invasion by Ca^{2+} waves for the nucleus. (Adapted from *Petersen OH, Pflugers Arch. 2012*) (182)

Acute Pancreatitis

Epidemiology and aetiology of acute pancreatitis

Acute pancreatitis (AP) (192,193) is a human disease which refers to an acute inflammatory disorder of the pancreas that frequently involves peripancreatic tissues and at times remote organ systems, usually occurred with abdominal pain and elevations of serum pancreatic enzymes. This disease is characterized by digestive proenzymes (i.e. trypsinogen) normally synthesized in the pancreatic acinar cells become active enzymes inside the cells, causing autodigestion of the pancreatic tissue and its surroundings and cell death (134,138,194). The prevalence of AP ranges from 13 to 45 per 100,000 people per year in the United States (195) and varies between 4.9 and 73.4 cases per 100,000 worldwide (196). The incidence of acute pancreatitis has increased globally, including a large rise in pediatric populations (197–199). AP is the single most frequent cause of hospital admissions for gastrointestinal (GI) disorders with health care costs of $2.5 billion (200) and there are more than 274,000 hospitalizations due to AP per year in the United States alone, which has increased by 12% from 2006 to 2012 (200,201). The mortality of AP is significant with more than 3000 deaths (1 out of 100,000) per year and approximately 1% in-hospital death (200,201). It has been widely accepted that repeated attacks of AP may cause chronic pancreatitis (CP) (Figure 1.14) (202–204). The annual incidence rate of CP is 5 to 12 per 100,000 people (205) and CP increases risk for development of pancreatic cancer (Figure 1.14), which is the second leading cause of death through gastrointestinal cancer and the fifth most common cause of cancer death, with extremely low 5-year survival rate which is about 3-4% (206,207).

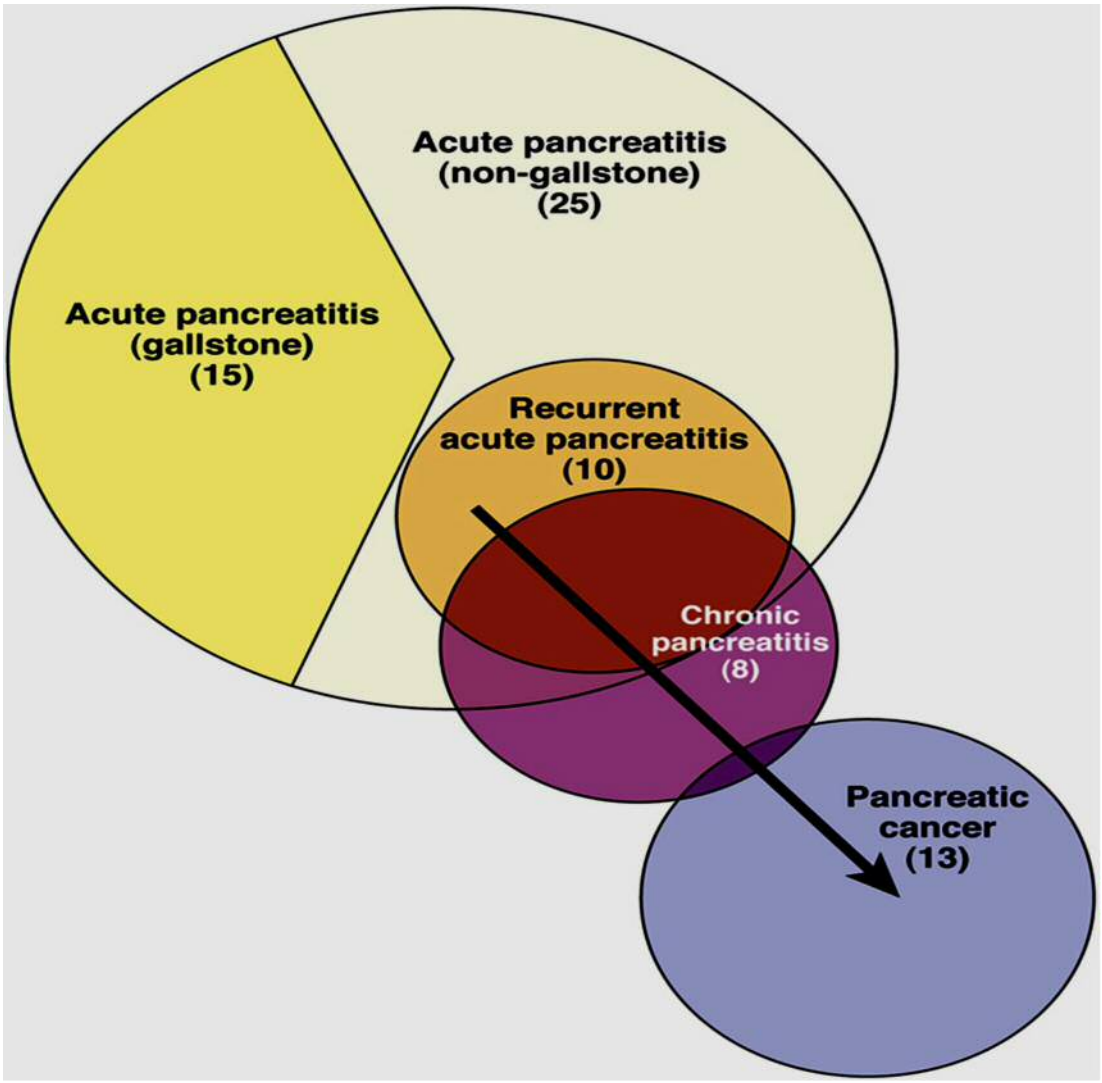

Figure 1.14 The annual incidence of pancreatitis and pancreatic cancer.

The sketch shows approximate incidence rates per 100,000 people per year and the arrow indicates the disease progression between benign (recurrent AP) and malignant (pancreatic cancer). (Adapted from *Yadav D& Lowenfels AB, Gastroenterology. 2013*) (195)

Table 1.3 lists the cause of acute pancreatitis. Biliary disease and alcohol abuse are the most common cause of acute pancreatitis, which accounts for up to 80% of cases of AP (138,202). Gallstones are a frequent cause of acute pancreatitis, which are believed that blockage of the pancreatic duct or obstruction of a common (bile-pancreatic) channel by the stone leads to reflux of bile into the pancreatic duct and cause pancreatic injury. Although the exact mechanisms due to gallstones initiate acute pancreatitis are presently not completely understood and the importance of this particular mechanism has been debated (208), it is nevertheless in any case that Ca^{2+}-dependent cell death is caused by transporter-mediated bile acid uptake in pancreatic acinar cells *in vitro* (209).

Alcohol abuse is the second leading cause of acute pancreatitis as well as a major cause of chronic pancreatitis. The risk of developing pancreatitis increases with excessive amounts of alcohol intake, but only a minority (<10%) of heavy drinkers develop pancreatitis (210). Alcohol appears to increase the sensitivity of the pancreas to injury caused by pancreatic stress (211). Prolonged alcohol use increases the risk for alcohol-related AP among persons who consumed more than 3 drinks daily over a period of more than 5 years (212). Compared with those without a history of alcoholism, subjects in the heavy-drinking groups increase about 4-fold in the prevalence of pancreatitis (213). Alcohol use is the single most common cause of CP, which is a proven risk factor for pancreatic cancer (212). It has been reported that the higher frequency of alcohol-related pancreatitis in men than in women, which is due to genetic background (214). The mechanisms of alcohol-related AP or CP are complex and include both direct toxicity and immunologic effects (215).

Other causes include drugs, hyperlipidemia, hypercalcemia, smoking, environmental toxins, morbid obesity, trauma, endoscopic retrograde cholangiopancreatography (ERCP) etc. (202,216–221). Genetic susceptibility

in a number of genes are associated with AP and CP, including mutations in the genes encoding cationic trypsinogen (PRSS1), serine protease inhibitor Kazal type 1 (SPINK1), cystic fibrosis transmembrane conductance regulator (CFTR), chymotrypsin C, calcium-sensing receptor (CaSR), and claudin-2 (222,223).

Table 1.3 Causes of Acute Pancreatitis. (Modified from *Forsmark CE et al, N Engl J Med, 2016)* (192)

Cause	Approximate Frequency
Gallstones	40%
Alcohol	30%
Hypertriglyceridemia	2–5%
Genetic causes	Not known
Drugs	<5%
Autoimmune cause	<1%
ERCP	5–10% (among patients under-going ERCP)
Trauma	<1%
Infection	<1%
Surgical complication	5–10% (among patients under-going cardiopulmonary bypass)
Obstruction	Rare
Associated conditions	Common (Diabetes, obesity, and smoking)

Clinical features and diagnosis of acute pancreatitis

Typical clinical manifestations of patient who suffers acute pancreatitis are characterised by rapid onset of epigastric or left upper quadrant pain, which is usually described as non-specific pain constantly radiating to the back, chest, or flanks. This is generally associated with fever, nausea, vomiting and abdominal tenderness. The intensity of the pain is usually severe, but can be variable. Therefore, clinical manifestations of acute pancreatitis vary greatly and may present as mild, self-limiting abdominal discomfort, or acute abdomen and shock. Complications include agonizing pain, extensive inflammation and subsequent necrosis of pancreatic and surrounding tissue leads to systemic inflammatory response syndrome (SIRS) proceeding to multiple organ dysfunction syndrome (MODS) with long hospitalization and deaths in up to 5% of cases (202). According to a recent international consensus and the recently published revised classification, acute pancreatitis may be classified as mild, moderate or severe based on laboratory values and radiological imaging (Table 1.4) (224).

Acute pancreatitis is diagnosed according to the Atlanta criteria if at least two of the following three criteria are fulfilled: clinical presentation (abdominal pain, often radiating to the back); serum lipase (or amylase) activity >3 times the upper limit of normal; or characteristic findings of acute pancreatitis on cross-sectional imaging - contrast-enhanced computed tomography (CECT) (Figure 1.15) (224).

Table 1.4 Definition of severity in acute pancreatitis (Revised Atlanta Classification 2012). (Modified from *Banks PA et al, Gut. 2013)* (224)

Grades of severity	Clinical features
Mild	No organ failure and no local or systemic complications
Moderately severe	Transient organ failure (<48 h) and/or local or systemic complications without persistent organ failure (>48 h)
Severe	Persistent organ failure (>48 h): single organ failure or multiple organ failure

A

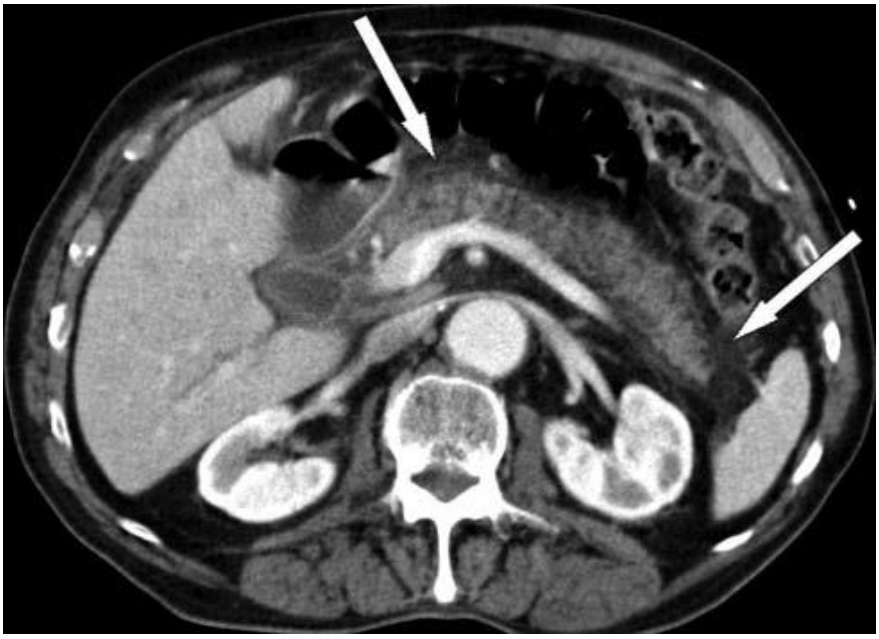

B

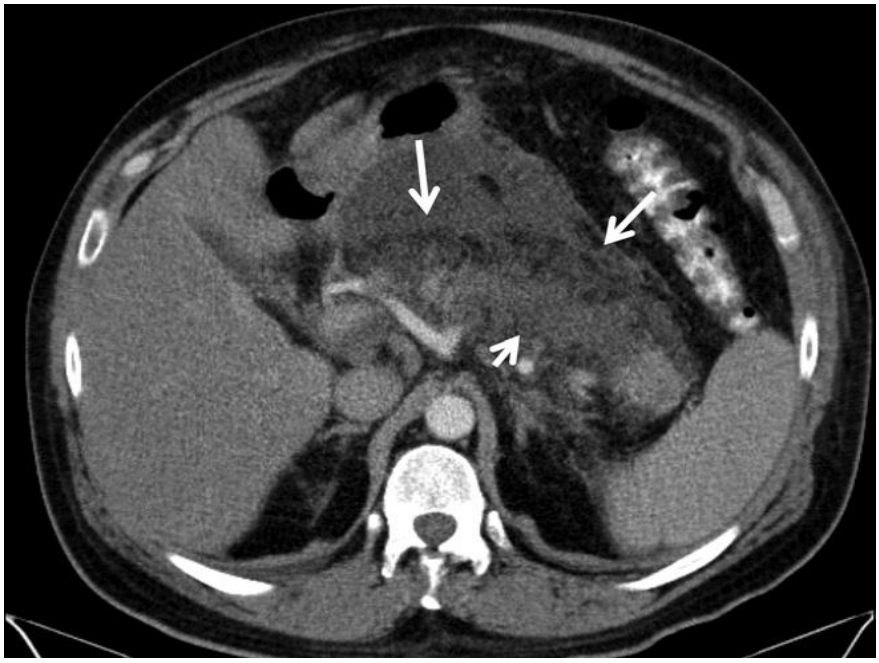

Figure 1.15 Contrast-enhanced computed tomography (CECT) imaging of acute pancreatitis. (Modified from *Banks PA et al, Gut. 2013* and *Wu BU & Banks PA, Gastroenterology. 2013*) (217,224)

(A) Acute interstitial oedematous pancreatitis. Peripancreatic fat stranding (arrows) is without an acute peripancreatic fluid collection. (B) Acute necrotic collection involves both the pancreas (large arrow) and peripancreatic tissue (arrowheads).

Pathogenesis of acute pancreatitis

Over the past few decades, the investigations based on animal models have provided substantial evidence for revealing the molecular mechanisms underlying the pathobiologic responses of acute pancreatitis (202). The sequence of initiating molecular steps resulting in the pathophysiological processes of acute pancreatitis has reached the consensus that intracellular protease activation is crucial in the initiation and onset of acute pancreatitis (136,138). This process is triggered by intracellular calcium overload which is characterized by global sustained $[Ca^{2+}]_i$ elevations (Figure 1.16) (225). This abnormal intracellular Ca^{2+} signalling depends on substantial release of Ca^{2+} from internal stores (ER and acidic store) followed by Ca^{2+} entry from the interstitial fluid, which can causes pancreatic acinar cell injury associated with abnormal intracellular enzyme activation, vacuolization and necrosis (134,194,226–228). It has also been found that intracellular vacuolization, which involves the zymogen granules being transformed into empty-looking vacuoles in the apical secretory granular pole, happens at the same time as protease activation (229).

It is clear that intracellular Ca^{2+} is an essential signal molecule (second messenger) involved in the regulation of almost all cellular functions. In the pancreas, the neurotransmitter ACh and the hormone CCK control exocytotic secretion of digestive proenzymes and the crucial fluid secretion in acinar cells. These agonists, at physiological concentrations, generate repetitive short-lasting Ca^{2+} spikes which are physiological Ca^{2+} signals that are transient and mostly confined to the granule-containing apical pole of the cells (80,230). Exocytosis of digestive enzymes and fluid secretion are activated by the local oscillatory Ca^{2+} spikes (50). These findings originally based on studies of animal models, specifically the link between the presence of functional CCK receptors and Ca^{2+} signalling, subsequently have been confirmed by a

detailed study on the preparation of the normal portions of human pancreas (231,232). Supraphysiologic doses of various pathological stimuli causing acute pancreatitis elicit global and sustained elevations of $[Ca^{2+}]_i$, which can be fatal (Figure 1.17) (133,233,234). Instead of causing sustained secretion of proteases, such pathological Ca^{2+} signals lead to release of cathepsin-B (235) and intracellular trypsin activation (209,229,236–240).

With regard to pathogenesis of AP, mitochondrial function associated with energy production is another very important aspect needs to be considered. As mention previously, three distinct groups of mitochondria are so specifically distributed in pancreatic acinar cells that production and demand of ATP are well tuned under physiological stimulation. Oscillating $[Ca^{2+}]_i$ responses induced by physiological concentration of ACh or CCK cause repeated spikes of $[Ca^{2+}]_m$ elevation that, in turn, activate Ca^{2+}-dependent Krebs-cycle dehydrogenases and stimulate mitochondrial ATP production (50,241), whereas a sustained $[Ca^{2+}]_i$ elevation evoked by overstimulation with caerulin or a high concentration of CCK only elicits one initial burst of $[Ca^{2+}]_m$ elevation and produce just one large NADH transient, which gives rise to one transient stimulation of ATP generation (50,185,186). In contrast, pathological stimulants implicated in pancreatitis such as non-oxidative alcohol metabolites - fatty acid ethyl esters and bile acids reduce both cytosolic and mitochondrial ATP (186,242). These pancreatitis-inducing stimulants induce calcium overload and ATP depletion in acinar cells, which eventually leads to necrosis (133,186).

Mitochondrial permeability transition pore (MPTP) is a protein formed in the inner membrane of the mitochondria (IMM) under certain pathological conditions such as cardiac ischemia–reperfusion injury (243–246). The mitochondrial permeability transition is a phenomenon that the IMM undergo abrupt increase of its permeability to solutes, which manifest a cut-off to

molecules of about 1.5 kDa (247). MPTP opening enables free passage into the mitochondria of molecules of <1.5 kDa including protons. The proton gradient utilized by complex V of the respiratory chain is responsible for ATP synthesis. In addition, this electrochemical gradient across the IMM generate the charge imbalance which forms the basis of the inner mitochondrial transmembrane potential ($\Delta\psi_m$). Therefore, the maintenance of the proton gradient is of the essence for cellular bioenergetics (248). Physiological stimulation may induce a transient loss of the $\Delta\psi_m$ (249), whereas long-lasting $\Delta\psi_m$ dissipation is often associated with cell death (250). This non-specific pore has been demonstrated as one of the crucial elements involved in mitochondrial pathophysiology of pancreatic injury (72,133,251,252). Calcium oscillations induced by stress and reactive oxygen species (ROS) can trigger MPTP opening and cell death (72,248,253,254). Mounting evidence suggests that Ca^{2+} overload and excessive generation of ROS as well as reactive nitrogen species (RNS) are involved in the pathophysiology of AP (133,202,255,256).

Pancreatitis is characterized by cell death, which consists of two major types: apoptosis and necrosis (133,257). It is clear that Ca^{2+} signalling and bioenergetics regulate physiological and pathological processes in the pancreatic acinar cell and influence both apoptotic and necrotic cell death pathways (50,133,134,258). Although the pathobiologic processes of AP is complex and various different mechanisms has been implicated in the involvement of this diseases (193,202,215,222,259–266), intracellular Ca^{2+} signalling and ATP level are central to the control of cell life and death, and are fundamentally influence the severity of AP.

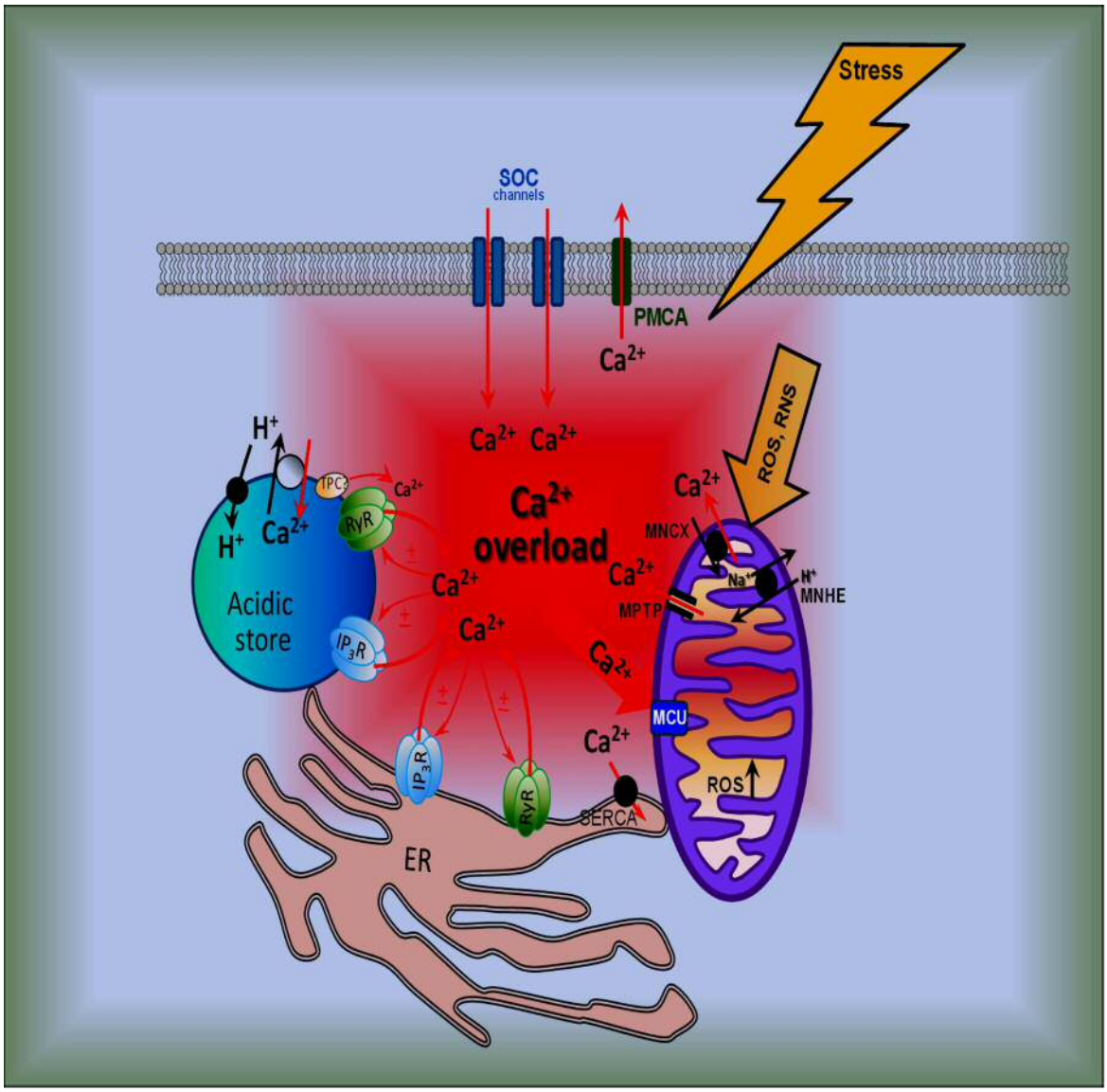

Figure 1.16 Pathological activity of Ca^{2+} overload in pancreatic acinar cells. (Modified from *Gerasimenko OV & Gerasimenko JV. Pflugers Arch. 2012*) (72)

Pancreatitis-associated toxins can induce stress to acinar cells which leads to a pathological Ca^{2+} response in the cytosol, primarily due to Ca^{2+} release from internal stores followed by excessive Ca^{2+} entry and decreased Ca^{2+} extrusion. Ca^{2+} overload and together with ROS/RNS cause mitochondrial stress, MPTP opening and cell death.

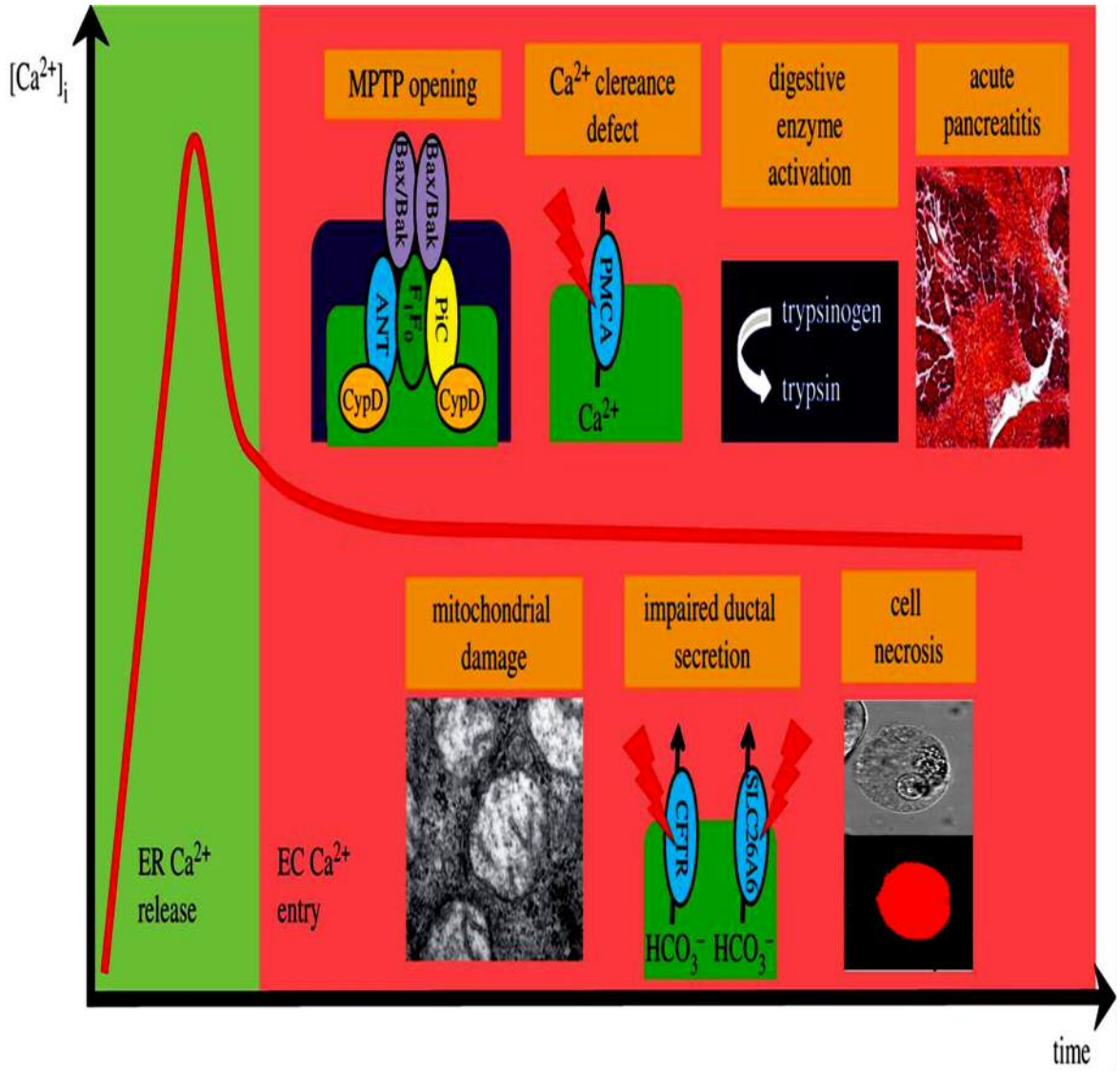

Figure 1.17 Pathological events in the pathogenesis of AP. (Modified from *Maléth J & Hegyi P, Philos Trans R Soc Lond B Biol Sci. 2016*) (240)

Pancreatitis-inducing stimulants (i.e. FAEEs and bile acids) release massive Ca^{2+} from intracellular stores and Ca^{2+} influx from the extracellular fluid occurred thereafter. This causes sustained $[Ca^{2+}]_i$ elevation which leads to mitochondrial damage and activation of digestive enzymes in acinar cells. Toxic Ca^{2+} signals and ATP depletion impairs functional pumps in both acinar cells and ductal cells, which eventually trigger necrosis and AP.

Asparaginase

Mechanism of action of asparaginase

In 1953, John G. Kidd first observed that normal guinea-pig serum had antitumor activity which resulted in regression of transplanted lymphomas in both rat and mice (267). This initiated the discovery and development of asparaginase as a drug to treat cancer. L-Asparaginase was discovered as an anti-cancer drug since 1960s (268,269). Unlike other chemotherapy agents, it can be given as an intramuscular, subcutaneous, or intravenous injection without tissue irritation. L-Asparaginase has been found in different types of bacteria including *Escherichia coli* (*E. coli*), *mycobacteria, Bacillus, Erwinia, Aspergillus, Salmonella, Pseudomonas,* and *Acinetobacter* species. However, not all asparaginases show anti-cancer activity apart from *E. coli* and *Erwinia chrysanthemi* asparaginases (270). They are the only preparations available for clinical use. There are currently three main clinical formulations of asparaginase have been used so far: two are derived from *E. coli*, i.e. the native L-asparaginase, and the pegylated form of the native *E. coli* asparaginase (PEG-asparaginase) (271). The third is derived from *Erwinia Chrysanthemi*, referred to as *Erwinia* asparaginase (271,272).

Given that most malignant transformed lymphoblasts are sometimes unable to synthesise sufficient asparagine for supporting their metabolism and growth, the depletion of the systemic asparagine pool caused by L-asparaginase via hydrolysis of L-asparagine to L-aspartic acid and ammonia will eventually lead to cell death (Figure 1.18) (273). However, resistant ALL leukaemic cells are not dependent on an exogenous L-asparagine source due to these cells contain L-asparagine synthetase, which converts aspartic acid into asparagine (Figure 1.18) (274,275).

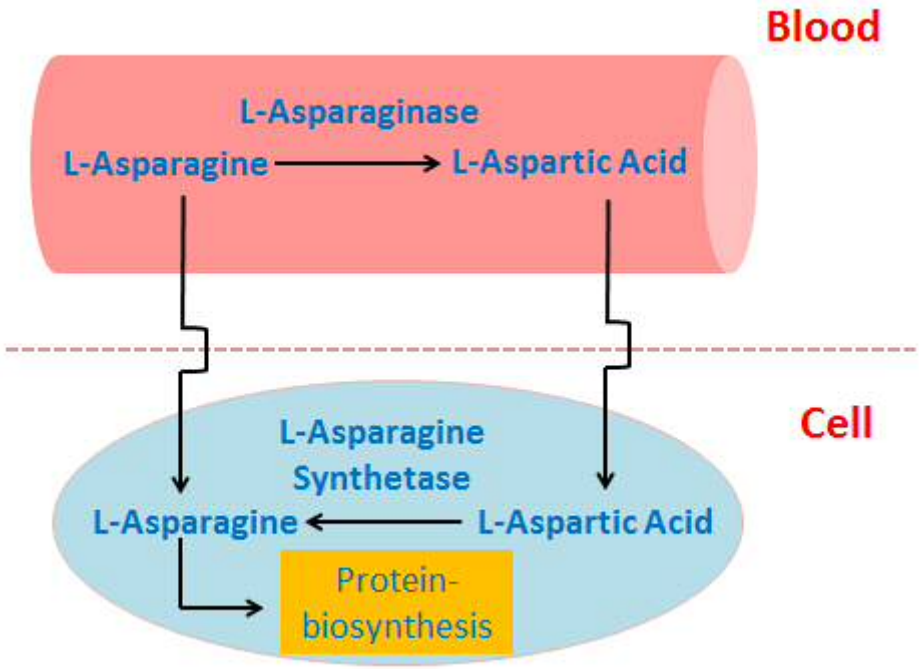

Figure 1.18 Mode of action of L-asparaginase. (Modified from *van den Berg H, Leuk Lymphoma. 2011*) (270)

This diagram shows the mechanism of L-asparaginase catalyzes the conversion of L-asparagine to L-aspartic acid in ALL.

Asparaginase toxicity

Acute lymphoblastic leukaemia (ALL) is the most common cancer in childhood (276–278). Given that relatively high rate of survival of ALL on contemporary protocols (279), attention is now shifting onto treatment-related side effects (280). L-Asparaginase is an essential element of combination chemotherapy in the treatment of ALL (281–283). It is feasible as part of an intensive multiagent chemotherapeutic regimen in ALL and appears associated with improved outcomes including disease-free survival (DFS) (284–288). However, asparaginase itself like other chemotherapeutic agents has toxicities associated with hypersensitivity, pancreatitis, hyperglycemia, thrombosis, encephalopathy, and liver dysfunction etc. The most common reason for stopping treatment with L-asparaginase is acute pancreatitis named as asparaginase-associated pancreatitis (AAP) (216,289–295). This occurs in about 5–10% of the cases according to the consensus among the studies (290). AAP is the most frequent cause of discontinuing the asparaginase treatment, for re-exposure of asparaginase leads to recurrence of pancreatitis (289,296,297).

Aims of the study

This study has the following aims;

1) To investigate and understand the mechanisms and the pathophysiology underlying the development of L-asparaginase-associated pancreatitis.

2) To determine the effects of calcium signalling and ATP in the pathogenesis of AAP in mouse models.

3) To develop and test new ways of reducing the side-effects of asparaginase treatments for both *in vitro* and *in vivo* studies.

Chapter 2

Materials and Methods

Materials

Reagents and chemicals

(±)-(3R*,4S*)-2-Oxo-4-phenyl-3-pyrollidinecarboxylic acid 2-[1-(3-bromophenyl)ethylidene]hydrazide (AC 264613)，from TOCRIS, UK. Made up to a 50 mM stock solution in DMSO and frozen in 20 µl aliquots at -20°C.

4-(2-Hydroxyethyl)piperazine-1-ethanesulfonic acid (HEPES), from Sigma-Aldrich, UK.

7-Chloro-5-(2-chlorophenyl)-1,5-dihydro-4,1-benzothiazepin-2(3H)-one (CGP-37157), Merck Millipore, UK. Made up to a 20 mM stock solution in DMSO and frozen in 30 µl aliquots at -20°C.

Acetylcholine (ACh), from Sigma-Aldrich, UK. Made up to a 10 mM stock solution in water and frozen in 50 µl aliquots at -20°C.

Asparaginase, from Abcam, UK. Made up to a 5000 IU/ml stock solution in water and and frozen in 40 µl aliquots at -80°C.

Atropine, from Sigma-Aldrich, UK. Made up to a 2 mM stock solution in water and kept refrigerated at 4°C.

Caffeine, from Sigma-Aldrich, UK. Made up to a 20 mM stock solution in water and kept refrigerated at 4°C.

Calcium chloride ($CaCl_2$), from Fluka, UK. 1 M stock solution kept in room temperature.

Carbonyl cyanide 3-chlorophenylhydrazone (CCCP), from Sigma-Aldrich, UK. Made up to a 10 mM stock solution in DMSO and frozen in 50 µl aliquots at -20°C.

Cholecystokinin, from Sigma-Aldrich, UK. Made up to a 5 µM stock solution in water and frozen in 50 µl aliquots at -80°C.

Collagenase, from Worthington, USA. Made up to a 222 IU/ml stock solution in NaHEPES buffer solution and frozen in 1 ml aliquots at -20°C.

Cyclopiazonic acid (CPA), from Merck Millipore, UK. Made up to a 20 mM stock solution in DMSO and frozen in 40 µl aliquots at -20°C.

D-galactose, from Sigma-Aldrich, UK.

D-glucose, from Sigma-Aldrich, UK.

Dimethyl Sulfoxide (DMSO), from Sigma-Aldrich, UK. Used as a diluent for hydrophobic chemicals.

Ethanol, absolute, from Sigma-Aldrich, UK.

Ethylene glycol-bis(β-aminoethyl ether)-*N,N,N′,N′*-tetraacetic acid (EGTA), from Sigma-Aldrich, UK. Made up to a 100 mM stock solution in NaOH and kept refrigerated at 4°C.

Fluo-4-AM, from Thermo Fisher Scientific, UK. Made up to a 2 mM stock solution in DMSO and frozen in 5 µl aliquots at -20°C.

Formaldehyde, from Sigma-Aldrich, UK. 37 - 38% stock solution kept in room

temperature.

Fructose, from Sigma-Aldrich, UK.

FSLLRY-NH_2 from TOCRIS, UK. Made up to a 1 mM stock solution in DMSO and frozen in 50 µl aliquots at -20°C.

Fura-2-AM, from Thermo Fisher Scientific, UK. Made up to a 2 mM stock solution in DMSO and frozen in 5 µl aliquots at -20°C.

GSK-7975A, from GlaxsoSmithKline, UK. Made up to a 10 mM stock solution in DMSO and frozen in 50 µl aliquots at -20°C.

Magnesium chloride ($MgCl_2$), from Sigma-Aldrich, UK.

Magnesium Green (MgGreen), from Thermo Fisher Scientific, UK. Made up to a 2 mM stock solution in DMSO and frozen in 6 µl aliquots at -20°C.

Oligomycin, from Merck Millipore, UK. Made up to a 5 mM stock solution in DMSO and frozen in 30 µl aliquots at -20°C.

Palmitoleic acid ethyl ester (POAEE), from Cayman Chemical, UK.

Phosphate-buffered saline (PBS), from Thermo Fisher Scientific, UK. 10X stock solution kept refrigerated at 4°C.

Potassium Chloride (KCl), from Calbiochem, UK.

Propidium iodide (PI), from Thermo Fisher Scientific, USA. 1 mg/ml stock solution kept refrigerated at 4°C.

Rhod-2-AM, from Thermo Fisher Scientific, UK. Made up to a 2 mM stock solution in DMSO and frozen in 10 µl aliquots at -20°C.

Sodium Chloride (NaCl), from Sigma-Aldrich, UK.

Sodium hydroxide (NaOH), from Sigma-Aldrich, UK. Made up to a 5 M stock solution in water and kept in room temperature.

Sodium iodoacetate, from Sigma-Aldrich, UK. Made up to a 0.2 M stock solution in water and frozen in 200 µl aliquots at -20°C.

Sodium pyruvate, from Sigma-Aldrich, UK. 100 mM stock solution kept refrigerated at 4°C.

Taurolithocholic acid 3-sulfate (TLC-S), from Sigma-Aldrich, UK. Made up to a 2 M stock solution in water and kept refrigerated at 4°C.

Tetramethylrhodamine, methyl ester, Perchlorate (TMRM), from Thermo Fisher Scientific, UK. Made up to a 10 mM stock solution in DMSO and frozen in 50 µl aliquots at -20°C.

Equipment

Analytical and Precision balances, from VWR International, UK.

Autoclave, from Tuttnauer, UK.

Calcium imaging system, from Scientifica, UK.

Centrifuge, from Eppendorf, UK.

Digital pH meter, from Infolab, UK.

Dissecting instruments (scissors and tweezers), from stock in the laboratory.

Fridges and biomedical freezers (-20°C and -80°C), from Bosch or Sanyo, UK.

Integral Water Purification System - Milli-Q, from Merck Millipore, UK.

Laser-scanning confocal microscope – Leica TCS SPE, from Leica, Germany.

Magnetic Stirrers, from stuart-equipment, UK.

Mini Centrifuge, from stuart-equipment, UK.

Mini Shakers, from VWR International, UK.

Osmometer - Osmomat 030, from gonotec, UK.

Oven and Drying Cabinet, from LTE Scientific, UK.

Vacuum pump - Welch™ LVS 110 Z Laboratory Vacuum System, from Fisher Scientific, UK.

Vortex mixer, from stuart-equipment, UK.

Water bath, Shaking & boiling baths, from Grant Instruments, UK.

Consumables

Aluminium foil, from Merck, UK.

Centrifuge tubes (15 ml), from Sarstedt, Germany.

Coverslips (32 x 32 mm, thickness No.1), from VWR International, UK.

Immersion oil for microscopy, from Sigma-Aldrich, UK.

Microcentrifuge tubes (0.5 ml and 1.5 ml), from Starlab, UK.

Pasteur Pipettes, from Fisher Scientific, UK.

Pipette tips (5 µl, 20 µl, 200 µl, 1 ml and 5 ml), from VWR International, UK.

Polypropylene containers (20 ml, 100 ml and 200 ml), from Starlab, UK.

Surgical Scalpel Blades, from Swann-Morton, UK.

Syringes (0.3 ml, 1 ml and 20 ml) and Needles, from BD, USA.

Weighting boats (46×46×8 mm and 140×140×22 mm), from VWR International, UK.

Animals

Wild type (WT) C57BL6/J male mice were purchased from Charles Rivers UK Ltd. They were fed standard laboratory chow and water in JBiosi of Cardiff University. Generally, mice between 4 and 6 weeks were used for experiments. Figure 2.1 shows WT C57BL6/J mouse used in this study.

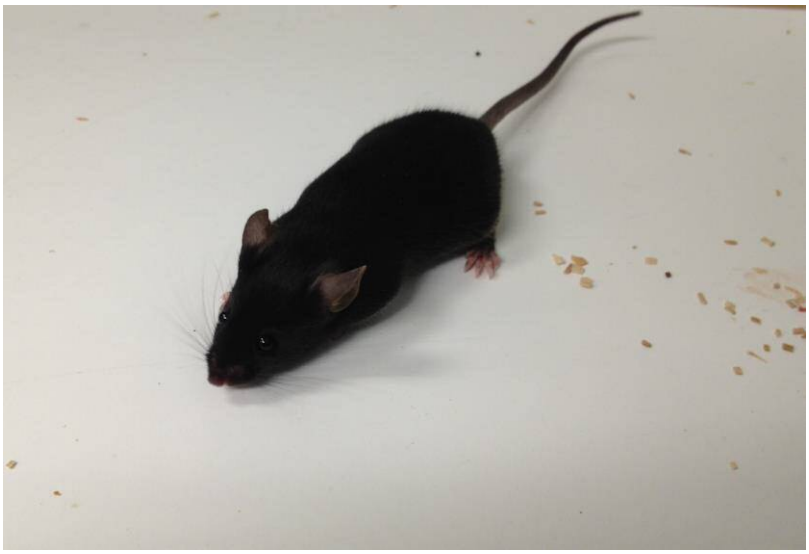

Figure 2.1 Wild type mouse.

The photograph shows a wild type mouse, which is used for pancreatic acinar cell isolation.

Methods

Preparation of solutions

The standard buffer solution of Sodium HEPES was practically used for all experiments (Table 2.1). This was made up with double distilled water into a buffer solution.

Table 2.1 Preparation of NaHEPES buffer (1 L)

NaCl	140 mM	8.18 g
KCl	4.7 mM	0.36 g
HEPES	10 mM	2.4 g
$MgCl_2$	1 mM	1 ml (from 1 M stock solution)
Glucose	10 mM	1.8 g

Osmolality and pH of the solution was adjusted to 290-300 osm/l and 7.3 by the addition of NaCl and NaOH (5 M), respectively. All further solution used the standard NaHEPES buffer as a base and 1 mM $CaCl_2$ was added when it was necessary.

Preparation of collagenase

18 ml of NaHEPES (supplemented with 1mM $CaCl_2$) buffer was added to 4 KU collagenase stock (Figure 2.2) and then mixed well by vortexing to produce a 222 IU/ml stock collagenase solution. After that, collagenase stock solution was divided into 1 ml aliquots in 18 tubes and frozen at -20°C.

Figure 2.2 Collagenase for pancreatic acinar cell isolation.

The photograph shows a stock of collagenase, which is used for pancreatic acinar cell isolation.

Preparation of fluorescent dyes

Fluo-4-AM

23 µl of DMSO was added to 50 µg Fluo-4-AM (Figure 2.3) and well mixed by vortexing. Then, the stock (2 mM) was aliquoted into 5 µl aliquots in 0.5 ml tubes and wrapped with aluminium foil in order to protect from light. All aliquots were stored at -20°C.

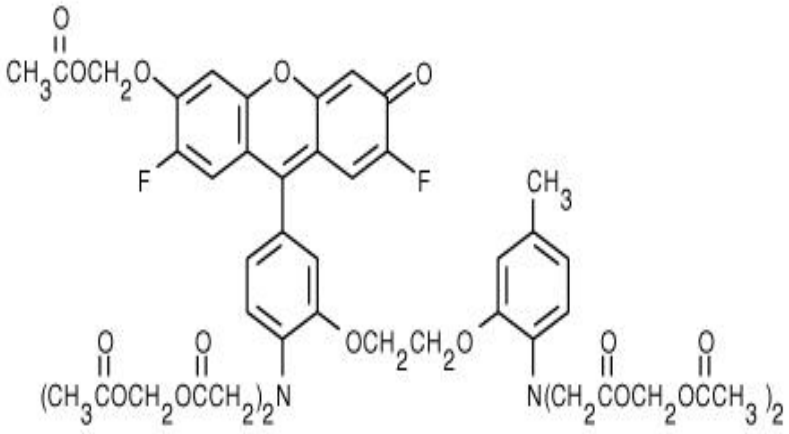

Figure 2.3 The chemical structure of Fluo-4.

Molecular formula: $C_{51}H_{50}F_2N_2O_{23}$. Molecular weight: 1096.95. (Modified from *Suzuki Y & Yokoyama K, Biosensors (Basel), 2015*) (298)

Fura-2-AM

25 µl of DMSO was added to 50 µg Fura-2-AM (Figure 2.4) and mixed well by vortexing. Then, the stock (2 mM) was aliquoted into 5 µl aliquots in 0.5 ml tubes and wrapped with aluminium foil in order to protect from light. All aliquots were stored at -20°C.

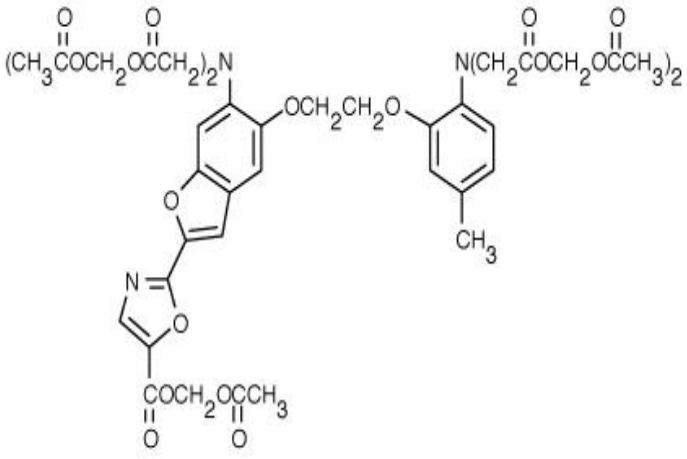

Figure 2.4 The chemical structure of Fura-2.

Molecular formula: $C_{44}H_{47}N_3O_{24}$. Molecular weight: 1001.86. (Modified from *Suzuki Y & Yokoyama K, Biosensors (Basel), 2015*) (298)

Rhod-2-AM

25 µl of DMSO was added to the sample of 50 µg Rhod-2-AM (Figure 2.5) and well mixed by vortexing. Then, the stock (2 mM) was aliquoted into 10 µl aliquots in 0.5 ml tubes and wrapped with aluminium foil in order to protect from light. All aliquots were stored at -20°C.

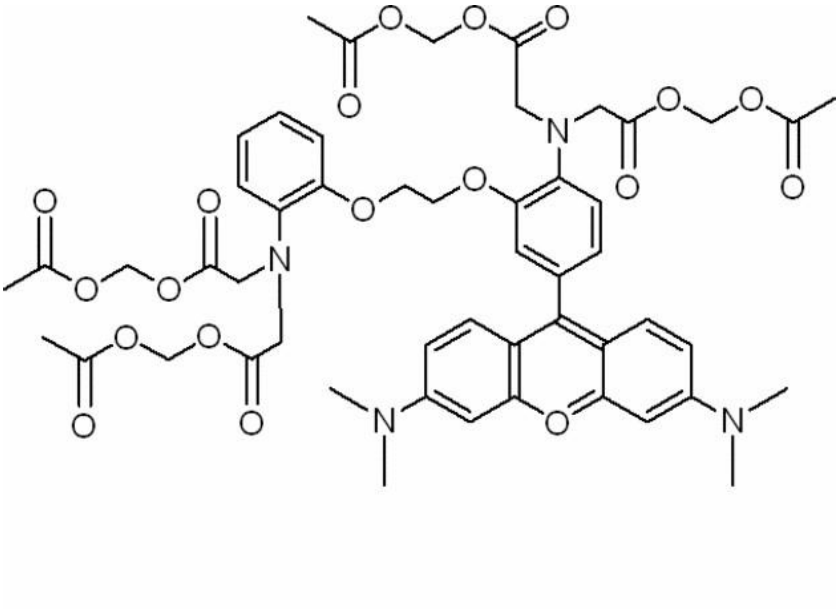

Figure 2.5 The chemical structure of Rhod-2.

Molecular formula: $C_{52}H_{59}BrN_4O_{19}$. Molecular weight: 1123.96. (Modified from *Minta A et al, J Biol Chem, 1989*) (299)

TMRM

25 µl of DMSO was added to the sample of 25 mg TMRM (Figure 2.6) and well mixed by vortexing. Then, the stock (10 mM) was aliquoted into 50 µl aliquots in 0.5 ml tubes and wrapped with aluminium foil in order to protect from light. All aliquots were stored at -20°C.

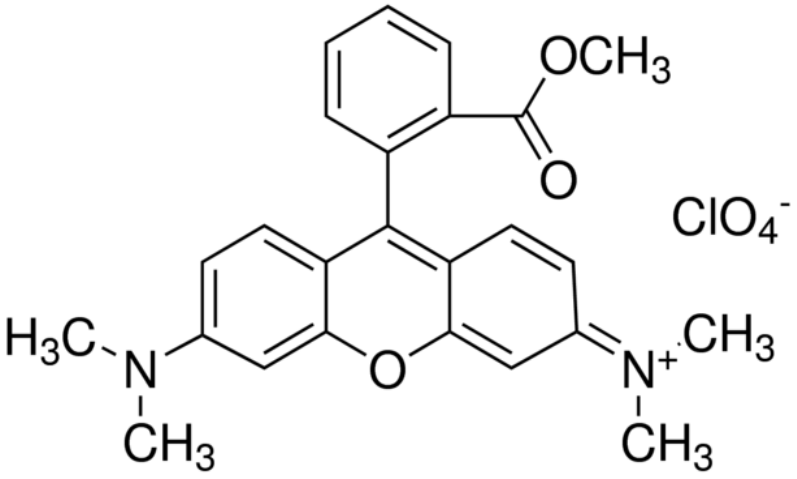

Figure 2.6 The chemical structure of TMRM.

Molecular formula: $C_{25}H_{25}N_2O_3 \cdot ClO_4$. Molecular weight: 500.93. (Modified from *Wang B et al, Analyst, 2015*) (300)

MgGreen

25 µl of DMSO was added to the sample of 50 µg MgGreen (Figure 2.7) and well mixed by vortexing. Then, the stock (2 mM) was aliquoted into 10 µl aliquots in 0.5 ml tubes and wrapped with aluminium foil in order to protect from light. All aliquots were stored at -20°C.

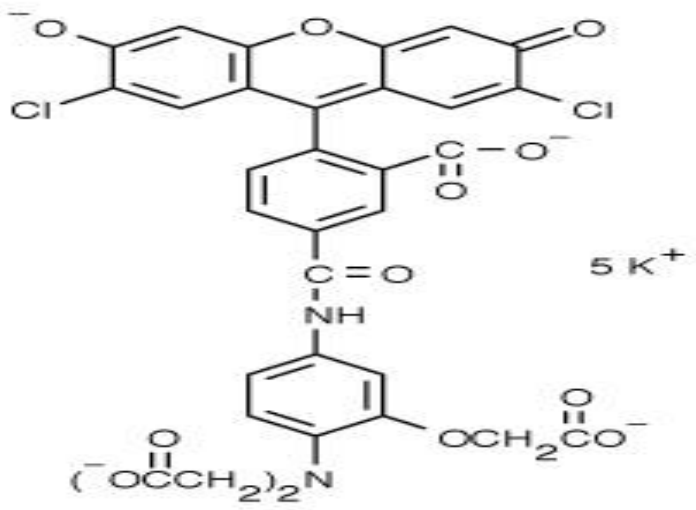

Figure 2.7 The chemical structure of MgGreen.

Molecular formula: $C_{33}H_{17}Cl_2K_5N_2O_{13}$. Molecular weight: 915.9004. (Modified from *Suzuki Y & Yokoyama K, Biosensors (Basel), 2015*) (298)

Preparation of isolated pancreatic acinar cells

Adult male C57BL6/J mice around 5 weeks old and 20-25g in weight were sacrificed by an approved schedule 1 procedure according to the Animal Scientific Procedures Act, 1986 and approved by the Ethical Review Committee of Cardiff University, that is, mice killed by cervical dislocation. The pancreas was excised via a left-sided laparotomy and placed immediately to a petri dish containing NaHEPES buffer solution supplemented with 1mM Ca^{2+}. The tissue was then washed twice by buffer and removed with excess fat. After that, the pancreatic tissue was transferred to an empty weighting boat and 1 ml of collagenase (222 IU/ml, worthington) was injected from different angles into the tissue. The injected tissue and collagenase was then collected into an eppendorf vial sealed with parafilm and incubated in a shaking water bath at 37°C for 16 – 18 min depending on the actual size of the pancreatic tissue. After incubation the tissue was disrupted by repeated manual aspiration with dispensing pipette tips of various diameters to produce preparation of single pancreatic acinar cell or small acinar clusters. The buffer with cells from the top of the eppendorf tube was collected and transferred to a 20 ml centrifuge tube and centrifuged for 1 min at 0.2 g-force. The supernatant was discarded and the cell pellet was re-suspended in fresh buffer. The cell suspension was spun again in order to wash the residual of collagenase and cell debris thoroughly. Finally, the cell pellet was re-suspended in NaHEPES buffer solution with 1 mM Ca^{2+} and the suspension of pancreatic acinar cells and clusters was ready for the fluorescent dye loading procedure.

Measurements of $[Ca^{2+}]_i$ in pancreatic acinar cells

For measurements of intracellular concentration ($[Ca^{2+}]_i$) in pancreatic acinar cells, two Ca^{2+} sensitive fluorescent probes, namely Fluo-4-AM and Fura-2-AM were used. In their esterified form, Fluo-4-AM and Fura-2-AM are uncharged and hydrophobic. Therefore, they can easily cross the cell membrane. Once the dyes are in the cytosol, acetoxymethyl (AM) esters are removed by cellular esterases, which regenerates the free acid forms of fluorescent Fluo-4 and Fura-2 and are trapped within the cell and cannot cross the cell membrane.

For measurements of $[Ca^{2+}]_i$ with fluorescent probe Fluo-4, pancreatic acinar cells were loaded with 5 μM Fluo-4-AM for 30 min at room temperature. Then cells were centrifuged for final wash and re-suspended in fresh NaHEPES buffer solution containing 1 mM Ca^{2+}. Fluo-4 is well-excited by the 488 nm line of the argon-ion laser and its emission wavelength of Ca^{2+}–bound form is the 506 nm (Figure 2.8) (301). Fluo-4 is a derivative of Fluo-3, however, it is brighter and more photostable. Its Ca^{2+} affinity (K_d ~345 nM) is a slightly higher than Fluo-3 (K_d ~390 nM). This makes Fluo-4 brighter at a lower dye concentration so that it has shorter incubation times and less phototoxic (302).

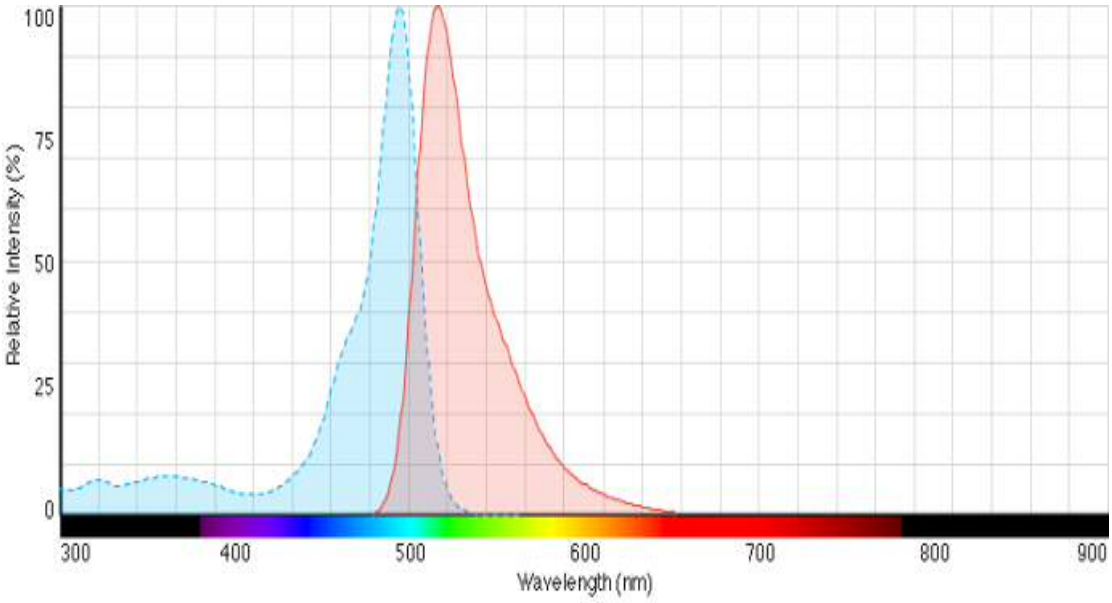

Figure 2.8 Fluorescence spectra of Fluo-4.

The graph shows spectra of excitation (blue trace) and emission (red trace) of Fluo-4 in the presence of Ca^{2+}. (Modified from *Gee KR et al, Cell Calcium. 2000*) (301)

Fura-2 is a ratiometric dye which is one of the most popular calcium indicators and has widely been used for quantitative measurement of intracellular $[Ca^{2+}]_i$. It is excited by ultraviolet light and its peak absorbance shifts from 380 nm in the Ca^{2+} free state to 340 nm in the Ca^{2+} bound state (Figure 2.9). In both states, the maximum emission intensity is at a wavelength of 510 nm. Fura-2 has a relative high Ca^{2+} affinity (K_d ~145 nM) that is similar to endogenous resting Ca^{2+} levels (303). Fura-2 is a dual excitation dye resistant to photo-bleaching and the advantage of the ratiometric measurement of $[Ca^{2+}]_i$ is that it automatically counteracts certain variables such as local differences in Fura-2 concentration or cell thickness. However, its main disadvantage is not suitable for confocal microscopy. In order to measure $[Ca^{2+}]_i$, freshly isolated pancreatic acinar cells were loaded with 2.5 μM Fura-2-AM for 45 min at room temperature. The cells were then washed and re-suspended in NaHEPES buffer containing 1 mM Ca^{2+}. The $[Ca^{2+}]_i$ change were recorded by scientifica imaging system with LED excitation 340 nm and 380 nm and the emission measured at 510 nm. The ratio signal allows for calculation of intracellular $[Ca^{2+}]_i$ according to the Grynkiewicz equation (304).

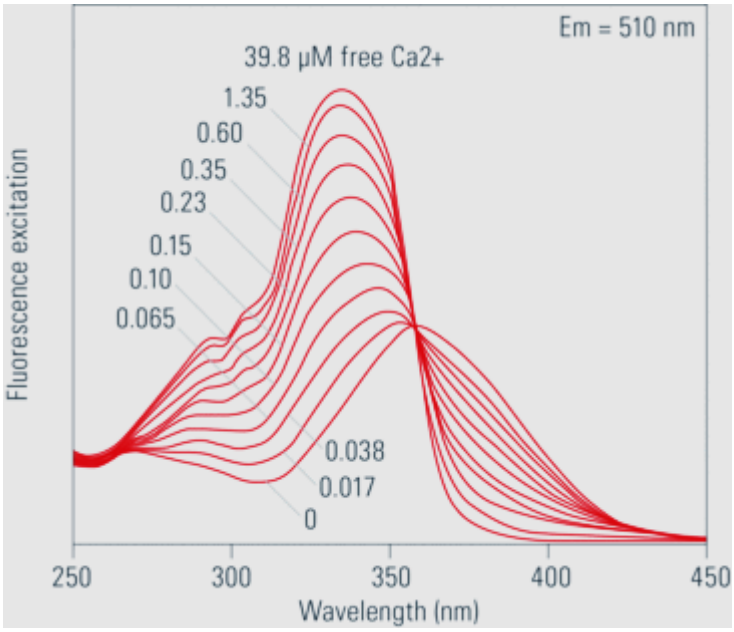

Figure 2.9 Fluorescence excitation spectra of Fura-2 at different calcium concentrations.

The graph shows spectra of excitation of Fura-2 in the presence and absence of Ca^{2+}. The response at 340 nm is much bigger than 380 nm on binding to Ca^{2+}. (Modified from *Grynkiewicz G et al, J Biol Chem.1985*) (304)

Measurements of $[Ca^{2+}]_m$ in pancreatic acinar cells

For mitochondrial calcium $[Ca^{2+}]_m$ measurements, freshly isolated pancreatic acinar cells were loaded with 10 μM Rhod-2-AM for 48 min at 30°C. The AM esters of this dye have a net positive charge, which promotes sequestration into mitochondria in many cells. Preferentially, Rhod-2 accumulate into the mitochondria, however, a substantial fraction of it is also present in the cytosol. After incubation the cells were centrifuged for 1 min and re-suspended for a final wash and re-suspended in fresh NaHEPES buffer solution containing 1 mM Ca^{2+}. The fluorescence of Rhod-2 was excited using an argon laser line at 535 nm, and the emitted light was collected using an LP560 filter. Peak excitation and emission wavelengths are 552 nm and 581nm for Rhod-2, respectively (Figure 2.10). Unlike Ca^{2+} sensitive dye Fura-2 and Fluo-4, the Ca^{2+} affinity is relatively low with K_d of ~570 nM for Rhod-2. Generally, the low affinity Ca^{2+} indicators are preferred choices to measure Ca^{2+} levels in the energy generating organelle such as mitochondria.

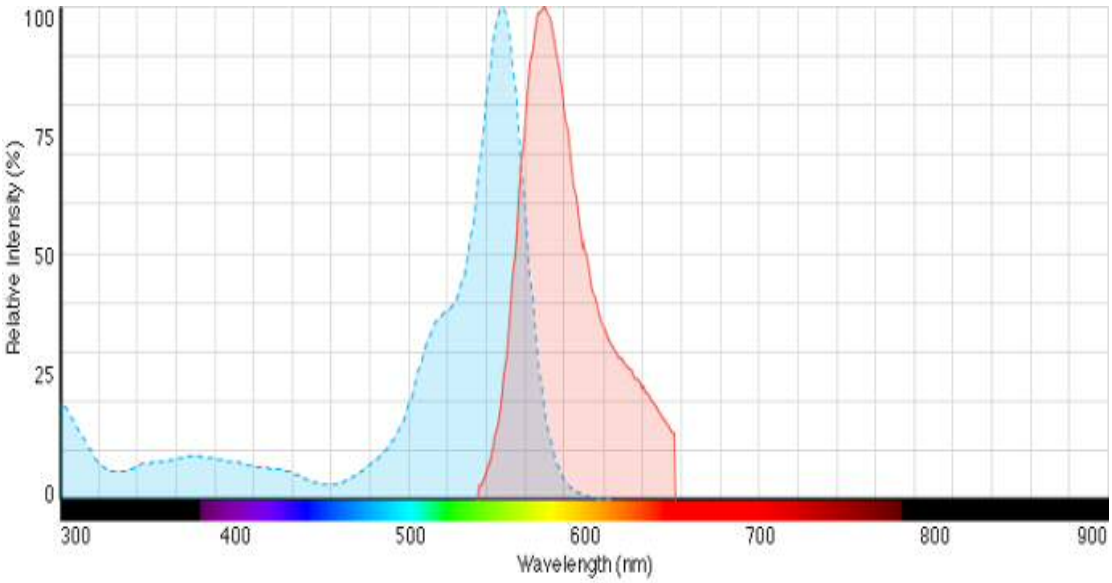

Figure 2.10 Fluorescence spectra of Rhod-2.

The graph shows spectra of excitation (blue trace) and emission (red trace) of Rhod-2 in the presence of Ca^{2+}. (Modified from *Ronzhina M et al, Physiol Res. 2013*) (305)

Measurements of $\Delta\psi_m$ in pancreatic acinar cells

For Measurements of mitochondrial membrane potential ($\Delta\psi_m$) in pancreatic acinar cells, the high concentration mode – dequench mode was used for the study, which is considered as a considerably more sensitive method of evaluation of $\Delta\psi_m$ that reflects depolarization of mitochondria (306,307). Freshly isolated pancreatic cells were loaded with 20 μM TMRM for 25 min at room temperature. One potential artifact in employing TMRM for measurements of $\Delta\psi_m$ is that translocation of the charged membrane-permeant indicator across the plasma membrane could influence the fluorescence (308). Because of the presence of calcium-dependent ionic channels in the plasma membrane, the pancreatic acinar cells are able to generate rapid changes of membrane potential during calcium responses (104). To avoid a possible artifact due to the redistribution of fluorescent dye across the plasma membrane, TMRM from the extracellular solution was removed prior to experiments, that is, cells were then washed and re-suspended in NaHEPES buffer solution containing 1 mM Ca^{2+}. Fluorescence was excited by a 535 nm argon laser line, and emission was collected above 560 nm. All these experiments were conducted by using a Leica TCS SPE confocal microscope with a 63x oil immersion objective. Whole cells as the regions of interest were chosen for analyzing the change of mitochondrial membrane potential of the dequench mode experiments. This is because of both the cytosol and the mitochondrial region responded to depolarization of mitochondria with an increase of fluorescence. (308).

Measurements of cellular ATP in pancreatic acinar cells

For measurements of intracellular ATP, this was performed with Magnesium Green-AM (MgGreen), which senses changes in $[Mg^{2+}]_i$ at concentrations around the resting $[Mg^{2+}]_i$ (approx. 0.9 mM). The cell-permeant Magnesium Green-AM exhibits a high affinity for Mg^{2+} (K_d ~ 1 mM) and the maximum fluorescence excitation/emission intensity on binding Mg^{2+} is ~506/531 nm. As most of the intracellular ATP is in the form of Mg-ATP, a reduction of the ATP concentration will increase the fluorescence intensity of MgGreen owing to the inevitable increase of $[Mg^{2+}]_i$. Therefore, this was used as an indirect approach to detect cytosolic ATP depletion (242,309). Pancreatic acinar cells were incubated with 4 µM MgGreen for 30 min at room temperature (excitation 488 nm). ATP depletion mixture (4 µM CCCP, 10 µM oligomycin and 2 mM iodoacetate) was applied for a final 10 min to induce maximum ATP depletion (310,311).

Necrotic cell death assay

Necrotic cell death assay was assessed by propidium iodide (PI) uptake on freshly isolated pancreatic acinar cells as previously described (312,313). PI is a popular red-fluorescent nuclear and chromosome counterstain. Since propidium iodide is not membrane permeant in viable cells, it is commonly used to detect dead cells and assess cell membrane rupture in a population. Once the dye is bound to DNA by intercalating between the bases, its fluorescence is enhanced 20- to 30-fold. In principle, freshly isolated cells were divided into three groups: negative control, positive control and treatment. Cells were incubated with various reagents in certain time period interval at room temperature and PI were added to every group until the incubation finished. Propidium iodide staining of necrotic cells was detected when excited by 535 nm laser light and the emission maximum is 617 nm. Multiple images (> 20) were taken in every group, and the viable and necrotic cells were counted afterwards. Generally, every protocol of necrotic cell death assay was repeated at least three times and the final data presented as bar chart with mean ± SEM.

In vivo model of experimental acute pancreatitis

All animal studies were ethically reviewed and conducted according to UK Animals (Scientific Procedures) Act of 1986, approved by the UK Home Office (PPL: 30/2956, PIL: I3087FFA9).The animal procedures and experimental protocols were approved by Animal Care and Ethics Committees at Cardiff school of biosciences, Cardiff University. Before and throughout the experiment unless otherwise denoted, mice were maintained in plastic cages with corn cob bedding; tap water and commercial pelleted diet were freely provided. To establish ASNase-induced AP (ASNase-AP), WT C57BL6/J mice received four daily intraperitoneal (IP) injections of Recombinant Asparaginase protein (ab73439, Abcam) in phosphate-buffered saline (PBS) at 20 IU/g. Control mice only received PBS IP injection. In ASNase-AP model, analgesia with 2.5 μg/ml buprenorphine hydrochloride (Temgesic) was orally administered. Treatment groups were defined as follows: galactose (180 mg/kg/day) fed (in drinking water 24 hours before the first ASNase IP injection and for the following days during injections) followed by ASNase injection (20 IU/g) or galactose (180 mg/kg/day) fed with galactose (180 mg/kg/day) simultaneously with the first injection of ASNase (20 IU/g; n ≥ 5 mice/group). Animals received injections at the same time each day and were sacrificed at 24 h after the final injection. Body weight was recorded at the first day and the day of euthanasia.

Histology and score

Preparation of tissue for light microscopy

Pancreas and lung tissue samples were fixed in 4% formaldehyde solution for 24 hours prior to processing. Fixed tissue samples were processed for paraffin embedding in Leica TP1050 fully enclosed automatic tissue processor (Figure 2.11) using the following schedule:

Step	Reagent	Time
01	70% Ethanol	1 h
02	90% Ethanol	1 h
03	100% Ethanol	1 h
04	100% Ethanol	1.5 h
05	100% Ethanol	1.5 h
06	Xylene	1 h
07	Xylene	1 h
08	Paraffin wax	1 h
09	Paraffin wax	2 h under vacuum
10	Paraffin wax	2 h under vacuum

After processing the samples were embedded in paraffin wax using a Leica EG1150H Embedding Centre (Figure 2.11), the blocks were then placed on a Leica EG1140C cold plate to allow the wax to harden rapidly.

Sections were cut at a thickness of 5µm using a Leica RM2235 rotary microtome (Figure 2.11), floated on warm water at 45^{o}C and mounted on Superfrost plus microscope slides. The sections were dried overnight at 45^{o}C.

Slides were stained with Hematoxylin and eosin (H&E) using an R.A. LAMB Histomate staining machine (Figure 2.11) using the following protocol.

Step	Reagent	Time
01	Xylene	3 min
02	Xylene	3 min
03	100% Ethanol	2 min
04	100% Ethanol	2 min
05	100% Ethanol	2 min
06	90% Ethanol	1 min
07	70% Ethanol	1 min
08	Running tap water	3 min
09	Mayer’s Haematoxylin	5 min
10	Water	5 min
11	1% Eosin	5 min
12	Water	30 sec
13	70% Ethanol	30 sec
14	90% Ethanol	30 sec
15	100% Ethanol	1 min
16	100% Ethanol	2 min
17	100% Ethanol	2 min
18	Xylene	1 min
19	Xylene	2 min
20	Xylene	2 min

Sections were mounted under a cover glass using DPX mountant.

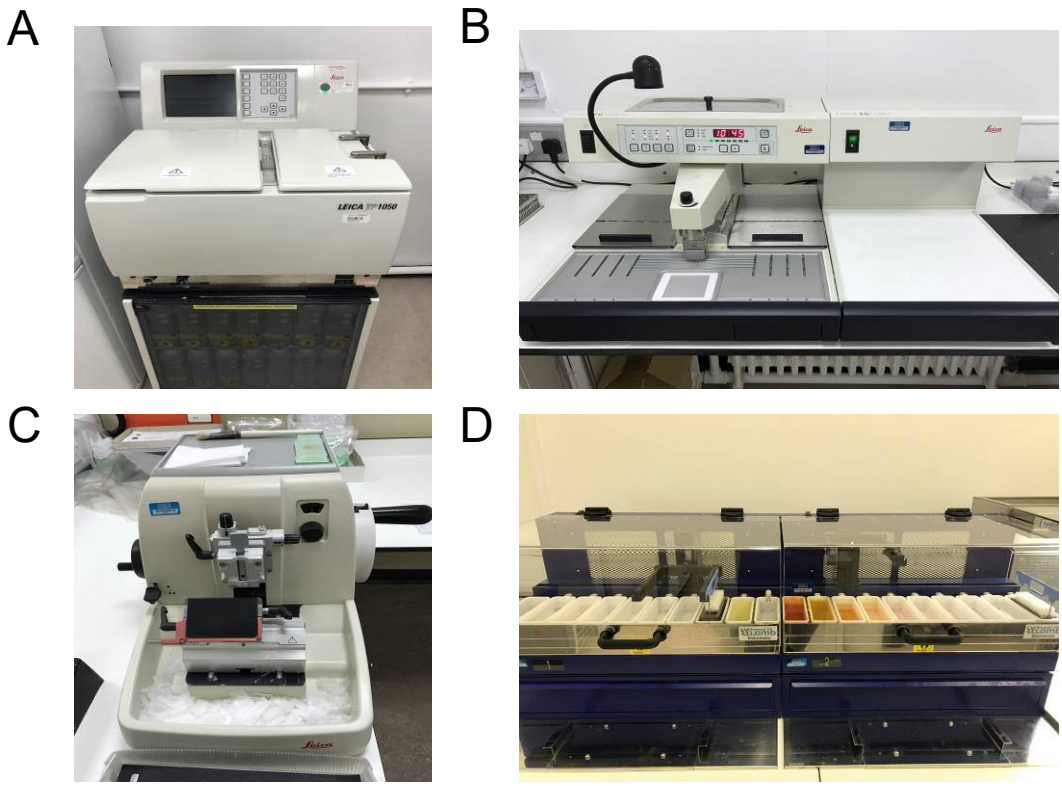

Figure 2.11 Main equipments for tissue preparation.

A. Tissue processing machine (Leica TP1050).

B. Embedding Centre (Leica EG1150H).

C. Rotary microtome (Leica RM2235).

D. H&E staining machine (R.A. LAMB Histomate).

Histological score

Histological assessment of tissue damage was performed after H&E staining of fixed pancreatic slices (4 μm thickness); 15 random fields per slide from all animal groups were graded in a blinded manner, without knowledge of the experimental design, according to severity and extent of edema, inflammatory cell infiltration and acinar necrosis from 0 to 3 by a histopathological grading system (Table 2.2) as previously described by Van Laetham *et al* (314,315).

Table 2.2 Grading criteria used for pancreatic histopathological score. (Modified from *Wildi S et al, Gut, 2007*) (315)

Parameter	Score	Indication
Edema	0	Absent
	1	Focally increased between lobules
	2	Diffusely increased
	3	Acini disrupted and separated
Inflammatory cell infiltrate	0	Absent
	1	In ducts (around ductal margins)
	2	In the parenchyma (< 50% of the lobules)
	3	In the parenchyma (> 50% of the lobules)
Acinar necrosis	0	Absent
	1	Periductal necrosis (< 5%)*
	2	Focal necrosis (5–20%)
	3	Diffuse parenchymal necrosis (20–50%)

*Approximate percentage of cells involved per field examined.

Statistical analysis

Statistical analysis was performed using IBM SPSS Statistics 20.0 software, which was issued and technically provided by Cardiff University IT office. Data were presented as mean ± SEM. Statistical significance and *p*-values were calculated using *t*-test or ANOVA, with $*p < 0.05$ was considered statistically significant and $**p < 0.01$ as highly significant.

Chapter 3

Asparaginase-induced pancreatic acinar cell death elicited via protease-activated receptor 2

Overview of protease-activated receptor 2

Proteinase-activated receptors (PARs) are a novel subfamily of seven-transmembrane G-protein-coupled receptors (GPCRs) superfamily in mammalian systems (316). Unlike the classic receptor being activated by simple ligand occupancy, PARs are uniquely and irreversibly activated enzymatically through proteolysis of the N terminus to reveal a tethered ligand of the receptor, that is, they are activated by cleavage of part of their extracellular domain (316,317). This proteolytic cleavage is specifically mediated by the serine proteases resulting in the generation of a new tethered ligand that interacts with the receptor within extracellular loop-2 (316,318). PARs are expressed predominantly in vascular (highly in platelets), immune and epithelial cells, astrocytes and neuron s and transmit cellular responses to extracellular proteases expressed in distinct tissues (319–321). There are four members of PARs known in mouse and human (322). Human PAR1 (323,324), PAR3 (325), and PAR4 (326,327) can be activated by thrombin (328). Whereas PAR2 is activated by trypsin (329) and tryptase (330) as well as by coagulation factors VIIa and Xa (331,332), but not by thrombin.

It was serendipitous that screening a mouse genomic library by using degenerate primers to the second and sixth transmembrane domains of the bovine neurokinin 2 receptor resulted in discovery and identification of PAR2 (329,333). Analysis of the PAR2 N-terminal amino acid sequence revealed a putative trypsin cleavage site SKGR^{34}↓S^{35}LIGKV (Figure 3.1) (329,333,334). The mechanism by which protease activates PAR2 has been investigated in detail. Trypsin cleaves PAR2 at R^{34}↓S^{35}LIGKV to reveal the NH_2-terminal tethered ligand SLIGKV in humans. This cleavage generates a new tethered ligand domain, which binds to conserved regions in the second extracellular loop of the cleaved receptor, resulting in the initiation of signal transduction (Figure 3.2). Cells derived from tissues e.g. kidney, pancreas, small intestine,

colon, and skin are shown to contain abundant mRNA in PAR-2 (334). They were also found to respond to trypsin or activating peptide corresponding to the tethered ligand domain e.g. SLIGKV (human) and SLIGRL (mouse) without the need for receptor cleavage, which furthermore confirmed the presence of a functionally and physiologically important receptor (334). Exposure of cells to trypsin leads to loss of immunoreactivity to an antibody against an NH_2-terminal epitope, which proves that trypsin cleaves intact PAR2 at the cell surface (335).

PAR2 activation via $G_q\alpha$ rather than G_i (336) generate IP_3 and mobilize Ca^{2+} in PAR2-transfected cell lines, enterocytes, keratinocytes, myocytes, neurons, astrocytes and tumor cells (329,334,337–342). PAR2 activation by proteases is an irreversible process that exposure of the tethered ligand domain by proteases cleavage is always available to interact with the cleaved receptor. The principal mechanism that terminates signaling of PARs is that ligand occupation of the GPCR induces the translocation of G protein receptor kinases (GRKs) from the cytosol to the activated receptor at the cell surface. GRKs are serine-threonine kinases that phosphorylate activated GPCR through its carboxy terminus or third intracellular loop. Phosphorylation triggers the membrane translocation of interaction with β-arrestins to interact with the phosphorylated GPCR, which mediate uncoupling of heterotrimeric G proteins and desensitization of GPCR, and thereby terminate signal transduction. It seems that PKC plays an important role in regulating PAR2 (335,336). However, the role of GRKs and β-arrestins in PAR2 desensitization is unknown.

PAR2 regulates pancreatic exocrine secretion and its activation stimulates the release of amylase from isolated rat pancreatic acini (337) and *in vivo* rat model (343). Furthermore, activation of PAR2 led to increased Ca^{2+}-activated Cl^- and K^+ conductance in pancreatic duct epithelial cells (344). In addition,

PAR2 is involved in inflammation and pain (345,346). However, the role of PAR2 in acute pancreatitis is still under debate (347–350).

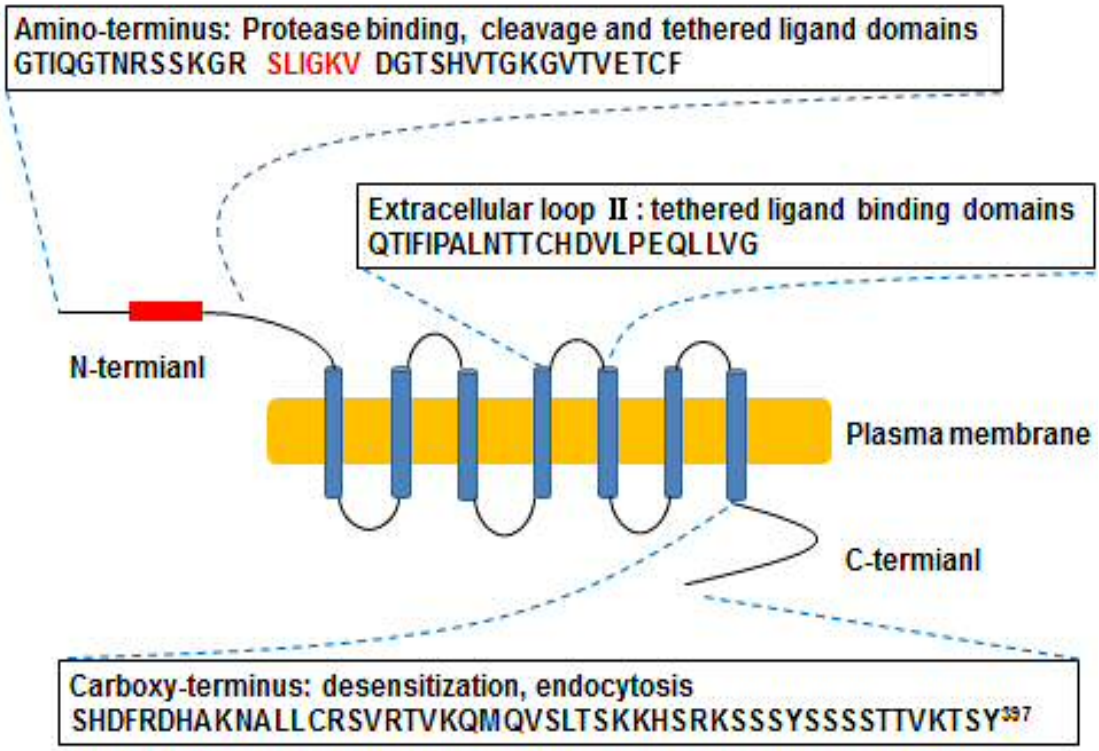

Figure 3.1 Structural and functional domains of PAR2.

The diagram shows alignment of functionally important domains in the amino terminus, second extracellular loop, and carboxy terminus of human PAR2. The key area of PAR2 receptor activation is highlighted. (Modified from *Ossovskaya VS & Bunnett NW, Physiol Rev. 2004*) (318)

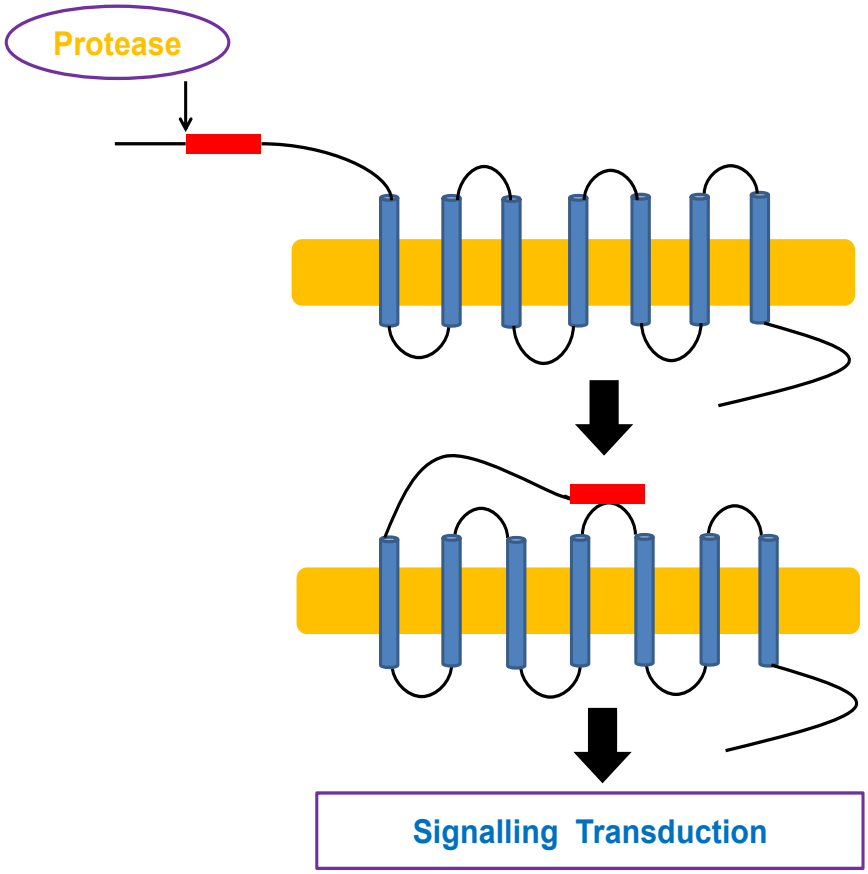

Figure 3.2 Mechanism of protease activation of PAR2.

Proteolytic cleavage the peptide bond between receptor residues Arg 34 and Ser 35 leads to the generation of a new tethered ligand designated by the filled section which docks intramolecularly with the extracellular loop-2 of the receptor to mediate transmembrane signalling. (Modified from *Macfarlane SR et al, Pharmacol Rev. 2001*) (316)

The study described in this chapter aimed to investigate the role of asparaginase on calcium signaling and evaluate the effects of the drugs CRAC channel blocker GSK-7975A and PAR2 antagonist FSLLRY-NH_2 on asparaginase-induced necrosis in pancreatic acinar cells.

Asparaginase increases $[Ca^{2+}]_i$ in pancreatic acinar cells

As mentioned above, studies on isolated pancreatic acinar cells or cell clusters have been showed remarkably helpful to understanding AP. Results *in vitro* have turned out to be excellent predictors of the outcomes of studies in *in vivo* AP models (351–354). Therefore our approach has been to study, for the first time, the effects of asparaginase on isolated mouse acinar cells or cell clusters are a natural starting point for investigations of the mechanism of AAP. Ca^{2+} has been known for playing the key role in the pathophysiology of AP (134,227,228,355,356). Pancreatitis-inducing agents, metabolites of ethanol and fatty acids - POAEE (239,242,310) or bile acids (238,354), are able to elicit $[Ca^{2+}]_i$ elevation in isolated acinar cells causing intracellular Ca^{2+} overload. This is due to Ca^{2+} release from internal stores triggering excessive store-operated Ca^{2+} entry (136,312). In order to identify the mechanism of action of asparaginase, the effects of asparaginase on $[Ca^{2+}]_i$ was initially tested over a wide concentration range. Time course is the one of the challenges inherent in this approach for a study on normal freshly isolated cells. Because AAP typically develops several days after several administrations (over many weeks) of asparaginase in the clinical situation (291). However, *in vitro* studies on isolated cells in the laboratory require observations of the effects of asparaginase within hours, which is quite different from clinical studies.

In the present study, we have tested the effects of different concentration of asparaginase on $[Ca^{2+}]_i$ and worked with the lowest concentration of asparaginase that reliably evoked similar cellular Ca^{2+} changes associated with AP as nonoxdative alcohol metabolites or bile acids did on pancreatic acinar cells. To measure $[Ca^{2+}]_i$, pancreatic acinar cells were isolated from pancreas of WT mice and loaded with calcium sensitive dye Fluo-4 (see

images of the cells in Figure 3.3A). The cells were subsequently exposed to asparaginase. We found that a low concentration of asparaginase (20 IU/ml) induced $[Ca^{2+}]_i$ oscillations only in a few cells (21%, 9 out of 42 cells; Figure 3.3D). Figure 3.3B shows a representative trace with repetitive Ca^{2+} spikes induced by asparaginase (20 IU/ml), whereas figure 3.3C represents the same concentration asparaginase failed to cause any change in $[Ca^{2+}]_i$ in majority of cells (79%, 33 out of 42 cells; Figure 3.3D).

A

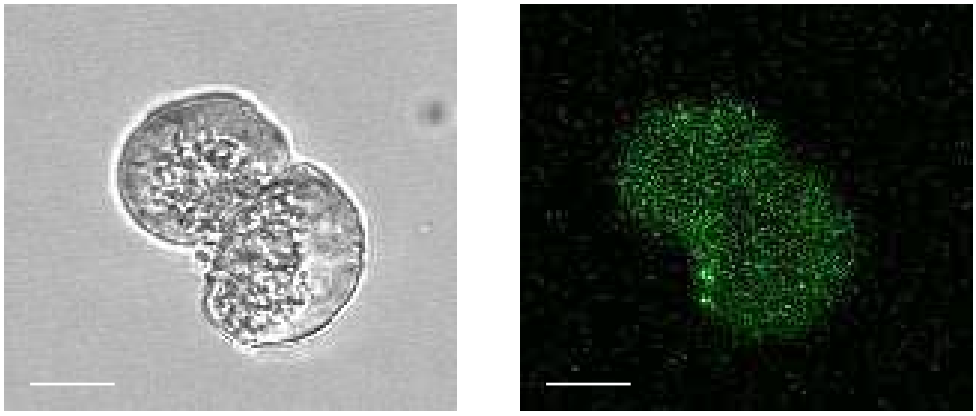

B

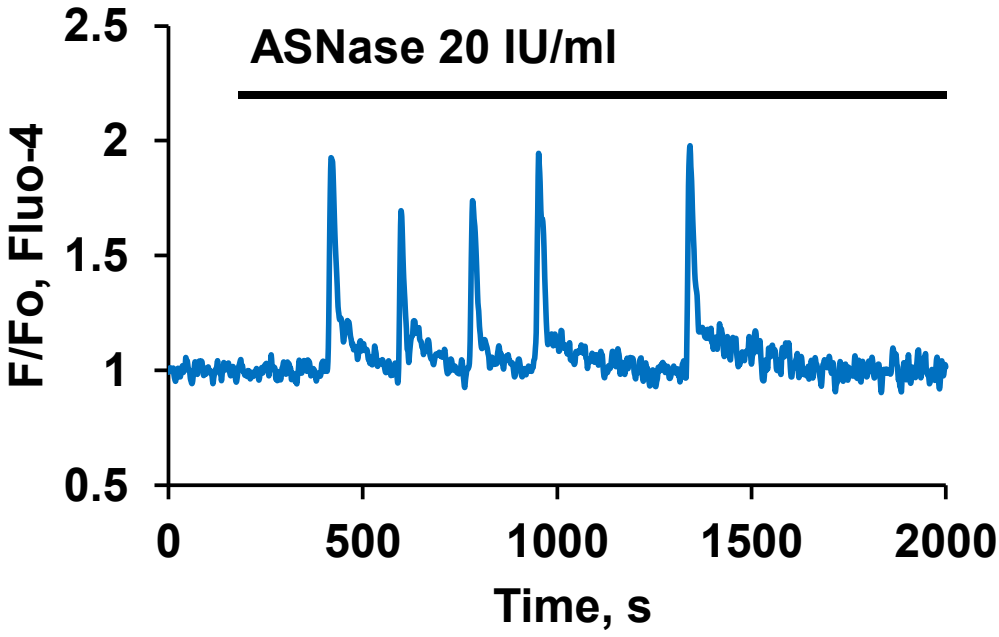

C

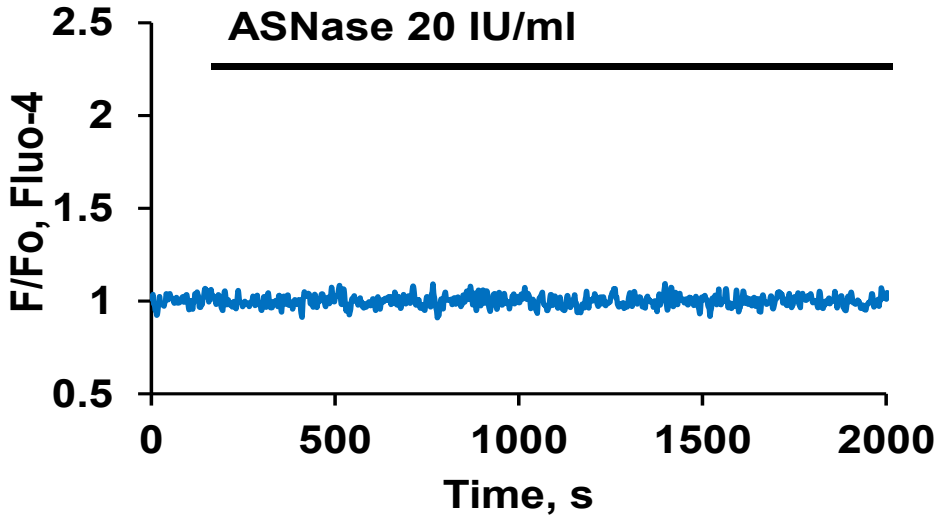

D

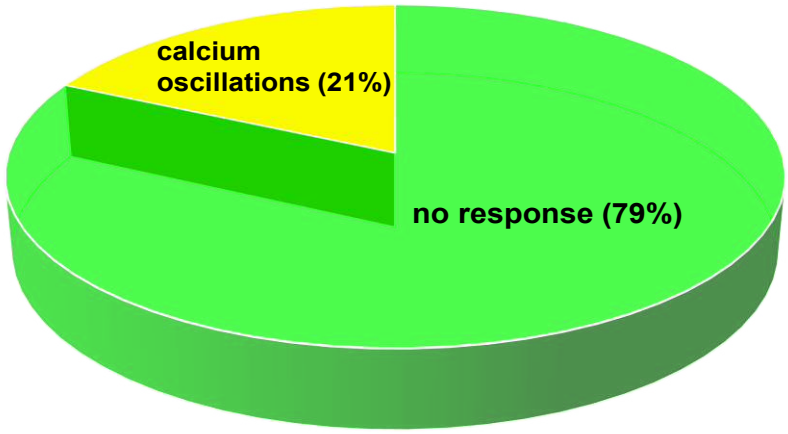

Figure 3.3 Asparaginase induces cytosolic Ca^{2+} signals in pancreatic acinar cells. (Modified from *Peng S et al, Philos Trans R Soc Lond B Biol Sci. 2016*) (313) (A) Images of a doublet of pancreatic acinar cells; transmitted light images (left part) and Fluo-4 fluorescence images (right part; scale bar: 10 μm). (B) The representative trace shows the low concentration of asparaginase (20 IU/ml) induces repetitive Ca^{2+} spikes in a minority (9 out of 42) of experiments. (C) Asparaginase (20 IU/ml) elicits no response in the majority (33 out of 42) of cases. (D) Pie chart shows percentage of cells responding to asparaginase (20 IU/ml) with oscillations or not responding at all.

A relatively higher concentration of asparaginase (200 IU/ml) was then used to test $[Ca^{2+}]_i$ in pancreatic acinar cells. The transmitted light picture of a cell under investigation is shown in Figure 3.4A1. After exposing the cell to Fluo-4-AM, the fluorescence intensity was generally weak, in the absence of stimulation, as shown in Figure 3.4A2. However, after a higher concentration of asparaginase (200 IU/ml) application, we found that sustained elevated $[Ca^{2+}]_i$ plateau with top of repetitive $[Ca^{2+}]_i$ oscillations was induced in pancreatic acinar cells (43 out of 55 cells; Figure 3.4B and C). The development of a sustained $[Ca^{2+}]_i$ elevation has previously been shown to be a distinctive characteristic of $[Ca^{2+}]_i$ changes induced by pathological concentrations of alcohol metabolites or bile acids. The small elevated $[Ca^{2+}]_i$ plateau was seen in the vast majority of cells (52 out of 55) stimulated by asparaginase (200 IU/ml) (Figure 3.4E). In some cases (12 out of 55), there were no, or very few, spikes superimposed on the elevated $[Ca^{2+}]_i$ plateau (Figure 3.4D). When the external solution was changed to Ca^{2+} free, the sustained $[Ca^{2+}]_i$ plateau gradually declined to the baseline. Therefore asparaginase (200 IU/ml)-induced $[Ca^{2+}]_i$ elevation depends on the continued presence of Ca^{2+} in the external solution.

A

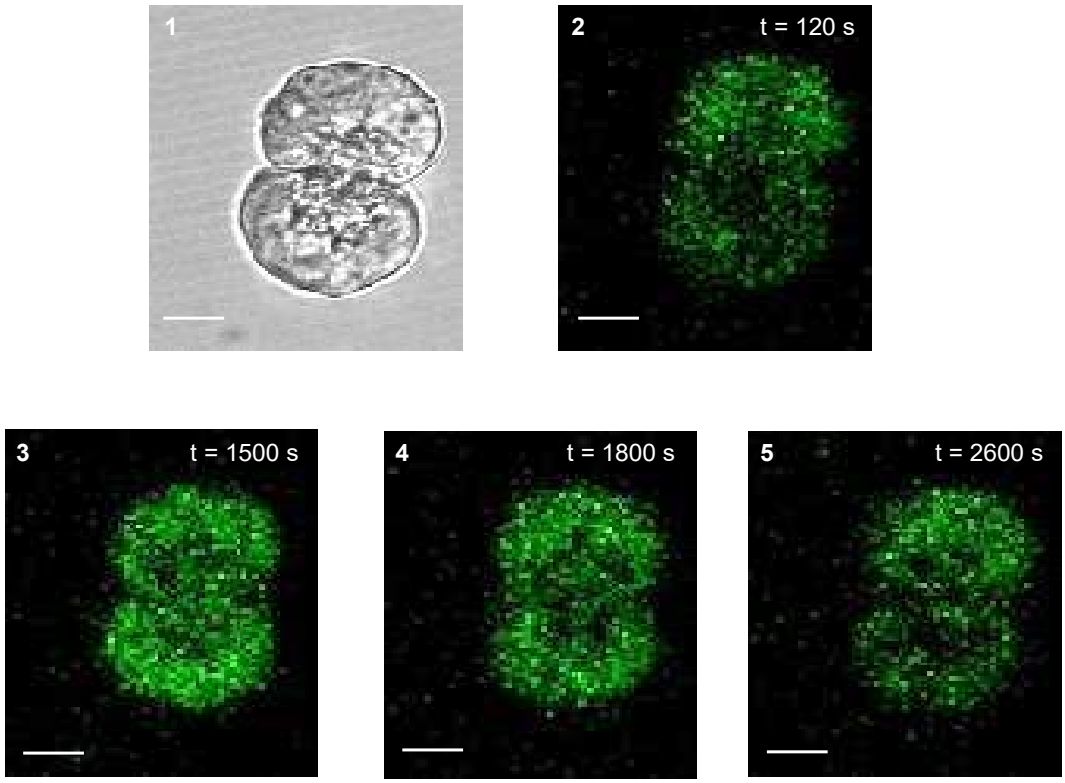
1
2
t = 120 s
3
t = 1500 s
4
t = 1800 s
5
t = 2600 s

B

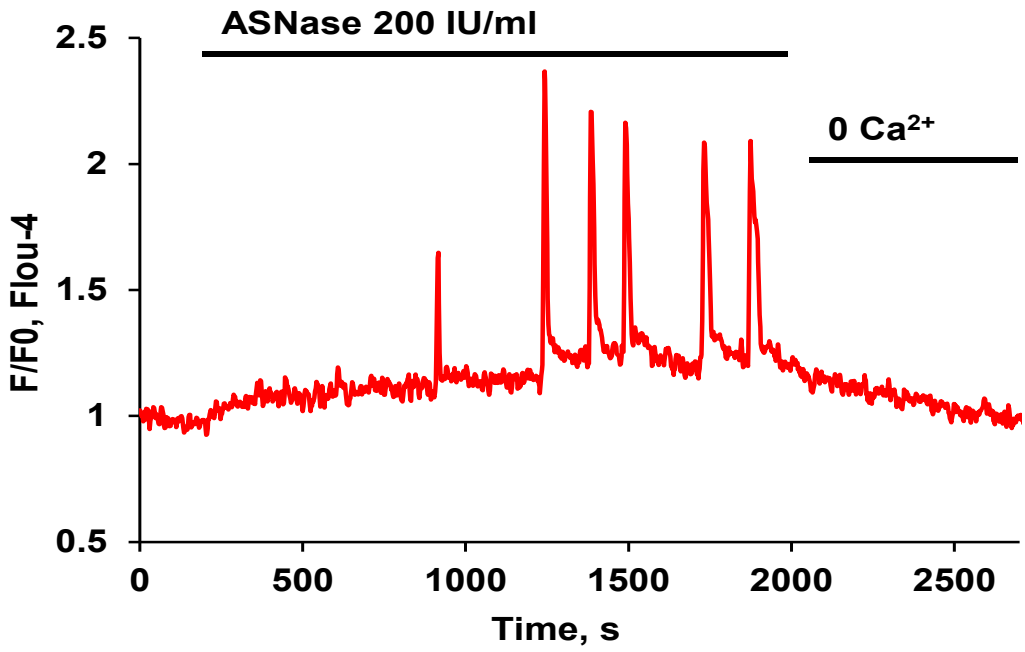
ASNase 200 IU/ml
0 Ca2+
F/F0, Flou-4
2.5
2
1.5
1
0.5
0
500
1000
1500
2000
2500
Time, s

C

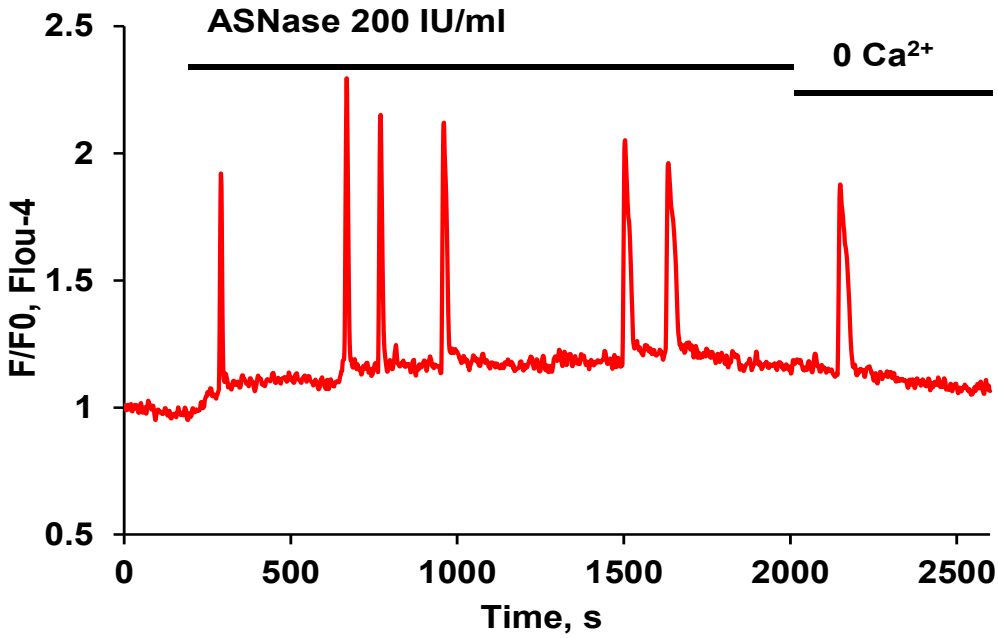
ASNase 200 IU/ml
0 Ca2+
F/F0, Flou-4
2.5
2
1.5
1
0.5
0
500
1000
1500
2000
2500
Time, s

D

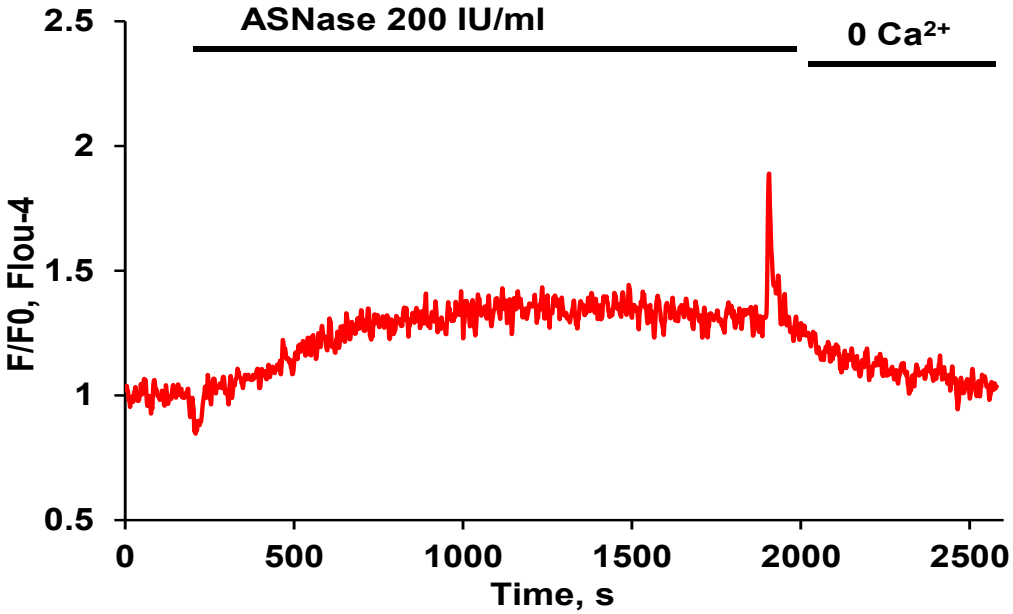
ASNase 200 IU/ml
0 Ca2+
F/F0, Flou-4
2.5
2
1.5
1
0.5
0
500
1000
1500
2000
2500
Time, s

E

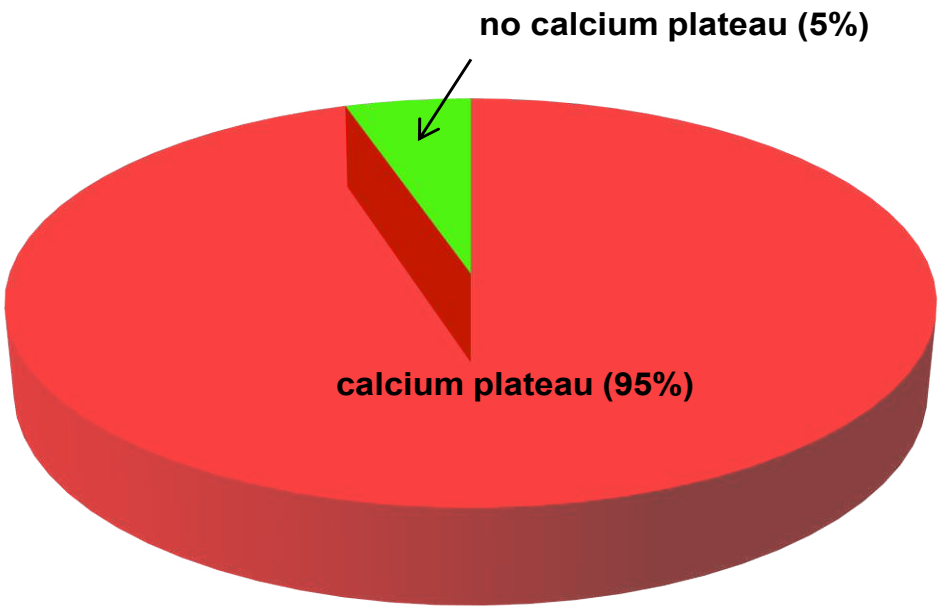

Figure 3.4 Asparaginase induces $[Ca^{2+}]_i$ changes in pancreatic acinar cells. (Modified from *Peng S et al, Philos Trans R Soc Lond B Biol Sci. 2016*) (313)

(A) Transmitted light micrograph and Fluo-4 fluorescence images showing the cells under investigation (scale bar: 10 μm). (B-D) A higher concentration of asparaginase (200 IU/ml) elicits an elevated $[Ca^{2+}]_i$ plateau in practically all cases (52 out of 55), often with repetitive Ca^{2+} transients on top of the plateau (43 out of 55) as shown in the representative trace B and C. But in some cases (12 out of 55) with no or very few spikes as shown in the representative trace D. (E) Pie chart shows percentage of cells responding to asparaginase (200 IU/ml) with or without elevated $[Ca^{2+}]_i$ plateau.

It has previously been shown that the cytosolic Ca^{2+} overload and ATP deprivation induced by fatty acid ethyl esters and bile acids lead to necrosis on pancreatic acinar cells, which is the hallmark of AP (136,138). We therefore tested if asparaginase also can induce necrosis on pancreatic acinar cells. Cell necrotic assays were performed on freshly isolated pancreatic acinar cells by propidium iodide (PI) staining. As seen in Figure 3.5, lower concentration of asparaginase (20 IU/ml) did not increase the level of necrosis (4.5 ± 0.7% of cells) more than the control level (4.6 ± 0.4% of cells, $p > 0.8$), whereas higher concentration of asparaginase (200 IU/ml) significantly induced the level of necrosis (15.4 ± 1.8% of cells). Asparaginase kills malignant lymphoblasts by depriving them of asparagine through hydrolysis of asparagine (Asn) to aspartic acid and ammonia (357). Given that most malignant lymphoblasts-unlike normal cells-cannot synthesize Asn by themselves (271,358,359). The effects of asparaginase on normal pancreatic acinar cells described in this study are therefore unlikely to be owing to Asn deprivation. We tested whether there was any difference between the ability of asparaginase to induce necrosis in the absence or presence of Asn. As seen in Figure 3.5, asparaginase did not significantly increase the level of necrosis (14.2 ± 0.8% of cells) in the presence of Asn (50 μM) (360,361) as compared with in the absence of Asn ($p > 0.6$).

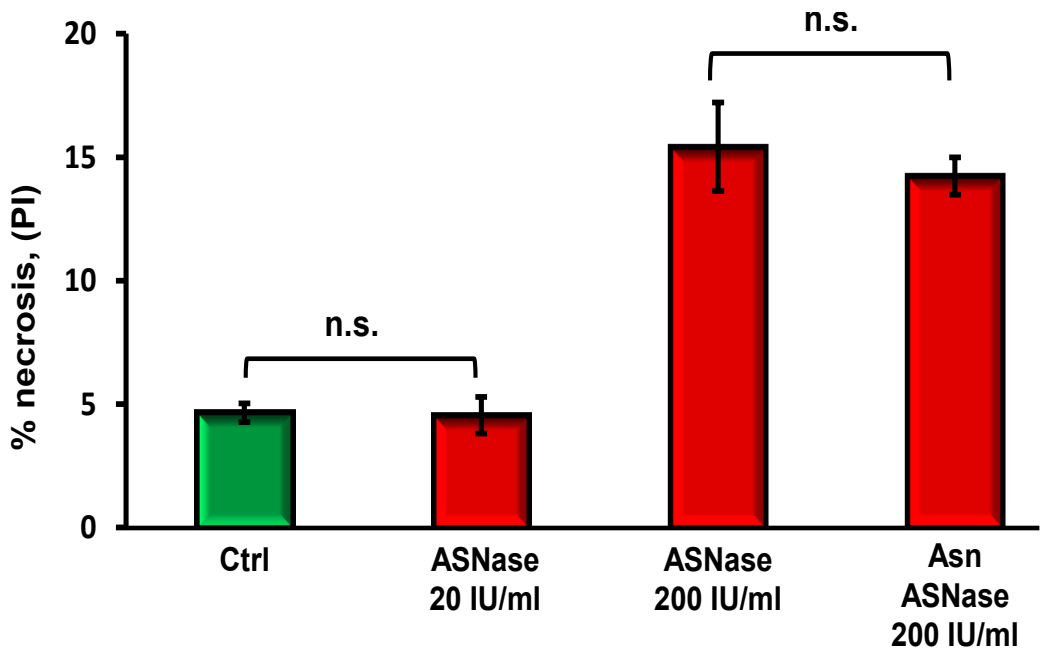

Figure 3.5 Asparaginase induces necrosis in pancreatic acinar cells, which is not dependent on asparagine. (Modified from *Peng S et al, Philos Trans R Soc Lond B Biol Sci. 2016*) (313)

A lower concentration of asparaginase (20 IU/ml) did not induce any significant change in the level of necrosis when compared with control (4.5 ± 0.7% and 4.6 ± 0.4%, respectively, $p > 0.8$, each test had four series of experiments with n > 130 of tested cells in each group). The presence or absence of asparagine (50 μM) made no difference to the level of asparaginase-induced necrosis ($p > 0.6$, three series of experiments with more than 70 cells in each sample).

Asparaginase-elicited Ca^{2+} release involves inositol 1,4,5-trisphosphate receptors

In order to investigate intracellular Ca^{2+} release mechanism involved in asparaginase-induced $[Ca^{2+}]_i$ elevations, caffeine was applied in the study. This substance has shown to reliably inhibit IP_3R-mediated intracellular Ca^{2+} release in pancreatic acinar cells (138,352,362,363). As described above, pancreatic acinar cells isolated from WT mice and loaded with calcium indicator Fluo-4 were used for measuring $[Ca^{2+}]_i$. In the whole series of experiments, pancreatic cells were exposed to Ca^{2+} free external solution. Cells were perfused with caffeine (20 mM) for 200 sec incubation and then asparaginase (200 IU/ml) was applied to the cells. As shown in Figure 3.6, caffeine (20 mM) substantially reduced the asparaginase-induced $[Ca^{2+}]_i$ elevations in a Ca^{2+}-free solution ($p < 0.003$; n = 8; compare with Figure 3.8 as the appropriate control). Because the asparaginase-elicited Ca^{2+} release from intracellular stores is dependent on functional IP_3Rs, we tested whether asparaginase acts by stimulating IP_3 production. The most widely used inhibitor of phospholipase C (PLC) is the aminosteroid compound U73122 (364,365). Although U73122 is a powerful PLC inhibitor, it has been reported that other effects including release of Ca^{2+} from IP_3-sensitive stores (364,366,367). We used U73122 at a concentration (10 μM) that abolishes cytosolic Ca^{2+} signal generation evoked by muscarinic receptor activation in many systems (364), including pancreatic acinar cells (368). Figure 3.7 shows U73122 (10 μM) also significantly blocked the asparaginase-induced Ca^{2+} release as well as the response to 1 μM ACh ($p < 0.001$; n = 11). Figure 3.9 compares Ca^{2+} responses in a form of a bar chart. Areas under the traces of application of asparaginase within 10 min from Figure 3.6, 3.7 and 3.8 were calculated. Both caffeine and U73122 markedly inhibited asparaginase-induced Ca^{2+} signals in pancreatic acinar cells.

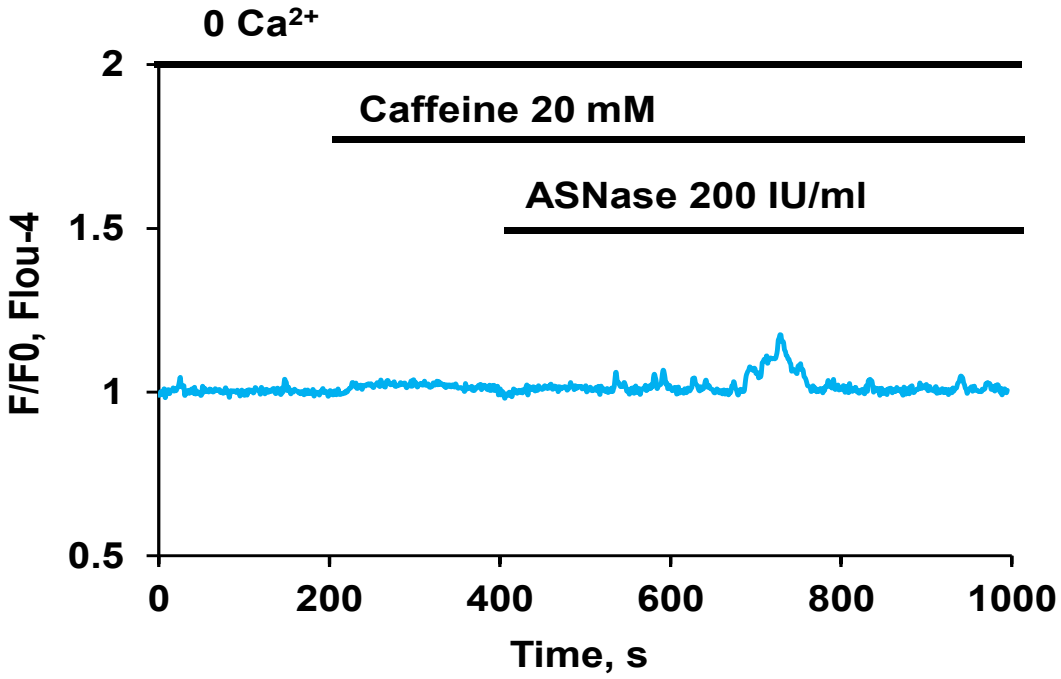

Figure 3.6 Caffeine inhibits asparaginase-induced cytosolic Ca^{2+} responses. (Modified from *Peng S et al, Philos Trans R Soc Lond B Biol Sci. 2016*) (313)

The representative trace shows the IP_3R blocker caffeine (20 mM) substantially reduced the asparaginase-induced $[Ca^{2+}]_i$ elevations in the absence of external Ca^{2+} in pancreatic acinar cells (n = 8).

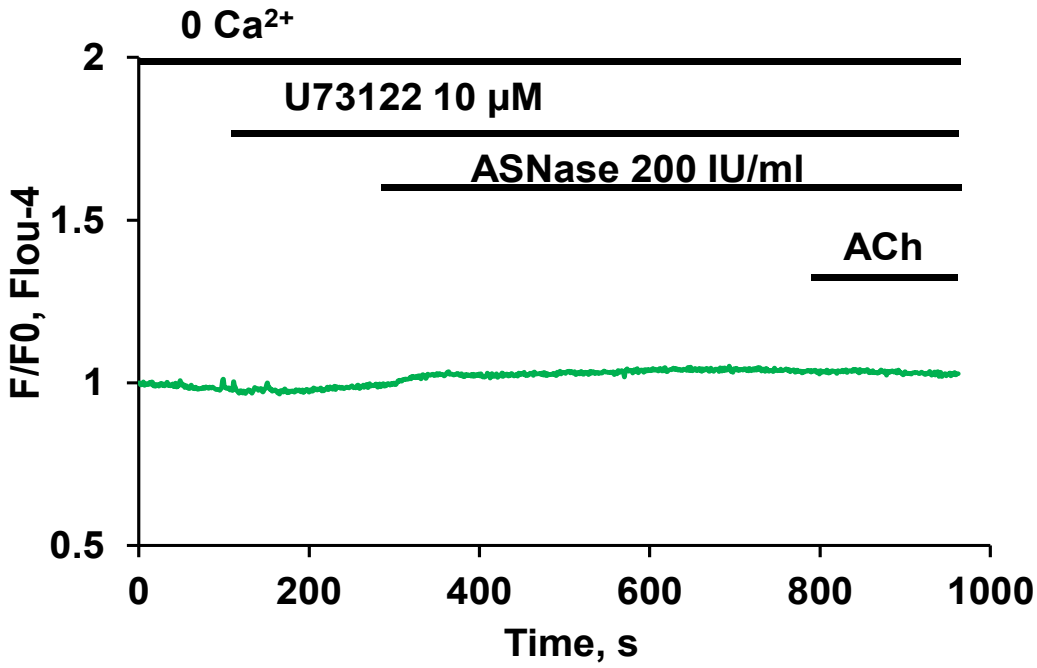

Figure 3.7 U73122 blocks asparaginase-induced cytosolic Ca^{2+} responses. (Modified from *Peng S et al, Philos Trans R Soc Lond B Biol Sci. 2016*) (313)

The representative trace shows the PLC inhibitor U73122 (10 µM) blocked the asparaginase-induced $[Ca^{2+}]_i$ elevation in the absence of external Ca^{2+} in pancreatic acinar cells (n = 11).

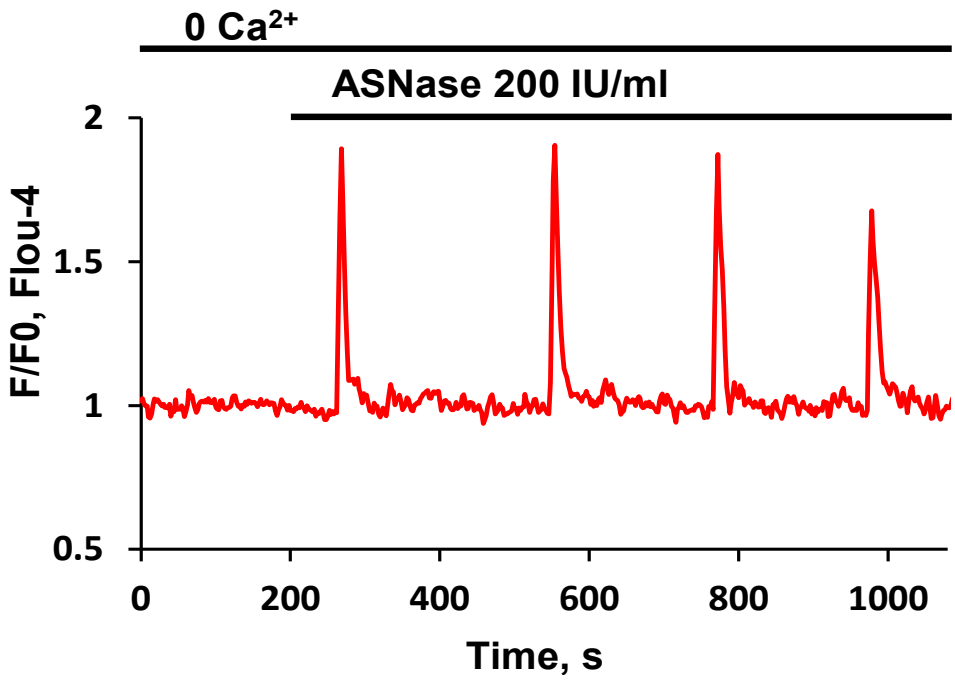

Figure 3.8 Cytosolic Ca^{2+} responses to asparaginase in Ca^{2+} free solution. (Modified from *Peng S et al, Philos Trans R Soc Lond B Biol Sci. 2016*) (313)

The representative trace shows asparaginase (200 IU/ml) induces Ca^{2+} oscillations in the absence of external Ca^{2+} in pancreatic acinar cells (n = 9).

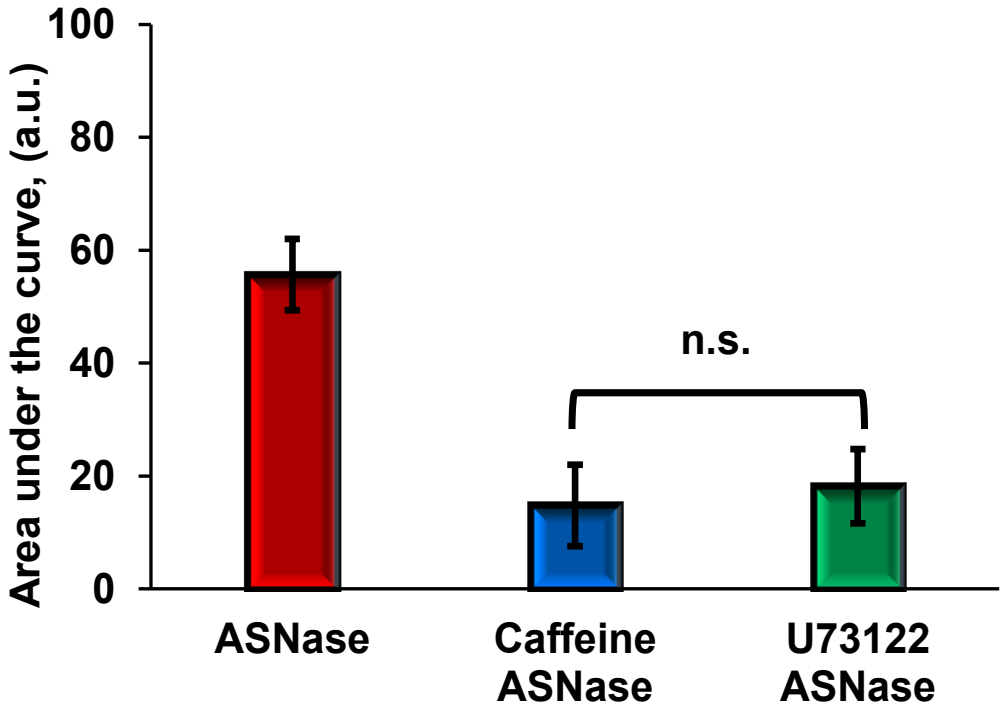

Figure 3.9 Pre-incubation of Caffeine or U73122 substantially reduced asparaginase-induced cytosolic Ca^{2+} responses. (Modified from *Peng S et al, Philos Trans R Soc Lond B Biol Sci. 2016*) (313)

The bar chart shows average area under the traces depicted in Figure 3.6, 3.7 and 3.8 of the recorded responses during the first 500 s of asparaginase application. Data represent mean ± SEM. IP_3R blocker caffeine (20 mM) and PLC inhibitor U73122 (10 μM) significantly blocked the asparaginase-induced $[Ca^{2+}]_i$ elevation in the absence of external Ca^{2+} in pancreatic acinar cells ($p < 0.003$).

The asparaginase-elicited sustained increase in $[Ca^{2+}]_i$ depends on the presence of external Ca^{2+}

It is clearly that Ca^{2+} entry plays an important role in the formation of the sustained elevated $[Ca^{2+}]_i$ plateau in pancreatic acinar cells (136,227). As we observed in the previous experiments, removal of external Ca^{2+} always terminated the elevated $[Ca^{2+}]_i$ plateau (Figure 3.4B,C,D). In order to assess extracellular Ca^{2+} contributing to the asparaginase-induced elevated $[Ca^{2+}]_i$ plateau, different protocols were designed to further characterise asparaginase-elicited $[Ca^{2+}]_i$ elevation by Ca^{2+} entry. We firstly tried simply removal of external Ca^{2+} and stimulating pancreatic acinar cells with asparaginase (200 IU/ml), and we found that cells only developed repetitive Ca^{2+} spikes without generation of sustained elevated $[Ca^{2+}]_i$ plateau (n = 28, Figure 3.10).

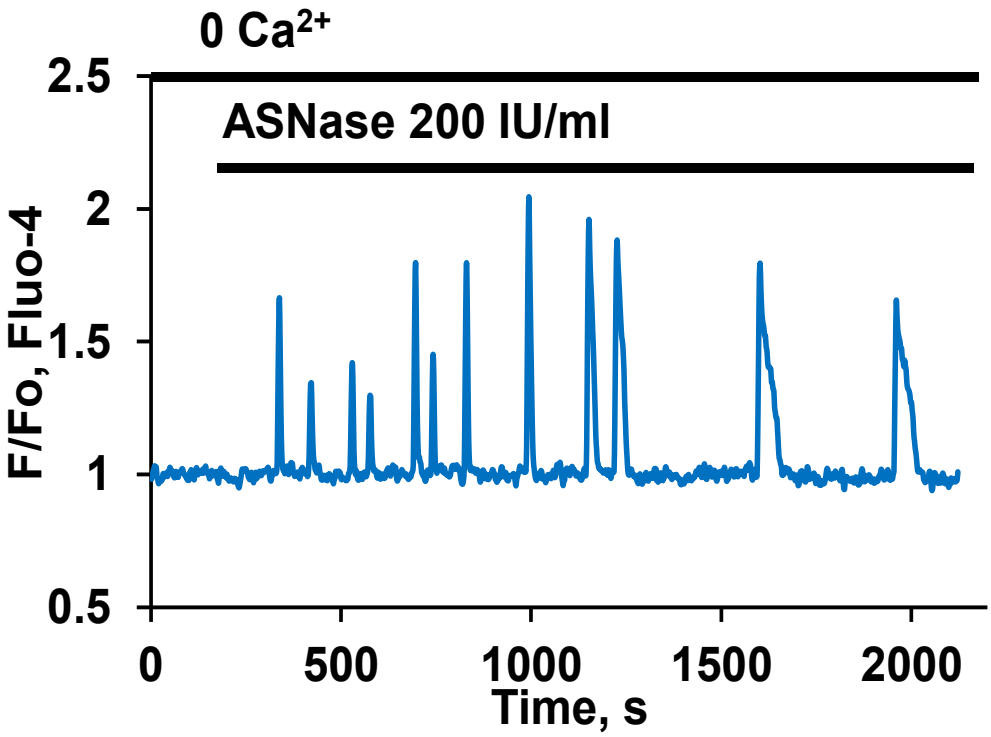

Figure 3.10 The effect of removal of external Ca^{2+} abrogates asparaginase-induced elevated $[Ca^{2+}]_i$ plateau. (Modified from *Peng S et al, Philos Trans R Soc Lond B Biol Sci. 2016*) (313)

Representative trace shows asparaginase induces repetitive Ca^{2+} transients in Ca^{2+} free solution without sustained $[Ca^{2+}]_i$ plateau (n = 28).

Another way to demonstrate asparaginase-elicited $[Ca^{2+}]_i$ elevation is dependent on external Ca^{2+} was to investigate the effect of a Ca^{2+} chelator EGTA (128) on asparaginase-elicited $[Ca^{2+}]_i$ change. Freshly isolated pancreatic acinar cells loaded with Fluo-4 were exposed to asparaginase (200 IU/ml) in the absence of external Ca^{2+} and then increasing the extracellular Ca^{2+} concentration to 2 mM during asparaginase stimulation. This caused a marked and sustained increase in $[Ca^{2+}]_i$ (n = 18, Figure 3.11). Subsequent extracellular solution was changed to Ca^{2+} free buffer containing the Ca^{2+} chelator EGTA (200 μM). As shown in Figure 3.11, elevated $[Ca^{2+}]_i$ plateau was rapidly decreased and abolished finally, whereas the Ca^{2+} oscillations continued for some time. Finally, pharmacological inhibition was performed by using selective CRAC channel blockers GSK-7975A (369,370). It has previously been proved that GSK-7975A can markedly inhibit excessive Ca^{2+} entry into pancreatic acinar cells induced by alcohol metabolites or bile acids and prevent their pathological effects on pancreatic acinar cells (312,354,371). We have therefore tested the effect of CRAC blockade on the asparaginase-induced sustained $[Ca^{2+}]_i$ elevation. Freshly isolated pancreatic acinar cells were preincubated with GSK-7975A (10 μM) for 10 min, and then asparaginase was applied to the cells. Figure 3.12 shows GSK-7975A abolished the elevated $[Ca^{2+}]_i$ plateau, although repetitive Ca^{2+} spiking was still observable within the time frame of the experiments (n = 32). Figure 3.13 summarizes the degree of inhibition, caused by removal of external Ca^{2+} or by GSK-7975A, of the integrated Ca^{2+} signal evoked by asparaginase.

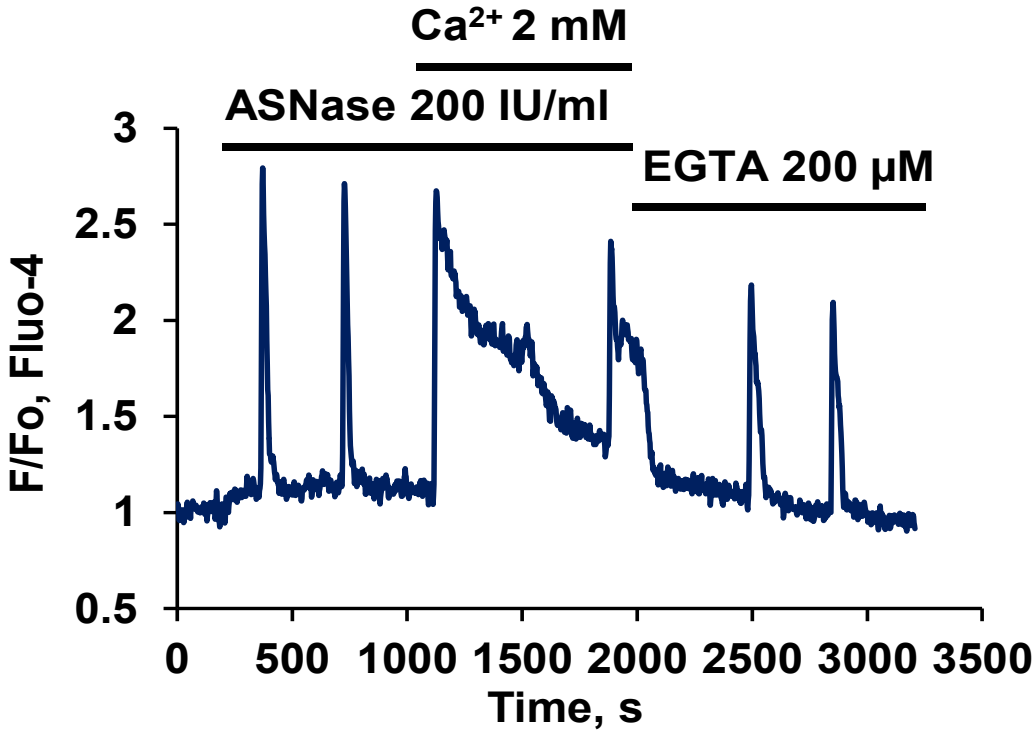

Figure 3.11 Increasing external calcium dramatically increases calcium plateau while calcium removal blocks asparaginase-induced elevated $[Ca^{2+}]_i$ plateau. (Modified from *Peng S et al, Philos Trans R Soc Lond B Biol Sci. 2016*) (313) Representative trace shows when the external Ca^{2+} concentration is increased from 1 to 2 mM, there is a marked transient $[Ca^{2+}]_i$ rise and a continuing elevated $[Ca^{2+}]_i$ plateau. When subsequently removal of external Ca^{2+} and addition of the Ca^{2+} chelator (EGTA), the plateau gradually disappears (n = 18).

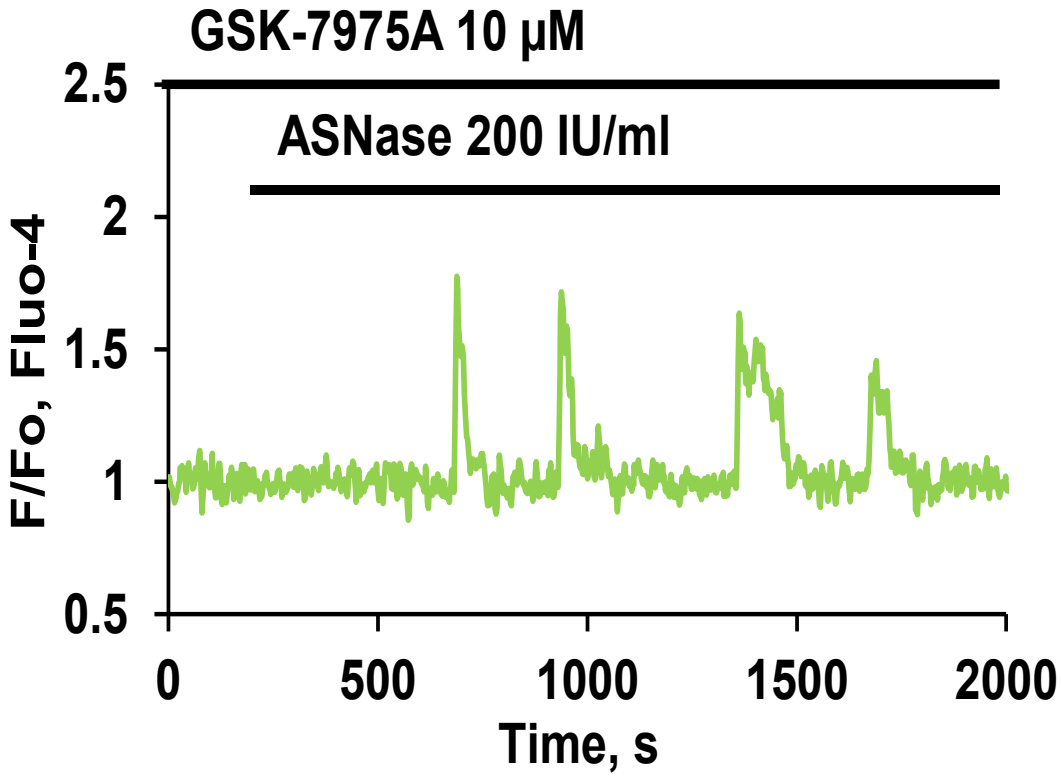

Figure 3.12 The effect of CRAC blockade on the asparaginase-induced elevated $[Ca^{2+}]_i$ plateau. (Modified from *Peng S et al, Philos Trans R Soc Lond B Biol Sci. 2016*) (313)

The typical trace shows in the presence of the CRAC channel blocker GSK-7975A (10 μM), asparaginase (200 IU/ml) evokes repetitive Ca^{2+} spikes without an elevated $[Ca^{2+}]_i$ plateau (n = 32).

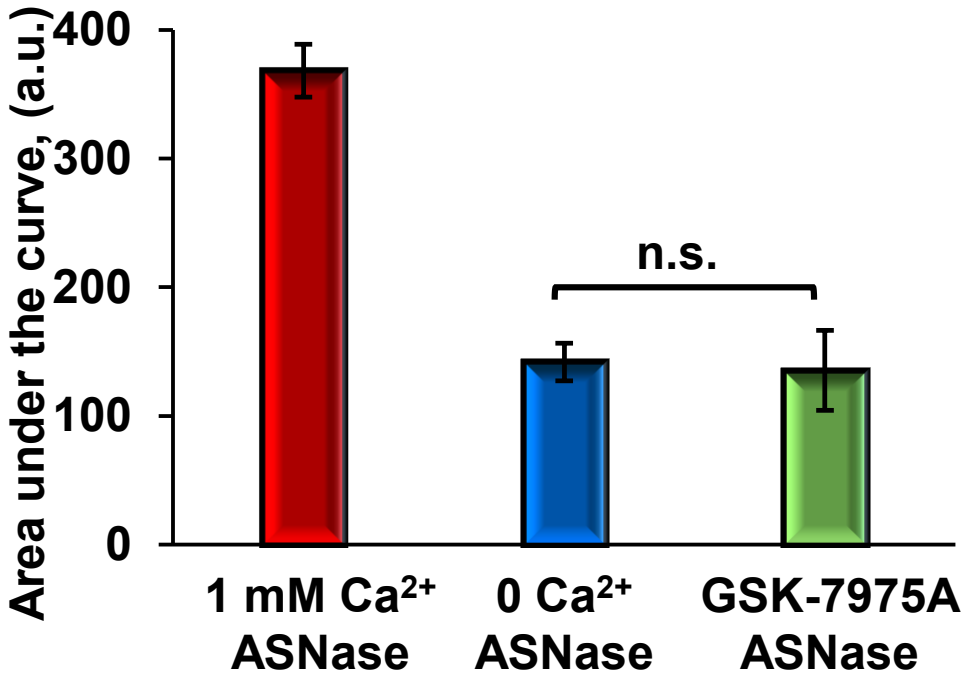

Figure 3.13 Comparison of asparaginase-elicited $[Ca^{2+}]_i$ response among presence or absence of external Ca^{2+} or CRAC blockade. (Modified from *Peng S et al, Philos Trans R Soc Lond B Biol Sci. 2016*) (313)

Comparison of the integrated Ca^{2+} signals ('area under the curve' from start of the Ca^{2+} signal until 30 min later), the bar chart shows that in the absence of external Ca^{2+} (n = 28) or in the presence of 1 mM external Ca^{2+} with the addition of the CRAC blocker GSK-7975A (n = 32) significantly (p < 0.0001 in both cases) reduced the responses to asparaginase (200 IU/ml) as compared to control in the presence of 1mM Ca^{2+} (n = 55; Figure 3.4). Bars represent mean ± SEM.

It is clear that excessive store-operated Ca^{2+} entry via CRAC channels is crucial for pathological Ca^{2+} signalling generation in pancreatic acinar cells, which leads to cell death (136,194,240,372). In the recent studies of store-operated Ca^{2+} influx, it has been shown that inhibition of Ca^{2+} entry into pancreatic acinar cells induced by non-oxidative product of combination of alcohol and fatty acids (fatty acid ethyl ester, FAEE), or bile acids could effectively protect against their pathological effects by the CRAC channel blocker GSK-7975A (312,354). We have therefore decided to check the effect of inhibition of Ca^{2+} entry channels by CRAC blocker (GSK-7975A, 10 μM) on the asparaginase- induced necrotic cell death pathway activation. Figure 3.14A shows representative images of some of the cells under the treatment protocols, together with the results of staining for PI. It is seen that asparaginase (200 IU/ml) elicited strong intracellular PI staining and that GSK-7975A provided protection against this. Pre-incubation of the CRAC channel inhibitor GSK-7975A (10 μM) (312,354) dramatically reduced the level of asparaginase-induced necrosis (5.8 ± 0.8% of cells) near to the control level (4.6 ± 0.8% of cells) (Figure 3.14B).

A

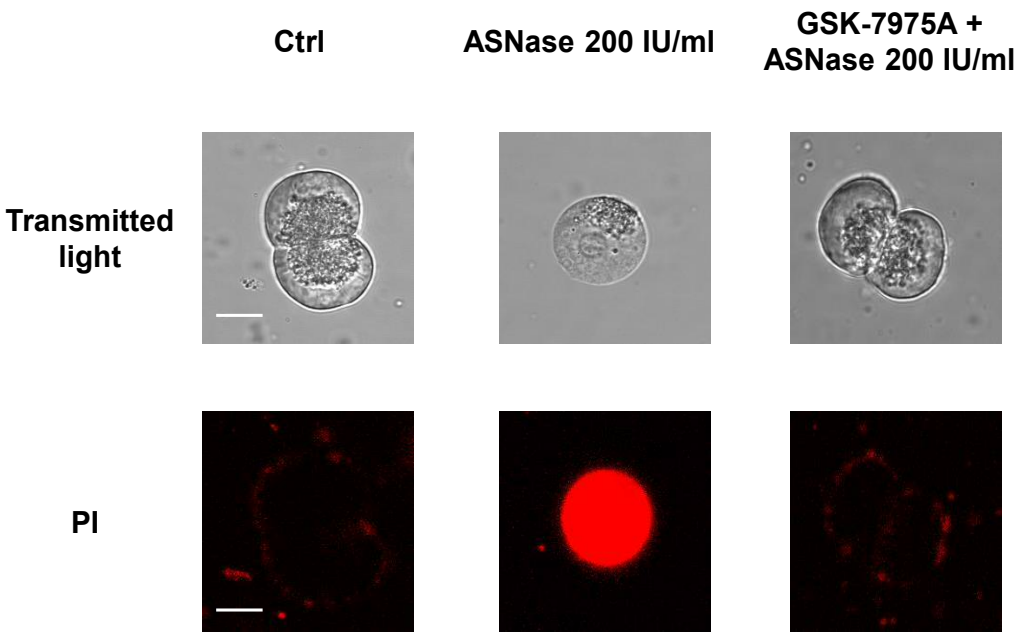
Ctrl
ASNase 200 IU/ml
GSK-7975A +
ASNase 200 IU/ml
Transmitted
light
PI

B

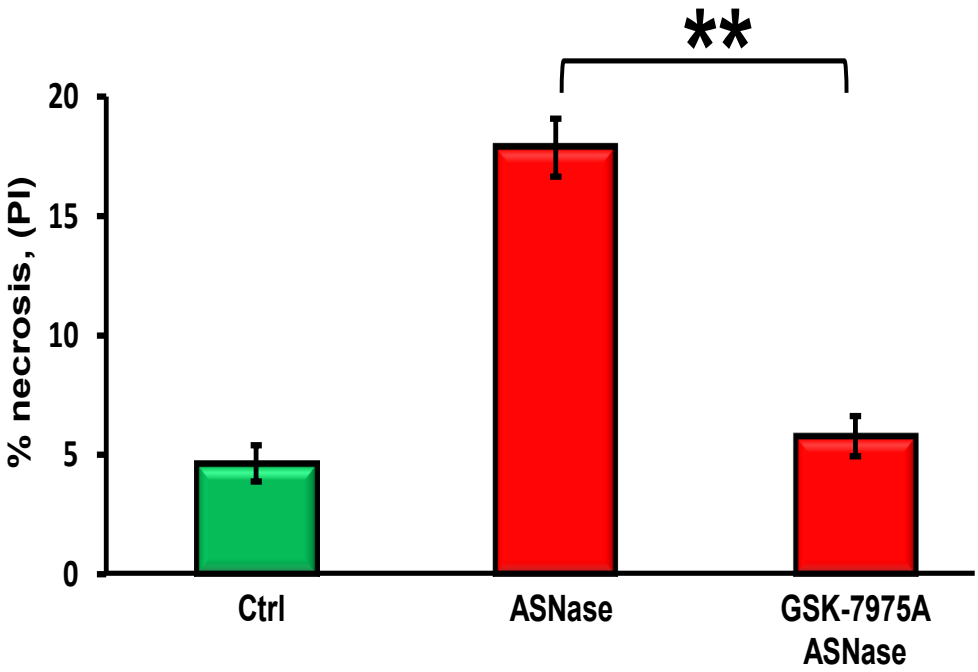
**
% necrosis, (PI)
20
15
10
5
0
Ctrl
ASNase
GSK-7975A
ASNase

Figure 3.14 Inhibition of CRAC channels by GSK-7975A dramatically reduces asparaginase-induced necrosis. (Modified from *Peng S et al, Philos Trans R Soc Lond B Biol Sci. 2016*) (313)

(A) Representative transmitted light images (upper row) and PI-stained fluorescence images (lower row; scale bar: 10 μm) of cells from the experiments shown in Figure 3.14B. (B) The CRAC channel inhibitor GSK-7975A (10 μM) essentially abolished asparaginase-induced necrosis to a level not significantly different from control ($p > 0.3$), while significantly ($p < 0.0001$, eight series, $n > 70$) lower than that caused by asparaginase (200 IU/ml) alone (17.8 ± 1.2% of cells).

Asparaginase-induced pathology depends on protease-activated receptor 2

As mentioned above, PAR2 is widely expressed in human and animal tissues, including the pancreas, lung, kidney, stomach, liver, colon, small intestine and immune and endothelial cells (329,337,373,374). PAR2 has previously been implicated in pain and inflammation (345,346) and contributions to gastrointestinal regulation in health and disease (375,376), including the pathology of AP (348–350). The activation of PAR family members is coupled to multiple heteromeric G proteins that lead to PLC activation and production of IP_3 and diacylglycerol, which can cause Ca^{2+} mobilization (317). Since the effect of asparaginase on Ca^{2+} signalling has been observed, we therefore tested the possibility that asparaginase could activate PAR2. Figure 3.15A,B shows the different concentrations (10 nM, 100 nM, 200 nM or 500 nM) of the potent PAR2 agonist AC-264613 (377) induced Ca^{2+} oscillations in pancreatic acinar cells. We then investigated the effect of the PAR2 blocker FSLLRY-NH_2 (378–381) on asparaginase-elicited $[Ca^{2+}]_i$ changes. As seen in Figure 3.16A, pre-incubation of FSLLRY-NH_2 (10 μM; n = 32) for 200 s before the addition of asparaginase significantly reduced the asparaginase-induced the sustained $[Ca^{2+}]_i$ elevation as well as $[Ca^{2+}]_i$ oscillations (n = 30, Figure 3.16B). Figure 3.16C and D show the mean values of all of the data from Figure3.16A and B. It is clear that PAR2 antagonist FSLLRY-NH_2 very markedly inhibits the $[Ca^{2+}]_i$ elevation ($p < 0.0001$) and oscillations ($p < 0.001$) normally evoked by 200 IU/ml asparaginase. Due to the effect of FSLLRY-NH_2 markedly inhibits sustained global $[Ca^{2+}]_i$ elevation evoked by asparaginase, thereby, we tested FSLLRY-NH_2 on necrotic death assay and we found that the PAR2 inhibitor FSLLRY-NH_2 (10 μM) significantly reduced the level of asparaginase-induced necrosis (6 ± 0.5% of cells) close to the control level (3.3 ± 0.2% of cells, $p < 0.0001$; Figure 3.16E).

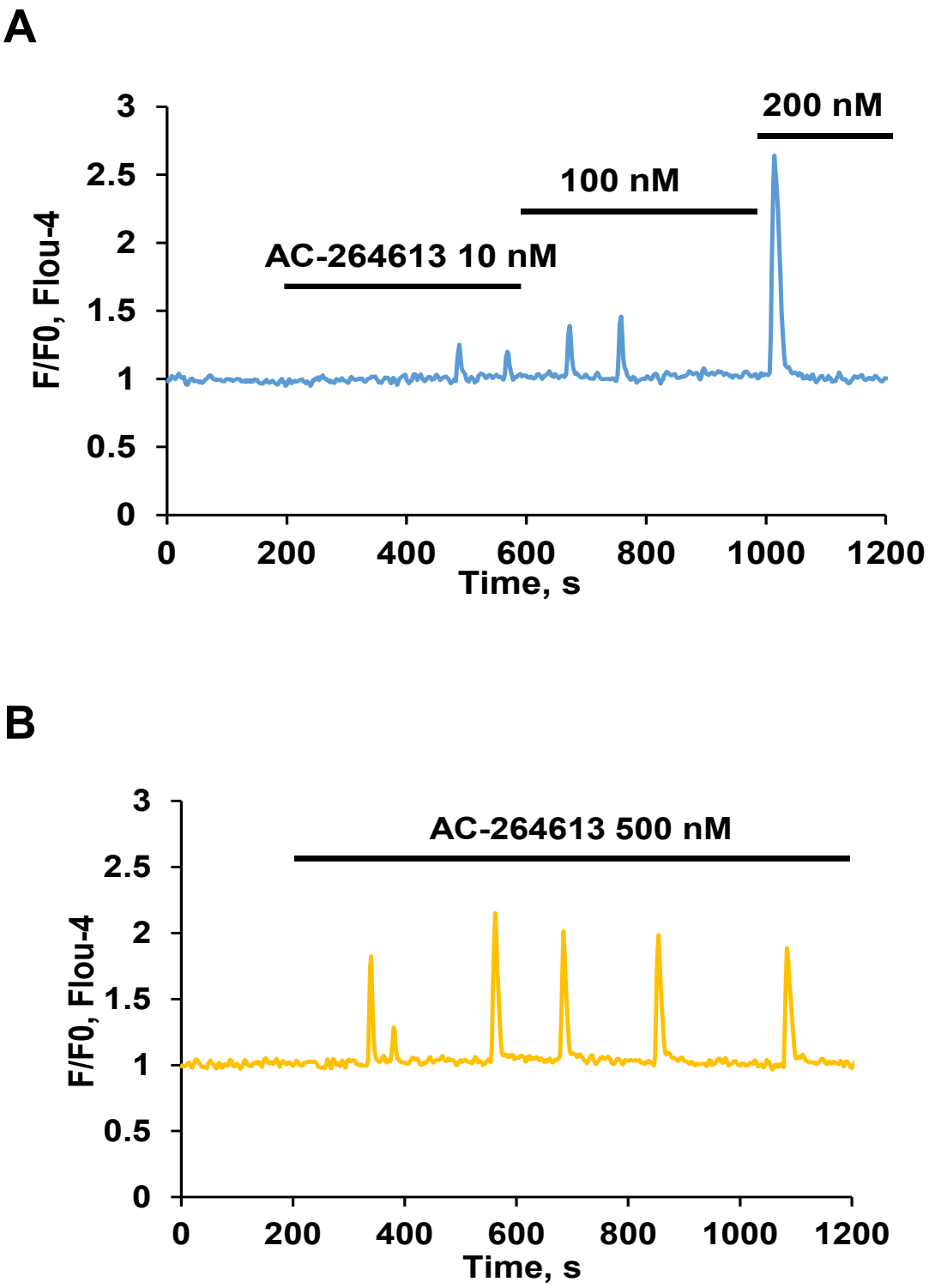

Figure 3.15 PAR2 agonist AC-264613-elicited $[Ca^{2+}]_i$ response. (Modified from *Peng S et al, Philos Trans R Soc Lond B Biol Sci. 2016*) (313)

(A) Representative trace shows AC-264613 (10 nM, 100 nM or 200 nM) induces $[Ca^{2+}]_i$ changes (n = 6). (B) AC-264613 (500 nM) elicits repetitive Ca^{2+} spike (n = 4).

A

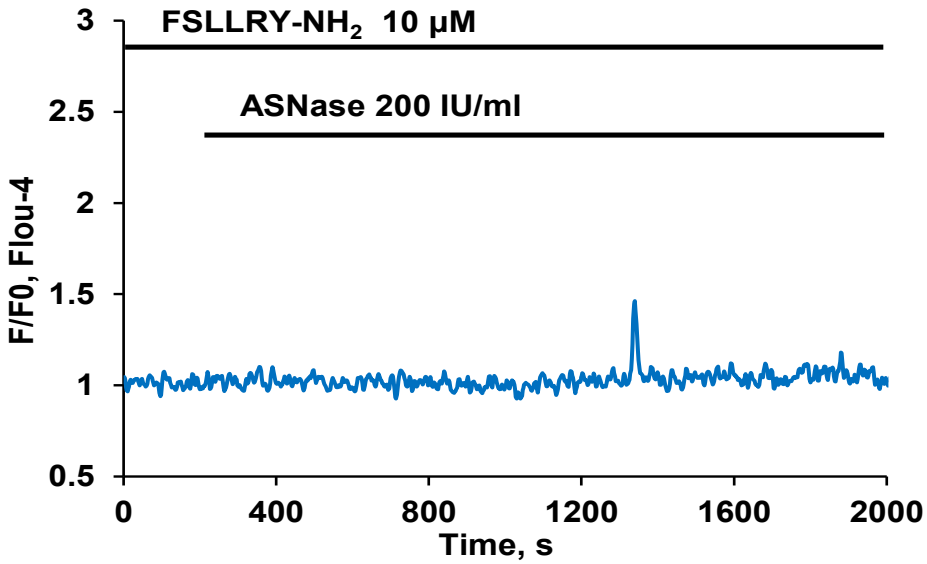
FSLLRY-NH2 10 μM
ASNase 200 IU/ml
F/F0, Flou-4
3
2.5
2
1.5
1
0.5
0
400
800
1200
1600
2000
Time, s

B

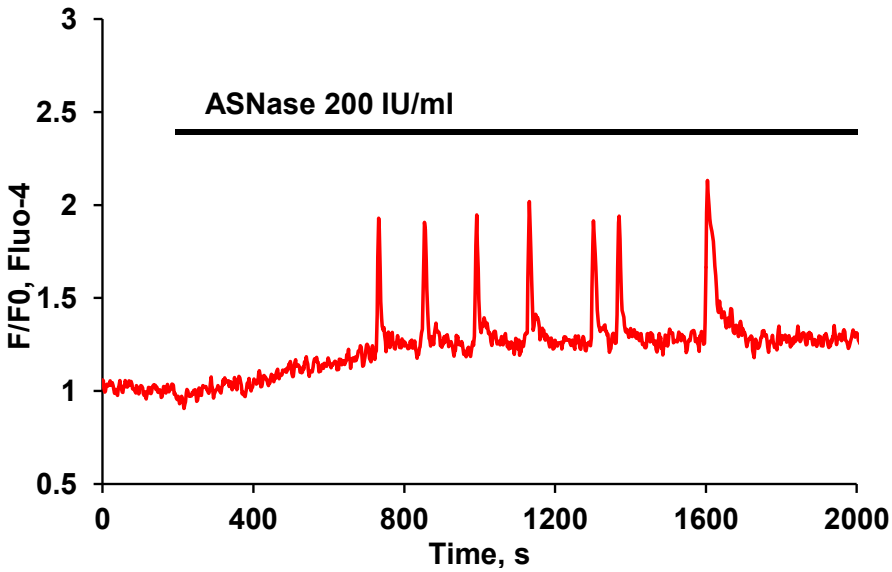
ASNase 200 IU/ml
F/F0, Fluo-4
3
2.5
2
1.5
1
0.5
0
400
800
1200
1600
2000
Time, s

C

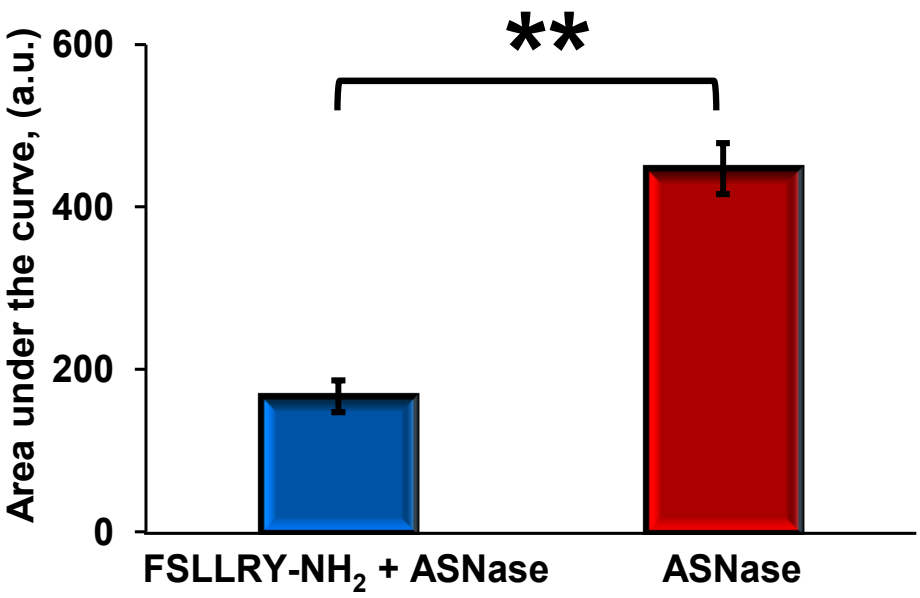
**
600
400
200
0
Area under the curve, (a.u.)
FSLLRY-NH2 + ASNase
ASNase

D

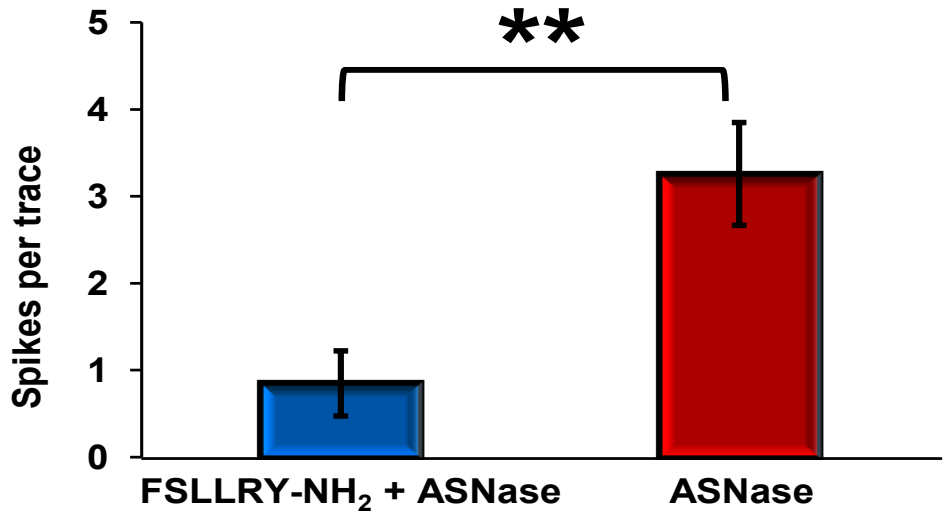
**
5
4
3
2
1
0
Spikes per trace
FSLLRY-NH2 + ASNase
ASNase

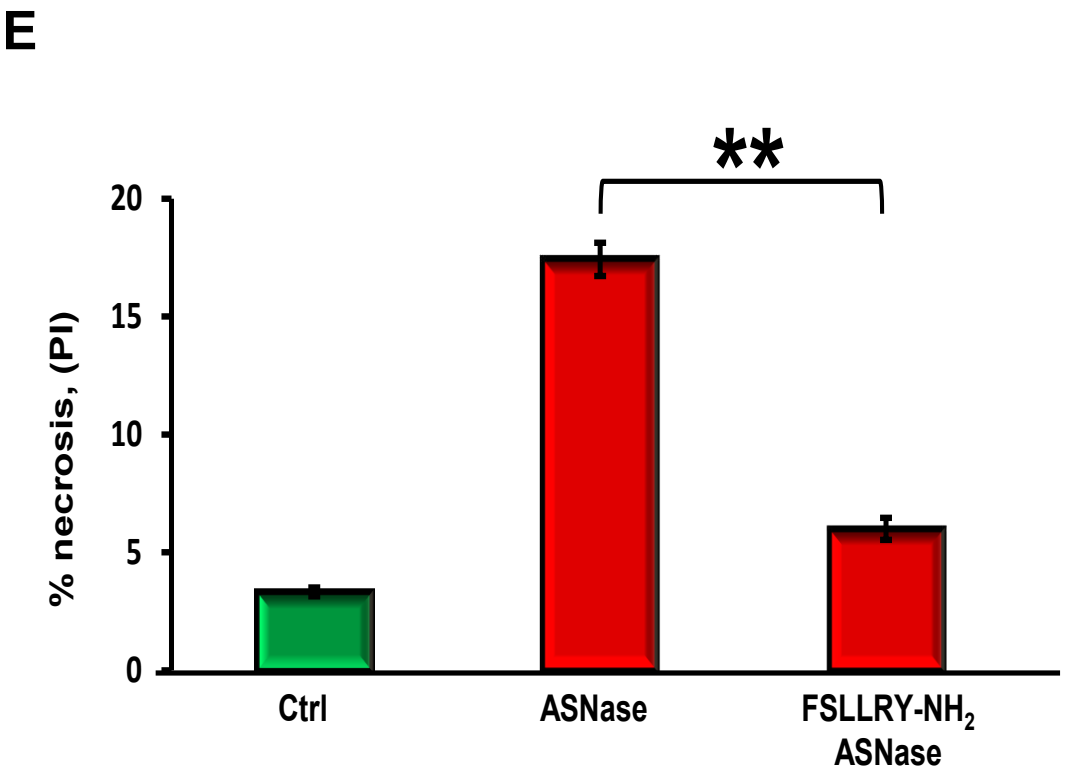

Figure 3.16 PAR2 antagonist FSLLRY-NH_2 significantly inhibited asparaginase-induced Ca^{2+} signals and necrosis. (Modified from *Peng S et al, Philos Trans R Soc Lond B Biol Sci. 2016*) (313)

The representative trace shows the asparaginase-induced Ca^{2+} signals (n = 30; Figure 3.16B) were eliminated by the PAR2 inhibitor FSLLRY-NH_2 (10 μM, n = 32; Figure 3.16A). (C) The bar chart shows average area under the traces depicted in Figure 3.16A and B between 200 s and 2000 s of the recorded responses. (p < 0.0001). (D) The bar chart shows FSLLRY-NH_2 reduces repetitive Ca^{2+} spike evoked by asparaginase (p < 0.001). Data presented as mean ± SEM. (E) The PAR2 inhibitor FSLLRY-NH_2 (10 μM) significantly blocked the asparaginase-induced necrosis (p < 0.0001; four series of experiments with n > 150 cells in each sample).

We tested whether asparaginase-elicited $[Ca^{2+}]_i$ response via muscarinic receptor (50,53). Pancreatic acinar cells were stimulated by ACh (50 nM) and then washed by NaHepes buffer. After that atropine (1 μM) (382–384) was applied to the acinar cells and incubated for 100 s and then re-exposed to ACh (50 nM). Atropine is the competitive nonselective antagonist at central and peripheral muscarinic acetylcholine receptors (385). There was not Ca^{2+} spikes developed after atropine application, which shows completely blockade of muscarinic receptors. Additional of asparaginase (200 IU/ml) after ACh washed out again, as shown in Figure 3.17A, evoked sustained $[Ca^{2+}]_i$ elevation response with Ca^{2+} oscillations (n = 22). Finally, CCK (50 pM) was applied into the acinar cells, which caused Ca^{2+} spike. Comparison of area under the response of asparaginase (n = 30, Figure 3.16B), inhibition of muscarinic receptors by atropine does not change asparaginase-induced $[Ca^{2+}]_i$ changes (Figure 3.17B; $p > 0.15$).

We also tested the effect of PAR2 antagonist FSLLRY-NH_2 on muscarinic receptor and we found that pre-incubation of FSLLRY-NH_2 (n = 36, Figure 3.18B) did not affect physiological concentration of ACh (50 nM)-induced $[Ca^{2+}]_i$ signals (n = 18, Figure 3.18A) in pancreatic acinar cells (Figure 3.18C; $p > 0.2$).

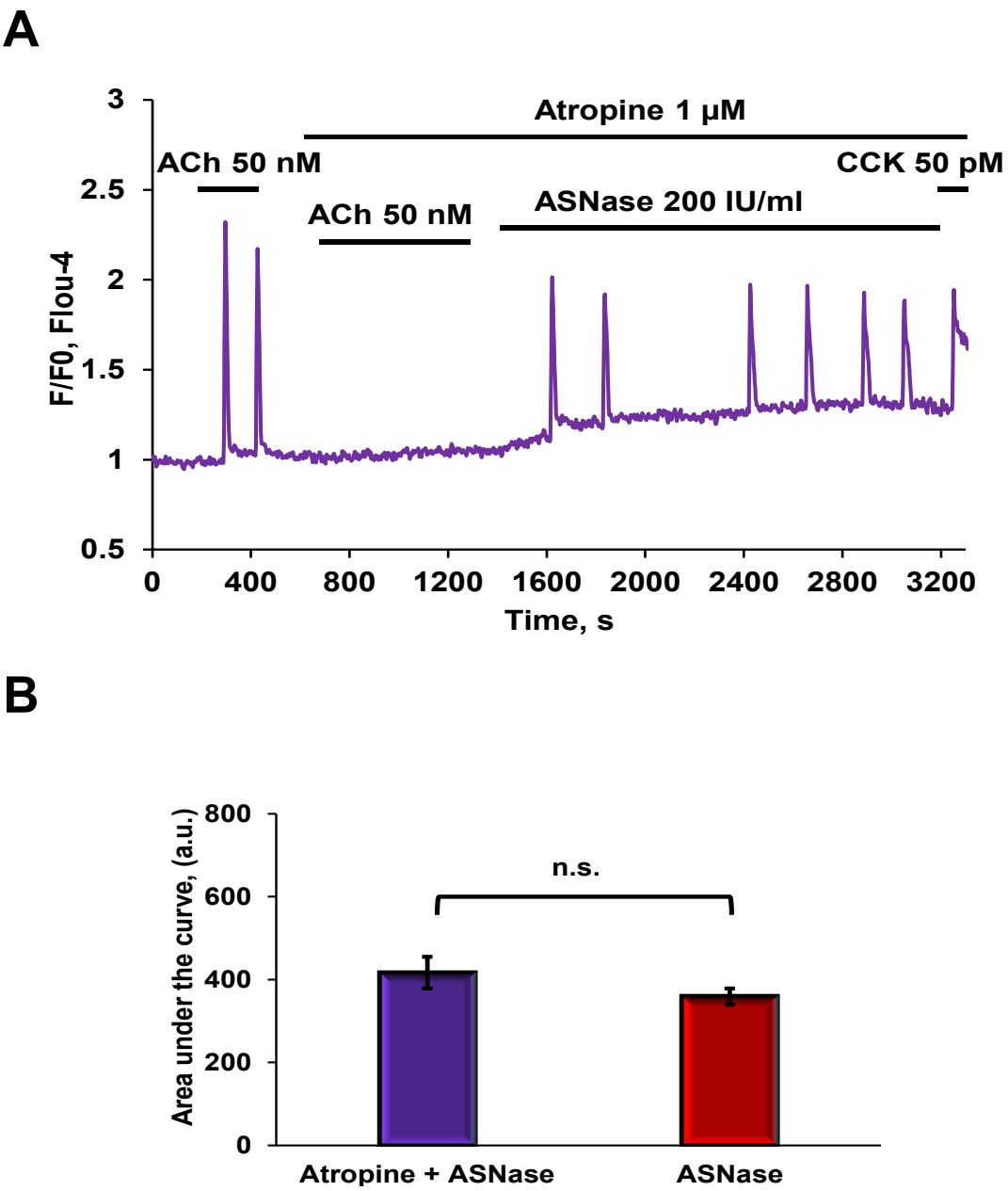

Figure 3.17 Asparaginase-induced Ca^{2+} signals do not depend on muscarinic receptor.

Nonselective muscarinic acetylcholine receptors antagonist atropine does not block asparaginase-induced $[Ca^{2+}]_i$ response (A; n = 22). The bar chart (C) shows comparison of the integrated Ca^{2+} signals elevation above the baseline (area under the curve) shown in A and Figure 3.16B (n = 30) recorded during the 30 min of asparaginase application. The mean values (± SEM) are not significantly different (p > 0.15).

A

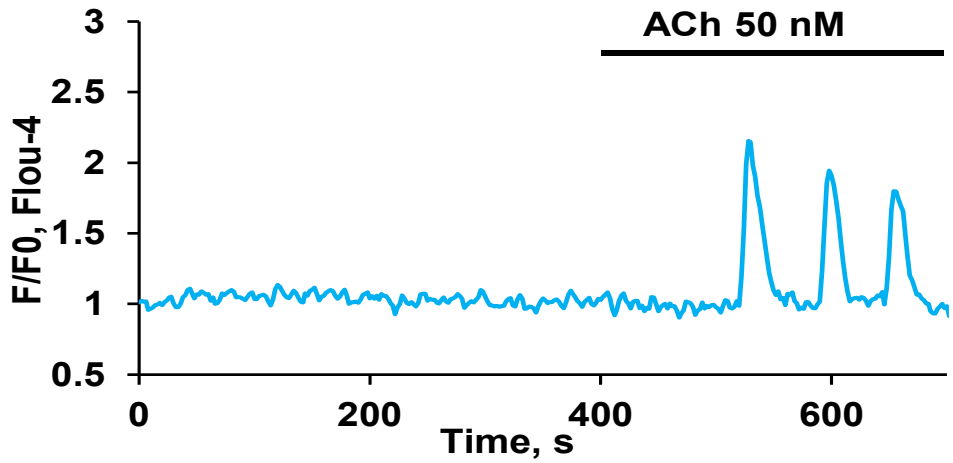
ACh 50 nM
F/F0, Flou-4
3
2.5
2
1.5
1
0.5
0
200
400
600
Time, s

B

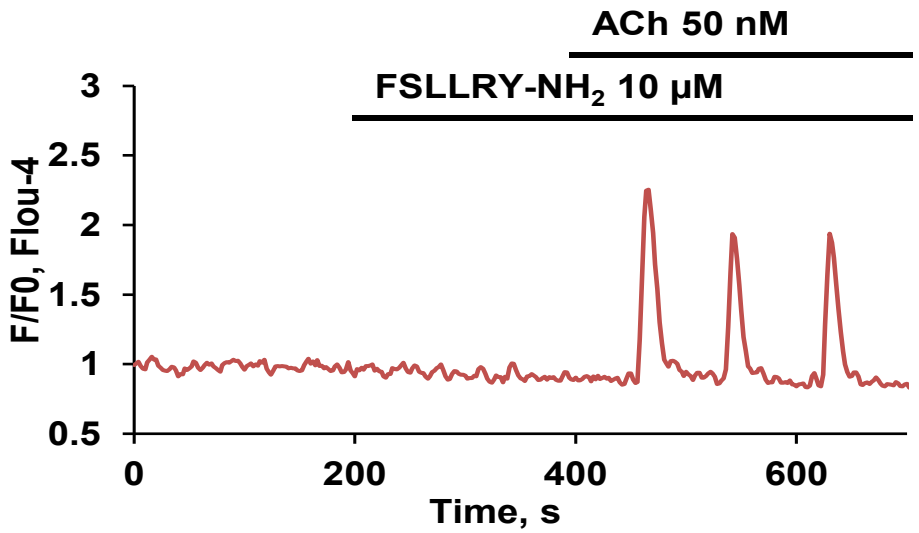
ACh 50 nM
FSLLRY-NH2 10 μM
F/F0, Flou-4
3
2.5
2
1.5
1
0.5
0
200
400
600
Time, s

C

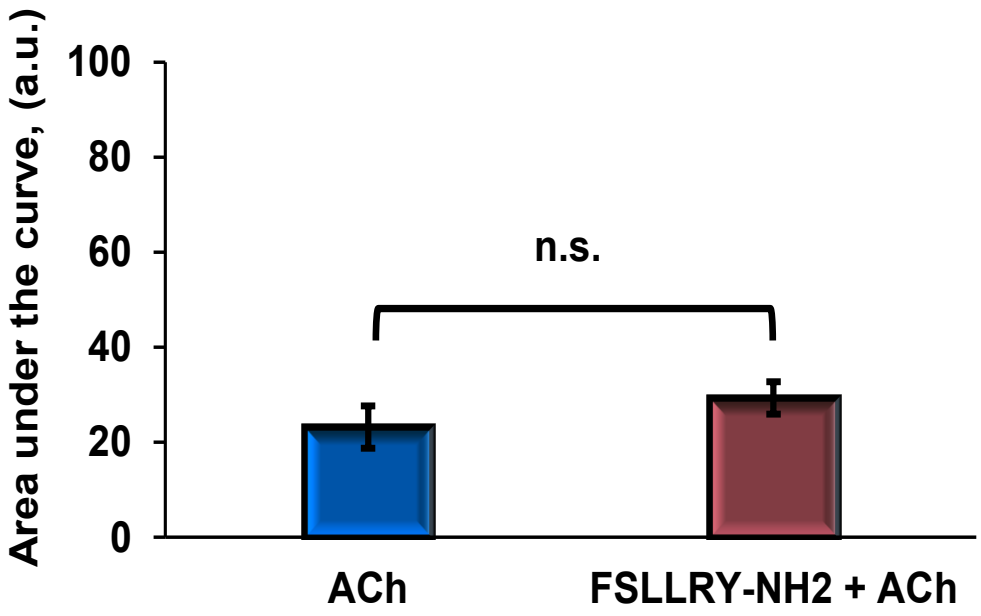

Figure 3.18 PAR2 antagonist FSLLRY-NH_2 does not affect ACh-induced Ca^{2+} signals.

(A) Typical trace shows ACh-induced Ca^{2+} signalling in pancreatic acinar cell (n = 18). (B) Pre-incubation of PAR2 antagonist FSLLRY-NH_2 does not block ACh-induced Ca^{2+} oscillations (n = 36). (C) The bar chart shows comparison of the integrated Ca^{2+} signals elevation above the baseline (area under the curve) shown in Figure A and B recorded during the 5 min of ACh application (p > 0.2). Data presented as mean ± SEM.

Ca^{2+} entry and extrusion mechanisms are affected by asparaginase

To study Ca^{2+} movements in more detail, a specific protocol routinely used to assess Ca^{2+} entry and extrusion have been applied. Our standard protocol for store-operated Ca^{2+} entry investigations consisted of first emptying the ER store of Ca^{2+} by applying the specific ER Ca^{2+} pump blocker cyclopiazonic acid (CPA) in a nominally Ca^{2+}-free solution. This caused a transient rise in $[Ca^{2+}]_i$ (Figure 3.19A). After $[Ca^{2+}]_i$ had returned to near its normal resting level, Ca^{2+} (2 mM) was added to the external solution for a short period and then removed. Additional of external Ca^{2+} resulted in a substantial rise in $[Ca^{2+}]_i$, which was sustained as long as Ca^{2+} was present outside the cell. In the presence of asparaginase (200 IU/ml), the Ca^{2+} entry following external Ca^{2+} admission was significantly increased (Figure 3.19A), assessed by both amplitude of the $[Ca^{2+}]_i$ change (Figure 3.19B) and the rate of $[Ca^{2+}]_i$ increase (half-time of the decrease, Figure 3.19C). However, the most obvious change seen in Figure 3.19A is quantitatively the most important effect of asparaginase which was to attenuate Ca^{2+} signals after removal of external Ca^{2+}. The half-time of $[Ca^{2+}]_i$ recovery of the cells treated with asparaginase (200 IU/ml) was more than three times longer than in the control cells (Figure 3.19D).

A

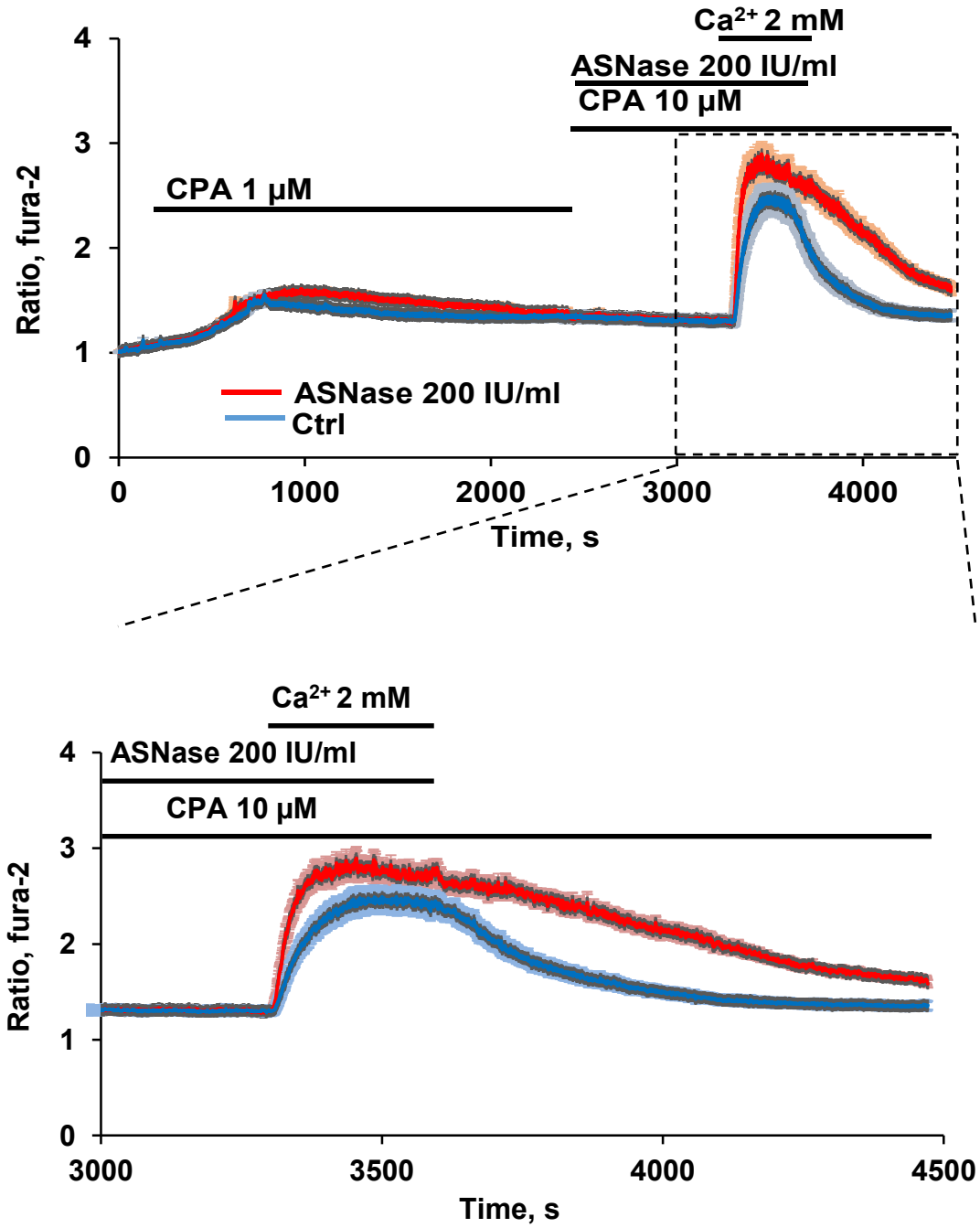
Ca2+ 2 mM
ASNase 200 IU/ml
CPA 10 µM
CPA 1 µM
ASNase 200 IU/ml
Ctrl
Ratio, fura-2
Time, s
0
1000
2000
3000
4000
0
1
2
3
4
Ca2+ 2 mM
ASNase 200 IU/ml
CPA 10 µM
Ratio, fura-2
Time, s
3000
3500
4000
4500

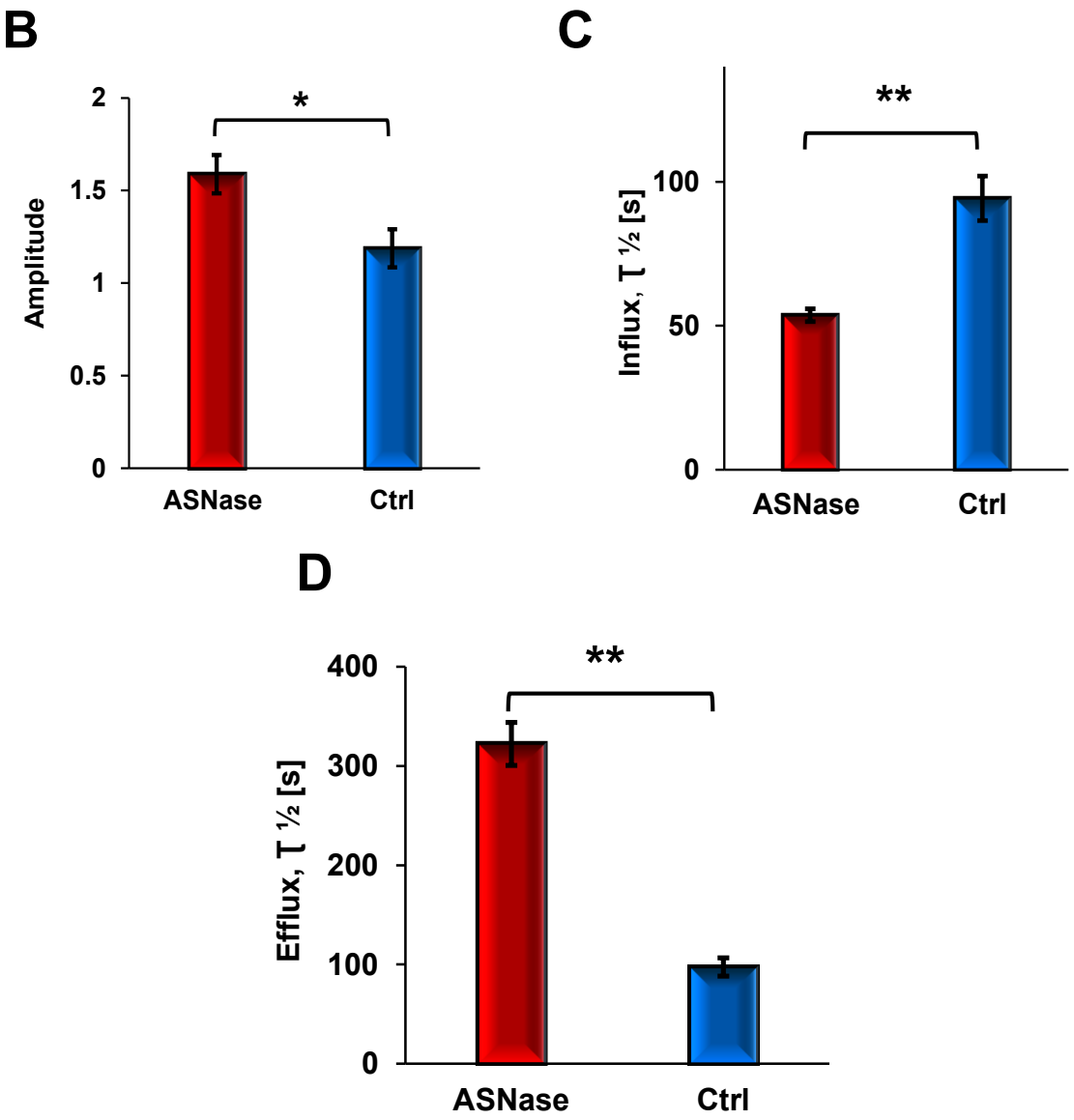

Figure 3.19 Asparaginase accelerates Ca^{2+} entry and substantially slows down Ca^{2+} extrusion. (Modified from *Peng S et al, Philos Trans R Soc Lond B Biol Sci. 2016*) (313)

(A) In the absence of external Ca^{2+}, CPA, a specific inhibitor of the Ca^{2+} pump in the ER membrane, causes a modest and largely transient $[Ca^{2+}]_i$ rise. When subsequently 2 mM Ca^{2+} is added to the external solution, there is a marked rise in $[Ca^{2+}]_i$, which then declines after removal of external Ca^{2+}. In the presence of asparaginase (red averaged trace, n = 32), the amplitude (B) and the rate of rise of $[Ca^{2+}]_i$ (C) are somewhat increased ($p < 0.05$ and $p < 0.0001$, respectively) when compared with control (A, blue averaged trace, n = 34). The extrusion of Ca^{2+} by the plasma membrane Ca^{2+} pumps, observed as the decline in $[Ca^{2+}]_i$ following removal of external Ca^{2+}, is very markedly and significantly ($p < 0.0001$) reduced in the presence of asparaginase (A,D).

Discussion

The findings presented in this chapter provide the first mechanistic insights into the process by which asparaginase treatment of ALL may cause acute pancreatitis. These insights also provide the first pointers to rational therapies that may prevent the currently necessary cessation of asparaginase treatment in cases of severe pancreatitis. Our data indicate that the asparaginase-induced pathological effects have much in common with those elicited by the 'classical' pancreatitis-inducing agents such as alcohol and fatty acids and, particularly, combinations of alcohol and fatty acids as well as bile acids (236,386,387). Ca^{2+} overloading, due to excessive intracellular Ca^{2+} release followed by excessive Ca^{2+} entry are central in all cases.

CRAC channels seem to be the most accessible therapeutic target for AAP (312,354,371,372,388). We have now shown that the asparaginase-induced Ca^{2+} elevations depend on CRAC-mediated Ca^{2+} entry and, therefore, are strongly inhibited by the CRAC channel inhibitor GSK-7975A (Figure 3.12 and 13). Consequently, asparaginase-induced necrosis can also be dramatically reduced to near control levels by GSK-7975A (Figure 3.14). Given the previously documented protective effects of Ca^{2+} entry channel inhibition against alcohol-related pancreatic pathology in isolated cell clusters, which including pancreatic acinar cells and stellate cells (389,390), and the more recent confirmation of its effectiveness *in vivo* in three different mouse pancreatitis models (354), our new data suggest very strongly that this therapeutic approach should also be successful against asparaginase-induced pancreatitis.

Interestingly, the asparaginase-induced pathological effects do not depend on the presence of the substrate of the enzyme, namely asparagine (Figure 3.5). Asparaginase induces $[Ca^{2+}]_i$ elevations, and thereby its pathological effects,

through protease activated receptor 2 (PAR2) rather than muscarinic receptor (Figure 3.17). PAR2 has previously been implicated in acute pancreatitis, although its exact role is still debatable (347–350). Blocking PAR2 in our experiments inhibited both the pathological $[Ca^{2+}]_i$ elevations and the asparaginase-induced necrosis (Figure 3.16), suggesting that PAR2 inhibitors in addition to, or in combination with, CRAC channel inhibitors (312,354,372) and calmodulin activators (119,391) could be a useful tool to supplement asparaginase ALL treatment in AAP cases.

Both Ca^{2+} entry and extrusion are significantly affected by asparaginase, leading to formation of the pathological elevated $[Ca^{2+}]_i$ plateau and this sustained elevation of $[Ca^{2+}]_i$ is somehow responsible for the necrosis. The demonstrated reduction of the intensity of Ca^{2+} extrusion (Figure 3.19) is clearly a key element and the simplest postulation and explanation for this is the reduction in the intracellular ATP level limiting the energy supply to the Ca^{2+} ATPase in the plasma membrane. In order to investigate this point, further experiments were undertaken using fluorescent probers for mitochondrial activity and ATP dynamics by confocal microscopy and these are described in next chapter.

Chapter 4

Asparaginase affects mitochondrial function and glucose metabolism in pancreatic acinar cells

Overview of mitochondrial functions

It has been universally acknowledged that mitochondria are important for cellular functions (392). The complex transport pathways play an essential role in mitochondrial function as well as cell physiology (393). Many digestive proenzymes are synthesized in the pancreatic acinar cells. These inactive enzymes are packaged into secretory (zymogen) granules and secreted by exocytosis upon the action of the neurotransmitter ACh (52,394) or the circulation hormone CCK (395). These secretagogues mobilize Ca^{2+} from internal stores and thus generate the physiological Ca^{2+} signalling that regulate exocytosis, which requires Ca^{2+}, Mg^{2+} and ATP (182,396). Therefore, Ca^{2+} homeostasis and energy demand made the functions of pancreatic acinar cells are highly dependent on the mitochondria. As a consequence, the pancreatic acinar cells have evolved in such a way that the mitochondria are distributed in very specific positions in the cells and play different roles at these different sites. Functionally, there are three distinct sets of mitochondria in pancreatic acinar cells (Figure 4.1) (71,109). The highest density of mitochondria was found on the border between the granular and baso-lateral regions. This so called mitochondrial belt is often referred to as the peri-granular mitochondria. The second group, called peripheral or sub-plasmalemmal, is located very close to the basolateral plasma membrane. Another set surrounds the nucleus, and these mitochondria are therefore named as perinuclear.

As mentioned above, mitochondria are mainly situated on the border between the apical granular region and the baso-lateral part of the cells (71). This special arrangement implicates a significant physiological role in pancreatic acinar cells. Since it was already known that physiological Ca^{2+} signals were initiated in the apical pole and mostly confined to the granular region (50,52,397), it seemed likely that the peri-granular mitochondrial belt could

confine physiological Ca^{2+} signals to the apical region as a Ca^{2+} buffer barrier. This hypothesis was demonstrated by Tinel et al (71). They observed that the IP_3-indcued physiological Ca^{2+} signal pattern consisting of repetitive local Ca^{2+} spikes was transformed into a global sustained $[Ca^{2+}]_i$ elevation by application of the ionophore CCCP, which indicated that Ca^{2+} released from the ER in the apical granular pole is rapidly taken into the peri-granular mitochondria and only released very slowly. Therefore, mitochondria belt by means of buffering Ca^{2+} to prevent the cytosolic Ca^{2+} wave spreading from apical granular pole into the basal region. The mitochondrial Ca^{2+} uniporter (MCU) (187) is mainly responsible for soaking up Ca^{2+} released from the ER and the Na^{+}/Ca^{2+} exchangers (398) extrude Ca^{2+} slowly from mitochondrial to the cytosol (399). Hence, this specific function of mitochondria on regulating Ca^{2+} signals in pancreatic acinar cells that enable the peri-granular mitochondrial belt to buffer Ca^{2+} and thereby confining the cytosolic Ca^{2+} spikes to the apical granular area (Figure 4.2).

The peripheral (sub-plasmalemmal) mitochondria are distributed just below the basolateral plasma membrane (Figure 4.1). Ca^{2+} uptake specifically into peripheral mitochondria during store-operated Ca^{2+} entry is essential for the function of peripheral mitochondria, that is, Ca^{2+} entry across the basal membrane lead to local mitochondrial Ca^{2+} uptake stimulating local ATP production (Figure 4.2). It is not clear that a major part of the store-operated Ca^{2+} entry is directed into the mitochondria or whether most of it goes directly into the ER. However, it has been shown that Ca^{2+} influx into the acinar cells through store-operated calcium channels (SOCs) in the basal membrane is immediately taken up into the ER by Ca^{2+} pumps (66). Moreover, electron microscopical images of the region just below the baso-lateral plasma membrane show ER is in closer contact with the surface membrane than the mitochondria (147). This indicates the most likely Ca^{2+} entry points and supports the point of view that Ca^{2+} is immediately taken up into the ER during

store-operated calcium entry. Nevertheless, Ca^{2+} uptake into the peripheral mitochondria are functionally important for ATP generation which is needed locally to fuel the ER Ca^{2+} pumps (Figure 4.2). There are also increasing evidences indicating that store-operated Ca^{2+} entry depends on the mitochondrial function (400–402).

The perinuclear mitochondria (Figure 4.1) have a lower density than the peri-granular mitochondria or peripheral mitochondria. The function of the perinuclear mitochondria is most likely to serve as a protection barrier for the nucleus in pancreatic acinar cells (Figure 4.2). In this scenario, exocytotic secretion-coupled Ca^{2+} signalling does not necessarily have to enter the nucleus. This is important because the nuclear pore complexes scarcely resist to Ca^{2+} flow (403,404). Although the function of perinuclear mitochondria remains elusive, it cannot be denied that the perinuclear mitochondria are helpful and effectively a special Ca^{2+} microdomain generation in the nucleus as a Ca^{2+} buffer barrier (109,405).

This chapter is aim to explore the effects of asparaginase on mitochondrial function and determine potential ways to intervene asparaginase-associated ATP depletion and mitochondrial Ca^{2+} overload in pancreatic acinar cells.

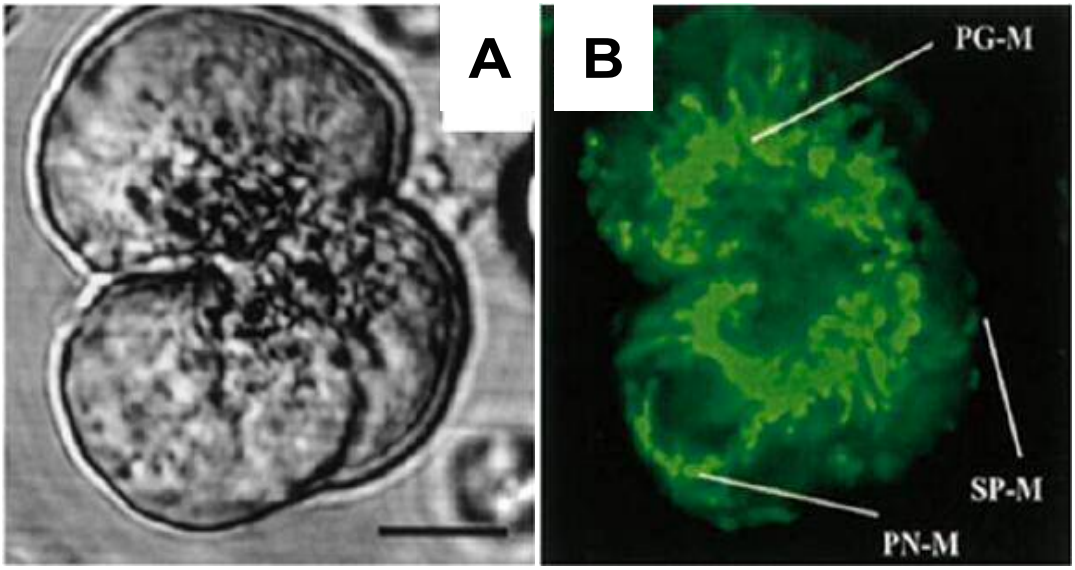

Figure 4.1 Distribution of mitochondria in pancreatic acinar cells.

Typical confocal images show a transmitted light micrograph (A) and a fluorescence image (B; mitotracker green), respectively, illustrating the distribution of all the mitochondria in an isolated triplet of pancreatic acinar cells [PG-M: peri-granular mitochondria; SP-M: sub-plasmalemmal (peripheral) mitochondria (very weakly represented in this image); PN-M: perinuclear mitochondria]. Scale bar is 10 μm. (Modified from *Johnson PR et al, Cell Tissue Res. 2003*) (181)

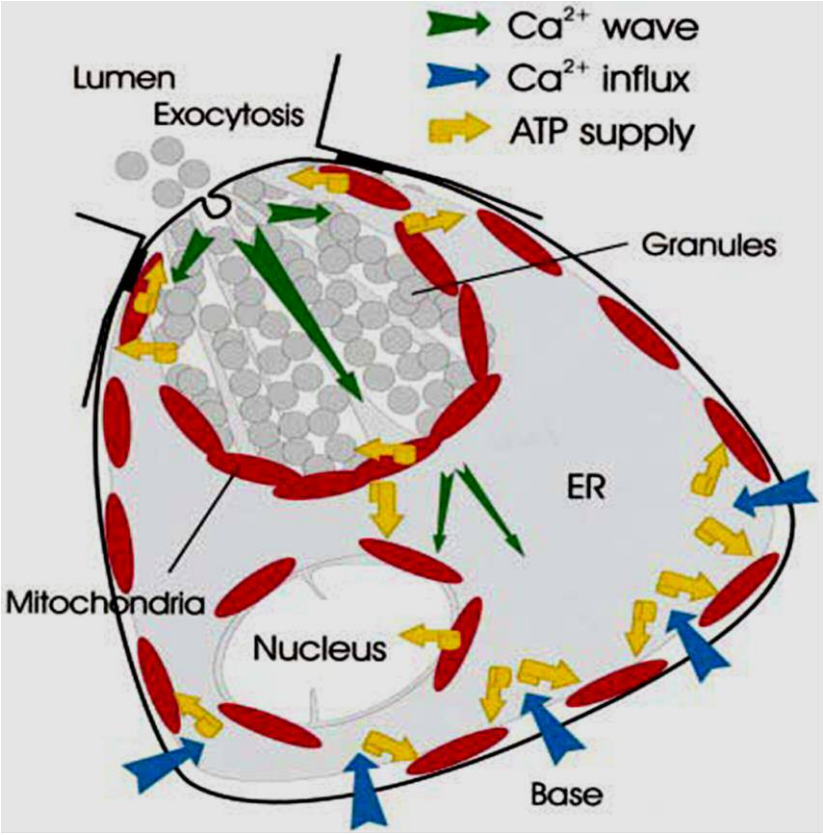

Figure 4.2 The location and function of three different groups of mitochondria in pancreatic acinar cell.

Schematic image illustrate three distinct sets of mitochondria in pancreatic acinar cells: the peri-granular mitochondria, the peripheral (sub-plasmalemmal) mitochondria and the perinuclear mitochondria. For the details of Ca^{2+} transport and ATP supply see the full description in text. (*Adapted from Park MK et al, EMBO J. 2001*) (109)

Asparaginase depletes intracellular adenosine triphosphate in pancreatic acinar cell

Ca^{2+} extrusion is an energy-demanding process, in which PMCA removes Ca^{2+} by the hydrolysis of adenosine triphosphate (ATP) (406). It has previously been found that Ca^{2+} extrusion was abnormal in pancreatic acinar cell pathologies as a result of disruption of mitochondrial metabolism and, therefore, reduction of ATP levels (311,407,408). To assess intracellular ATP concentration changes in pancreatic acinar cells, indirect measurements by using Magnesium Green (MgGreen) fluorescence (Figure 4.3A) was conducted in our study. Because both ATP and Mg^{2+} are mutually and strongly buffered in the cytosol, most of the intracellular ATP forms biologically functional unit as Mg-ATP complexes to compose (409). Hence, a reduction of the ATP concentration will increase the fluorescence intensity of MgGreen owing to the inevitable increase of $[Mg^{2+}]_i$ (242,410,411). Using the MgGreen technique, asparaginase (200 IU/ml) induced a substantial reduction of intracellular ATP levels superseded only by the full ATP depletion caused by a mixture of the protonophore CCCP, oligomycin and iodoacetate (n = 39; Figure 4.3B) (311) . Because Ca^{2+} entry was contributed to Ca^{2+} overload and the cytoplasmic and mitochondrial effects induced by asparaginase, we therefore tested if inhibition of Ca^{2+} entry channels (312,354,371) could affect the ATP loss evoked by asparaginase. Blocking Ca^{2+} entry by GSK-7975A (10 μM) markedly reduced the asparaginase-induced ATP depletion (n = 21, $p < 0.0001$; Figure 4.3C and E). It has been previously reported that ethyl pyruvate, aliphatic ester derived from pyruvic acid (412), had protective effect in the *in vivo* biliary pancreatitis mode and attenuated the severe AP induced by sodium taurocholate in rats (413–415). We next wanted to investigate whether this was due to preservation of ATP, and therefore tested the effect of pyruvate on asparaginase-induced ATP loss. Additional of pyruvate (1 mM) in the external solution resulted in the asparaginase-induced ATP loss substantially

reduced as compared with control experiments (n = 8, $p < 0.0001$; Figure 4.3D and E).

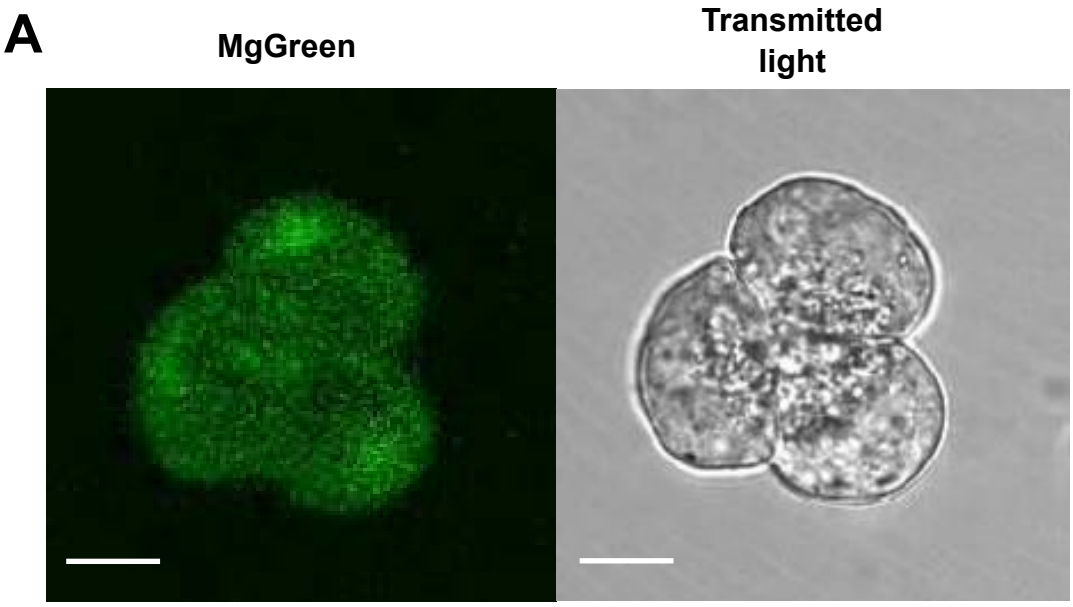

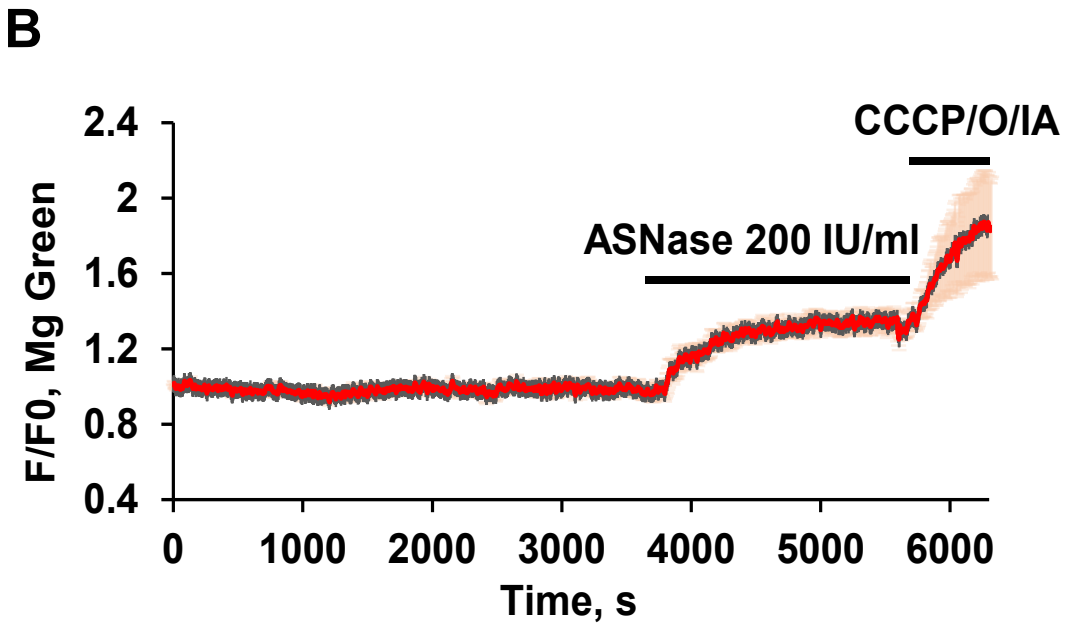

C

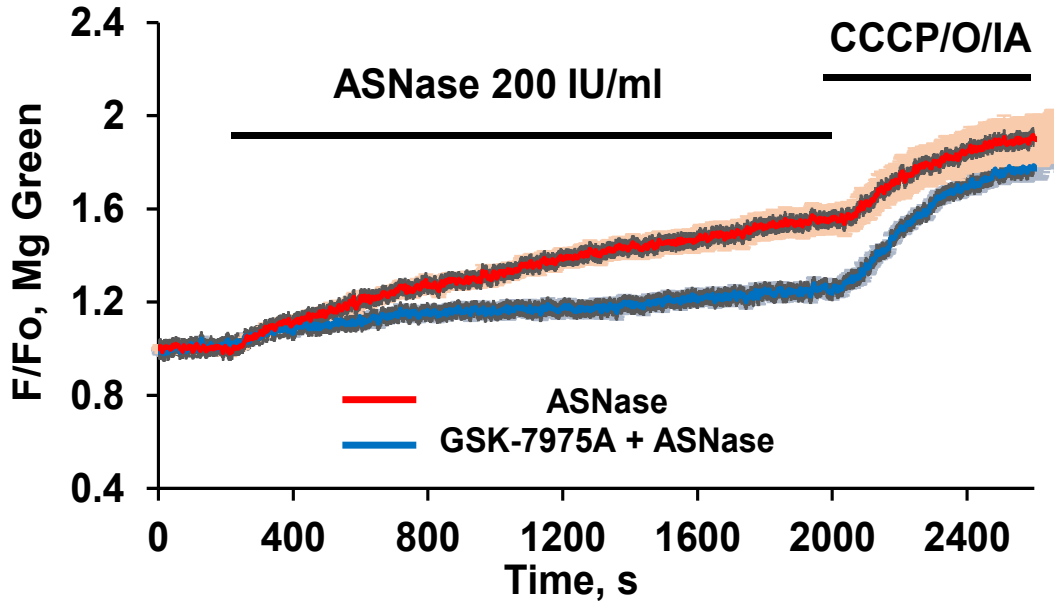
2.4
2
1.6
1.2
0.8
0.4
F/Fo, Mg Green
ASNase 200 IU/ml
CCCP/O/IA
ASNase
GSK-7975A + ASNase
0
400
800
1200
1600
2000
2400
Time, s

D

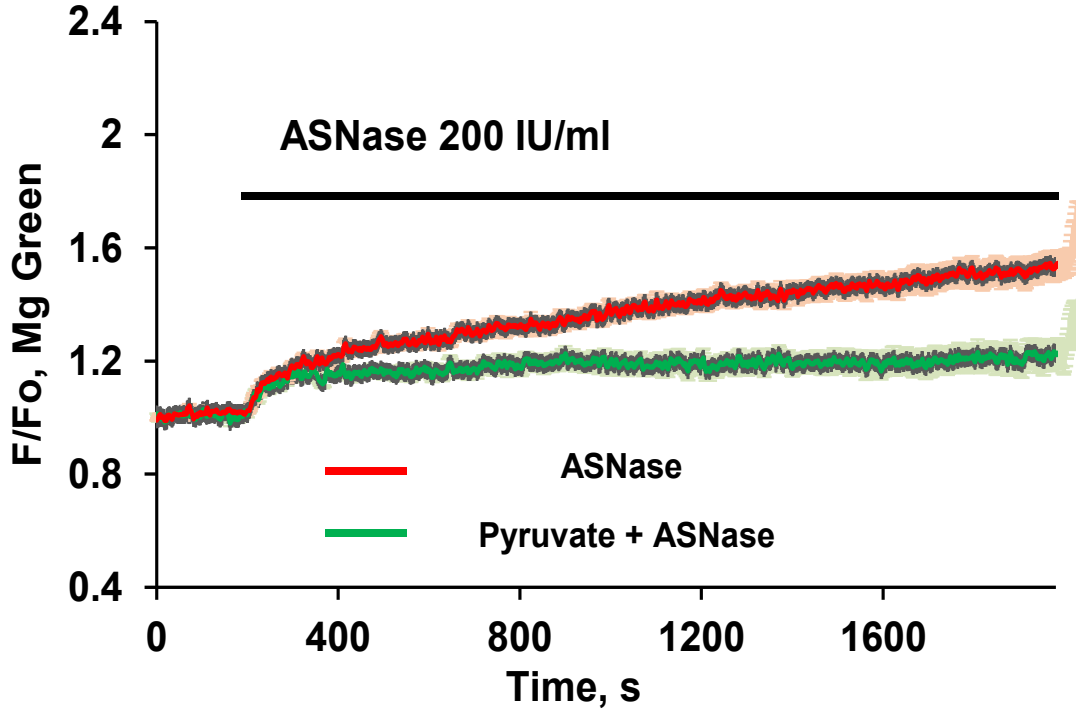
2.4
2
1.6
1.2
0.8
0.4
F/Fo, Mg Green
ASNase 200 IU/ml
ASNase
Pyruvate + ASNase
0
400
800
1200
1600
Time, s

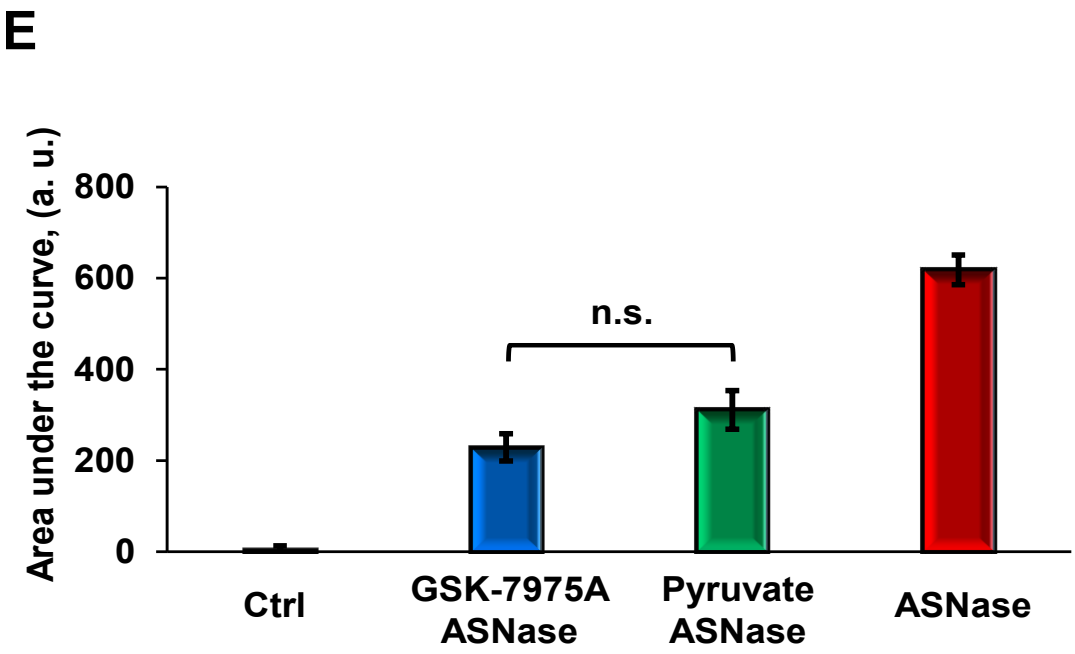

Figure 4.3 Asparaginase reduces intracellular ATP levels as assessed by increases in $[Mg^{2+}]_i$. (Modified from *Peng S et al, Philos Trans R Soc Lond B Biol Sci. 2016*) (313)

Confocal images of a cluster of pancreatic acinar cells; the left part represents the confocal image of MgGreen fluorescence, and the right part shows the transmitted image of the cells (Figure 4.3A; scale bar: 10 μm). Asparaginase (200 IU/ml) markedly increased $[Mg^{2+}]_i$ and a further rise occurred after poisoning mitochondrial function with a cocktail of CCCP (4 μM), oligomycin (10 μM) and sodium iodoacetate (2 mM) (n = 39; Figure 4.3B). Average traces show the relative MgGreen fluorescence (F/F0) in response to Asparaginase (200 IU/ml) followed by the "ATP depletion" mixture in GSK-7975A-treated cells (n = 21; Figure 4.3C) and pyruvate-treated cells (n = 8; Figure 4.3D). Comparisons of the integrated responses ('areas under the curve' from the start of the responses until 1800 s later) show that GSK-7975A or pyruvate significantly reduced the asparaginase-induced ATP depletion ($p < 0.0001$ for both treatments).

Asparaginase affects mitochondrial membrane potential in pancreatic acinar cell

In the previous chapter (Chapter 3), we have demonstrated that asparaginase dramatically slowing down Ca^{2+} extrusion in pancreatic acinar cells (Figure 3.19). Since Ca^{2+} extrusion in pancreatic acinar cell is the ATP dependent process, we decided to investigate more details of asparaginase acting on mitochondria. The high concentration mode of TMRM (dequench mode) measurements is highly sensitive reflecting the changes in mitochondrial membrane potential ($\Delta\psi_m$) (308) and therefore dequench mode was applied in our experiments.

Figure 4.4A shows a typical dequench mode of high concentration of TMRM (10 μM) loading in pancreatic acinar cells. Application of asparaginase (200 IU/ml) resulted in increases of fluorescence in cells (n = 33; Figure 4.4B). The subsequent addition of 5 nM CCCP resulted in fast and large further increases of fluorescence in all cells.

Since the protective effect of pyruvate in asparaginase-induced pancreatic acinar cell necrosis was observed, we therefore applied pyruvate in the dequench mode. As seen in Figure 4.4C, pre-incubation of pyruvate (1 mM) markedly abolished the fluorescence intensity increasing induced by asparaginase (n = 12, $p < 0.01$).

A

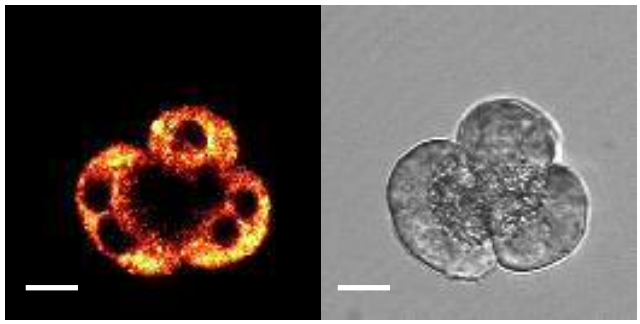
TMRM
Transmitted light

B

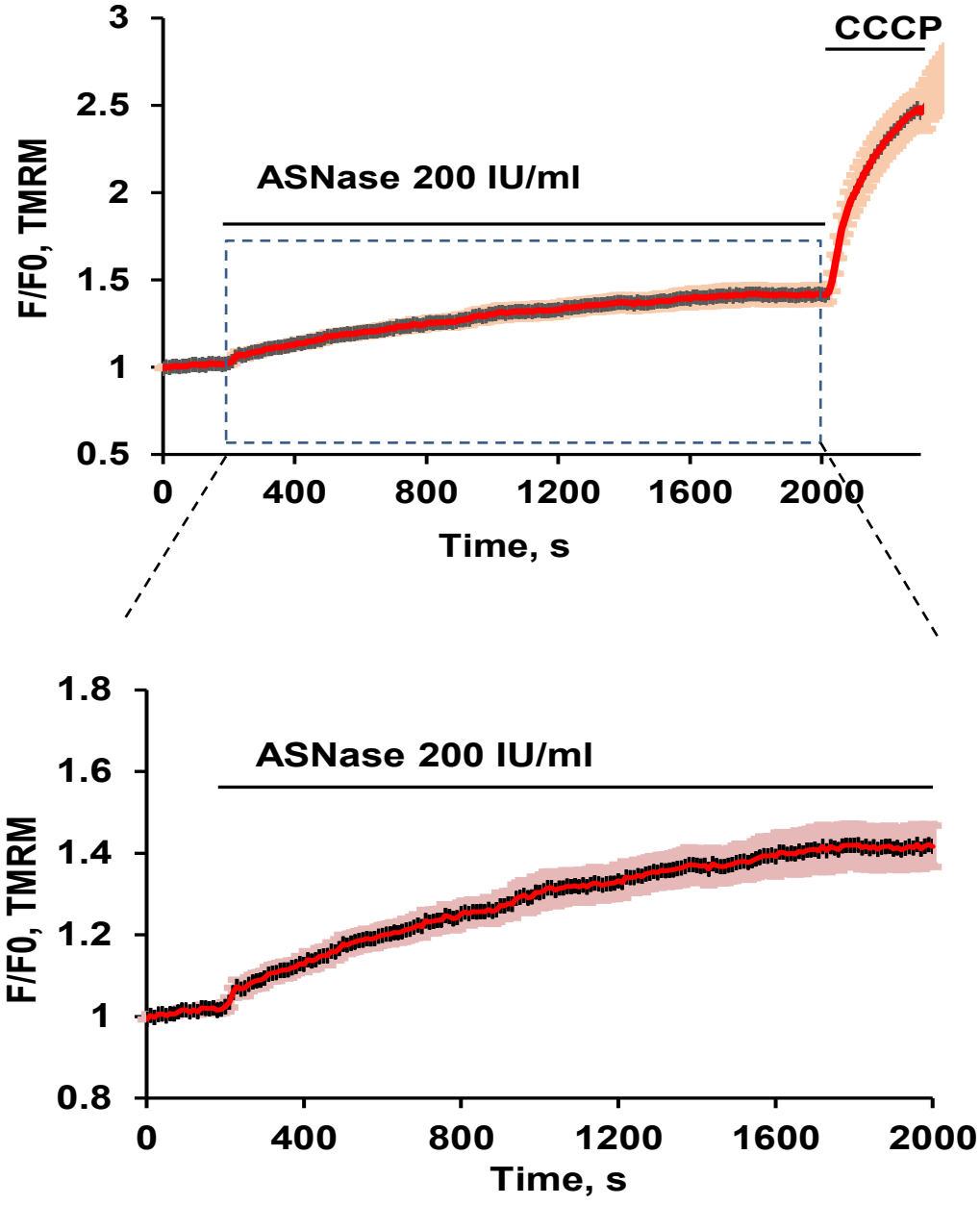
CCCP
ASNase 200 IU/ml
F/F0, TMRM
Time, s
ASNase 200 IU/ml
F/F0, TMRM
Time, s

C

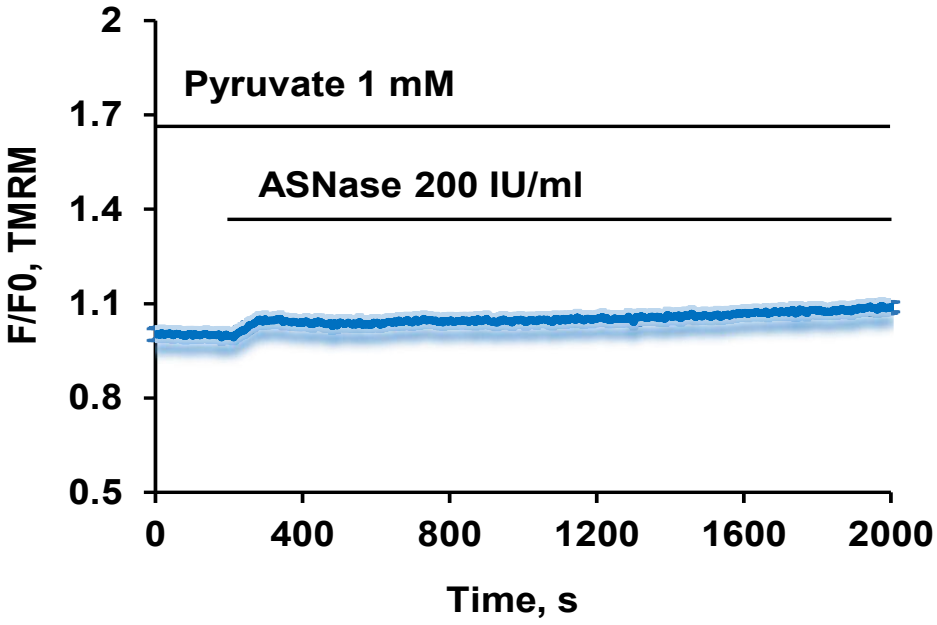
2
1.7
1.4
1.1
0.8
0.5
F/F0, TMRM
Pyruvate 1 mM
ASNase 200 IU/ml
0
400
800
1200
1600
2000
Time, s

D

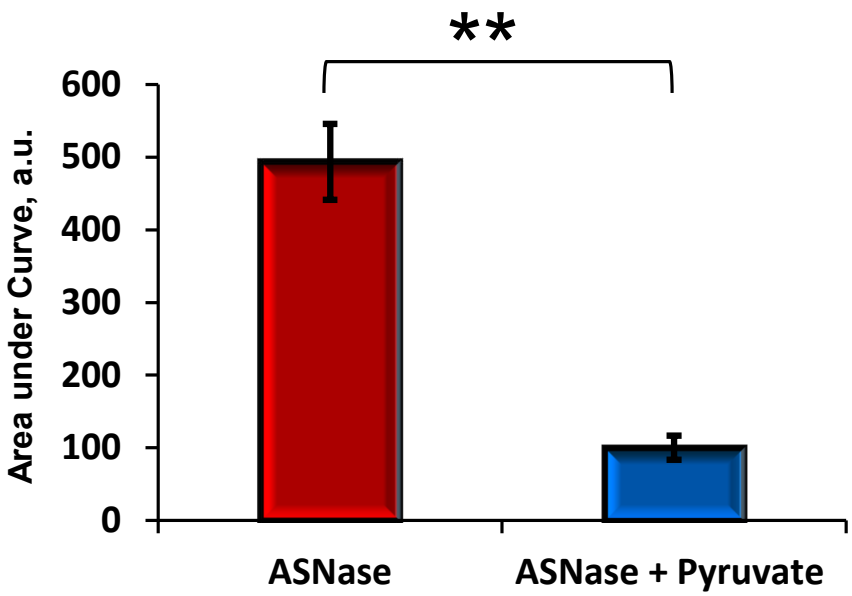
**
600
500
400
300
200
100
0
Area under Curve, a.u.
ASNase
ASNase + Pyruvate

Figure 4.4 Asparaginase induces mitochondrial depolarization.

(A) Confocal images of a cluster of pancreatic acinar cells; the left part represents the confocal image of TMRM distribution, and the right part shows the transmitted image of the cells (scale bar: 10 μm). (B) Responses of the mitochondrial membrane potential probe TMRM to asparaginase. The average traces show effects of asparaginase followed by CCCP on mitochondrial membrane potential to pancreatic acinar cells loaded with 10 μM TMRM (dequench mode, n = 33). (C) The average traces show protective effects of ATP supplementation with 1mM pyruvate (n = 16) on asparaginase-induced change of mitochondrial membrane potential. (D) Comparisons of the integrated responses ('areas under the curve' from the start of the responses of application of asparaginase) show that pyruvate significantly reduced the asparaginase-induced change of mitochondrial membrane potential. ($p < 0.05$).

Asparaginase affects mitochondrial calcium in pancreatic acinar cell

Mitochondrial Ca^{2+} plays an essential role in regulating mitochondrial metabolism (184) and has a direct role in driving ATP production (416). Since the effect of asparaginase-induced mitochondria depolarization and ATP depletion have been observed above, here we have investigated how mitochondrial Ca^{2+} concentration ($[Ca^{2+}]_m$) affect the response to asparaginase by pancreatic acinar cells. To image mitochondria and measure $[Ca^{2+}]_m$ in freshly isolated pancreatic acinar cells, Ca^{2+} dye Rhod-2 (299,417) was applied in the experiments, for this dye is concentrated in cellular compartments with a high negative voltage. As shown in Figure 4.5A, the polarized doublet pancreatic acinar cells has the strongest staining located as a ring surrounding in granular area with some staining in periphery. It has been demonstrated that ER-derived $[Ca^{2+}]_i$ increase results in mitochondrial Ca^{2+} uptake immediately (418). After Rhod-2 loaded cells exposed to asparaginase (200 IU/ml), we found that $[Ca^{2+}]_m$ immediately increase and gradually reach to the sustained plateau (n = 14; Figure 4.5B). When ACh (1 μM) was applied to the cells, there was no more $[Ca^{2+}]_m$ response to be elicited.

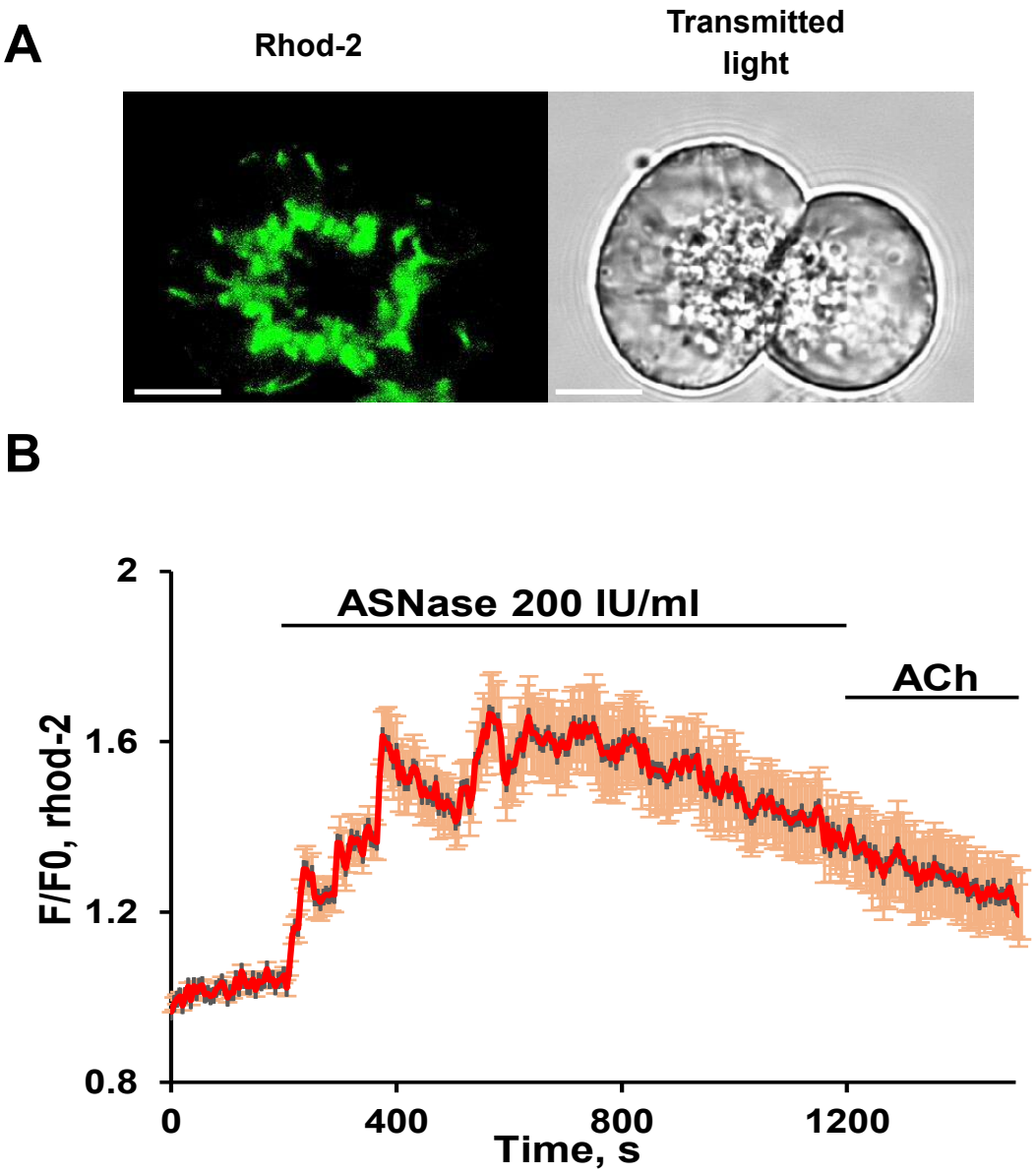

Figure 4.5 Asparaginase induces $[Ca^{2+}]_m$ elevation in pancreatic acinar cells.

(A) Confocal images of a cluster of pancreatic acinar cells; the left part represents the confocal image of Rhod-2 fluorescence, and the right part shows the transmitted image of the cells (scale bar: 10 μm). (B) The average trace shows the effects of ASNase (200 IU/ml) markedly induces $[Ca^{2+}]_m$ elevation followed by 1 μM ACh (n = 14).

Since we found that pre-incubation of pyruvate could reduce the mitochondria depolarization in pancreatic acinar cells, it is naturally to check the effect of pyruvate on $[Ca^{2+}]_m$ dynamics induced by asparaginase. Freshly isolated pancreatic acinar cells were treated with pyruvate (1 mM) for 5 min, and then the same protocol, as it was done in Figure 4.5B, was used to monitor $[Ca^{2+}]_m$ change. Figure 4.6A shows the pre-incubation of pyruvate markedly decrease the $[Ca^{2+}]_m$ response induced by asparaginase (200 IU/ml) (n = 17, $p < 0.01$). ACh (1 μM) could elicit $[Ca^{2+}]_m$ elevation when cells were treated with pyruvate, which is the major difference from the cells exposed to asparaginase without any treatment (Figure 4.5B).

Mitochondrial Ca^{2+} is essential for the regulation of the metabolism, because they modulate dehydrogenases (191,419). Accumulated evidences suggest that pancreatic acinar cell death is an ATP dependent process (133,134). Galactose is a monosaccharide sugar that is converted via the Leloir pathway to glucose 6-phosphate (420) and finally is metabolized to pyruvate via the glycolytic pathway. Thus galactose enters glycolysis bypassing hexokinase at a slower rate than glucose (421). Since the protective effect of pyruvate has been found in our experiments, we next tested whether galactose exerts the same effect as pyruvate does in pancreatic acinar cells when challenged by asaparginase. To examine this, the same protocol was applied in this trial. Freshly isolated cells were pre-incubated with galactose (1 mM) for 15 min and then were exposed to asparaginase (200 IU/ml). As shown in Figure 4.6B, although small $[Ca^{2+}]_m$ plateau with mitochondrial Ca^{2+} transient developed in Rhod-2 loaded cells, pre-incubation of galactose significantly decrease the $[Ca^{2+}]_m$ response induced by asparaginase (200 IU/ml) followed by ACh responses at the end of experiments (n = 6, $p < 0.01$). Figure 4.6C summarizes the degree of inhibition, caused by pre-incubation of pyruvate or galactose of the integrated mitochondrial Ca^{2+} signals evoked by asparaginase.

A

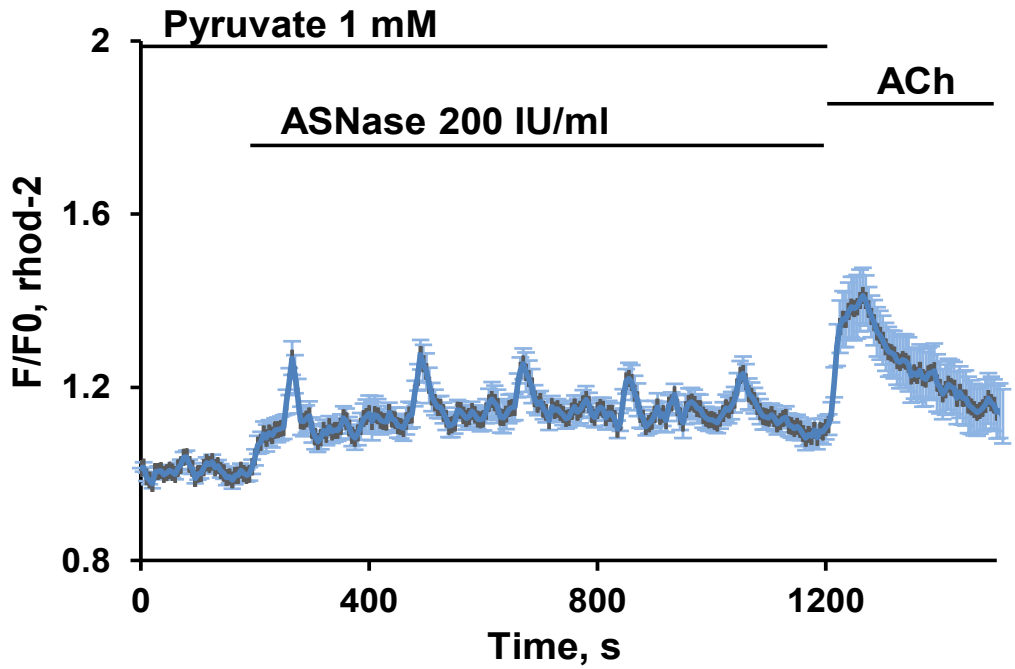
Pyruvate 1 mM
ACh
ASNase 200 IU/ml
F/F0, rhod-2
2
1.6
1.2
0.8
0
400
800
1200
Time, s

B

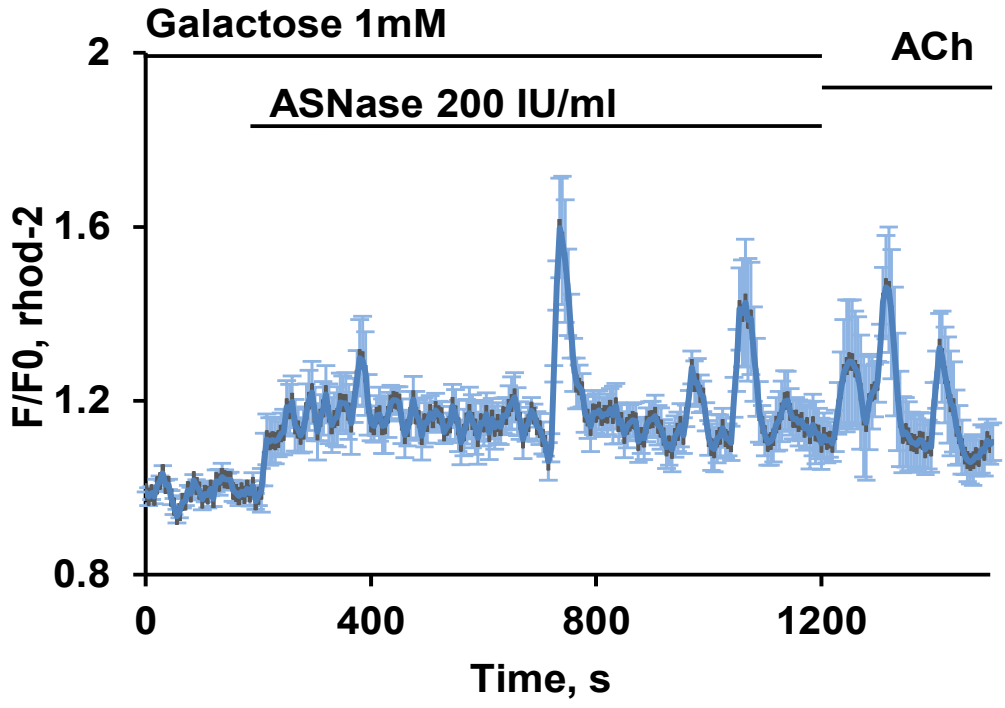
Galactose 1mM
ACh
ASNase 200 IU/ml
F/F0, rhod-2
2
1.6
1.2
0.8
0
400
800
1200
Time, s

C

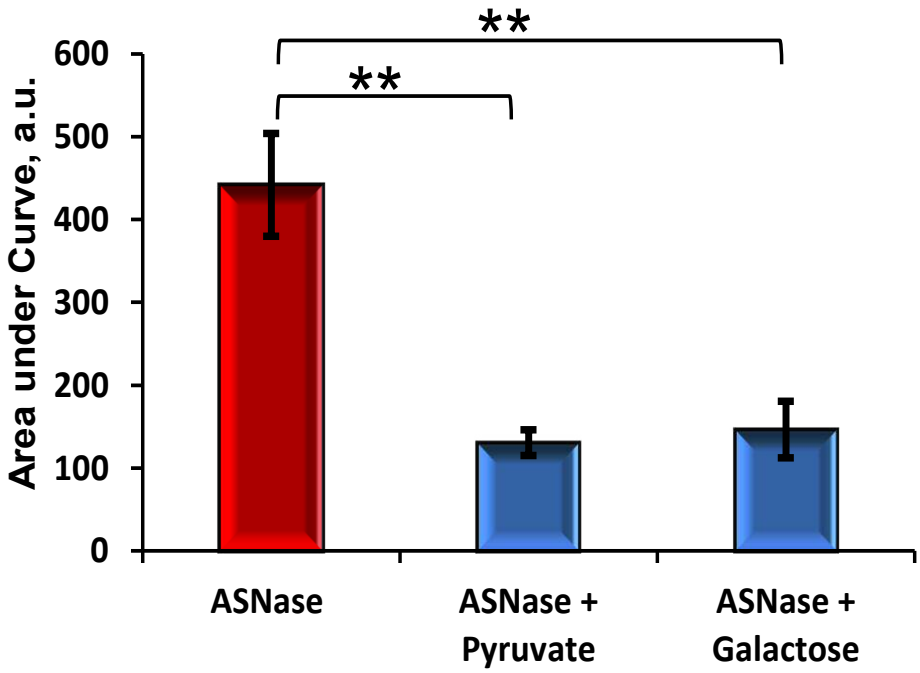

Figure 4.6 Pyruvate or galactose reduces mitochondrial Ca^{2+} response induced by asparaginase.

The average traces show the effect of asparaginase (200 IU/ml) on mitochondrial calcium response are significantly decreased by 5 min preincubation of 1 mM pyruvate (A, n = 17) or 15 min preincubation of 1 mM galactose (B, n = 6) in pancreatic acinar cells. Quantitative analysis of experiments of the type shown in Figure 4.5A and B by comparing the integrated mitochondrial calcium change above the baseline (area under the curve) recorded during the first 1000 sec of asparaginase application (C; $p < 0.01$ for all cases). Bars represent mean ± SEM.

As mentioned previously, Ca^{2+} entry is extremely important for physiology as well as pathophysiology of pancreatic acinar cells (50). To investigate whether extracellular Ca^{2+} contributes to asparaginase-induced $[Ca^{2+}]_m$ response in pancreatic acinar cells, we removed external Ca^{2+} in the buffer and applied asparaginase (200 IU/ml) to Rhod-2 loaded cells. As shown in Figure 4.7A, the much slower $[Ca^{2+}]_m$ elevation was observed in first 10 min when compare with the experiments done with 1 mM external Ca^{2+} shown in Figure 4.5B (n = 10, $p < 0.01$; Figure 4.7B).

Mitochondrial Ca^{2+} efflux is mainly regulated by mitochondrial Na^+/Ca^{2+} exchanger, which is together with mitochondrial Ca^{2+} uniporter control the mitochondrial Ca^{2+} homeostasis (422,423), oxidative phosphorylation (424), and Ca^{2+} crosstalk among mitochondria, cytoplasm, and the ER (425). Here we examined the effect of mitochondrial Na^+/Ca^{2+} exchanger – CGP-37157 (251,426) in our experiments. Pre-incubation of CGP-37157 (20 μM) for 100 s could practically block mitochondrial Ca^{2+} extrusion and application of ACh (1 μM) did not elicit further mitochondrial Ca^{2+} response (n = 6; Figure 4.8).

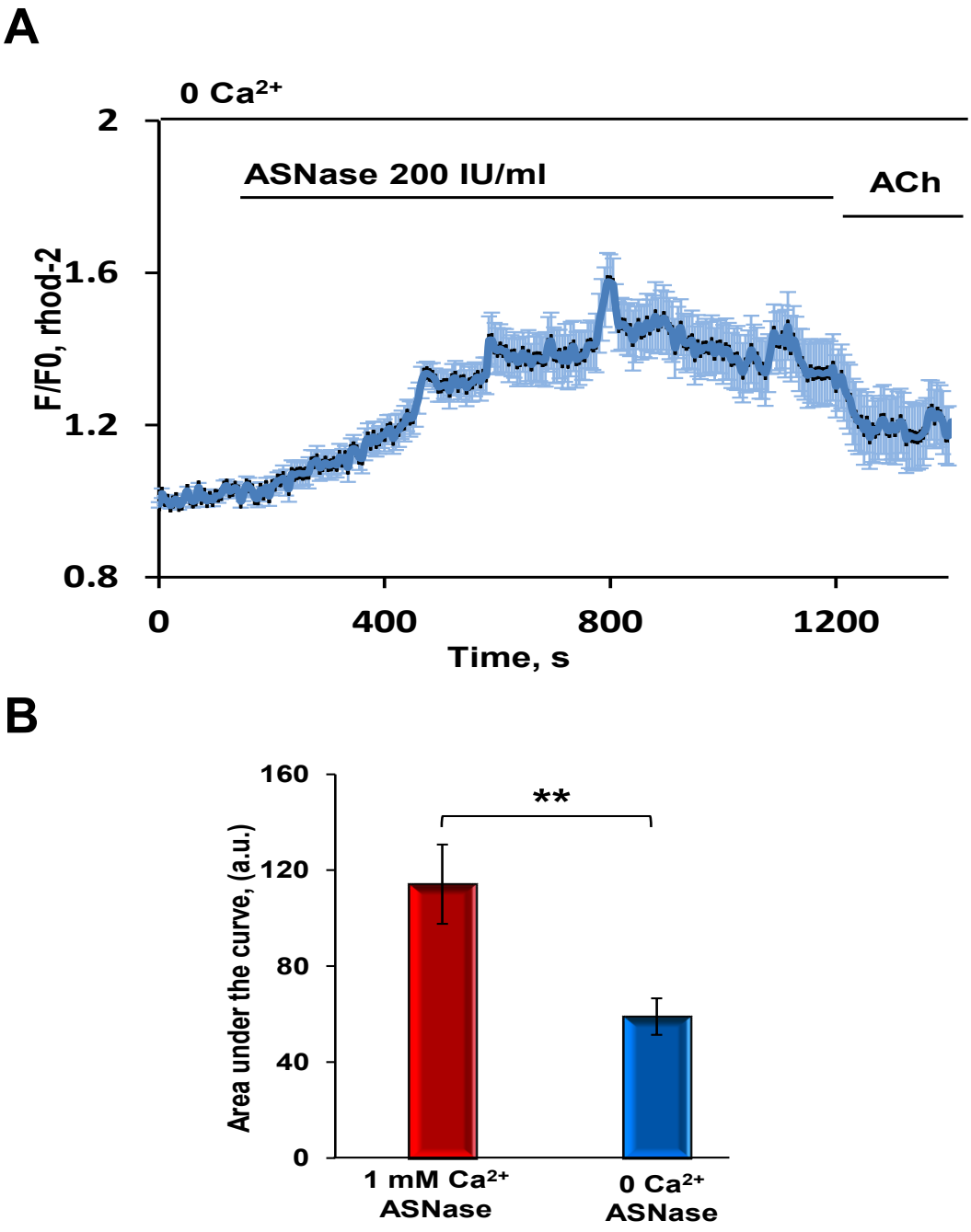

Figure 4.7 External Ca^{2+} accelerates $[Ca^{2+}]_m$ plateau induced by asparaginase. (A) The average trace shows effects of ASNase (200 IU/ml) in the absence of extracellular Ca^{2+} followed by 1 μM ACh on mitochondrial calcium (n = 10). (B) Bar chart comparing first 10 min of the mitochondrial calcium change in the presence of calcium (red bar; Figure 4.5B) or absence of external calcium (blue bar), $p < 0.01$.

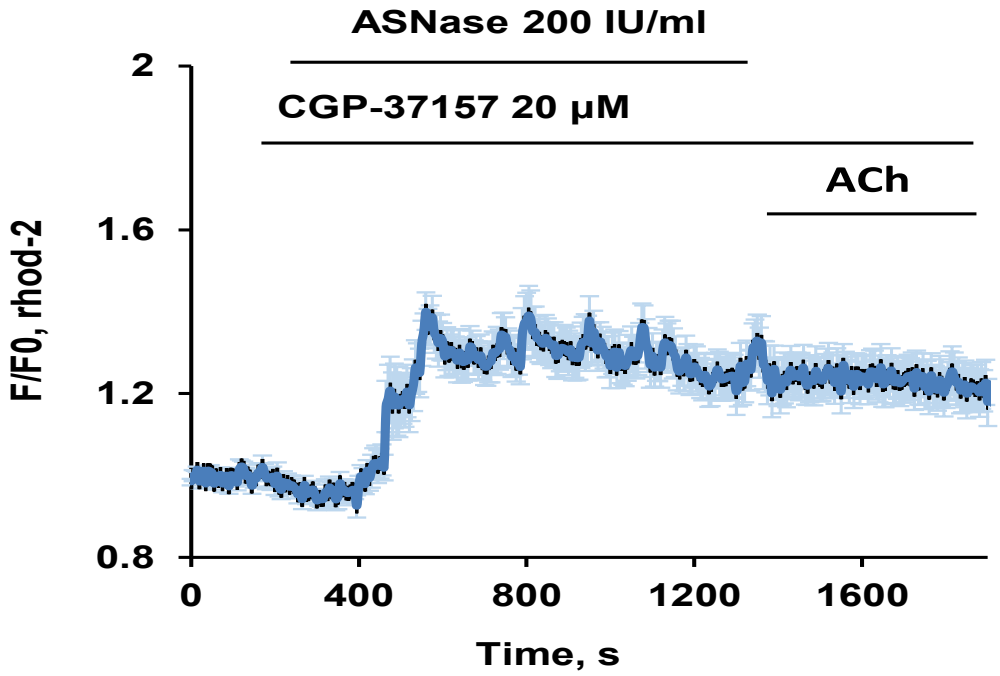

Figure 4.8 Na^+/Ca^{2+} exchanger inhibitor CGP-37157 facilitates $[Ca^{2+}]_m$ plateau induced by asparaginase.

The average trace shows asparaginase (200 IU/ml) elicits the plateau on mitochondrial calcium with 100 sec treatment of mitochondrial Na^+/Ca^{2+} exchanger inhibitor CGP-37157 (20 μM) followed by 1 μM ACh (n = 6).

Asparaginase affects glucose metabolism in pancreatic acinar cell

Glucose is converted into pyruvate by the metabolic pathway called glycolysis. As the results shown above, it has been found that pyruvate was quite effective against mitochondrial ATP depletion. Also, galactose has been shown to reduce $[Ca^{2+}]_m$ elevation induced by asparaginase significantly. Based on these evidences, we speculated that glucose metabolism can be affected by asparaginase. To test this hypothesis, we carried out experiments by using permutation and combination for glucose and pyruvate in extracellular solution. We found that pre-incubation of pyruvate (1 mM) for 5 min with or without glucose (10 mM) substantially reduced increasing of MgGreen fluorescence intensity compared with the cells in the absence of pyruvate in external solution (Figure 4.9A). Comparison of the response area (area under the curve; Figure 4.9B) and the amplitude of the traces at 2000 s (Figure 4.9C) were shown in the presence of pyruvate (1 mM) had more protection against ATP depletion than the cells was not treated with pyruvate. These results indicated that the metabolic pathway from glucose to pyruvate is interfered by asparaginase.

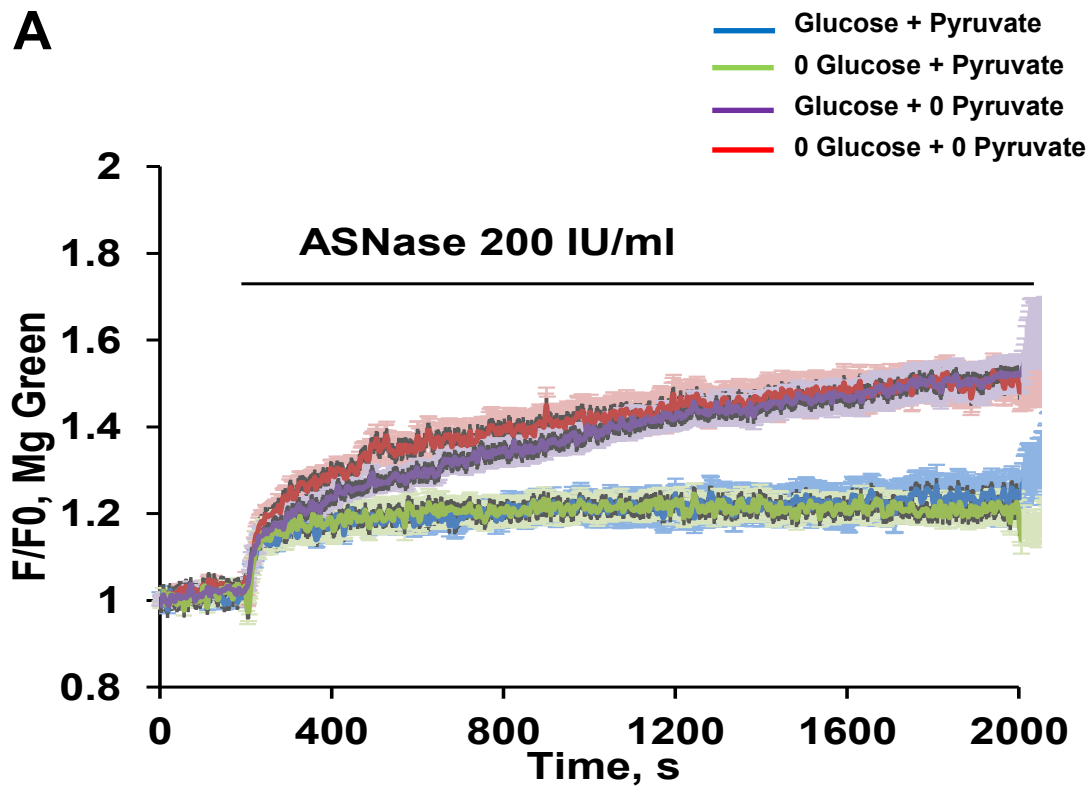
A
Glucose + Pyruvate
0 Glucose + Pyruvate
Glucose + 0 Pyruvate
0 Glucose + 0 Pyruvate
ASNase 200 IU/ml
F/F0, Mg Green
2
1.8
1.6
1.4
1.2
1
0.8
0
400
800
1200
1600
2000
Time, s

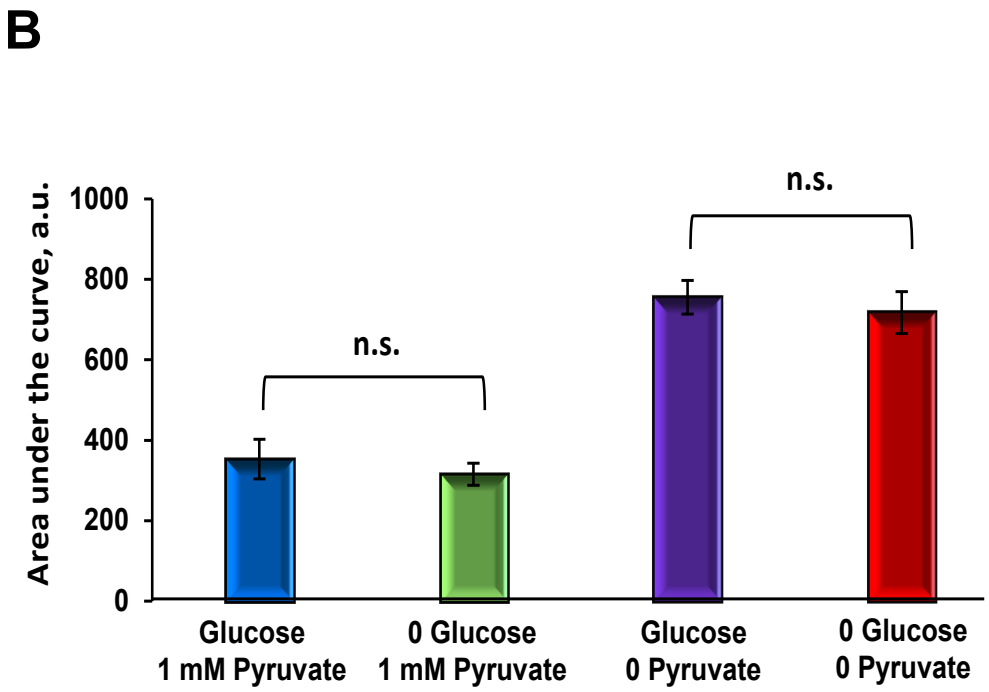
B
Area under the curve, a.u.
1000
800
600
400
200
0
n.s.
n.s.
Glucose
1 mM Pyruvate
0 Glucose
1 mM Pyruvate
Glucose
0 Pyruvate
0 Glucose
0 Pyruvate

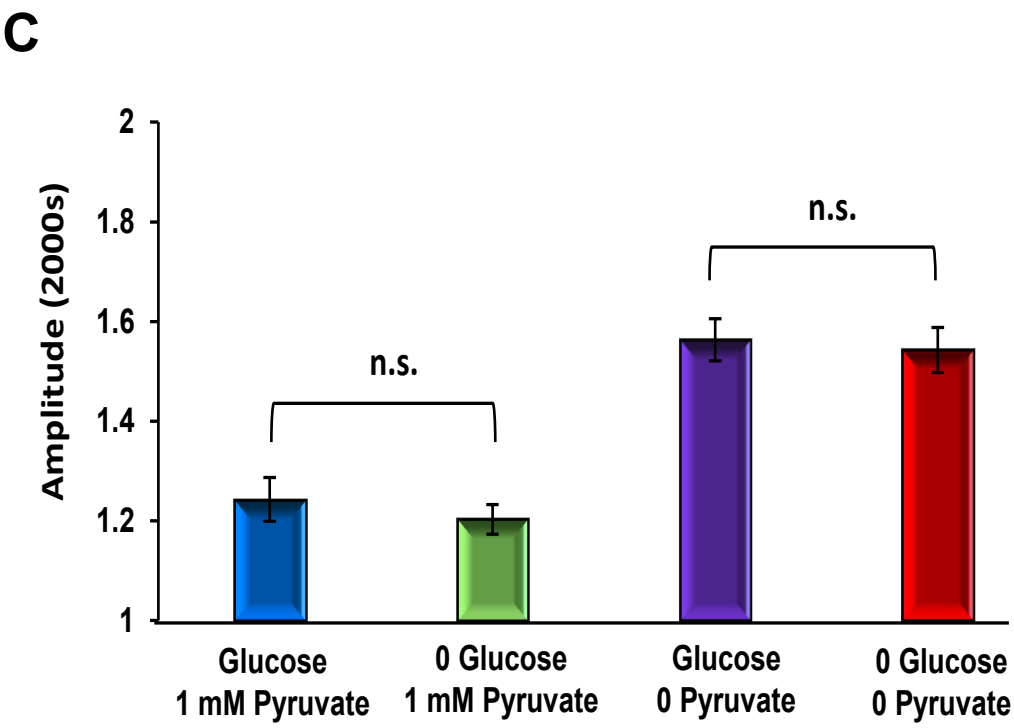

Figure 4.9 Pyruvate effectively protects against ATP depletion induced by asparaginase.

(A) Cellular ATP was assessed by using MgGreen fluorescence. Average traces show ASNase (200 IU/ml) markedly increased $[Mg^{2+}]_i$ in the absence of pyruvate (1 mM) when extracellular glucose (10 mM) was presence (purple trace, n = 21) or absence (red trace, n = 17). In contrast, pancreatic acinar cells exposure to pyruvate (1 mM) significantly decreased $[Mg^{2+}]_i$ induced by ASNase (200 IU/ml) when extracellular glucose (10 mM) was presence (blue trace, n = 14) or absence (green trace, n = 16). (B) Quantitative analysis of experiments shown in A by comparing the cellular ATP depletion above the baseline (area under the curve). Pyruvate (blue bar and green bar) is highly effective against cellular ATP depletion induced by asparaginase (purple bar and red bar), $p < 0.0001$. (C) Bar chart comparing amplitude at 2000 s shown in A. In the absence of pyruvate, the amplitude is higher than the presence of pyruvate induced by ASNase in pancreatic acinar cells, $p < 0.0001$.

In order to investigate the phenomenon further that we observed above, two different sugars – fructose and galactose were applied in the study. Firstly, we tested ATP dynamic changes without extracellular glucose in pancreatic acinar cells. Figure 4.10 shows that ATP gradually and slowly was reduced inside the pancreatic acinar cells when glucose was not provided in the external solution. Therefore, glucose was replaced by pyruvate (10 mM), fructose (10 mM) or galactose (10 mM) in the buffer for freshly isolated cells and all cells were incubated with pyruvate, fructose or galactose for 1 hour before the additional of asparaginase (200 IU/ml). We found that cells treated with pyruvate (green trace, n = 19; Figure 4.11A), fructose (blue trace, n = 33; Figure 4.11A) or galactose (purple trace, n = 16; Figure 4.11A) substantially reduced ATP depletion compared with the cells exposed to glucose (red trace, n = 22; Figure 4.11A). The areas of responses are compared in Figure 4.11B, which shows the fully substitution of glucose by pyruvate, fructose or galactose could diminish a reduction in the intracellular ATP level induced by asparaginase in pancreatic acinar cells ($p < 0.001$).

In the other protocol, pyruvate (1 mM), fructose (1 mM) or galactose (1 mM) was supplemented in the extracellular solution with glucose (10 mM) for freshly isolated cells. When these cells are exposed to asparaginase (200 IU/ml), the cells treated with pyruvate (green bar, n = 14; Figure 4.11C), fructose (blue bar, n = 9; Figure 4.11C) or galactose (purple bar, n = 16; Figure 4.11C) exerts the similar effect as 10 times concentration of them did on cellular ATP level changes. In other words, pyruvate (1 mM), fructose (1 mM) or galactose (1 mM) effectively reduces ATP depletion induced by asparaginase ($p < 0.05$).

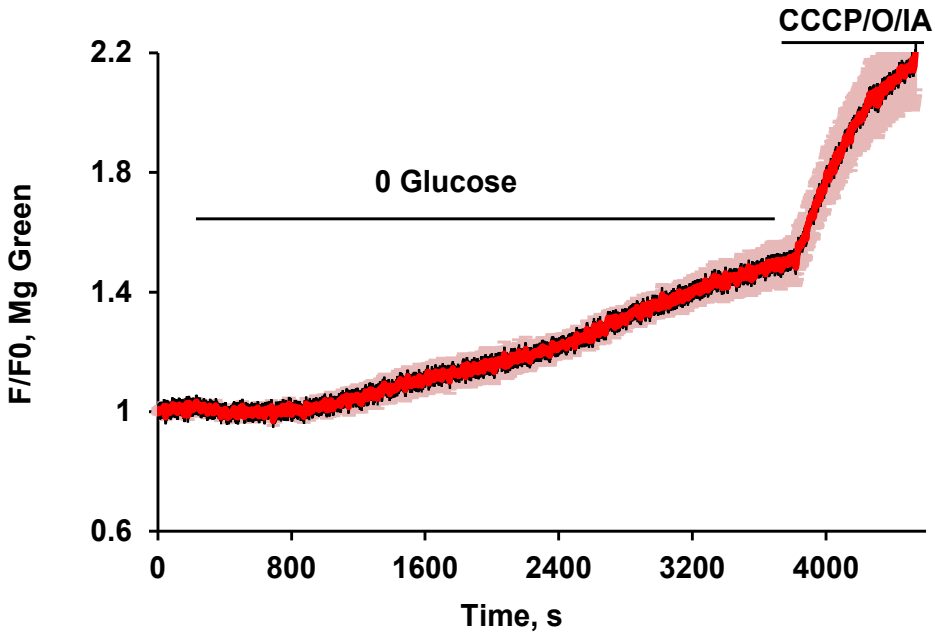

Figure 4.10 ATP depletion induced by the absence of extracellular glucose in pancreatic acinar cells.

Average trace shows $[Mg^{2+}]_i$ change in the absence of glucose within 1 h followed by ATP depletion cocktail of CCCP (4 μM), oligomycin (10 μM) and sodium iodoacetate (2 mM) (n = 14).

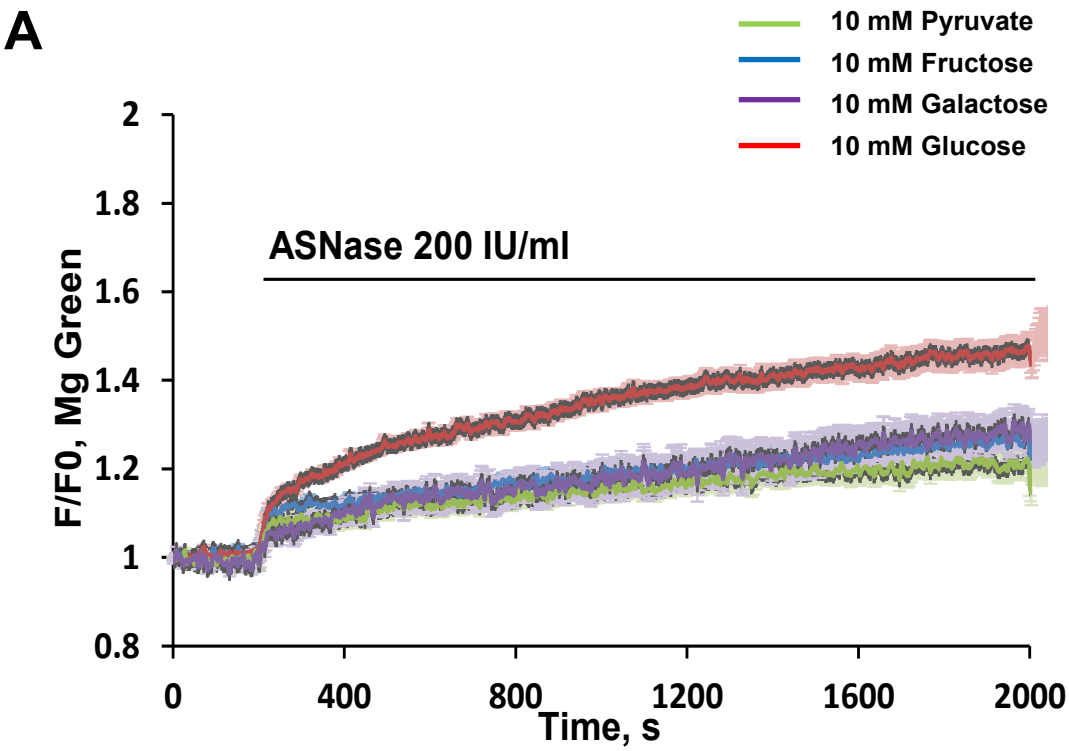
A
10 mM Pyruvate
10 mM Fructose
10 mM Galactose
10 mM Glucose
ASNase 200 IU/ml
F/F0, Mg Green
2
1.8
1.6
1.4
1.2
1
0.8
0
400
800
1200
1600
2000
Time, s

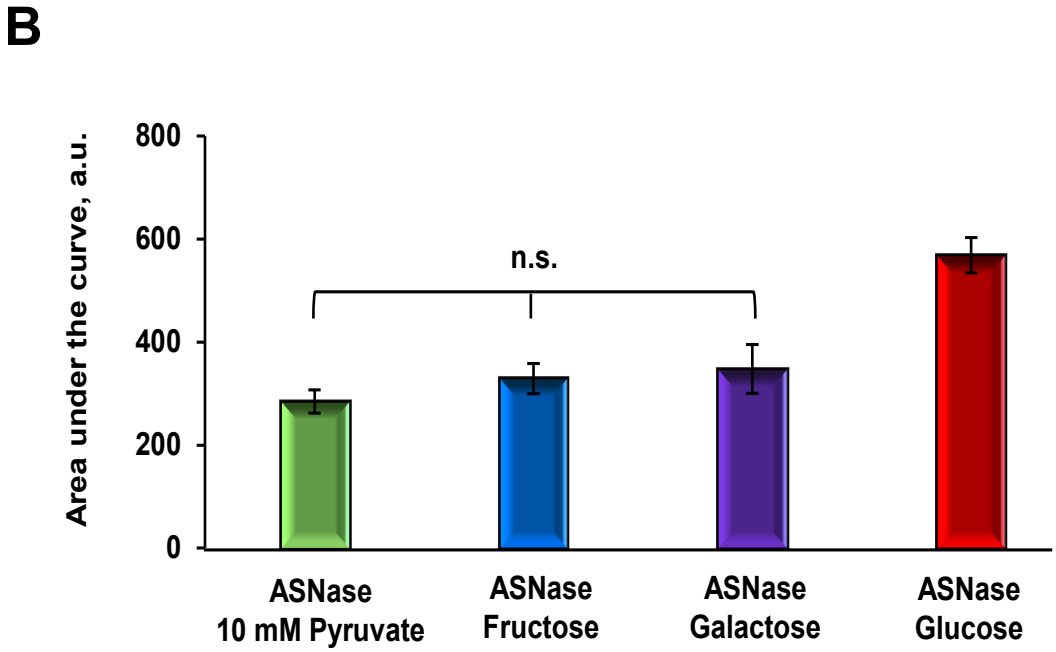
B
Area under the curve, a.u.
800
600
400
200
0
n.s.
ASNase
10 mM Pyruvate
ASNase
Fructose
ASNase
Galactose
ASNase
Glucose

C

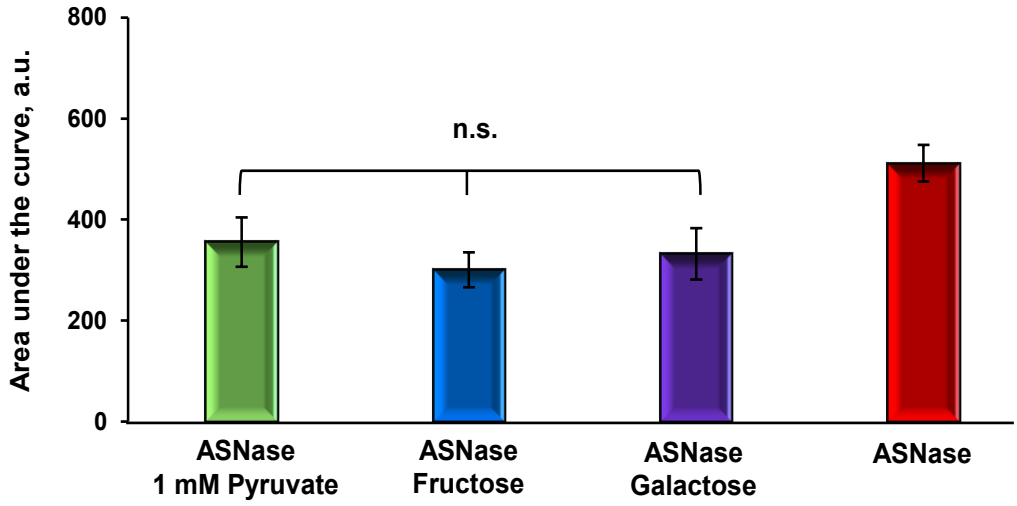

Figure 4.11 Pyruvate, fructose or galactose reduces ATP depletion caused by asparaginase in pancreatic acinar cells.

(A) Average traces show fully substitution of extracellular 10 mM glucose with 10 mM pyruvate (green trace, n = 19), 10 mM fructose (blue trace, n = 33) or 10 mM galactose (purple trace, n = 16) for 1 hour in pancreatic acinar cells could also highly against $[Mg^{2+}]_i$ change induce by asparaginase (200 IU/ml) (red trace, n = 22). (B) Quantitative analysis of experiments of the type shown in A by comparing the integrated $[Mg^{2+}]_i$ change above the baseline (area under the curve) recorded during the 30 min of ASNase application.($p < 0.001$ for all cases). (C) Quantitative analysis of experiments for the additional of 1 mM pyruvate (n = 14), 1 mM fructose (n = 9) or 1 mM galactose (n = 16) in external solution by comparing the integrated $[Mg^{2+}]_i$ change above the baseline (area under the curve) recorded during the 30 min of ASNase application.($p < 0.05$ for all cases).

As previously mentioned, ATP metabolism is highly related to Ca^{2+} signalling in pancreatic acinar cells (97,178,184,195). Since the effect of both pyruvate and galactose has been identified that they are protective for ATP reduction induced by asparaginase, thereafter we examined whether pyruvate or galactose could modulate asparaginase elicited aberrant Ca^{2+} signals. Pre-incubation of pyruvate (1 mM) for 5 min (n = 33; Figure 4.12B and D) or galactose (1 mM) for 15 min (n = 17; Figure 4.12C and D) eliminated asparaginase (200 IU/ml)-induced sustained $[Ca^{2+}]_i$ elevation (n = 35; Figure 4.12A and D) in Fluo-4 loaded pancreatic acinar cells. Figure 4.12E summarizes comparisons of the integrated responses ('areas under the curve' from the start of the responses until 30 min) showing that pyruvate or galactose significantly reduced the responses to asparaginase ($p < 0.001$ for both treatments).

A

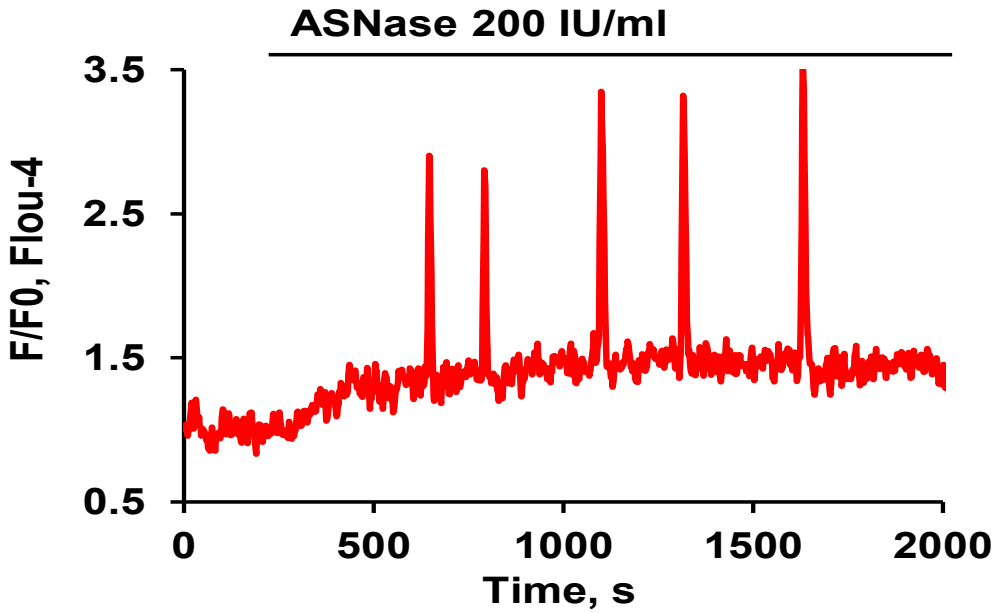
ASNase 200 IU/ml
3.5
2.5
1.5
0.5
F/F0, Flou-4
0
500
1000
1500
2000
Time, s

B

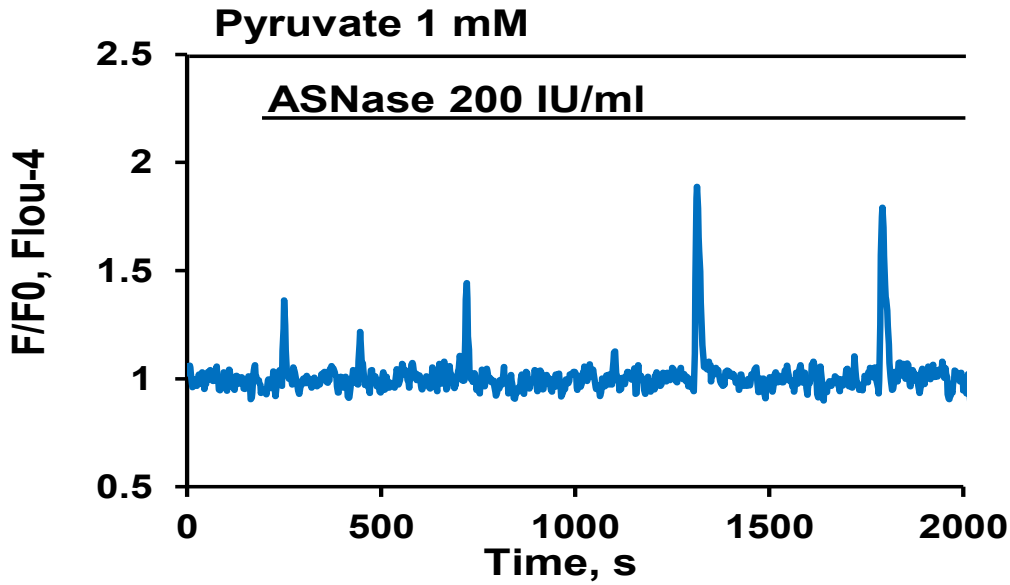
Pyruvate 1 mM
ASNase 200 IU/ml
2.5
2
1.5
1
0.5
F/F0, Flou-4
0
500
1000
1500
2000
Time, s

C

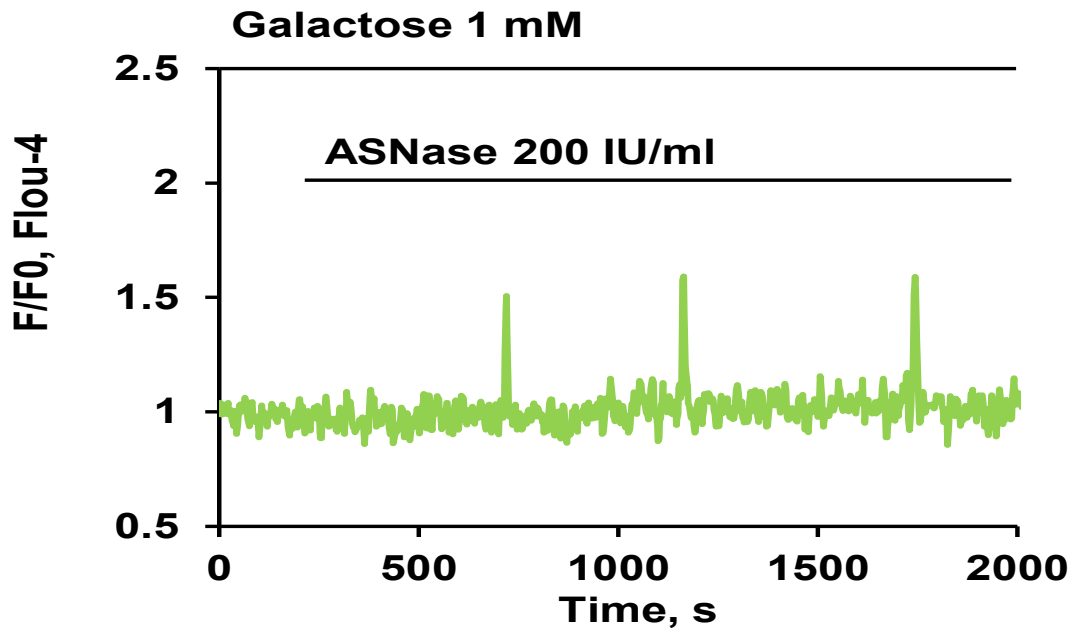
Galactose 1 mM
ASNase 200 IU/ml
F/F0, Flou-4
2.5
2
1.5
1
0.5
0
500
1000
1500
2000
Time, s

D

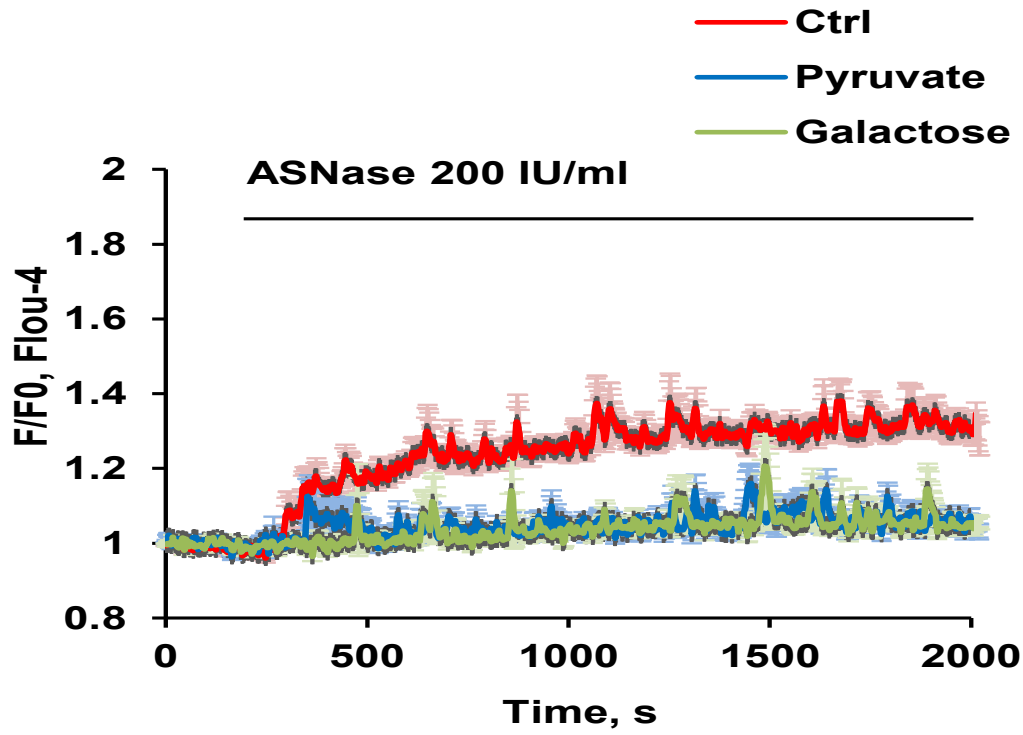
Ctrl
Pyruvate
Galactose
ASNase 200 IU/ml
F/F0, Flou-4
2
1.8
1.6
1.4
1.2
1
0.8
0
500
1000
1500
2000
Time, s

E

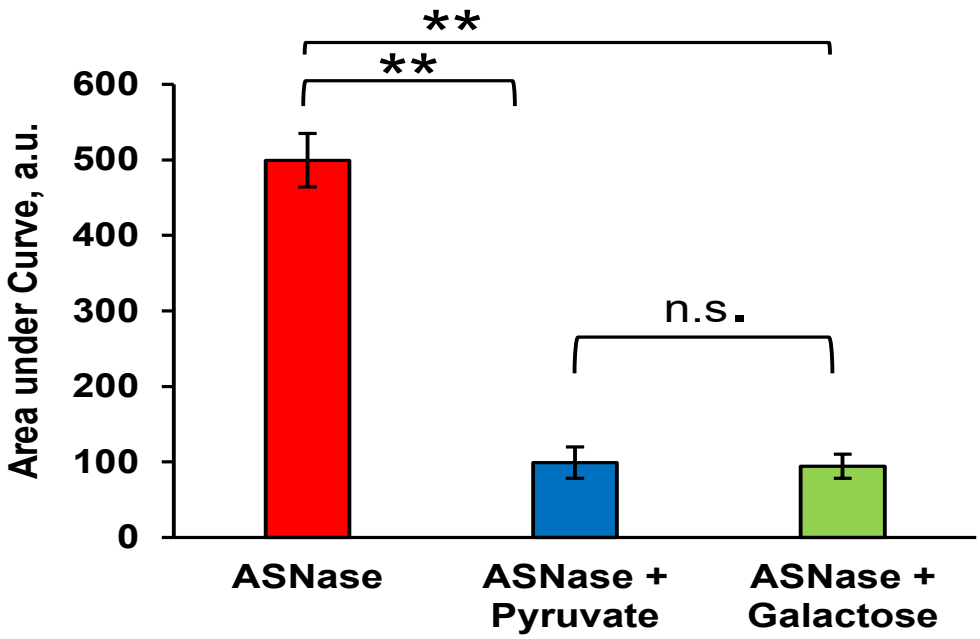

Figure 4.12 Pyruvate or galactose reduces $[Ca^{2+}]_i$ responses to asparaginase in pancreatic acinar cells.

Measurements of the cytosolic calcium were performed using the fluorescence probes Fluo-4-AM. Asparaginase (200 IU/ml) elicits an elevated $[Ca^{2+}]_i$ plateau with repetitive Ca^{2+} transients on top of the plateau in practically all cases (n = 35; A). The trace shows Pancreatic acinar cells were pre-incubated with pyruvate (1 mM) for 5 min (n = 33; B) or galactose (1 mM) for 15 min (n = 17; C), there is no elevated $[Ca^{2+}]_i$ plateau in the majority of cases. Average traces (D) show the changes in $[Ca^{2+}]_i$ in response to ASNase (200 IU/ml) in the presence of pyruvate (1 mM) or galactose (1 mM). Bar chart (E) comparing first 30min of the $[Ca^{2+}]_i$ change in presence of pyruvate (blue bar) or galactose (green bar) in respond to ASNase (200 IU/ml) (red bar). (p < 0.001 for both treatments).

We finally tested pyruvate, fructose and galactose in cell necrotic assay on pancreatic acinar cells. Figure 4.13A shows representative images of some of the treated cells as well as the results of PI staining. It is seen that asparaginase (200 IU/ml)-induced pancreatic acinar necrosis is stimulated with strong intracellular PI staining. In contrast, the treatment groups are not stained by PI. As seen in Figure 4.13B, in the absence of extracellularl glucose, asparaginase (200 IU/ml) induced the comparable level of necrosis (18.4 ± 0.2% of cells) to the group treated with asparaginase (200 IU/ml) in the presence of glucose (16.6 ± 0.3% of cells, $p = 0.48$). Replacement of external glucose with pyruvate (10 mM), fructose (10 mM) or galactose (10 mM) substantially reduced the level of asparaginase-induced necrosis close to the control level ($p < 0.001$). Furthermore, pyruvate (1 mM), fructose (1 mM) or galactose (1 mM) was supplemented in the standard buffer for freshly isolated cells and then all cells were treated with asparaginase (200 IU/ml). As shown in figure 4.13C, additional of pyruvate (1 mM), fructose (1 mM) or galactose (1 mM) significantly protected against asparaginase-induced necrosis.

A

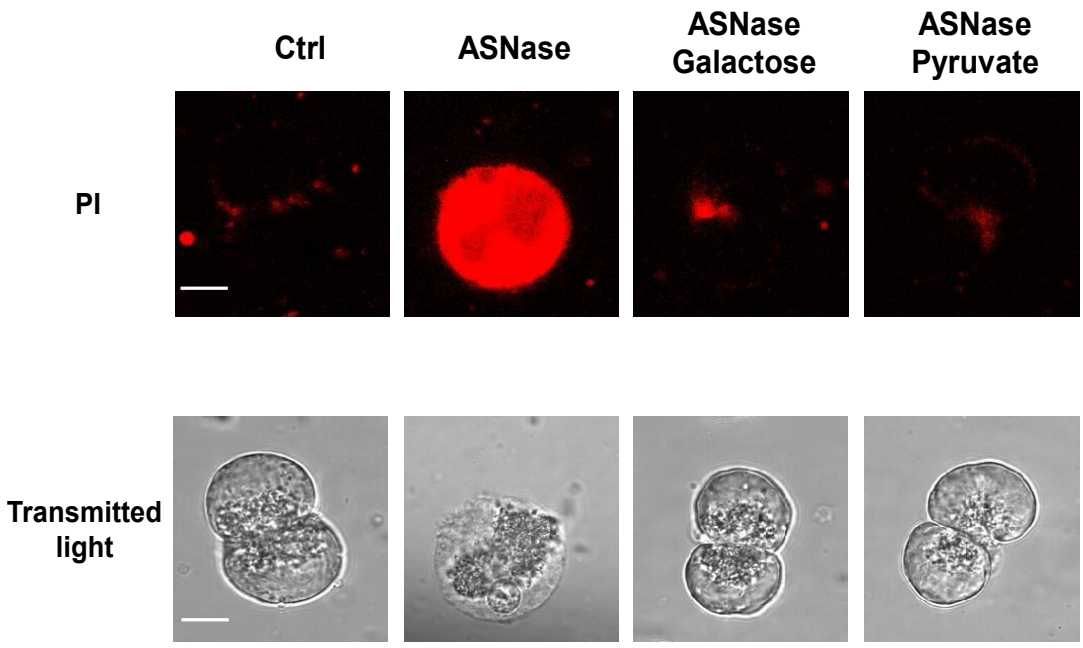
Ctrl
ASNase
ASNase Galactose
ASNase Pyruvate
PI
Transmitted light

B

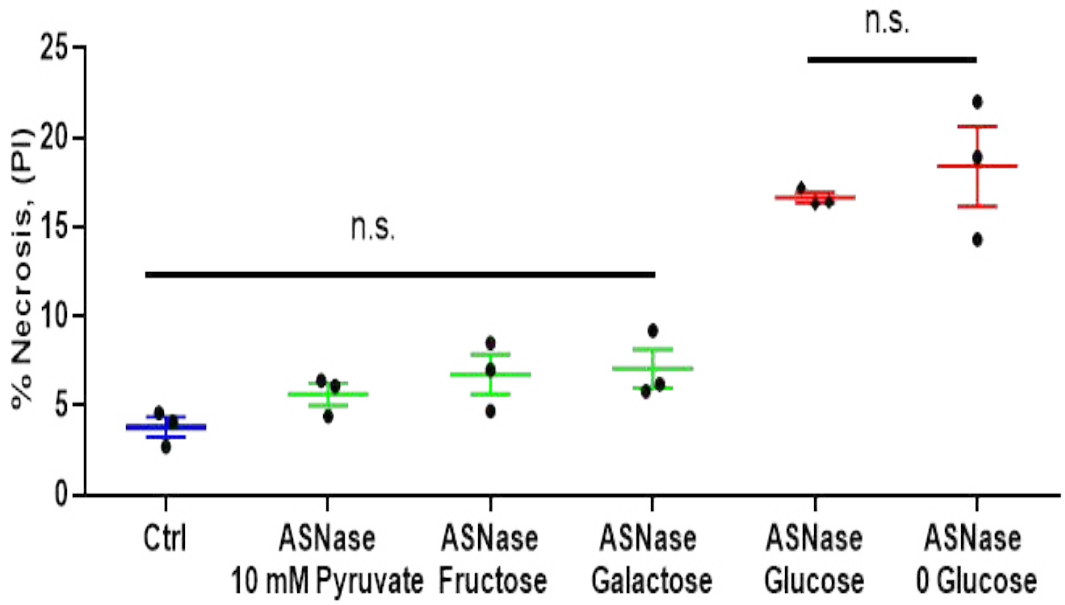
% Necrosis, (PI)
25
20
15
10
5
0
n.s.
n.s.
Ctrl
ASNase 10 mM Pyruvate
ASNase Fructose
ASNase Galactose
ASNase Glucose
ASNase 0 Glucose

C

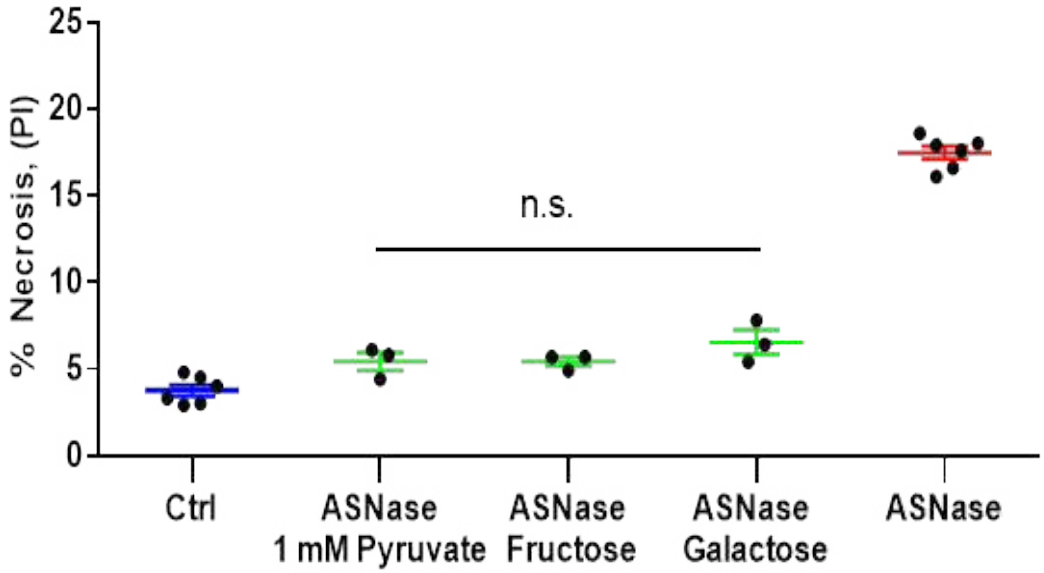

Figure 4.13 Pyruvate, fructose or galactose protects against asparaginase-induced pancreatic acinar necrosis.

(A) Representative images of cells from some of the experiments shown in (B and C). PI-stained fluorescence images (upper row) and transmitted light images (lower row). (B) The level of necrosis induced by 200 IU/ml of ASNase (16.6 ± 0.3%, three series with n > 300) is similar to the absence of glucose in pancreatic acinar cell induce by ASNase (18.4 ± 2.2%, three series with n > 300), $p = 0.48$. Whereas, fully substitution of extracellular 10 mM glucose with 10 mM pyruvate (5.6 ± 0.6%, three series with n > 300, $p < 0.001$), 10 mM fructose (6.7 ± 1.1%, three series with n > 300, $p < 0.001$) or 10 mM galactose (7.1 ± 1.1%, three series with n > 300, $p < 0.001$) markedly protect against necrosis to the control level (3.8 ± 0.6%, three series with n > 300). (C) In the presence of 1 mM pyruvate (5.4 ± 0.5%, three series with n > 300, $p < 0.001$), 1 mM fructose (5.4 ± 0.3%, three series with n > 300, $p < 0.001$) or 1 mM galactose (6.5 ± 0.7%, three series with n > 300, $p < 0.001$) could also reduce the necrosis level induce by 200 IU/ml of ASNase (17.5 ± 0.4%, six series with n > 300).

Discussion

The findings presented in this chapter provide the first mechanistic insights into both mitochondrial function and glucose metabolism are affected by asparaginase. Our data demonstrate that asparaginase lead to mitochondrial depolarization and sustained $[Ca^{2+}]_m$ elevation, which are consistent with the results showing ATP reduction caused by asparaginase. Pre-incubation of pyruvate resulted in reduction of mitochondrial membrane potential and $[Ca^{2+}]_m$ changes as well as pancreatic acinar necrotic cell death pathway activation when pancreatic acinar cells exposed to asparaginase, which indicates that energy supplement may protect against asparaginase-induced pancreatic acinar cell death.

Interestingly, extracellular glucose and pyruvate used by the manner of permutation and combination demonstrate that glycolysis pathway in pancreatic acinar cells is disrupted by asparaginase, and subsequently fully substitution of pyruvate, fructose and galactose or additional of these three energy supplement confirmed that glucose metabolism via glycolysis is interfered by asparaginase. Furthermore, asparaginase-induced cytosolic Ca^{2+} overload is weakened by pre-incubation of pyruvate or galactose, which is together with the data showing that treatment with pyruvate, fructose and galactose significantly protect against pancreatic acinar necrosis suggest that the AAP patients can benefit from such treatment. However, whether there would be protective effects of this treatment in *in vivo* models remains to be determined. This is described in next chapter.

Chapter 5

In vivo model of asparaginase-induced acute pancreatitis

Overview of asparaginase-associated pancreatitis

Patients suffering from acute lymphoblastic leukaemia (ALL) who are receiving asparaginase treatment can develop acute pancreatitis, which is defined as asparaginase-associated pancreatitis (AAP) (290). This is the most common complication of the asparaginase treatment in childhood ALL (427–431). No matter what the preparation is, or dosage and ways of administration of asparaginase, the incidence of AAP remains unchanged (289,293,296,432,433). The incidence of AAP according to the retrospective studies is 5-10% of cases (289,291–293,296,432,434,435).

The pathogenesis and pathophysiology underlying the development of AAP so far is still elusive. Genetic predispositions are likely to play a role in AAP. It has been reported that the CPA2 gene encoding carboxypeptidase A2 in human (436) and eukaryotic initiation factor 2 (eIF2) kinase, general control nonderepressible 2 (GCN2) in mouse (437) are highly related to AAP. Despite of the genetic risk factors, independent risk factors for AAP during ALL treatment include older age, higher exposure to asparaginase, combination therapy with other anti-cancer drugs and higher Native American ancestry (436).

The study described in this chapter was designed to investigate the effects of asparaginase on experimental AP *in vivo* and evaluate the effects of two different therapies by using galactose in experimental AP.

A novel *in vivo* model of asparaginase-induced acute pancreatitis

To establish a novel *in vivo* model of asparaginase-associated pancreatitis - ASNase-AP, C57BL/6J mice given four daily injections of recombinant *Escherichia Coli* L-asparaginase (Abcam) in sterile phosphate-buffered saline (PBS) at 20 IU/g. Animals received injections at the same time each day and were humanely sacrificed 24 h after the final injection. We observed that intraperitoneal injections of asparaginase (20 IU/g) induced pancreatic damage in histological slices taken 24 h after the final application, with extensive acinar cell edema, neutrophil infiltration and necrosis (Figure 5.1). Whereas in control group, mice also received four daily intraperitoneal injections of the same volume of PBS and the histological slices did not show any apparent histopathological changes (Figure 5.1).

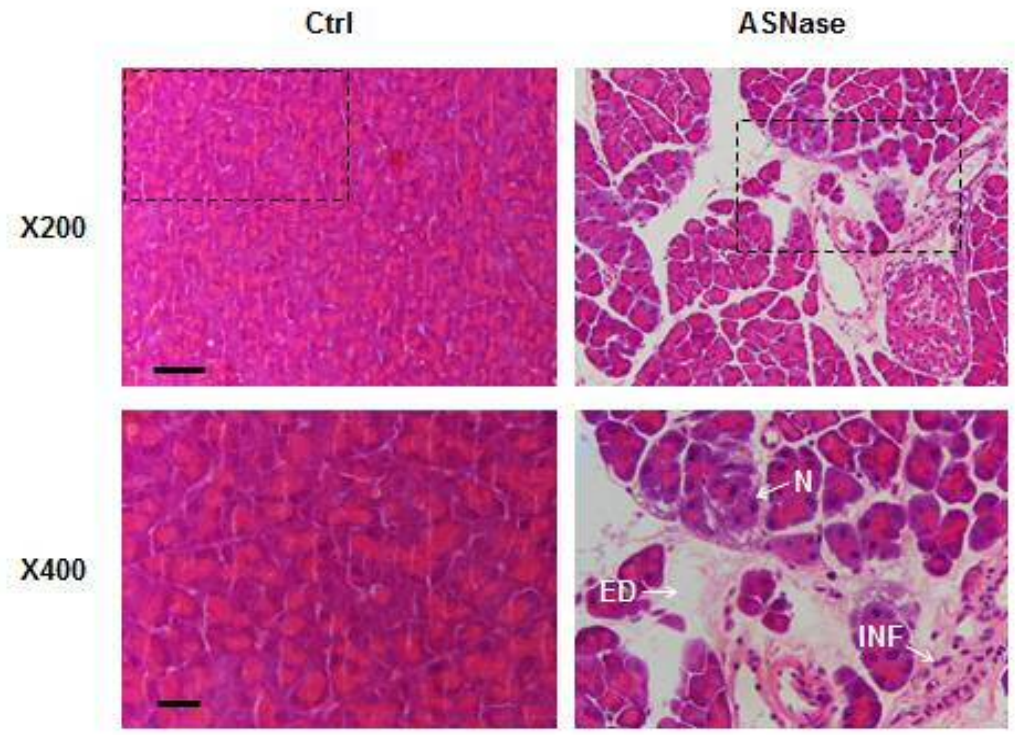

Figure 5.1 Typical histopathology from ASNase-AP.

Representative histological images of hematoxylin-eosin (H&E)-stained pancreatic acinar tissue sections show low magnification (x200, Scale bar: 50 μm; upper row) and high magnification (x400, Scale bar: 20 μm; lower row) of normal pancreatic histology and typical histopathology from ASNase-AP. ED, edema; N, necrosis; INF, inflammation.

Potential treatments for ASNase-AP

As glucose metabolism affected by asparaginase were found in the *in vitro* study (Figure 4.9), herein, galactose was tested in mouse models of ASNase-AP to evaluate its effect *in vivo*. We designed two different manners of the treatments. In the first treatment group, mice were orally fed by water with galactose (180 mg/kg/day). In the other treatment group, galactose (180 mg/kg/day) was administered intraperitoneally prior to asparaginase injection for the mice. Water containing galactose (10 mM) was also supplied daily for this group. Both ways of administration of galactose were protective on pancreatic histopathology (Figure 5.2), showing significant reduction of edema, inflammatory infiltration, necrosis and histopathology scores ($p < 0.01$; Figure 5.3).

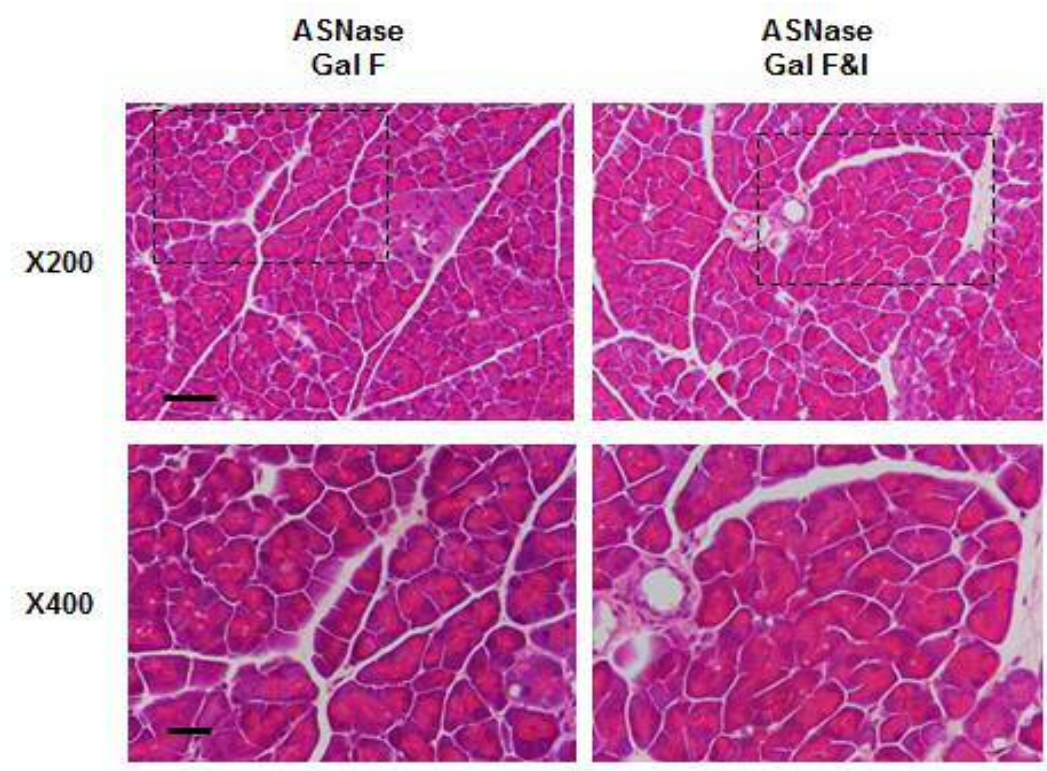

Figure 5.2 Typical histopathology of ASNase-AP following galactose feeding (Gal F) or feeding+injections (Gal F&I).

Representative histological images of hematoxylin-eosin (H&E)-stained pancreatic acinar tissue sections show low magnification (x200, Scale bar: 50 μm; upper row) and high magnification (x400, Scale bar: 20 μm; lower row) of typical histopathology from ASNase-AP with treatments of either oral feeding of galactose (Gal F) or oral feeding of galactose with once intraperitoneal injection of galactose (Gal F&I).

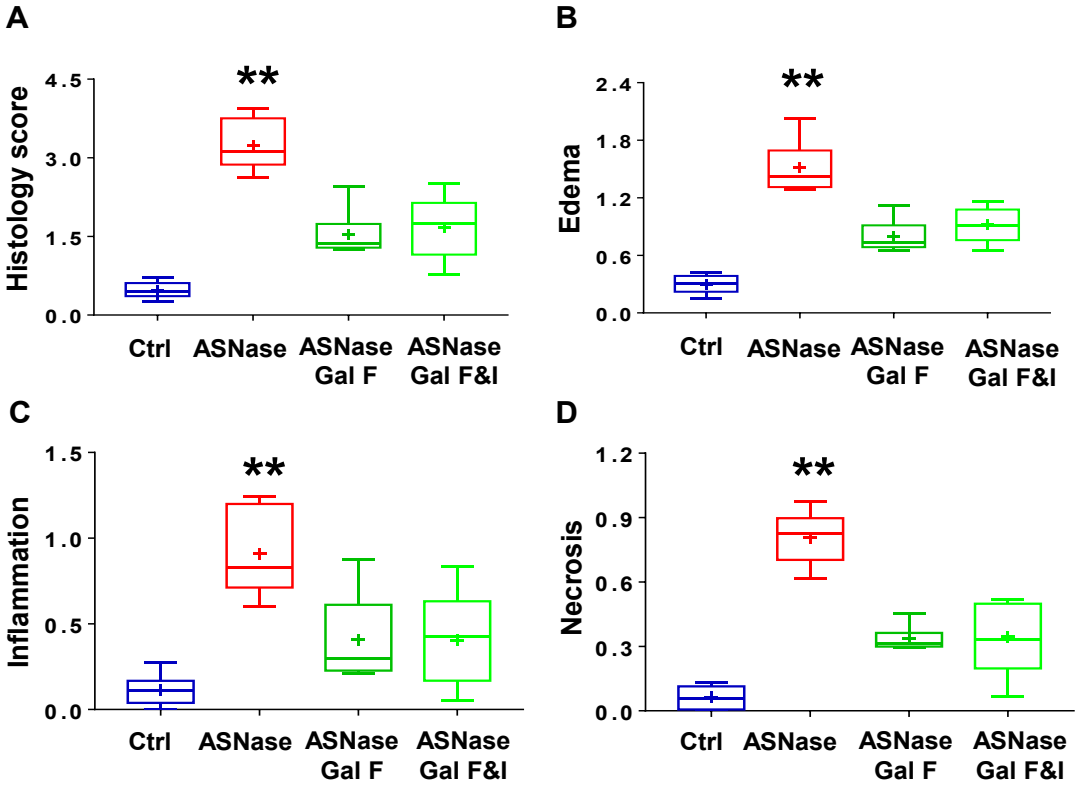

Figure 5.3 Histopathological scores from ASNase-AP.

ASNase-AP results in substantial increase in (A) histology score (B) edema, (C) inflammation, and (D) necrosis. Oral feeding of galactose (Gal F) or oral feeding of galactose with once intraperitoneal injection of galactose (Gal F&I) significantly reduced pancreatic damage, approaching control levels (mean ± SEM, ≥5 mice/group; $^{**}p < 0.01$). Box-and-whisker plots indicate the median (line), mean (cross), IQR (box), and whiskers (min to max) in all figures.

Discussion

The findings presented in this chapter provide a novel *in vivo* model of asparaginase-associated pancreatitis - ASNase-AP. The data demonstrated both orally feeding with and intraperitoneal administrations of galactose (180 mg/kg/day) together significantly reduced a broad range of histopathological parameters in ASNase-AP. These findings are consistent with previous findings *in vitro* that galactose can attenuate effect of asparaginase–induced calcium overload, ATP loss and necrosis in pancreatic acinar cells (Chapter 2). Although both treatments did not decrease all histopathological parameters to the control level, these data nevertheless have very strong clinical implication and provide preclinical validation of energy supplement by galactose as a therapeutic approach for treating ASNase-AP.

Chapter 6

Conclusions and general discussion

Summary

L-Asparaginase is an essential element in the successful treatment of Acute Lymphoblastic Leukaemia (ALL), the most common type of cancer to affect children. However, asparaginase treatment can result in acute pancreatitis (AAP). This occurs in about 5–10% of cases and AAP is the most frequent cause of having to discontinue asparaginase treatment. Acute pancreatitis is a dangerous human disease characterized by premature activation of digestive enzymes inside the pancreatic acinar cells that leads to high levels of necrosis, digestion of the pancreatic tissue and its surroundings with no specific therapy. This study aims to investigate the molecular mechanisms underlying the development of AAP. Understanding the pathogenesis of AAP could lead to effective therapies for this complication, potentially reducing toxicity and allowing re-exposure to continued treatment with asparaginase.

Confocal microscopy was used to investigate *in vitro* asparaginase-induced pathophysiological changes in cytosolic calcium, mitochondrial potential and calcium, ATP loss and necrosis. Both pharmacological inhibition of protease activated receptor 2 (PAR2) or calcium entry with GSK-7975A reduced calcium overload and necrosis in pancreatic acinar cells. Moreover, energy supplements i.e. adding pyruvate, fructose or galactose as a source of ATP had significantly reduced calcium signals, mitochondrial depolarization, mitochondrial calcium responses, ATP depletion and necrosis. We further developed the novel animal model of asparaginase-induced acute pancreatitis (i.e. intraperitoneal injections of asparaginase) and compared these protective effects followed by comparison of histological analysis.

We conclude that combining inhibition of calcium overload with energy supplements could be potentially beneficial for AAP treatments.

General discussion

In humans, the pancreas is the central and highly interconnected organ acting on both exocrine and endocrine functions, which is associated with the digestive and endocrine systems for normal physiological activity of metabolism. However, the pancreas is not only the target but also the effector critically involved in local and systemic inflammation. Pancreatic disorders including acute and chronic pancreatitis and pancreatic cancer are the main and fatal gastrointestinal diseases, which significantly affect the health of all mankind and reduce patients' quality of life (200,201). The incidence of acute pancreatitis accounts for a large proportion in pancreatic diseases and even in gastrointestinal diseases. According to the epidemiological investigation, the annual incidence of acute pancreatitis (AP) affects up to 420 patients per million populations and has a 5 % mortality rate even in mild cases (195,205). The number of admissions and discharges with AP as principal diagnosis have increased by up to 30% over the last ten years (192,193). AP is undoubtedly the most common and the leading cause of hospital admissions for GI disorders, which costs approximately $2.63 billion per year (200). This is absolutely a source of substantial burden and cost for medical care of the society. Hence, the development of treatments for AP conducted by both laboratory and clinical studies is the best strategy to meet the challenge of this disease.

Acute pancreatitis is a dangerous human disease characterized by premature activation of digestive enzymes inside the pancreatic acinar cells that leads to high levels of necrosis, digestion of the pancreatic tissue and its surroundings with no specific therapy (138). Repeated attacks of AP, in particular alcohol-related pancreatitis, may result in the development of chronic pancreatitis, which is likely to contribute to develop pancreatic cancer

(194,195). Obviously, these pancreatic disorders have seriously endangered human health. There is currently no specific drug to treat AP clinically. Therefore, there is pressing need to understand the mechanisms underlying AP and identify the potential biological target for the treatment of AP. This could prevent the recurrence of AAP and the possible transition from acute to chronic pancreatitis and pancreatic cancer.

Asparaginase is the anti-leukaemic drug, forming an essential component of combination chemotherapy for the treatment of acute lymphoblastic leukaemia (ALL) in most young leukaemia patients (282). ALL is the most commonly diagnosed childhood cancer, accounting for 26% and 8% of cancers diagnosed in children and adolescents, respectively (438). During the last few decades, it has been demonstrated and supported by extensive clinical trials that intensive asparaginase treatment in pediatric ALL has dramatically improved of the long-term survival of ALL patients (272,282,285,439,440). However, in 5% to 10% of pediatric patients the asparaginase treatment has to be truncated due to development of acute pancreatitis (289,293,441). Asparaginase-associated pancreatitis (AAP) occurs after one or a few administrations of asparaginase. Re-exposure to asparaginase after the occurrence of AAP is associated with a high risk of recurrence. In this situation, further treatment of asparaginase is often discontinued, which may negatively impact event-free survival. The pathogenesis and pathophysiology underlying AAP is completely unknown.

Evolutionally, various forms of life existed on Earth employ calcium ions (Ca^{2+}) and adenosine triphosphate (ATP) to maintain the most basic living activity and control life, death and cellular signalling (180,442,443). These two molecules are profoundly interconnected and interdependent. This is because a low cytosolic Ca^{2+} concentration ($[Ca^{2+}]_i$) is required by ATP metabolism. In order to maintain such $[Ca^{2+}]_i$, the Ca^{2+} signalling system using the immense

transmembrane Ca^{2+} gradients utterly demand ATP-dependent Ca^{2+} transport (444). Therefore, these two molecules are tethered together to regulate multiple vital functions.

Ca^{2+} is a ubiquitous intracellular signal, which has been known for decades of its importance in controlling secretion. Under physiological stimulations, changes of $[Ca^{2+}]_i$ results in cellular responses of molecular cascades. However, aberrant Ca^{2+} signalling contributes to numerous diseases including pancreatitis, cardiovascular disease and nervous system disorders (236,445,446). In pancreatic acinar cells, physiological Ca^{2+} signals consist of repetitive $[Ca^{2+}]_i$ spikes and often these are confined to the apical pole. Local Ca^{2+} signalling induced by physiological concentration of ACh or CCK can only be transient, whereas sustained $[Ca^{2+}]_i$ elevations evoked by pathological stimuli (combinations of alcohol and fatty acids or bile acids) always become global and lead to inflammation of the pancreas. The latter pattern of Ca^{2+} signals is toxic, because intracellular Ca^{2+} overload not only invades some sub-cellular spaces where only requires local Ca^{2+} regulation, but also decrease mitochondrial ATP production due to depolarization of the inner mitochondrial membrane caused by opening of the MPTP (447). Cytosolic Ca^{2+} overloading initiates negative event loop that overloading of mitochondria with Ca^{2+} reduce markedly in mitochondrial ATP synthesis will affect Ca^{2+} pumps and prevent Ca^{2+} movements across the plasmalemma and the endomembranes, which eventually cause further $[Ca^{2+}]_i$ elevation.

The aims of this thesis were to understand the mechanism underlying the asparaginase-associated pancreatitis (AAP). Moreover, we have also explored potential molecular therapeutic targets. We further aimed to develop therapeutic approaches by using novel *in vivo* mouse model of AAP to probe a new effective treatment for AAP.

Effects of asparaginase on calcium signalling in pancreatic acinar cells

Intracellular Ca^{2+} plays a critical role in the initiation of acute pancreatitis. The process of this disease is Ca^{2+} dependent, in which digestive proenzymes are prematurely activated inside the pancreatic acinar cells causing necrosis of acinar cells and autodigestion of pancreatic tissue (138,202,448). Studies on isolated murine cells or cell clusters are enormously useful methods in understanding AP (312,354,371,449). Furthermore, results obtained from *in vitro* experiments have turned out to predict accurately the outcome of *in vivo* studies of real AP (351–354). Hence, acute studies of the effects of asparaginase on isolated mouse acinar cells or cell clusters was our approach, for the first time, to investigate the mechanism of AAP. However, time course is one of the challenges inherent in this approach. This is because the time course needed in the clinical situation for the development of AAP typically requires several weeks after a few administration of asparaginase (290), which is quite different from the time course needed for *in vitro* study to observe the effects of asparaginase on normal freshly isolated acinar cells within hours .

The results presented in this thesis indicate that Ca^{2+} overload is the critical trigger in the pathophysiology of AAP and is responsible for asparaginase-elicited pancreatic acinar injury. This probably can explain the development process of AAP, which share some similarities with AP induced by fatty acid ethyl esters (FAEE) as well as bile acids (134,136,138). Asparaginase generate toxic Ca^{2+} signals by eliciting Ca^{2+} release from intracellular stores and then followed by store-operated Ca^{2+} entry through CRAC channels. However, the sustained $[Ca^{2+}]_i$ elevations evoked by FAEE or bile acids are somewhat larger than that induced by asparaginase. This is consistent with our results shown that the level of necrosis induced by asparaginase is somewhat lower than that caused by the alcohol metabolite

POAEE or the bile acid taurolithocholic acid 3-sulfate (TLC-S).

In pancreatic acinar cells, IP_3R types 2 and 3 are predominantly expressed in the apical region and responsible for physiological Ca^{2+} signalling and enzyme secretion (69,450). IP_3Rs-mediated excessive Ca^{2+} release from intracellular stores is evoked by various stimuli such as supramaximal dose of CCK, FAEE and TLC-S. This effect could be inhibited by double knockout of IP_3Rs (451). Our data show that the intracellular messengers IP_3 and the intracellular receptors IP_3Rs are involved in asparaginase-induced Ca^{2+} release from intracellular stores, which is due to activation of a signal transduction mechanism via G-protein–coupled protease-activated receptor 2 (PAR2). Despite the fact that the importance of PAR2 activation in triggering inflammatory responses has been well defined, the signal transduction mechanisms involved in PAR2-mediated mobilization of cytosolic Ca^{2+} and effector responses remain to be unraveled (345,376). Blocking PAR2 by selective antagonist FSLLRY-NH_2 alleviated asparaginase-evoked cytosolic Ca^{2+} overload and blocking muscarinic receptor by nonselective antagonist atropine did not affect pathological Ca^{2+} response stimulated by asparaginase. Together with the data showing that FSLLRY-NH_2 had no effect on muscarinic receptor, our results suggest that asparaginase-induced $[Ca^{2+}]_i$ elevations is elicited via PAR2. Although the results indicate that PAR2 is linked to the development of AAP, it is still not fully understood how PAR-2 activation drive inflammatory responses in acinar cells, which is associated with pancreatic acinar necrosis. Interestingly, it has been recently reported that PAR2-activated Ca^{2+} signalling and cytokine production are regulated by CRAC channels in human airway epithelial cells (452). We may speculate that stimulation of PAR2 by asparaginase triggers opening of CRAC channels in pancreatic acinar cells, in turn, leads to the release of numerous inflammatory mediators. More studies using knockout mice would be needed to test this issue.

Ca^{2+} entry plays a critical role in the formation of the pathologically elevated $[Ca^{2+}]_i$ plateau in pancreatic acinar cells and is crucial for the initiation of acinar cell injury (312). Removal of external Ca^{2+}, adding Ca^{2+} chelator EGTA in buffer or pharmacological CRAC blockade by GSK-7975A show the sustained $[Ca^{2+}]_i$ elevations induced by asparaginase are markedly reduced. These results confirm Ca^{2+} entry is indispensable and responsible for Ca^{2+} overload and CRAC channels are involved in the pathophysiological process of AAP. The specific CRAC channel blocker GSK-7975A markedly reduces the asparaginase-evoked sustained $[Ca^{2+}]_i$ plateau, which is consistent with the previous finding that the main pathway of store-operated Ca^{2+} influx and Ca^{2+} entry currents is CRAC channel (312) rather than transient receptor potential (TRP) channel (453,454) in pancreatic acinar cells. Nevertheless, Ca^{2+} entry mediated by TRP channels, mainly by TRPC3, is contributed to the damage of the pancreas. Either genetic or pharmacological inhibition of TRPC3 showed protective effect to against pancreatic inflammatory responses (453,454).

Based on a specific protocol routinely used to assess Ca^{2+} influx and efflux (312), we observed that asparaginase significantly affect both Ca^{2+} entry and extrusion in acinar cells. However, the slowing down of the rate of Ca^{2+} extrusion is quantitatively the most important effect of asparaginase on acinar cells. This indicates that intracellular ATP level of acinar cells is reduced by asparaginase treatment which, in turn, limits the energy supply to the Ca^{2+} ATPase in the plasma membrane (PMCA). It has been demonstrated that Ca^{2+} extrusion is mainly regulated by PMCA rather than NCX in the plasma membrane in pancreatic acinar cells (96,97) and the processes of Ca^{2+} across the plasma membrane is energy-dependent (99). Therefore, it is a strong implication that asparaginase could deplete cellular ATP in acinar cells.

We further investigated the effect of asparaginase on mitochondrial Ca^{2+} handling. Mounting evidence suggests that mitochondria are extremely helpful

in regulating spatio-temporal patterns of intracellular Ca^{2+} signalling (455,456). Mitochondrial Ca^{2+} homeostasis is very complex. This is because numerous Ca^{2+} channels, pumps and exchangers are involved to regulate this dynamic process. It is not surprising that the result presented here shows asparaginase evoke prolonged elevation of $[Ca^{2+}]_m$ in acinar cells. This is likely due to relatively fast Ca^{2+} uptake and slower Ca^{2+} extrusion by mitochondria so that $[Ca^{2+}]_i$ transients can be blunted and transformed into long term $[Ca^{2+}]_i$ elevations. Moreover, long lasting cytosolic Ca^{2+} overload is able to induce such effect in mitochondria of pancreatic acinar cells. Inhibition of the mitochondrial Na^+/Ca^{2+} exchanger with CGP-37157 results in prolonged $[Ca^{2+}]_m$ plateau, which indicate that the mechanism of Ca^{2+} extrusion of mitochondria is mainly controlled by Na^+/Ca^{2+} exchanger. This is consistent with the observation in another type of excitable cell — chromaffin cells (457). Interestingly, both pyruvate or galactose reduce asparaginase-induced $[Ca^{2+}]_m$ response, which is implicated in metabolic demands for ATP production and energy expenditure in the cell. Mitochondrial Ca^{2+} uptake plays a crucial role in the modulation of cellular Ca^{2+} homeostasis and bioenergetics (458,459), thereby, it is necessary to conduct experiments on mitochondrial Ca^{2+} handling during the action of asparaginase for further studies.

Effects of asparaginase on ATP metabolism in pancreatic acinar cell

ATP production via the metabolic pathways of glycolysis (Figure 6.1) and oxidative phosphorylation is critical for physiological functions of the pancreas (72,180,182). Calcium signalling machinery includes Ca^{2+} release from internal stores via IP_3R and RyR, Ca^{2+} entry from the extracellular solution via store-operated channels, Ca^{2+} uptake and Ca^{2+} extrusion by Ca^{2+} pumps. All components of this machinery are influenced by mitochondria and cellular ATP level. On the other hand, Ca^{2+} movement process is energy dependent and cellular Ca^{2+} homeostasis is associated with ATP dynamics. Accumulating evidence from past decades demonstrate that ATP is essential not only for secretion in pancreatic acinar cells, but also for pathogenesis of acute pancreatitis (133,134).

Our data show that Ca^{2+} extrusion is significantly affected by the treatment of asparaginase in acinar cells. As the process of Ca^{2+} extrusion is ATP-demanding, therefore, we assessed asparaginase on intracellular ATP changes in pancreatic acinar cells. The results show that asparaginase markedly reduces the intracellular ATP levels and induces mitochondrial depolarization, which support the hypothesis that Ca^{2+} extrusion slowed down by asparaginase due to the reduction in the intracellular ATP level limit the energy supply to the PMCA.

Pyruvate is a product of glycolysis. This chemical compound is efficiently imported and utilized by mitochondria to supply energy to cells through the Krebs cycle (460). Previous studies show the effects of pyruvate modulate Ca^{2+} signalling, which highlight another critical and clearly underexplored link between Ca^{2+}-channel function and energy demand (461,462). The results presented here demonstrate that the asparaginase-induced ATP loss was

substantially reduced by the addition of pyruvate to pancreatic acinar cells. Moreover, the addition of fructose or galactose also exerts the similar effect as pyruvate in protecting against ATP loss. Further, replacing glucose with pyruvate, fructose or galactose in extracellular medium markedly reduce the ATP depletion evoked by asparaginase. These results indicate that supplement with energy source such as pyruvate, fructose and galactose could boost energy production *in vitro* to counteract the toxic effects of asparaginase. Our data also show that both pyruvate and galactose very markedly reduced the asparaginase-elicited $[Ca^{2+}]_i$ rise and $[Ca^{2+}]_m$ elevation. Interestingly, we observed that the ATP loss was substantially higher in the absence of pyruvate regardless of the presence or absence of glucose. Taken these results together, it suggests that asparaginase may interrupt intermediary metabolism and hexokinase activity is inhibited by asparaginase. Therefore, hexokinase dysfunction could be the likely explanation of the ATP loss in AAP. To explore the potential effects of asparaginase affecting hexokinase activity will be the subject of follow-up studies.

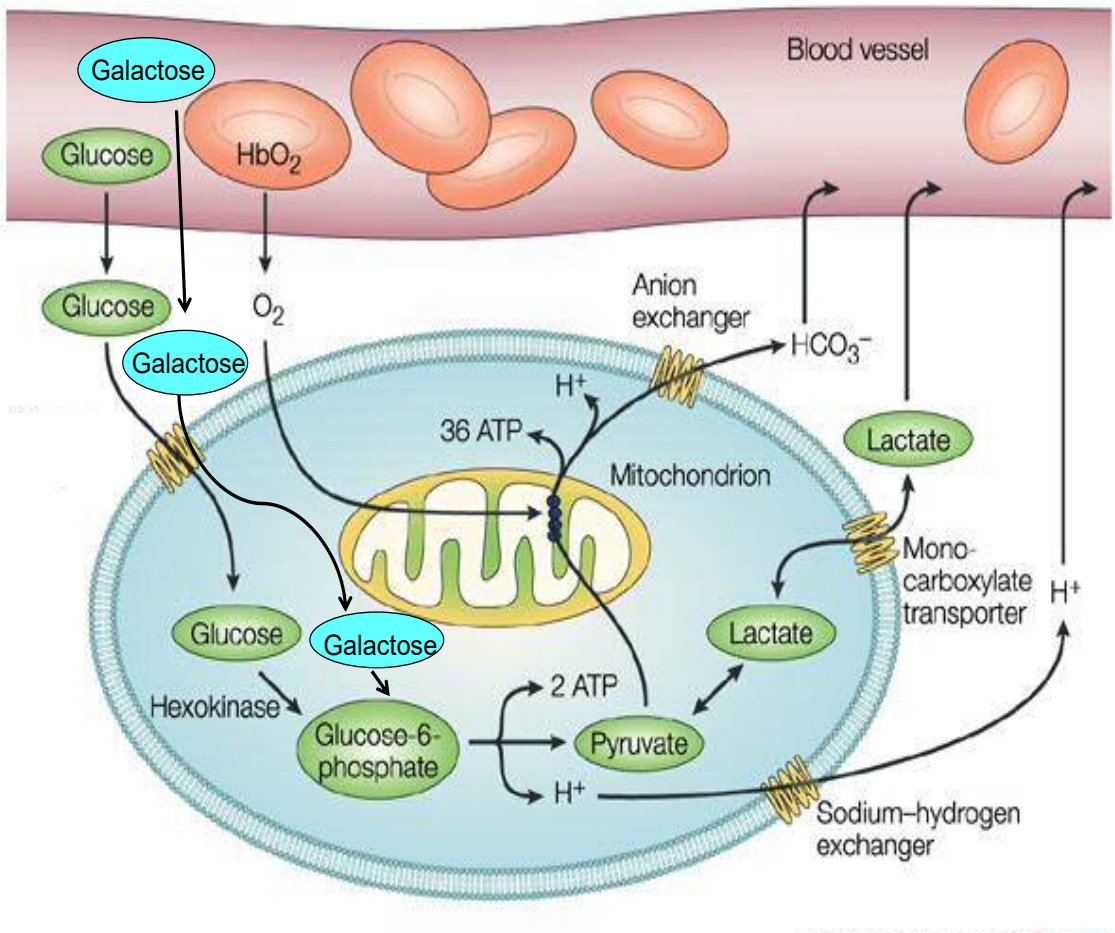

Figure 6.1 Simplified schematic diagram of glycolysis.

(Modified from *Gatenby RA & Gillies RJ., Nat Rev Cancer. 2004*) (463)

The diagram shows the metabolic pathway of glycolysis. Both glucose and galactose can be transported into glycolysis pathway and eventually forms pyruvate in pancreatic acinar cells.

Potential targets and therapies for asparaginase-associated pancreatitis

The clinical presentation and complications in asparaginase-associated pancreatitis (AAP) do not differ significantly from acute pancreatitis (AP) in other pediatric populations (290). Therefore, AAP can be diagnosed by the same diagnostic procedures as AP if at least two of the following three criteria are met: typical upper abdominal pain, serum amylase or lipase at least three times the upper limit of normal and confirmatory findings from cross-sectional imaging analysis (192,193,217). Although AAP can be monitored by clinicians, there is a lack of specific therapy for patients who developed AAP in the course of receiving asparaginase treatment. This also significantly affects re-administration of asparaginase after the occurrence of AAP, which dramatically decreases event-free survival in childhood ALL. Understanding the mechanisms underlying the development of AAP leads to the development of new therapeutic approaches for reducing the side-effects of asparaginase treatments.

Current strategies for managing AP are supportive, which includes fluid resuscitation, analgesia and enteral nutritional support. However, these treatments do not deal with the root cause of the disease. The current consensus of the initiation step of AP is that intracellular proteases are activated inside the pancreatic acinar cell by toxic Ca^{2+} signals evoked by, for example, non-oxidative alcohol metabolites or bile acids (138,202,235). However, there are now opportunities for new therapeutic intervention based on recent advances in our understanding of Ca^{2+} handling and bioenergetics in pancreatic acinar cells of AAP.

It is now clear that pancreatitis-inducing stimulants release Ca^{2+} from both the ER and acidic stores primarily via IP_3 receptors and that the depletion of

internal Ca^{2+} stores causes opening of store-operated Ca^{2+} channels in the plasma membrane, mediating the sustained Ca^{2+} entry mainly by CRAC channel into the cells during prolonged stimulation of the pancreatic acinar cells (136). Cytosolic Ca^{2+} overload is a crucial feature of AP, thereby, inhibition of the primary Ca^{2+} release and Ca^{2+} entry, enhancement of Ca^{2+} extrusion are all attractive and potential targets for the treatment of AP. The results presented in this thesis demonstrate that AAP is owing to toxic Ca^{2+} signal generation and the primary site of asparaginase acting on pancreatic acinar cells seems to be PAR2. Accumulating evidence suggest that PAR2 has been most prominently implicated in the pathogenesis of AP, although its exact role is still debated (347–350). The controversy about the role of PAR2 in AP is due to the observation obtained from two pancreatitis models: bile salt-induced model and caerulein-induced model. In the bile salt-induced pancreatitis model, PAR2 activation triggers the pathological Ca^{2+} signals. Consequently, pancreatic injury become worse via a series of downstream events including acinar cell injury and c-Jun N-terminal kinase (JNK) activation (349). In contrast, PAR2 activation reduces the severity of pancreatic injury in caerulein-induced pancreatitis model by the similar mechanisms as the bile salt-induced pancreatitis model and by stimulating the secretion of activated digestive zymogens from acinar cells as well as by reducing the translocation of extracellular-signal regulated kinase (ERK)1/2, but this does not involve an alteration in the generation of $[Ca^{2+}]_i$ elevation (348,350,464,465). Due to different responses observed in dissimilar models and in the absence of clinical studies, we believe that the induction of the clinical relevant model should direct interpretation of the results. Moreover, pharmacologic activation of PAR2 could trigger profound hypotension and activation of neutrophils and generation of IL-8, which contribute to the MODS (348). Interestingly, it has been reported that activation of PAR2 receptors stimulate neural pathways linked to pain in the pancreas (466,467). Our data indicate that blocking PAR2 leads to the reduced level of asparaginase-elicited intracellular Ca^{2+} overload

and necrosis, which support the hypothesis that asparaginase-induced PAR2 activation is the onset of AAP. These results are consistent with the studies in airway epithelial cells and the emerging idea that acute responses to PAR2 tend to be protective largely, whereas more sustained responses to PAR2 activation result in proinflammatory effect (452,468,469) and pain. From our perspective, we suggest that interventions designed to interfere with PAR2 activation would favorably affect the outcome of AAP.

Pancreatic acinar cell is the electrically non-excitable cell, which do not possess voltage-gated Ca^{2+} channels. Hence, CRAC channels constitute the main Ca^{2+} entry pathway and contribute to both physiological and pathological Ca^{2+} signalling in acinar cells. The previous studies show that CRAC channel inhibition both *in vitro* and *in vivo* by GSK-7975A dramatically reduces Ca^{2+} toxicity and effectively eliminates necrosis in pancreatic acinar cells (312,354). Here, our results indicate that asparaginase-induced pathological Ca^{2+} signals depend on CRAC-mediated Ca^{2+} entry are markedly inhibited by the CRAC channel blocker GSK-7975A and also that, consequently, asparaginase-induced necrosis and ATP loss are significantly reduced. CRAC channels are widely expressed in the body, thereby, there is an argument about CRAC inhibition as a potential treatment against, for example, asthma (470) or pancreatitis (240,312,313), because it is likely to occur unintended side-effects in the course of the treatment of CRAC blockade. Nevertheless, it has recently been demonstrated that inhibition of CRAC channels by GSK-7975A or CM_128 is the remarkably effective way to treat experimental pancreatitis in three different *in vivo* mouse models (354). CRAC channel inhibitors have mainly been designed and developed to deal with immunological disorders (369,370,471–475). Hence, they also inhibit Ca^{2+} entry into various immune cells such as neutrophils (476–478) invade and infiltrate pancreatic tissue in the early stages of AP, which exacerbate the development of this disease. In this situation, inhibition of immune cell

activation by blocking Ca^{2+} entry would be beneficial and advantageous to limit the inflammatory responses to the pancreas. Interestingly, pancreatic stellate cells have been implicated in the amplification the effects of pancreatitis-inducing agents (POAEE and bile acids) on the acinar cells (389,390,479,480). CRAC channel blockade would diminish toxic Ca^{2+} signal generation in both acinar and stellate cells, and this may explain the remarkable success of such inhibition in preventing pancreatic acinar injury in three experimental pancreatitis *in vivo* models. Although the primary intracellular Ca^{2+} release sites could be the potential target to be developed against AP (352,391), however, it may be more profitable to focus on store-operated Ca^{2+} entry channels as this would not necessarily consider about efficient delivery of drug into the cells. Clearly, future study would need to test the effectiveness of CRAC channel blocker in an *in vivo* AAP mouse model.

In terms of bioenergetics in pancreatic acinar cells, we focused our investigations on the effects of galactose, an essential component of human breast milk (481), as this sugar has already been included as part of human trials for the treatment of the glycogen storage disease type 1b (Fabry's disease), nephrotic syndrome, congenital disorders of glycosylation etc. and has not shown to have any negative effects (482–485). In view of the remarkable protective effects of galactose against asparaginase-induced intracellular toxic Ca^{2+} signals, ATP loss and necrosis from our results, we tested the effect of galactose in a novel *in vivo* AAP model. Galactose is quite stable in solution, relatively slowly metabolised as compared to pyruvate or fructose and has been used in both IV injection as well as feeding (drink) protocols (486–488). Our results show galactose markedly changed the histology score and the degrees of edema, inflammation and necrosis towards more normal values in both feeding and injection plus feeding protocols and with very similar efficiency. Therefore, potentially, galactose could become a

new effective treatment for AAP.

Clearly, both Ca^{2+} and ATP play key roles in the pathophysiology of pancreatic disorder and therapeutic strategies should take both into account and must be based on Ca^{2+} transport systems and cellular bioenergetics. Overall, the findings present in this thesis indicate that inhibition of PAR2, CRAC channel blockade or boosting cellular energy production by administering galactose has the potential to become a valuable and effective therapy in the acute early stage of AAP (Figure 6.2).

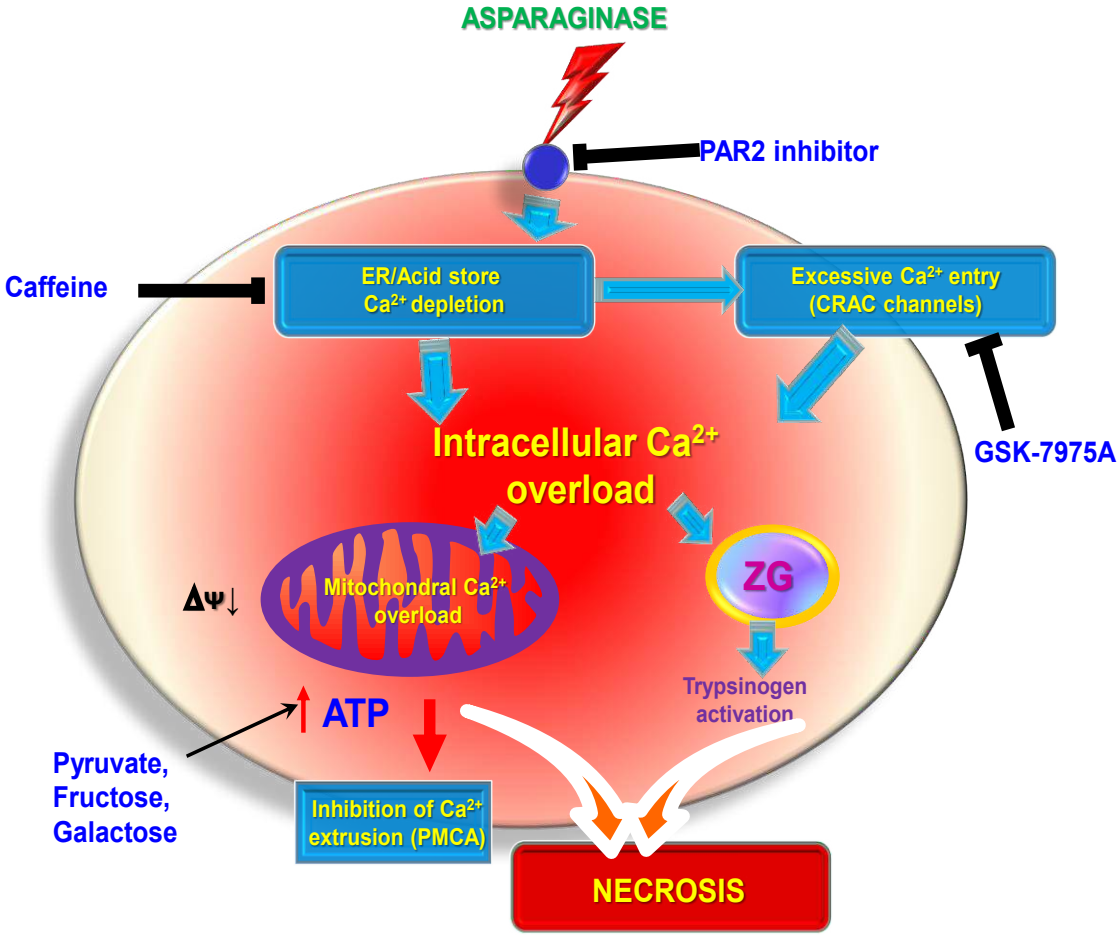

Figure 6.2 Potential sites for therapeutic intervention of AAP.

(Modified from *Peng S et al, Philos Trans R Soc Lond B Biol Sci. 2016*) (313)

Schematic diagram illustrating the mechanisms of asparaginase-induced necrotic cell death pathway activation on pancreatic acinar cells and the potential drug targets for the treatment of AAP.

Bibliography

1. Howard JM, Hess W. History of the Pancreas: Mysteries of a Hidden Organ. Springer Science & Business Media; 2012. 1089 p.

2. McClusky DA, Skandalakis LJ, Colborn GL, Skandalakis JE. Harbinger or hermit? Pancreatic anatomy and surgery through the ages--part 1. World J Surg. 2002 Sep;26(9):1175–85.

3. Ceranowicz P, Cieszkowski J, Warzecha Z, Kuśnierz-Cabala B, Dembiński A. The Beginnings of Pancreatology as a Field of Experimental and Clinical Medicine. BioMed Res Int. 2015;2015:128095.

4. Busnardo AC, DiDio LJ, Tidrick RT, Thomford NR. History of the pancreas. Am J Surg. 1983 Nov;146(5):539–50.

5. Flati G, Andrén-Sandberg A. Wirsung and Santorini: the men behind the ducts. Pancreatol Off J Int Assoc Pancreatol IAP Al. 2002;2(1):4–11.

6. Cid-Arregui A, Juarez V. Perspectives in the treatment of pancreatic adenocarcinoma. World J Gastroenterol. 2015 Aug 21;21(31):9297–316.

7. Chandra R, Liddle RA. Neural and hormonal regulation of pancreatic secretion. Curr Opin Gastroenterol. 2009 Sep;25(5):441–6.

8. Saito K, Iwama N, Takahashi T. Morphometrical analysis on topographical difference in size distribution, number and volume of islets in the human pancreas. Tohoku J Exp Med. 1978 Feb;124(2):177–86.

9. Röder PV, Wu B, Liu Y, Han W. Pancreatic regulation of glucose homeostasis. Exp Mol Med. 2016 Mar 11;48:e219.

10. Hauge-Evans AC, King AJ, Carmignac D, Richardson CC, Robinson ICAF, Low MJ, et al. Somatostatin secreted by islet delta-cells fulfills multiple roles as a paracrine regulator of islet function. Diabetes. 2009 Feb;58(2):403–11.

11. Batterham RL, Le Roux CW, Cohen MA, Park AJ, Ellis SM, Patterson M, et al. Pancreatic polypeptide reduces appetite and food intake in humans. J Clin Endocrinol Metab. 2003 Aug;88(8):3989–92.

12. Katsuura G, Asakawa A, Inui A. Roles of pancreatic polypeptide in regulation of food intake. Peptides. 2002 Feb;23(2):323–9.

13. Wierup N, Svensson H, Mulder H, Sundler F. The ghrelin cell: a novel developmentally regulated islet cell in the human pancreas. Regul Pept. 2002 Jul 15;107(1–3):63–9.

14. Brissova M, Fowler MJ, Nicholson WE, Chu A, Hirshberg B, Harlan DM,

et al. Assessment of human pancreatic islet architecture and composition by laser scanning confocal microscopy. J Histochem Cytochem Off J Histochem Soc. 2005 Sep;53(9):1087–97.

15. Cabrera O, Berman DM, Kenyon NS, Ricordi C, Berggren P-O, Caicedo A. The unique cytoarchitecture of human pancreatic islets has implications for islet cell function. Proc Natl Acad Sci U S A. 2006 Feb 14;103(7):2334–9.

16. Dolenšek J, Rupnik MS, Stožer A. Structural similarities and differences between the human and the mouse pancreas. Islets. 2015;7(1):e1024405.

17. Karamanou M, Protogerou A, Tsoucalas G, Androutsos G, Poulakou-Rebelakou E. Milestones in the history of diabetes mellitus: The main contributors. World J Diabetes. 2016 Jan 10;7(1):1–7.

18. Jörgens V. Oskar Minkowski (1858-1931). An outstanding master of diabetes research. Horm Athens Greece. 2006 Dec;5(4):310–1.

19. Luft R. Oskar Minkowski: discovery of the pancreatic origin of diabetes, 1889. Diabetologia. 1989 Jul;32(7):399–401.

20. Sakula A. Paul Langerhans (1847-1888): a centenary tribute. J R Soc Med. 1988 Jul;81(7):414–5.

21. Banting FG, Best CH, Collip JB, Campbell WR, Fletcher AA. Pancreatic extracts in the treatment of diabetes mellitus: preliminary report. 1922. CMAJ Can Med Assoc J J Assoc Medicale Can. 1991 Nov 15;145(10):1281–6.

22. Polonsky KS. The past 200 years in diabetes. N Engl J Med. 2012 Oct 4;367(14):1332–40.

23. Modlin IM. Regnier de Graaf: Paris, purging, and the pancreas. J Clin Gastroenterol. 2000 Mar;30(2):109–13.

24. DiMagno EP. A short, eclectic history of exocrine pancreatic insufficiency and chronic pancreatitis. Gastroenterology. 1993 May;104(5):1255–62.

25. Rodriguez de Romo AC, Borgstein J. Claude Bernard and pancreatic function revisited after 150 years. Vesalius Acta Int Hist Med. 1999 Jun;5(1):18–24.

26. Smith GP. Pavlov and integrative physiology. Am J Physiol Regul Integr Comp Physiol. 2000 Sep;279(3):R743-755.

27. Henderson J. Ernest Starling and ‘Hormones’: an historical commentary. J Endocrinol. 2005 Jan;184(1):5–10.

28. Modlin IM, Kidd M. Ernest Starling and the discovery of secretin. J Clin Gastroenterol. 2001 Mar;32(3):187–92.

29. Hirst BH. Secretin and the exposition of hormonal control. J Physiol. 2004 Oct 15;560(Pt 2):339.

30. Ceranowicz P, Warzecha Z, Dembinski A. Peptidyl hormones of endocrine cells origin in the gut--their discovery and physiological relevance. J Physiol Pharmacol Off J Pol Physiol Soc. 2015 Feb;66(1):11–27.

31. Harper AA, Raper HS. Pancreozymin, a stimulant of the secretion of pancreatic enzymes in extracts of the small intestine. J Physiol. 1943 Jun 30;102(1):115–25.

32. Jorpes E, Mutt V. Cholecystokinin and pancreozymin, one single hormone? Acta Physiol Scand. 1966 Feb;66(1):196–202.

33. Chandra R, Liddle RA. Neurohormonal regulation of pancreatic secretion. Curr Opin Gastroenterol. 2012 Sep;28(5):483–7.

34. Chandra R, Liddle RA. Recent advances in the regulation of pancreatic secretion. Curr Opin Gastroenterol. 2014 Sep;30(5):490–4.

35. White TW, Paul DL. Genetic diseases and gene knockouts reveal diverse connexin functions. Annu Rev Physiol. 1999;61:283–310.

36. Iwatsuki N, Petersen OH. Electrical coupling and uncoupling of exocrine acinar cells. J Cell Biol. 1978 Nov;79(2 Pt 1):533–45.

37. Meda P, Findlay I, Kolod E, Orci L, Petersen OH. Short and reversible uncoupling evokes little change in the gap junctions of pancreatic acinar cells. J Ultrastruct Res. 1983 Apr;83(1):69–84.

38. Palade G. Intracellular aspects of the process of protein synthesis. Science. 1975 Aug 1;189(4200):347–58.

39. Douglas WW, Rubin RP. The role of calcium in the secretory response of the adrenal medulla to acetylcholine. J Physiol. 1961 Nov;159:40–57.

40. Douglas WW, Rubin RP. Mechanism of nicotinic action at the adrenal medulla: calcium as a link in stimulus-secretion coupling. Nature. 1961 Dec 16;192:1087–9.

41. Douglas WW. Stimulus-secretion coupling: the concept and clues from

chromaffin and other cells. Br J Pharmacol. 1968 Nov;34(3):451–74.

42. Hille B, Billiard J, Babcock DF, Nguyen T, Koh DS. Stimulation of exocytosis without a calcium signal. J Physiol. 1999 Oct 1;520 Pt 1:23–31.

43. Petersen OH, Ueda N. Pancreatic acinar cells: the role of calcium in stimulus-secretion coupling. J Physiol. 1976 Jan;254(3):583–606.

44. Logsdon CD, Ji B. The role of protein synthesis and digestive enzymes in acinar cell injury. Nat Rev Gastroenterol Hepatol. 2013 Jun;10(6):362–70.

45. Bolender RP. Stereological analysis of the guinea pig pancreas. I. Analytical model and quantitative description of nonstimulated pancreatic exocrine cells. J Cell Biol. 1974 May;61(2):269–87.

46. Gerasimenko OV, Gerasimenko JV, Rizzuto RR, Treiman M, Tepikin AV, Petersen OH. The distribution of the endoplasmic reticulum in living pancreatic acinar cells. Cell Calcium. 2002 Dec;32(5–6):261–8.

47. Whitmore TE, Holloway JL, Lofton-Day CE, Maurer MF, Chen L, Quinton TJ, et al. Human secretin (SCT): gene structure, chromosome location, and distribution of mRNA. Cytogenet Cell Genet. 2000;90(1–2):47–52.

48. Chey WY, Chang T-M. Secretin, 100 years later. J Gastroenterol. 2003;38(11):1025–35.

49. Kim CD, Li P, Lee KY, Coy DH, Chey WY. Effect of [(CH2NH)4,5]secretin on pancreatic exocrine secretion in guinea pigs and rats. Am J Physiol. 1993 Nov;265(5 Pt 1):G805-810.

50. Petersen OH, Tepikin AV. Polarized calcium signaling in exocrine gland cells. Annu Rev Physiol. 2008;70:273–99.

51. Ashby MC, Craske M, Park MK, Gerasimenko OV, Burgoyne RD, Petersen OH, et al. Localized Ca2+ uncaging reveals polarized distribution of Ca2+-sensitive Ca2+ release sites: mechanism of unidirectional Ca2+ waves. J Cell Biol. 2002 Jul 22;158(2):283–92.

52. Thorn P, Lawrie AM, Smith PM, Gallacher DV, Petersen OH. Local and global cytosolic Ca2+ oscillations in exocrine cells evoked by agonists and inositol trisphosphate. Cell. 1993 Aug 27;74(4):661–8.

53. Iwatsuki N, Petersen OH. Pancreatic acinar cells: localization of acetylcholine receptors and the importance of chloride and calcium for acetylcholine-evoked depolarization. J Physiol. 1977 Aug;269(3):723–

33.

54. Philpott HG, Petersen OH. Extracellular but not intracellular application of peptide hormones activates pancreatic acinar cells. Nature. 1979 Oct 25;281(5733):684–6.

55. Gerasimenko JV, Sherwood M, Tepikin AV, Petersen OH, Gerasimenko OV. NAADP, cADPR and IP3 all release Ca2+ from the endoplasmic reticulum and an acidic store in the secretory granule area. J Cell Sci. 2006 Jan 15;119(Pt 2):226–38.

56. Nielsen SP, Petersen OH. Transport of calcium in the perfused submandibular gland of the cat. J Physiol. 1972 Jun;223(3):685–97.

57. Case RM, Clausen T. The relationship between calcium exchange and enzyme secretion in the isolated rat pancreas. J Physiol. 1973 Nov;235(1):75–102.

58. Matthews EK, Petersen OH, Williams JA. Pancreatic acinar cells: acetylcholine-induced membrane depolarization, calcium efflux and amylase release. J Physiol. 1973 Nov;234(3):689–701.

59. Streb H, Irvine RF, Berridge MJ, Schulz I. Release of Ca2+ from a nonmitochondrial intracellular store in pancreatic acinar cells by inositol-1,4,5-trisphosphate. Nature. 1983 Nov 3;306(5938):67–9.

60. Berridge MJ. Inositol trisphosphate and calcium signalling. Nature. 1993 Jan 28;361(6410):315–25.

61. Kasai H, Augustine GJ. Cytosolic Ca2+ gradients triggering unidirectional fluid secretion from exocrine pancreas. Nature. 1990 Dec 20;348(6303):735–8.

62. Toescu EC, Lawrie AM, Petersen OH, Gallacher DV. Spatial and temporal distribution of agonist-evoked cytoplasmic Ca2+ signals in exocrine acinar cells analysed by digital image microscopy. EMBO J. 1992 Apr;11(4):1623–9.

63. Kasai H, Li YX, Miyashita Y. Subcellular distribution of Ca2+ release channels underlying Ca2+ waves and oscillations in exocrine pancreas. Cell. 1993 Aug 27;74(4):669–77.

64. Gerasimenko OV, Gerasimenko JV, Petersen OH, Tepikin AV. Short pulses of acetylcholine stimulation induce cytosolic Ca2+ signals that are excluded from the nuclear region in pancreatic acinar cells. Pflugers Arch. 1996 Oct;432(6):1055–61.

65. Petersen OH, Tepikin A, Park MK. The endoplasmic reticulum: one continuous or several separate Ca(2+) stores? Trends Neurosci. 2001 May;24(5):271–6.

66. Mogami H, Nakano K, Tepikin AV, Petersen OH. Ca2+ flow via tunnels in polarized cells: recharging of apical Ca2+ stores by focal Ca2+ entry through basal membrane patch. Cell. 1997 Jan 10;88(1):49–55.

67. Nathanson MH, Fallon MB, Padfield PJ, Maranto AR. Localization of the type 3 inositol 1,4,5-trisphosphate receptor in the Ca2+ wave trigger zone of pancreatic acinar cells. J Biol Chem. 1994 Feb 18;269(7):4693–6.

68. Lee MG, Xu X, Zeng W, Diaz J, Wojcikiewicz RJ, Kuo TH, et al. Polarized expression of Ca2+ channels in pancreatic and salivary gland cells. Correlation with initiation and propagation of [Ca2+]i waves. J Biol Chem. 1997 Jun 20;272(25):15765–70.

69. Futatsugi A, Nakamura T, Yamada MK, Ebisui E, Nakamura K, Uchida K, et al. IP3 receptor types 2 and 3 mediate exocrine secretion underlying energy metabolism. Science. 2005 Sep 30;309(5744):2232–4.

70. Park MK, Lomax RB, Tepikin AV, Petersen OH. Local uncaging of caged Ca(2+) reveals distribution of Ca(2+)-activated Cl(-) channels in pancreatic acinar cells. Proc Natl Acad Sci U S A. 2001 Sep 11;98(19):10948–53.

71. Tinel H, Cancela JM, Mogami H, Gerasimenko JV, Gerasimenko OV, Tepikin AV, et al. Active mitochondria surrounding the pancreatic acinar granule region prevent spreading of inositol trisphosphate-evoked local cytosolic Ca(2+) signals. EMBO J. 1999 Sep 15;18(18):4999–5008.

72. Gerasimenko OV, Gerasimenko JV. Mitochondrial function and malfunction in the pathophysiology of pancreatitis. Pflüg Arch Eur J Physiol. 2012 Jul;464(1):89–99.

73. Carafoli E. Calcium signaling: a tale for all seasons. Proc Natl Acad Sci U S A. 2002 Feb 5;99(3):1115–22.

74. Clapham DE. Calcium signaling. Cell. 2007 Dec 14;131(6):1047–58.

75. Berridge MJ, Bootman MD, Roderick HL. Calcium signalling: dynamics, homeostasis and remodelling. Nat Rev Mol Cell Biol. 2003 Jul;4(7):517–29.

76. Miller DJ. Sydney Ringer; physiological saline, calcium and the contraction of the heart. J Physiol. 2004 Mar 16;555(Pt 3):585–7.

77. Berridge MJ. Unlocking the secrets of cell signaling. Annu Rev Physiol. 2005;67:1–21.

78. Burgoyne RD. Neuronal calcium sensor proteins: generating diversity in neuronal Ca2+ signalling. Nat Rev Neurosci. 2007 Mar;8(3):182–93.

79. Brini M, Carafoli E, Calì T. The plasma membrane calcium pumps: focus on the role in (neuro)pathology. Biochem Biophys Res Commun. 2017 Feb 19;483(4):1116–24.

80. Petersen OH. Ca2+ signalling and Ca2+-activated ion channels in exocrine acinar cells. Cell Calcium. 2005 Oct;38(3–4):171–200.

81. Monteith GR, McAndrew D, Faddy HM, Roberts-Thomson SJ. Calcium and cancer: targeting Ca2+ transport. Nat Rev Cancer. 2007 Jul;7(7):519–30.

82. Rash BG, Ackman JB, Rakic P. Bidirectional radial Ca(2+) activity regulates neurogenesis and migration during early cortical column formation. Sci Adv. 2016 Feb;2(2):e1501733.

83. Berridge MJ, Lipp P, Bootman MD. The versatility and universality of calcium signalling. Nat Rev Mol Cell Biol. 2000 Oct;1(1):11–21.

84. Lamprecht R, LeDoux J. Structural plasticity and memory. Nat Rev Neurosci. 2004 Jan;5(1):45–54.

85. Joseph SK, Hajnóczky G. IP3 receptors in cell survival and apoptosis: Ca2+ release and beyond. Apoptosis Int J Program Cell Death. 2007 May;12(5):951–68.

86. Gilman AG. G proteins: transducers of receptor-generated signals. Annu Rev Biochem. 1987;56:615–49.

87. King N, Hittinger CT, Carroll SB. Evolution of key cell signaling and adhesion protein families predates animal origins. Science. 2003 Jul 18;301(5631):361–3.

88. Vassilatis DK, Hohmann JG, Zeng H, Li F, Ranchalis JE, Mortrud MT, et al. The G protein-coupled receptor repertoires of human and mouse. Proc Natl Acad Sci U S A. 2003 Apr 15;100(8):4903–8.

89. Wettschureck N, Offermanns S. Mammalian G proteins and their cell type specific functions. Physiol Rev. 2005 Oct;85(4):1159–204.

90. Overington JP, Al-Lazikani B, Hopkins AL. How many drug targets are there? Nat Rev Drug Discov. 2006 Dec;5(12):993–6.

91. Strehler EE, Treiman M. Calcium pumps of plasma membrane and cell interior. Curr Mol Med. 2004 May;4(3):323–35.

92. Blaustein MP, Lederer WJ. Sodium/calcium exchange: its physiological implications. Physiol Rev. 1999 Jul;79(3):763–854.

93. Brini M, Calì T, Ottolini D, Carafoli E. The plasma membrane calcium pump in health and disease. FEBS J. 2013 Nov;280(21):5385–97.

94. Brini M, Carafoli E. The plasma membrane Ca^2+ ATPase and the plasma membrane sodium calcium exchanger cooperate in the regulation of cell calcium. Cold Spring Harb Perspect Biol. 2011 Feb 1;3(2).

95. Berberián G, Podjarny A, DiPolo R, Beaugé L. Metabolic regulation of the squid nerve Na^+/Ca^{2+} exchanger: recent kinetic, biochemical and structural developments. Prog Biophys Mol Biol. 2012 Jan;108(1–2):47–63.

96. Ferdek PE, Gerasimenko JV, Peng S, Tepikin AV, Petersen OH, Gerasimenko OV. A novel role for Bcl-2 in regulation of cellular calcium extrusion. Curr Biol CB. 2012 Jul 10;22(13):1241–6.

97. Petersen OH. Localization and regulation of Ca2+ entry and exit pathways in exocrine gland cells. Cell Calcium. 2003 Jun;33(5–6):337–44.

98. Tidow H, Poulsen LR, Andreeva A, Knudsen M, Hein KL, Wiuf C, et al. A bimodular mechanism of calcium control in eukaryotes. Nature. 2012 Nov 15;491(7424):468–72.

99. Brini M, Carafoli E. Calcium pumps in health and disease. Physiol Rev. 2009 Oct;89(4):1341–78.

100. Bokvist K, Eliasson L, Ammälä C, Renström E, Rorsman P. Co-localization of L-type Ca2+ channels and insulin-containing secretory granules and its significance for the initiation of exocytosis in mouse pancreatic B-cells. EMBO J. 1995 Jan 3;14(1):50–7.

101. Maruyama Y, Inooka G, Li YX, Miyashita Y, Kasai H. Agonist-induced localized Ca2+ spikes directly triggering exocytotic secretion in exocrine pancreas. EMBO J. 1993 Aug;12(8):3017–22.

102. Maruyama Y, Petersen OH. Delay in granular fusion evoked by repetitive cytosolic Ca2+ spikes in mouse pancreatic acinar cells. Cell Calcium. 1994 Nov;16(5):419–30.

103. Dean PM, Matthews EK. Electrical activity in pancreatic islet cells.

Nature. 1968 Jul 27;219(5152):389–90.

104. Petersen OH. Stimulus-secretion coupling: cytoplasmic calcium signals and the control of ion channels in exocrine acinar cells. J Physiol. 1992 Mar;448:1–51.

105. Tepikin AV, Voronina SG, Gallacher DV, Petersen OH. Acetylcholine-evoked increase in the cytoplasmic Ca2+ concentration and Ca2+ extrusion measured simultaneously in single mouse pancreatic acinar cells. J Biol Chem. 1992 Feb 25;267(6):3569–72.

106. Parekh AB, Putney JW. Store-operated calcium channels. Physiol Rev. 2005 Apr;85(2):757–810.

107. Feske S. CRAC channelopathies. Pflugers Arch. 2010 Jul;460(2):417–35.

108. Dolman NJ, Gerasimenko JV, Gerasimenko OV, Voronina SG, Petersen OH, Tepikin AV. Stable Golgi-mitochondria complexes and formation of Golgi Ca(2+) gradients in pancreatic acinar cells. J Biol Chem. 2005 Apr 22;280(16):15794–9.

109. Park MK, Ashby MC, Erdemli G, Petersen OH, Tepikin AV. Perinuclear, perigranular and sub-plasmalemmal mitochondria have distinct functions in the regulation of cellular calcium transport. EMBO J. 2001 Apr 17;20(8):1863–74.

110. Nakamura K, Hamada K, Terauchi A, Matsui M, Nakamura T, Okada T, et al. Distinct roles of M1 and M3 muscarinic acetylcholine receptors controlling oscillatory and non-oscillatory [Ca2+]i increase. Cell Calcium. 2013 Aug;54(2):111–9.

111. Williams JA, Sankaran H, Roach E, Goldfine ID. Quantitative electron microscope autoradiographs of 125I-cholecystokinin in pancreatic acini. Am J Physiol. 1982 Oct;243(4):G291-296.

112. Dufresne M, Seva C, Fourmy D. Cholecystokinin and gastrin receptors. Physiol Rev. 2006 Jul;86(3):805–47.

113. Yamasaki M, Thomas JM, Churchill GC, Garnham C, Lewis AM, Cancela J-M, et al. Role of NAADP and cADPR in the induction and maintenance of agonist-evoked Ca2+ spiking in mouse pancreatic acinar cells. Curr Biol CB. 2005 May 10;15(9):874–8.

114. Thorn P, Gerasimenko O, Petersen OH. Cyclic ADP-ribose regulation of ryanodine receptors involved in agonist evoked cytosolic Ca2+ oscillations in pancreatic acinar cells. EMBO J. 1994 May 1;13(9):2038–

43.

115. Cancela JM, Petersen OH. The cyclic ADP ribose antagonist 8-NH2-cADP-ribose blocks cholecystokinin-evoked cytosolic Ca2+ spiking in pancreatic acinar cells. Pflüg Arch Eur J Physiol. 1998 Apr;435(5):746–8.

116. Menteyne A, Burdakov A, Charpentier G, Petersen OH, Cancela J-M. Generation of specific Ca(2+) signals from Ca(2+) stores and endocytosis by differential coupling to messengers. Curr Biol CB. 2006 Oct 10;16(19):1931–7.

117. Yamasaki M, Masgrau R, Morgan AJ, Churchill GC, Patel S, Ashcroft SJH, et al. Organelle selection determines agonist-specific Ca2+ signals in pancreatic acinar and beta cells. J Biol Chem. 2004 Feb 20;279(8):7234–40.

118. Gerasimenko OV, Gerasimenko JV, Belan PV, Petersen OH. Inositol trisphosphate and cyclic ADP-ribose-mediated release of Ca2+ from single isolated pancreatic zymogen granules. Cell. 1996 Feb 9;84(3):473–80.

119. Gerasimenko J, Peng S, Gerasimenko O. Role of acidic stores in secretory epithelia. Cell Calcium. 2014 Jun;55(6):346–54.

120. Gerasimenko JV, Maruyama Y, Yano K, Dolman NJ, Tepikin AV, Petersen OH, et al. NAADP mobilizes Ca2+ from a thapsigargin-sensitive store in the nuclear envelope by activating ryanodine receptors. J Cell Biol. 2003 Oct 27;163(2):271–82.

121. Calcraft PJ, Ruas M, Pan Z, Cheng X, Arredouani A, Hao X, et al. NAADP mobilizes calcium from acidic organelles through two-pore channels. Nature. 2009 May 28;459(7246):596–600.

122. Brailoiu E, Churamani D, Cai X, Schrlau MG, Brailoiu GC, Gao X, et al. Essential requirement for two-pore channel 1 in NAADP-mediated calcium signaling. J Cell Biol. 2009 Jul 27;186(2):201–9.

123. Gerasimenko JV, Charlesworth RM, Sherwood MW, Ferdek PE, Mikoshiba K, Parrington J, et al. Both RyRs and TPCs are required for NAADP-induced intracellular Ca(2+) release. Cell Calcium. 2015 Sep;58(3):237–45.

124. Li Q, Luo X, Muallem S. Functional mapping of Ca2+ signaling complexes in plasma membrane microdomains of polarized cells. J Biol Chem. 2004 Jul 2;279(27):27837–40.

125. Fitzsimmons TJ, Gukovsky I, McRoberts JA, Rodriguez E, Lai FA, Pandol SJ. Multiple isoforms of the ryanodine receptor are expressed in rat pancreatic acinar cells. Biochem J. 2000 Oct 1;351(Pt 1):265–71.

126. Cancela JM, Gerasimenko OV, Gerasimenko JV, Tepikin AV, Petersen OH. Two different but converging messenger pathways to intracellular Ca(2+) release: the roles of nicotinic acid adenine dinucleotide phosphate, cyclic ADP-ribose and inositol trisphosphate. EMBO J. 2000 Jun 1;19(11):2549–57.

127. Petersen OH, Petersen CC, Kasai H. Calcium and hormone action. Annu Rev Physiol. 1994;56:297–319.

128. Mogami H, Tepikin AV, Petersen OH. Termination of cytosolic Ca2+ signals: Ca2+ reuptake into intracellular stores is regulated by the free Ca2+ concentration in the store lumen. EMBO J. 1998 Jan 15;17(2):435–42.

129. Hofer AM, Landolfi B, Debellis L, Pozzan T, Curci S. Free [Ca2+] dynamics measured in agonist-sensitive stores of single living intact cells: a new look at the refilling process. EMBO J. 1998 Apr 1;17(7):1986–95.

130. Tepikin AV, Voronina SG, Gallacher DV, Petersen OH. Pulsatile Ca2+ extrusion from single pancreatic acinar cells during receptor-activated cytosolic Ca2+ spiking. J Biol Chem. 1992 Jul 15;267(20):14073–6.

131. Park MK, Petersen OH, Tepikin AV. The endoplasmic reticulum as one continuous Ca(2+) pool: visualization of rapid Ca(2+) movements and equilibration. EMBO J. 2000 Nov 1;19(21):5729–39.

132. Nicotera P, Bellomo G, Orrenius S. Calcium-mediated mechanisms in chemically induced cell death. Annu Rev Pharmacol Toxicol. 1992;32:449–70.

133. Criddle DN, Gerasimenko JV, Baumgartner HK, Jaffar M, Voronina S, Sutton R, et al. Calcium signalling and pancreatic cell death: apoptosis or necrosis? Cell Death Differ. 2007 Jul;14(7):1285–94.

134. Petersen OH, Gerasimenko OV, Gerasimenko JV. Pathobiology of acute pancreatitis: focus on intracellular calcium and calmodulin. F1000 Med Rep. 2011;3:15.

135. Toescu EC, Petersen OH. Region-specific activity of the plasma membrane Ca2+ pump and delayed activation of Ca2+ entry characterize the polarized, agonist-evoked Ca2+ signals in exocrine cells. J Biol Chem. 1995 Apr 14;270(15):8528–35.

136. Gerasimenko JV, Gerasimenko OV, Petersen OH. The role of Ca2+ in the pathophysiology of pancreatitis. J Physiol. 2014 Jan 15;592(Pt 2):269–80.

137. Belan PV, Gerasimenko OV, Tepikin AV, Petersen OH. Localization of Ca2+ extrusion sites in pancreatic acinar cells. J Biol Chem. 1996 Mar 29;271(13):7615–9.

138. Petersen OH, Sutton R. Ca2+ signalling and pancreatitis: effects of alcohol, bile and coffee. Trends Pharmacol Sci. 2006 Feb;27(2):113–20.

139. Camello P, Gardner J, Petersen OH, Tepikin AV. Calcium dependence of calcium extrusion and calcium uptake in mouse pancreatic acinar cells. J Physiol. 1996 Feb 1;490 (Pt 3):585–93.

140. Burgoyne RD, Morgan A. Secretory granule exocytosis. Physiol Rev. 2003 Apr;83(2):581–632.

141. Parekh AB, Penner R. Store depletion and calcium influx. Physiol Rev. 1997 Oct;77(4):901–30.

142. Prakriya M, Lewis RS. Store-Operated Calcium Channels. Physiol Rev. 2015 Oct;95(4):1383–436.

143. Parekh AB. Functional consequences of activating store-operated CRAC channels. Cell Calcium. 2007 Aug;42(2):111–21.

144. Parekh AB. On the activation mechanism of store-operated calcium channels. Pflugers Arch. 2006 Dec;453(3):303–11.

145. Lewis RS. The molecular choreography of a store-operated calcium channel. Nature. 2007 Mar 15;446(7133):284–7.

146. Feske S, Gwack Y, Prakriya M, Srikanth S, Puppel S-H, Tanasa B, et al. A mutation in Orai1 causes immune deficiency by abrogating CRAC channel function. Nature. 2006 May 11;441(7090):179–85.

147. Lur G, Haynes LP, Prior IA, Gerasimenko OV, Feske S, Petersen OH, et al. Ribosome-free terminals of rough ER allow formation of STIM1 puncta and segregation of STIM1 from IP(3) receptors. Curr Biol CB. 2009 Oct 13;19(19):1648–53.

148. Liou J, Kim ML, Heo WD, Jones JT, Myers JW, Ferrell JE, et al. STIM is a Ca2+ sensor essential for Ca2+-store-depletion-triggered Ca2+ influx. Curr Biol CB. 2005 Jul 12;15(13):1235–41.

149. Roos J, DiGregorio PJ, Yeromin AV, Ohlsen K, Lioudyno M, Zhang S, et

al. STIM1, an essential and conserved component of store-operated Ca2+ channel function. J Cell Biol. 2005 May 9;169(3):435–45.

150. Vig M, Peinelt C, Beck A, Koomoa DL, Rabah D, Koblan-Huberson M, et al. CRACM1 is a plasma membrane protein essential for store-operated Ca2+ entry. Science. 2006 May 26;312(5777):1220–3.

151. Zhang SL, Yu Y, Roos J, Kozak JA, Deerinck TJ, Ellisman MH, et al. STIM1 is a Ca2+ sensor that activates CRAC channels and migrates from the Ca2+ store to the plasma membrane. Nature. 2005 Oct 6;437(7060):902–5.

152. Zhang SL, Yeromin AV, Zhang XH-F, Yu Y, Safrina O, Penna A, et al. Genome-wide RNAi screen of Ca(2+) influx identifies genes that regulate Ca(2+) release-activated Ca(2+) channel activity. Proc Natl Acad Sci U S A. 2006 Jun 13;103(24):9357–62.

153. Hoth M, Penner R. Depletion of intracellular calcium stores activates a calcium current in mast cells. Nature. 1992 Jan 23;355(6358):353–6.

154. Prakriya M, Feske S, Gwack Y, Srikanth S, Rao A, Hogan PG. Orai1 is an essential pore subunit of the CRAC channel. Nature. 2006 Sep 14;443(7108):230–3.

155. Yeromin AV, Zhang SL, Jiang W, Yu Y, Safrina O, Cahalan MD. Molecular identification of the CRAC channel by altered ion selectivity in a mutant of Orai. Nature. 2006 Sep 14;443(7108):226–9.

156. Vig M, Beck A, Billingsley JM, Lis A, Parvez S, Peinelt C, et al. CRACM1 multimers form the ion-selective pore of the CRAC channel. Curr Biol CB. 2006 Oct 24;16(20):2073–9.

157. Yamashita M, Navarro-Borelly L, McNally BA, Prakriya M. Orai1 mutations alter ion permeation and Ca2+-dependent fast inactivation of CRAC channels: evidence for coupling of permeation and gating. J Gen Physiol. 2007 Nov;130(5):525–40.

158. McNally BA, Yamashita M, Engh A, Prakriya M. Structural determinants of ion permeation in CRAC channels. Proc Natl Acad Sci U S A. 2009 Dec 29;106(52):22516–21.

159. Hou X, Pedi L, Diver MM, Long SB. Crystal structure of the calcium release-activated calcium channel Orai. Science. 2012 Dec 7;338(6112):1308–13.

160. Wu MM, Buchanan J, Luik RM, Lewis RS. Ca2+ store depletion causes STIM1 to accumulate in ER regions closely associated with the plasma

membrane. J Cell Biol. 2006 Sep 11;174(6):803–13.

161. Baba Y, Hayashi K, Fujii Y, Mizushima A, Watarai H, Wakamori M, et al. Coupling of STIM1 to store-operated Ca2+ entry through its constitutive and inducible movement in the endoplasmic reticulum. Proc Natl Acad Sci U S A. 2006 Nov 7;103(45):16704–9.

162. Muik M, Frischauf I, Derler I, Fahrner M, Bergsmann J, Eder P, et al. Dynamic coupling of the putative coiled-coil domain of ORAI1 with STIM1 mediates ORAI1 channel activation. J Biol Chem. 2008 Mar 21;283(12):8014–22.

163. Park CY, Hoover PJ, Mullins FM, Bachhawat P, Covington ED, Raunser S, et al. STIM1 clusters and activates CRAC channels via direct binding of a cytosolic domain to Orai1. Cell. 2009 Mar 6;136(5):876–90.

164. Yuan JP, Zeng W, Dorwart MR, Choi Y-J, Worley PF, Muallem S. SOAR and the polybasic STIM1 domains gate and regulate Orai channels. Nat Cell Biol. 2009 Mar;11(3):337–43.

165. Zhou Y, Meraner P, Kwon HT, Machnes D, Oh-hora M, Zimmer J, et al. STIM1 gates the store-operated calcium channel ORAI1 in vitro. Nat Struct Mol Biol. 2010 Jan;17(1):112–6.

166. Shen W-W, Demaurex N. Morphological and functional aspects of STIM1-dependent assembly and disassembly of store-operated calcium entry complexes. Biochem Soc Trans. 2012 Feb;40(1):112–8.

167. Lewis RS. Store-operated calcium channels: new perspectives on mechanism and function. Cold Spring Harb Perspect Biol. 2011 Dec 1;3(12).

168. Manji SS, Parker NJ, Williams RT, van Stekelenburg L, Pearson RB, Dziadek M, et al. STIM1: a novel phosphoprotein located at the cell surface. Biochim Biophys Acta. 2000 Aug 31;1481(1):147–55.

169. Mignen O, Thompson JL, Shuttleworth TJ. STIM1 regulates Ca2+ entry via arachidonate-regulated Ca2+-selective (ARC) channels without store depletion or translocation to the plasma membrane. J Physiol. 2007 Mar 15;579(Pt 3):703–15.

170. Mercer JC, Dehaven WI, Smyth JT, Wedel B, Boyles RR, Bird GS, et al. Large store-operated calcium selective currents due to co-expression of Orai1 or Orai2 with the intracellular calcium sensor, Stim1. J Biol Chem. 2006 Aug 25;281(34):24979–90.

171. Luik RM, Wu MM, Buchanan J, Lewis RS. The elementary unit of

store-operated Ca2+ entry: local activation of CRAC channels by STIM1 at ER-plasma membrane junctions. J Cell Biol. 2006 Sep 11;174(6):815–25.

172. Xu P, Lu J, Li Z, Yu X, Chen L, Xu T. Aggregation of STIM1 underneath the plasma membrane induces clustering of Orai1. Biochem Biophys Res Commun. 2006 Dec 1;350(4):969–76.

173. Derler I, Jardin I, Romanin C. Molecular mechanisms of STIM/Orai communication. Am J Physiol Cell Physiol. 2016 Apr 15;310(8):C643-662.

174. Putney JW. Pharmacology of store-operated calcium channels. Mol Interv. 2010 Aug;10(4):209–18.

175. Covington ED, Wu MM, Lewis RS. Essential role for the CRAC activation domain in store-dependent oligomerization of STIM1. Mol Biol Cell. 2010 Jun 1;21(11):1897–907.

176. Liou J, Fivaz M, Inoue T, Meyer T. Live-cell imaging reveals sequential oligomerization and local plasma membrane targeting of stromal interaction molecule 1 after Ca2+ store depletion. Proc Natl Acad Sci U S A. 2007 May 29;104(22):9301–6.

177. Wu MM, Covington ED, Lewis RS. Single-molecule analysis of diffusion and trapping of STIM1 and Orai1 at endoplasmic reticulum-plasma membrane junctions. Mol Biol Cell. 2014 Nov 5;25(22):3672–85.

178. Smyth JT, Dehaven WI, Bird GS, Putney JW. Ca2+-store-dependent and -independent reversal of Stim1 localization and function. J Cell Sci. 2008 Mar 15;121(Pt 6):762–72.

179. Shim AH-R, Tirado-Lee L, Prakriya M. Structural and functional mechanisms of CRAC channel regulation. J Mol Biol. 2015 Jan 16;427(1):77–93.

180. Petersen OH, Verkhratsky A. Calcium and ATP control multiple vital functions. Philos Trans R Soc Lond B Biol Sci. 2016 Aug 5;371(1700).

181. Johnson PR, Dolman NJ, Pope M, Vaillant C, Petersen OH, Tepikin AV, et al. Non-uniform distribution of mitochondria in pancreatic acinar cells. Cell Tissue Res. 2003 Jul;313(1):37–45.

182. Petersen OH. Specific mitochondrial functions in separate sub-cellular domains of pancreatic acinar cells. Pflugers Arch. 2012 Jul;464(1):77–87.

183. Ying W. NAD+/NADH and NADP+/NADPH in cellular functions and cell death: regulation and biological consequences. Antioxid Redox Signal. 2008 Feb;10(2):179–206.

184. Hajnóczky G, Robb-Gaspers LD, Seitz MB, Thomas AP. Decoding of cytosolic calcium oscillations in the mitochondria. Cell. 1995 Aug 11;82(3):415–24.

185. Voronina S, Sukhomlin T, Johnson PR, Erdemli G, Petersen OH, Tepikin A. Correlation of NADH and Ca2+ signals in mouse pancreatic acinar cells. J Physiol. 2002 Feb 15;539(Pt 1):41–52.

186. Voronina SG, Barrow SL, Simpson AWM, Gerasimenko OV, da Silva Xavier G, Rutter GA, et al. Dynamic changes in cytosolic and mitochondrial ATP levels in pancreatic acinar cells. Gastroenterology. 2010 May;138(5):1976–87.

187. De Stefani D, Raffaello A, Teardo E, Szabò I, Rizzuto R. A forty-kilodalton protein of the inner membrane is the mitochondrial calcium uniporter. Nature. 2011 Jun 19;476(7360):336–40.

188. Kamer KJ, Mootha VK. The molecular era of the mitochondrial calcium uniporter. Nat Rev Mol Cell Biol. 2015 Sep;16(9):545–53.

189. Oxenoid K, Dong Y, Cao C, Cui T, Sancak Y, Markhard AL, et al. Architecture of the mitochondrial calcium uniporter. Nature. 2016 12;533(7602):269–73.

190. Denton RM, McCormack JG. The calcium sensitive dehydrogenases of vertebrate mitochondria. Cell Calcium. 1986 Dec;7(5–6):377–86.

191. McCormack JG, Halestrap AP, Denton RM. Role of calcium ions in regulation of mammalian intramitochondrial metabolism. Physiol Rev. 1990 Apr;70(2):391–425.

192. Forsmark CE, Vege SS, Wilcox CM. Acute Pancreatitis. N Engl J Med. 2016 17;375(20):1972–81.

193. Lankisch PG, Apte M, Banks PA. Acute pancreatitis. Lancet Lond Engl. 2015 Jul 4;386(9988):85–96.

194. Petersen O. Can specific calcium channel blockade be the basis for a drug-based treatment of acute pancreatitis? Expert Rev Gastroenterol Hepatol. 2014 May;8(4):339–41.

195. Yadav D, Lowenfels AB. The epidemiology of pancreatitis and pancreatic cancer. Gastroenterology. 2013 Jun;144(6):1252–61.

196. Tenner S, Baillie J, DeWitt J, Vege SS, American College of Gastroenterology. American College of Gastroenterology guideline: management of acute pancreatitis. Am J Gastroenterol. 2013 Sep;108(9):1400–1415; 1416.

197. Hazra N, Gulliford M. Evaluating pancreatitis in primary care: a population-based cohort study. Br J Gen Pract J R Coll Gen Pract. 2014 May;64(622):e295-301.

198. Spanier BWM, Bruno MJ, Dijkgraaf MGW. Incidence and mortality of acute and chronic pancreatitis in the Netherlands: a nationwide record-linked cohort study for the years 1995-2005. World J Gastroenterol. 2013 May 28;19(20):3018–26.

199. Pant C, Deshpande A, Olyaee M, Anderson MP, Bitar A, Steele MI, et al. Epidemiology of acute pancreatitis in hospitalized children in the United States from 2000-2009. PloS One. 2014;9(5):e95552.

200. Peery AF, Crockett SD, Barritt AS, Dellon ES, Eluri S, Gangarosa LM, et al. Burden of Gastrointestinal, Liver, and Pancreatic Diseases in the United States. Gastroenterology. 2015 Dec;149(7):1731–1741.e3.

201. Peery AF, Dellon ES, Lund J, Crockett SD, McGowan CE, Bulsiewicz WJ, et al. Burden of gastrointestinal disease in the United States: 2012 update. Gastroenterology. 2012 Nov;143(5):1179-1187.e1-3.

202. Pandol SJ, Saluja AK, Imrie CW, Banks PA. Acute pancreatitis: bench to the bedside. Gastroenterology. 2007 Mar;132(3):1127–51.

203. Yadav D, O'Connell M, Papachristou GI. Natural history following the first attack of acute pancreatitis. Am J Gastroenterol. 2012 Jul;107(7):1096–103.

204. Lankisch PG, Breuer N, Bruns A, Weber-Dany B, Lowenfels AB, Maisonneuve P. Natural history of acute pancreatitis: a long-term population-based study. Am J Gastroenterol. 2009 Nov;104(11):2797–2805; quiz 2806.

205. Yadav D, Whitcomb DC. The role of alcohol and smoking in pancreatitis. Nat Rev Gastroenterol Hepatol. 2010 Mar;7(3):131–45.

206. Maisonneuve P, Lowenfels AB. Chronic pancreatitis and pancreatic cancer. Dig Dis Basel Switz. 2002;20(1):32–7.

207. Everhart JE, Ruhl CE. Burden of digestive diseases in the United States Part III: Liver, biliary tract, and pancreas. Gastroenterology. 2009 Apr;136(4):1134–44.

208. Lerch MM, Aghdassi AA. The role of bile acids in gallstone-induced pancreatitis. Gastroenterology. 2010 Feb;138(2):429–33.

209. Kim JY, Kim KH, Lee JA, Namkung W, Sun A-Q, Ananthanarayanan M, et al. Transporter-mediated bile acid uptake causes Ca2+-dependent cell death in rat pancreatic acinar cells. Gastroenterology. 2002 Jun;122(7):1941–53.

210. Pandol SJ, Lugea A, Mareninova OA, Smoot D, Gorelick FS, Gukovskaya AS, et al. Investigating the pathobiology of alcoholic pancreatitis. Alcohol Clin Exp Res. 2011 May;35(5):830–7.

211. Pandol SJ, Gukovsky I, Satoh A, Lugea A, Gukovskaya AS. Emerging concepts for the mechanism of alcoholic pancreatitis from experimental models. J Gastroenterol. 2003;38(7):623–8.

212. Coté GA, Yadav D, Slivka A, Hawes RH, Anderson MA, Burton FR, et al. Alcohol and smoking as risk factors in an epidemiology study of patients with chronic pancreatitis. Clin Gastroenterol Hepatol Off Clin Pract J Am Gastroenterol Assoc. 2011 Mar;9(3):266–273; quiz e27.

213. Yadav D, Eigenbrodt ML, Briggs MJ, Williams DK, Wiseman EJ. Pancreatitis: prevalence and risk factors among male veterans in a detoxification program. Pancreas. 2007 May;34(4):390–8.

214. Whitcomb DC, LaRusch J, Krasinskas AM, Klei L, Smith JP, Brand RE, et al. Common genetic variants in the CLDN2 and PRSS1-PRSS2 loci alter risk for alcohol-related and sporadic pancreatitis. Nat Genet. 2012 Dec;44(12):1349–54.

215. Apte MV, Pirola RC, Wilson JS. Mechanisms of alcoholic pancreatitis. J Gastroenterol Hepatol. 2010 Dec;25(12):1816–26.

216. Badalov N, Baradarian R, Iswara K, Li J, Steinberg W, Tenner S. Drug-induced acute pancreatitis: an evidence-based review. Clin Gastroenterol Hepatol Off Clin Pract J Am Gastroenterol Assoc. 2007 Jun;5(6):648–661; quiz 644.

217. Wu BU, Banks PA. Clinical management of patients with acute pancreatitis. Gastroenterology. 2013 Jun;144(6):1272–81.

218. Sadr-Azodi O, Andrén-Sandberg Å, Orsini N, Wolk A. Cigarette smoking, smoking cessation and acute pancreatitis: a prospective population-based study. Gut. 2012 Feb;61(2):262–7.

219. Sadr-Azodi O, Orsini N, Andrén-Sandberg Å, Wolk A. Abdominal and total adiposity and the risk of acute pancreatitis: a population-based

prospective cohort study. Am J Gastroenterol. 2013 Jan;108(1):133–9.

220. Wang AY, Strand DS, Shami VM. Prevention of Post-Endoscopic Retrograde Cholangiopancreatography Pancreatitis: Medications and Techniques. Clin Gastroenterol Hepatol Off Clin Pract J Am Gastroenterol Assoc. 2016 Nov;14(11):1521–1532.e3.

221. Jin S, Orabi AI, Le T, Javed TA, Sah S, Eisses JF, et al. Exposure to Radiocontrast Agents Induces Pancreatic Inflammation by Activation of Nuclear Factor-κB, Calcium Signaling, and Calcineurin. Gastroenterology. 2015 Sep;149(3):753–764.e11.

222. Whitcomb DC. Genetic risk factors for pancreatic disorders. Gastroenterology. 2013 Jun;144(6):1292–302.

223. Whitcomb DC, Gorry MC, Preston RA, Furey W, Sossenheimer MJ, Ulrich CD, et al. Hereditary pancreatitis is caused by a mutation in the cationic trypsinogen gene. Nat Genet. 1996 Oct;14(2):141–5.

224. Banks PA, Bollen TL, Dervenis C, Gooszen HG, Johnson CD, Sarr MG, et al. Classification of acute pancreatitis--2012: revision of the Atlanta classification and definitions by international consensus. Gut. 2013 Jan;62(1):102–11.

225. Ward JB, Petersen OH, Jenkins SA, Sutton R. Is an elevated concentration of acinar cytosolic free ionised calcium the trigger for acute pancreatitis? Lancet Lond Engl. 1995 Oct 14;346(8981):1016–9.

226. Criddle DN, Sutton R, Petersen OH. Role of Ca2+ in pancreatic cell death induced by alcohol metabolites. J Gastroenterol Hepatol. 2006 Oct;21 Suppl 3:S14-17.

227. Parekh AB. Calcium signaling and acute pancreatitis: specific response to a promiscuous messenger. Proc Natl Acad Sci U S A. 2000 Nov 21;97(24):12933–4.

228. Gerasimenko OV, Petersen OH, Gerasimenko JV. Role of intracellular acid Ca(2+) stores in pathological pancreatic protease activation. Expert Rev Gastroenterol Hepatol. 2012 Apr;6(2):129–31.

229. Raraty M, Ward J, Erdemli G, Vaillant C, Neoptolemos JP, Sutton R, et al. Calcium-dependent enzyme activation and vacuole formation in the apical granular region of pancreatic acinar cells. Proc Natl Acad Sci U S A. 2000 Nov 21;97(24):13126–31.

230. Ashby MC, Tepikin AV. Polarized calcium and calmodulin signaling in secretory epithelia. Physiol Rev. 2002 Jul;82(3):701–34.

231. Murphy JA, Criddle DN, Sherwood M, Chvanov M, Mukherjee R, McLaughlin E, et al. Direct activation of cytosolic Ca2+ signaling and enzyme secretion by cholecystokinin in human pancreatic acinar cells. Gastroenterology. 2008 Aug;135(2):632–41.

232. Liang T, Dolai S, Xie L, Winter E, Orabi AI, Karimian N, et al. Ex vivo human pancreatic slice preparations offer a valuable model for studying pancreatic exocrine biology. J Biol Chem. 2017 Apr 7;292(14):5957–69.

233. Orrenius S, Zhivotovsky B, Nicotera P. Regulation of cell death: the calcium-apoptosis link. Nat Rev Mol Cell Biol. 2003 Jul;4(7):552–65.

234. Montell C. The latest waves in calcium signaling. Cell. 2005 Jul 29;122(2):157–63.

235. Talukdar R, Sareen A, Zhu H, Yuan Z, Dixit A, Cheema H, et al. Release of Cathepsin B in Cytosol Causes Cell Death in Acute Pancreatitis. Gastroenterology. 2016 Oct;151(4):747–758.e5.

236. Petersen OH, Tepikin AV, Gerasimenko JV, Gerasimenko OV, Sutton R, Criddle DN. Fatty acids, alcohol and fatty acid ethyl esters: toxic Ca2+ signal generation and pancreatitis. Cell Calcium. 2009 Jun;45(6):634–42.

237. Krüger B, Albrecht E, Lerch MM. The role of intracellular calcium signaling in premature protease activation and the onset of pancreatitis. Am J Pathol. 2000 Jul;157(1):43–50.

238. Voronina S, Longbottom R, Sutton R, Petersen OH, Tepikin A. Bile acids induce calcium signals in mouse pancreatic acinar cells: implications for bile-induced pancreatic pathology. J Physiol. 2002 Apr 1;540(Pt 1):49–55.

239. Criddle DN, Raraty MGT, Neoptolemos JP, Tepikin AV, Petersen OH, Sutton R. Ethanol toxicity in pancreatic acinar cells: mediation by nonoxidative fatty acid metabolites. Proc Natl Acad Sci U S A. 2004 Jul 20;101(29):10738–43.

240. Maléth J, Hegyi P. Ca2+ toxicity and mitochondrial damage in acute pancreatitis: translational overview. Philos Trans R Soc Lond B Biol Sci. 2016 Aug 5;371(1700).

241. Denton RM. Regulation of mitochondrial dehydrogenases by calcium ions. Biochim Biophys Acta. 2009 Nov;1787(11):1309–16.

242. Criddle DN, Murphy J, Fistetto G, Barrow S, Tepikin AV, Neoptolemos JP, et al. Fatty acid ethyl esters cause pancreatic calcium toxicity via inositol

trisphosphate receptors and loss of ATP synthesis. Gastroenterology. 2006 Mar;130(3):781–93.

243. Halestrap AP. What is the mitochondrial permeability transition pore? J Mol Cell Cardiol. 2009 Jun;46(6):821–31.

244. Bernardi P, Di Lisa F. The mitochondrial permeability transition pore: molecular nature and role as a target in cardioprotection. J Mol Cell Cardiol. 2015 Jan;78:100–6.

245. Galluzzi L, Kepp O, Trojel-Hansen C, Kroemer G. Mitochondrial control of cellular life, stress, and death. Circ Res. 2012 Oct 12;111(9):1198–207.

246. Halestrap AP. Calcium, mitochondria and reperfusion injury: a pore way to die. Biochem Soc Trans. 2006 Apr;34(Pt 2):232–7.

247. Bernardi P. The mitochondrial permeability transition pore: a mystery solved? Front Physiol. 2013;4:95.

248. Kroemer G, Galluzzi L, Brenner C. Mitochondrial membrane permeabilization in cell death. Physiol Rev. 2007 Jan;87(1):99–163.

249. Kroemer G, Dallaporta B, Resche-Rigon M. The mitochondrial death/life regulator in apoptosis and necrosis. Annu Rev Physiol. 1998;60:619–42.

250. Zamzami N, Larochette N, Kroemer G. Mitochondrial permeability transition in apoptosis and necrosis. Cell Death Differ. 2005 Nov;12 Suppl 2:1478–80.

251. Baumgartner HK, Gerasimenko JV, Thorne C, Ferdek P, Pozzan T, Tepikin AV, et al. Calcium elevation in mitochondria is the main Ca2+ requirement for mitochondrial permeability transition pore (mPTP) opening. J Biol Chem. 2009 Jul 31;284(31):20796–803.

252. Gerasimenko JV, Gerasimenko OV, Palejwala A, Tepikin AV, Petersen OH, Watson AJM. Menadione-induced apoptosis: roles of cytosolic Ca(2+) elevations and the mitochondrial permeability transition pore. J Cell Sci. 2002 Feb 1;115(Pt 3):485–97.

253. Green DR, Galluzzi L, Kroemer G. Cell biology. Metabolic control of cell death. Science. 2014 Sep 19;345(6203):1250256.

254. Kokoszka JE, Waymire KG, Levy SE, Sligh JE, Cai J, Jones DP, et al. The ADP/ATP translocator is not essential for the mitochondrial permeability transition pore. Nature. 2004 Jan 29;427(6973):461–5.

255. Leung PS, Chan YC. Role of oxidative stress in pancreatic inflammation. Antioxid Redox Signal. 2009 Jan;11(1):135–65.

256. Booth DM, Murphy JA, Mukherjee R, Awais M, Neoptolemos JP, Gerasimenko OV, et al. Reactive oxygen species induced by bile acid induce apoptosis and protect against necrosis in pancreatic acinar cells. Gastroenterology. 2011 Jun;140(7):2116–25.

257. Gukovskaya AS, Gukovsky I. Which way to die: the regulation of acinar cell death in pancreatitis by mitochondria, calcium, and reactive oxygen species. Gastroenterology. 2011 Jun;140(7):1876–80.

258. Petersen OH, Sutton R, Criddle DN. Failure of calcium microdomain generation and pathological consequences. Cell Calcium. 2006 Dec;40(5–6):593–600.

259. Gukovsky I, Pandol SJ, Mareninova OA, Shalbueva N, Jia W, Gukovskaya AS. Impaired autophagy and organellar dysfunction in pancreatitis. J Gastroenterol Hepatol. 2012 Mar;27 Suppl 2:27–32.

260. Gaisano HY, Lutz MP, Leser J, Sheu L, Lynch G, Tang L, et al. Supramaximal cholecystokinin displaces Munc18c from the pancreatic acinar basal surface, redirecting apical exocytosis to the basal membrane. J Clin Invest. 2001 Dec;108(11):1597–611.

261. Perides G, Laukkarinen JM, Vassileva G, Steer ML. Biliary acute pancreatitis in mice is mediated by the G-protein-coupled cell surface bile acid receptor Gpbar1. Gastroenterology. 2010 Feb;138(2):715–25.

262. Gukovskaya AS, Perkins P, Zaninovic V, Sandoval D, Rutherford R, Fitzsimmons T, et al. Mechanisms of cell death after pancreatic duct obstruction in the opossum and the rat. Gastroenterology. 1996 Mar;110(3):875–84.

263. Hofbauer B, Saluja AK, Bhatia M, Frossard JL, Lee HS, Bhagat L, et al. Effect of recombinant platelet-activating factor acetylhydrolase on two models of experimental acute pancreatitis. Gastroenterology. 1998 Nov;115(5):1238–47.

264. Gukovsky I, Cheng JH, Nam KJ, Lee OT, Lugea A, Fischer L, et al. Phosphatidylinositide 3-kinase gamma regulates key pathologic responses to cholecystokinin in pancreatic acinar cells. Gastroenterology. 2004 Feb;126(2):554–66.

265. Chen X, Ji B, Han B, Ernst SA, Simeone D, Logsdon CD. NF-kappaB activation in pancreas induces pancreatic and systemic inflammatory response. Gastroenterology. 2002 Feb;122(2):448–57.

266. Satoh A, Gukovskaya AS, Edderkaoui M, Daghighian MS, Reeve JR, Shimosegawa T, et al. Tumor necrosis factor-alpha mediates pancreatitis responses in acinar cells via protein kinase C and proline-rich tyrosine kinase 2. Gastroenterology. 2005 Aug;129(2):639–51.

267. Kidd JG. Regression of transplanted lymphomas induced in vivo by means of normal guinea pig serum. I. Course of transplanted cancers of various kinds in mice and rats given guinea pig serum, horse serum, or rabbit serum. J Exp Med. 1953 Dec;98(6):565–82.

268. Broome JD. Evidence that the L-asparaginase of guinea pig serum is responsible for its antilymphoma effects. I. Properties of the L-asparaginase of guinea pig serum in relation to those of the antilymphoma substance. J Exp Med. 1963 Jul;118:99–120.

269. Broome JD. L-asparaginase: the evolution of a new tumor inhibitory agent. Trans N Y Acad Sci. 1968 Mar;30(5):690–704.

270. van den Berg H. Asparaginase revisited. Leuk Lymphoma. 2011 Feb;52(2):168–78.

271. Müller HJ, Boos J. Use of L-asparaginase in childhood ALL. Crit Rev Oncol Hematol. 1998 Aug;28(2):97–113.

272. Duval M, Suciu S, Ferster A, Rialland X, Nelken B, Lutz P, et al. Comparison of Escherichia coli-asparaginase with Erwinia-asparaginase in the treatment of childhood lymphoid malignancies: results of a randomized European Organisation for Research and Treatment of Cancer-Children's Leukemia Group phase 3 trial. Blood. 2002 Apr 15;99(8):2734–9.

273. Broome JD. L-Asparaginase: discovery and development as a tumor-inhibitory agent. Cancer Treat Rep. 1981;65 Suppl 4:111–4.

274. Ho DH, Whitecar JP, Luce JK, Frei E. L-asparagine requirement and the effect of L-asparaginase on the normal and leukemic human bone marrow. Cancer Res. 1970 Feb;30(2):466–72.

275. Iwamoto S, Mihara K, Downing JR, Pui C-H, Campana D. Mesenchymal cells regulate the response of acute lymphoblastic leukemia cells to asparaginase. J Clin Invest. 2007 Apr;117(4):1049–57.

276. Pui C-H, Relling MV, Downing JR. Acute lymphoblastic leukemia. N Engl J Med. 2004 Apr 8;350(15):1535–48.

277. Pui C-H, Robison LL, Look AT. Acute lymphoblastic leukaemia. Lancet Lond Engl. 2008 Mar 22;371(9617):1030–43.

278. Inaba H, Greaves M, Mullighan CG. Acute lymphoblastic leukaemia. Lancet Lond Engl. 2013 Jun 1;381(9881):1943–55.

279. Schmiegelow K, Forestier E, Hellebostad M, Heyman M, Kristinsson J, Söderhäll S, et al. Long-term results of NOPHO ALL-92 and ALL-2000 studies of childhood acute lymphoblastic leukemia. Leukemia. 2010 Feb;24(2):345–54.

280. Schmiegelow K, Attarbaschi A, Barzilai S, Escherich G, Frandsen TL, Halsey C, et al. Consensus definitions of 14 severe acute toxic effects for childhood lymphoblastic leukaemia treatment: a Delphi consensus. Lancet Oncol. 2016 Jun;17(6):e231-239.

281. Jaffe N, Traggis D, Das L, Moloney WC, Hann HW, Kim BS, et al. L-asparaginase in the treatment of neoplastic diseases in children. Cancer Res. 1971 Jul;31(7):942–9.

282. Silverman LB, Gelber RD, Dalton VK, Asselin BL, Barr RD, Clavell LA, et al. Improved outcome for children with acute lymphoblastic leukemia: results of Dana-Farber Consortium Protocol 91-01. Blood. 2001 Mar 1;97(5):1211–8.

283. Whitecar JP, Bodey GP, Harris JE, Freireich EJ. L-asparaginase. N Engl J Med. 1970 Mar 26;282(13):732–4.

284. Wetzler M, Sanford BL, Kurtzberg J, DeOliveira D, Frankel SR, Powell BL, et al. Effective asparagine depletion with pegylated asparaginase results in improved outcomes in adult acute lymphoblastic leukemia: Cancer and Leukemia Group B Study 9511. Blood. 2007 May 15;109(10):4164–7.

285. Pession A, Valsecchi MG, Masera G, Kamps WA, Magyarosy E, Rizzari C, et al. Long-term results of a randomized trial on extended use of high dose L-asparaginase for standard risk childhood acute lymphoblastic leukemia. J Clin Oncol Off J Am Soc Clin Oncol. 2005 Oct 1;23(28):7161–7.

286. Kobrinsky NL, Sposto R, Shah NR, Anderson JR, DeLaat C, Morse M, et al. Outcomes of treatment of children and adolescents with recurrent non-Hodgkin's lymphoma and Hodgkin's disease with dexamethasone, etoposide, cisplatin, cytarabine, and l-asparaginase, maintenance chemotherapy, and transplantation: Children's Cancer Group Study CCG-5912. J Clin Oncol Off J Am Soc Clin Oncol. 2001 May 1;19(9):2390–6.

287. Steinherz PG, Gaynon P, Miller DR, Reaman G, Bleyer A, Finklestein J,

et al. Improved disease-free survival of children with acute lymphoblastic leukemia at high risk for early relapse with the New York regimen--a new intensive therapy protocol: a report from the Childrens Cancer Study Group. J Clin Oncol Off J Am Soc Clin Oncol. 1986 May;4(5):744–52.

288. Clavell LA, Gelber RD, Cohen HJ, Hitchcock-Bryan S, Cassady JR, Tarbell NJ, et al. Four-agent induction and intensive asparaginase therapy for treatment of childhood acute lymphoblastic leukemia. N Engl J Med. 1986 Sep 11;315(11):657–63.

289. Kearney SL, Dahlberg SE, Levy DE, Voss SD, Sallan SE, Silverman LB. Clinical course and outcome in children with acute lymphoblastic leukemia and asparaginase-associated pancreatitis. Pediatr Blood Cancer. 2009 Aug;53(2):162–7.

290. Raja RA, Schmiegelow K, Frandsen TL. Asparaginase-associated pancreatitis in children. Br J Haematol. 2012 Oct;159(1):18–27.

291. Raja RA, Schmiegelow K, Albertsen BK, Prunsild K, Zeller B, Vaitkeviciene G, et al. Asparaginase-associated pancreatitis in children with acute lymphoblastic leukaemia in the NOPHO ALL2008 protocol. Br J Haematol. 2014 Apr;165(1):126–33.

292. Samarasinghe S, Dhir S, Slack J, Iyer P, Wade R, Clack R, et al. Incidence and outcome of pancreatitis in children and young adults with acute lymphoblastic leukaemia treated on a contemporary protocol, UKALL 2003. Br J Haematol. 2013 Sep;162(5):710–3.

293. Alvarez OA, Zimmerman G. Pegaspargase-induced pancreatitis. Med Pediatr Oncol. 2000 Mar;34(3):200–5.

294. Wolthers BO, Frandsen TL, Abrahamsson J, Albertsen BK, Helt LR, Heyman M, et al. Asparaginase-associated pancreatitis: a study on phenotype and genotype in the NOPHO ALL2008 protocol. Leukemia. 2017 Feb;31(2):325–32.

295. Lankisch PG, Dröge M, Gottesleben F. Drug induced acute pancreatitis: incidence and severity. Gut. 1995 Oct;37(4):565–7.

296. Knoderer HM, Robarge J, Flockhart DA. Predicting asparaginase-associated pancreatitis. Pediatr Blood Cancer. 2007 Oct 15;49(5):634–9.

297. Hijiya N, van der Sluis IM. Asparaginase-associated toxicity in children with acute lymphoblastic leukemia. Leuk Lymphoma. 2016;57(4):748–57.

298. Suzuki Y, Yokoyama K. Development of Functional Fluorescent Molecular Probes for the Detection of Biological Substances. Biosensors. 2015 Jun 18;5(2):337–63.

299. Minta A, Kao JP, Tsien RY. Fluorescent indicators for cytosolic calcium based on rhodamine and fluorescein chromophores. J Biol Chem. 1989 May 15;264(14):8171–8.

300. Wang B, Zhang X, Wang C, Chen L, Xiao Y, Pang Y. Bipolar and fixable probe targeting mitochondria to trace local depolarization via two-photon fluorescence lifetime imaging. The Analyst. 2015 Aug 21;140(16):5488–94.

301. Gee KR, Brown KA, Chen WN, Bishop-Stewart J, Gray D, Johnson I. Chemical and physiological characterization of fluo-4 Ca(2+)-indicator dyes. Cell Calcium. 2000 Feb;27(2):97–106.

302. Paredes RM, Etzler JC, Watts LT, Zheng W, Lechleiter JD. Chemical calcium indicators. Methods San Diego Calif. 2008 Nov;46(3):143–51.

303. Hurley TW, Ryan MP, Brinck RW. Changes of cytosolic Ca2+ interfere with measurements of cytosolic Mg2+ using mag-fura-2. Am J Physiol. 1992 Aug;263(2 Pt 1):C300-307.

304. Grynkiewicz G, Poenie M, Tsien RY. A new generation of Ca2+ indicators with greatly improved fluorescence properties. J Biol Chem. 1985 Mar 25;260(6):3440–50.

305. Ronzhina M, Cmiel V, Janoušek O, Kolářová J, Nováková M, Babula P, et al. Application of the optical method in experimental cardiology: action potential and intracellular calcium concentration measurement. Physiol Res. 2013;62(2):125–37.

306. Duchen MR, Surin A, Jacobson J. Imaging mitochondrial function in intact cells. Methods Enzymol. 2003;361:353–89.

307. Perry SW, Norman JP, Barbieri J, Brown EB, Gelbard HA. Mitochondrial membrane potential probes and the proton gradient: a practical usage guide. BioTechniques. 2011 Feb;50(2):98–115.

308. Voronina SG, Barrow SL, Gerasimenko OV, Petersen OH, Tepikin AV. Effects of secretagogues and bile acids on mitochondrial membrane potential of pancreatic acinar cells: comparison of different modes of evaluating DeltaPsim. J Biol Chem. 2004 Jun 25;279(26):27327–38.

309. Mankad P, James A, Siriwardena AK, Elliott AC, Bruce JIE. Insulin protects pancreatic acinar cells from cytosolic calcium overload and

inhibition of plasma membrane calcium pump. J Biol Chem. 2012 Jan 13;287(3):1823–36.

310. Samad A, James A, Wong J, Mankad P, Whitehouse J, Patel W, et al. Insulin protects pancreatic acinar cells from palmitoleic acid-induced cellular injury. J Biol Chem. 2014 Aug 22;289(34):23582–95.

311. Baggaley EM, Elliott AC, Bruce JIE. Oxidant-induced inhibition of the plasma membrane Ca2+-ATPase in pancreatic acinar cells: role of the mitochondria. Am J Physiol Cell Physiol. 2008 Nov;295(5):C1247-1260.

312. Gerasimenko JV, Gryshchenko O, Ferdek PE, Stapleton E, Hébert TOG, Bychkova S, et al. Ca2+ release-activated Ca2+ channel blockade as a potential tool in antipancreatitis therapy. Proc Natl Acad Sci U S A. 2013 Aug 6;110(32):13186–91.

313. Peng S, Gerasimenko JV, Tsugorka T, Gryshchenko O, Samarasinghe S, Petersen OH, et al. Calcium and adenosine triphosphate control of cellular pathology: asparaginase-induced pancreatitis elicited via protease-activated receptor 2. Philos Trans R Soc Lond B Biol Sci. 2016 Aug 5;371(1700).

314. Van Laethem JL, Robberecht P, Résibois A, Devière J. Transforming growth factor beta promotes development of fibrosis after repeated courses of acute pancreatitis in mice. Gastroenterology. 1996 Feb;110(2):576–82.

315. Wildi S, Kleeff J, Mayerle J, Zimmermann A, Böttinger EP, Wakefield L, et al. Suppression of transforming growth factor beta signalling aborts caerulein induced pancreatitis and eliminates restricted stimulation at high caerulein concentrations. Gut. 2007 May;56(5):685–92.

316. Macfarlane SR, Seatter MJ, Kanke T, Hunter GD, Plevin R. Proteinase-activated receptors. Pharmacol Rev. 2001 Jun;53(2):245–82.

317. Soh UJK, Dores MR, Chen B, Trejo J. Signal transduction by protease-activated receptors. Br J Pharmacol. 2010 May;160(2):191–203.

318. Ossovskaya VS, Bunnett NW. Protease-activated receptors: contribution to physiology and disease. Physiol Rev. 2004 Apr;84(2):579–621.

319. Coughlin SR. Protease-activated receptors in hemostasis, thrombosis and vascular biology. J Thromb Haemost JTH. 2005 Aug;3(8):1800–14.

320. Russo A, Soh UJK, Trejo J. Proteases display biased agonism at protease-activated receptors: location matters! Mol Interv. 2009

Apr;9(2):87–96.

321. D'Andrea MR, Saban MR, Nguyen N-B, Andrade-Gordon P, Saban R. Expression of protease-activated receptor-1, -2, -3, and -4 in control and experimentally inflamed mouse bladder. Am J Pathol. 2003 Mar;162(3):907–23.

322. Arora P, Ricks TK, Trejo J. Protease-activated receptor signalling, endocytic sorting and dysregulation in cancer. J Cell Sci. 2007 Mar 15;120(Pt 6):921–8.

323. Vu TK, Hung DT, Wheaton VI, Coughlin SR. Molecular cloning of a functional thrombin receptor reveals a novel proteolytic mechanism of receptor activation. Cell. 1991 Mar 22;64(6):1057–68.

324. Rasmussen UB, Vouret-Craviari V, Jallat S, Schlesinger Y, Pagès G, Pavirani A, et al. cDNA cloning and expression of a hamster alpha-thrombin receptor coupled to Ca2+ mobilization. FEBS Lett. 1991 Aug 19;288(1–2):123–8.

325. Ishihara H, Connolly AJ, Zeng D, Kahn ML, Zheng YW, Timmons C, et al. Protease-activated receptor 3 is a second thrombin receptor in humans. Nature. 1997 Apr 3;386(6624):502–6.

326. Xu WF, Andersen H, Whitmore TE, Presnell SR, Yee DP, Ching A, et al. Cloning and characterization of human protease-activated receptor 4. Proc Natl Acad Sci U S A. 1998 Jun 9;95(12):6642–6.

327. Kahn ML, Zheng YW, Huang W, Bigornia V, Zeng D, Moff S, et al. A dual thrombin receptor system for platelet activation. Nature. 1998 Aug 13;394(6694):690–4.

328. Coughlin SR. Thrombin signalling and protease-activated receptors. Nature. 2000 Sep 14;407(6801):258–64.

329. Nystedt S, Emilsson K, Wahlestedt C, Sundelin J. Molecular cloning of a potential proteinase activated receptor. Proc Natl Acad Sci U S A. 1994 Sep 27;91(20):9208–12.

330. Molino M, Barnathan ES, Numerof R, Clark J, Dreyer M, Cumashi A, et al. Interactions of mast cell tryptase with thrombin receptors and PAR-2. J Biol Chem. 1997 Feb 14;272(7):4043–9.

331. Camerer E, Huang W, Coughlin SR. Tissue factor- and factor X-dependent activation of protease-activated receptor 2 by factor VIIa. Proc Natl Acad Sci U S A. 2000 May 9;97(10):5255–60.

332. Riewald M, Ruf W. Mechanistic coupling of protease signaling and initiation of coagulation by tissue factor. Proc Natl Acad Sci U S A. 2001 Jul 3;98(14):7742–7.

333. Nystedt S, Larsson AK, Aberg H, Sundelin J. The mouse proteinase-activated receptor-2 cDNA and gene. Molecular cloning and functional expression. J Biol Chem. 1995 Mar 17;270(11):5950–5.

334. Nystedt S, Emilsson K, Larsson AK, Strömbeck B, Sundelin J. Molecular cloning and functional expression of the gene encoding the human proteinase-activated receptor 2. Eur J Biochem. 1995 Aug 15;232(1):84–9.

335. Böhm SK, Khitin LM, Grady EF, Aponte G, Payan DG, Bunnett NW. Mechanisms of desensitization and resensitization of proteinase-activated receptor-2. J Biol Chem. 1996 Sep 6;271(36):22003–16.

336. DeFea KA, Zalevsky J, Thoma MS, Déry O, Mullins RD, Bunnett NW. beta-arrestin-dependent endocytosis of proteinase-activated receptor 2 is required for intracellular targeting of activated ERK1/2. J Cell Biol. 2000 Mar 20;148(6):1267–81.

337. Bohm SK, Kong W, Bromme D, Smeekens SP, Anderson DC, Connolly A, et al. Molecular cloning, expression and potential functions of the human proteinase-activated receptor-2. Biochem J. 1996 Mar 15;314 (Pt 3):1009–16.

338. Corvera CU, Déry O, McConalogue K, Böhm SK, Khitin LM, Caughey GH, et al. Mast cell tryptase regulates rat colonic myocytes through proteinase-activated receptor 2. J Clin Invest. 1997 Sep 15;100(6):1383–93.

339. Corvera CU, Déry O, McConalogue K, Gamp P, Thoma M, Al-Ani B, et al. Thrombin and mast cell tryptase regulate guinea-pig myenteric neurons through proteinase-activated receptors-1 and -2. J Physiol. 1999 Jun 15;517 (Pt 3):741–56.

340. Kong W, McConalogue K, Khitin LM, Hollenberg MD, Payan DG, Böhm SK, et al. Luminal trypsin may regulate enterocytes through proteinase-activated receptor 2. Proc Natl Acad Sci U S A. 1997 Aug 5;94(16):8884–9.

341. Santulli RJ, Derian CK, Darrow AL, Tomko KA, Eckardt AJ, Seiberg M, et al. Evidence for the presence of a protease-activated receptor distinct from the thrombin receptor in human keratinocytes. Proc Natl Acad Sci U

S A. 1995 Sep 26;92(20):9151–5.

342. Ubl JJ, Vöhringer C, Reiser G. Co-existence of two types of [Ca2+]i-inducing protease-activated receptors (PAR-1 and PAR-2) in rat astrocytes and C6 glioma cells. Neuroscience. 1998 Sep;86(2):597–609.

343. Kawabata A, Nishikawa H, Kuroda R, Kawai K, Hollenberg MD. Proteinase-activated receptor-2 (PAR-2): regulation of salivary and pancreatic exocrine secretion in vivo in rats and mice. Br J Pharmacol. 2000 Apr;129(8):1808–14.

344. Nguyen TD, Moody MW, Steinhoff M, Okolo C, Koh DS, Bunnett NW. Trypsin activates pancreatic duct epithelial cell ion channels through proteinase-activated receptor-2. J Clin Invest. 1999 Jan;103(2):261–9.

345. Cottrell GS, Amadesi S, Schmidlin F, Bunnett N. Protease-activated receptor 2: activation, signalling and function. Biochem Soc Trans. 2003 Dec;31(Pt 6):1191–7.

346. Fiorucci S, Distrutti E. Role of PAR2 in pain and inflammation. Trends Pharmacol Sci. 2002 Apr;23(4):153–5.

347. Gorelick F. Pancreatic protease-activated receptors: friend and foe. Gut. 2007 Jul;56(7):901–2.

348. Namkung W, Han W, Luo X, Muallem S, Cho KH, Kim KH, et al. Protease-activated receptor 2 exerts local protection and mediates some systemic complications in acute pancreatitis. Gastroenterology. 2004 Jun;126(7):1844–59.

349. Laukkarinen JM, Weiss ER, van Acker GJD, Steer ML, Perides G. Protease-activated receptor-2 exerts contrasting model-specific effects on acute experimental pancreatitis. J Biol Chem. 2008 Jul 25;283(30):20703–12.

350. Singh VP, Bhagat L, Navina S, Sharif R, Dawra RK, Saluja AK. Protease-activated receptor-2 protects against pancreatitis by stimulating exocrine secretion. Gut. 2007 Jul;56(7):958–64.

351. Huang W, Booth DM, Cane MC, Chvanov M, Javed MA, Elliott VL, et al. Fatty acid ethyl ester synthase inhibition ameliorates ethanol-induced Ca2+-dependent mitochondrial dysfunction and acute pancreatitis. Gut. 2014 Aug;63(8):1313–24.

352. Huang W, Cane MC, Mukherjee R, Szatmary P, Zhang X, Elliott V, et al. Caffeine protects against experimental acute pancreatitis by inhibition of inositol 1,4,5-trisphosphate receptor-mediated Ca2+ release. Gut. 2017

Feb;66(2):301–13.

353. Mukherjee R, Mareninova OA, Odinokova IV, Huang W, Murphy J, Chvanov M, et al. Mechanism of mitochondrial permeability transition pore induction and damage in the pancreas: inhibition prevents acute pancreatitis by protecting production of ATP. Gut. 2015 Jun 12;

354. Wen L, Voronina S, Javed MA, Awais M, Szatmary P, Latawiec D, et al. Inhibitors of ORAI1 Prevent Cytosolic Calcium-Associated Injury of Human Pancreatic Acinar Cells and Acute Pancreatitis in 3 Mouse Models. Gastroenterology. 2015 Aug;149(2):481–492.e7.

355. Frick TW. The role of calcium in acute pancreatitis. Surgery. 2012 Sep;152(3 Suppl 1):S157-163.

356. Niederau C, Luthen R, Klonowski-Stumpe H, Schreiber R, Soika I, Sata N, et al. The role of calcium in pancreatitis. Hepatogastroenterology. 1999 Oct;46(29):2723–30.

357. Broome JD. Studies on the mechanism of tumor inhibition by L-asparaginase. Effects of the enzyme on asparagine levels in the blood, normal tissues, and 6C3HED lymphomas of mice: differences in asparagine formation and utilization in asparaginase-sensitive and -resistant lymphoma cells. J Exp Med. 1968 Jun 1;127(6):1055–72.

358. Hill JM, Roberts J, Loeb E, Khan A, MacLellan A, Hill RW. L-asparaginase therapy for leukemia and other malignant neoplasms. Remission in human leukemia. JAMA. 1967 Nov 27;202(9):882–8.

359. Oettgen HF, Old LJ, Boyse EA, Campbell HA, Philips FS, Clarkson BD, et al. Inhibition of leukemias in man by L-asparaginase. Cancer Res. 1967 Dec;27(12):2619–31.

360. Cooney DA, Capizzi RL, Handschumacher RE. Evaluation of L-asparagine metabolism in animals and man. Cancer Res. 1970 Apr;30(4):929–35.

361. Canepa A, Filho JCD, Gutierrez A, Carrea A, Forsberg A-M, Nilsson E, et al. Free amino acids in plasma, red blood cells, polymorphonuclear leukocytes, and muscle in normal and uraemic children. Nephrol Dial Transplant Off Publ Eur Dial Transpl Assoc - Eur Ren Assoc. 2002 Mar;17(3):413–21.

362. Wakui M, Osipchuk YV, Petersen OH. Receptor-activated cytoplasmic Ca2+ spiking mediated by inositol trisphosphate is due to Ca2(+)-induced Ca2+ release. Cell. 1990 Nov 30;63(5):1025–32.

363. Toescu EC, O'Neill SC, Petersen OH, Eisner DA. Caffeine inhibits the agonist-evoked cytosolic Ca2+ signal in mouse pancreatic acinar cells by blocking inositol trisphosphate production. J Biol Chem. 1992 Nov 25;267(33):23467–70.

364. Horowitz LF, Hirdes W, Suh B-C, Hilgemann DW, Mackie K, Hille B. Phospholipase C in living cells: activation, inhibition, Ca2+ requirement, and regulation of M current. J Gen Physiol. 2005 Sep;126(3):243–62.

365. Macmillan D, McCarron JG. The phospholipase C inhibitor U-73122 inhibits Ca(2+) release from the intracellular sarcoplasmic reticulum Ca(2+) store by inhibiting Ca(2+) pumps in smooth muscle. Br J Pharmacol. 2010 Jul;160(6):1295–301.

366. Mogami H, Lloyd Mills C, Gallacher DV. Phospholipase C inhibitor, U73122, releases intracellular Ca2+, potentiates Ins(1,4,5)P3-mediated Ca2+ release and directly activates ion channels in mouse pancreatic acinar cells. Biochem J. 1997 Jun 1;324 (Pt 2):645–51.

367. Jan CR, Ho CM, Wu SN, Tseng CJ. The phospholipase C inhibitor U73122 increases cytosolic calcium in MDCK cells by activating calcium influx and releasing stored calcium. Life Sci. 1998;63(10):895–908.

368. Yule DI, Williams JA. U73122 inhibits Ca2+ oscillations in response to cholecystokinin and carbachol but not to JMV-180 in rat pancreatic acinar cells. J Biol Chem. 1992 Jul 15;267(20):13830–5.

369. Derler I, Schindl R, Fritsch R, Heftberger P, Riedl MC, Begg M, et al. The action of selective CRAC channel blockers is affected by the Orai pore geometry. Cell Calcium. 2013 Feb;53(2):139–51.

370. Rice LV, Bax HJ, Russell LJ, Barrett VJ, Walton SE, Deakin AM, et al. Characterization of selective Calcium-Release Activated Calcium channel blockers in mast cells and T-cells from human, rat, mouse and guinea-pig preparations. Eur J Pharmacol. 2013 Mar 15;704(1–3):49–57.

371. Voronina S, Collier D, Chvanov M, Middlehurst B, Beckett AJ, Prior IA, et al. The role of Ca2+ influx in endocytic vacuole formation in pancreatic acinar cells. Biochem J. 2015 Feb 1;465(3):405–12.

372. Hegyi P. Blockade of calcium entry provides a therapeutic window in acute pancreatitis. J Physiol. 2016 Jan 15;594(2):257.

373. Vergnolle N. Review article: proteinase-activated receptors - novel signals for gastrointestinal pathophysiology. Aliment Pharmacol Ther. 2000 Mar;14(3):257–66.

374. D'Andrea MR, Derian CK, Leturcq D, Baker SM, Brunmark A, Ling P, et al. Characterization of protease-activated receptor-2 immunoreactivity in normal human tissues. J Histochem Cytochem Off J Histochem Soc. 1998 Feb;46(2):157–64.

375. Amadesi S, Bunnett N. Protease-activated receptors: protease signaling in the gastrointestinal tract. Curr Opin Pharmacol. 2004 Dec;4(6):551–6.

376. Kawabata A, Matsunami M, Sekiguchi F. Gastrointestinal roles for proteinase-activated receptors in health and disease. Br J Pharmacol. 2008 Mar;153 Suppl 1:S230-240.

377. Seitzberg JG, Knapp AE, Lund BW, Mandrup Bertozzi S, Currier EA, Ma J-N, et al. Discovery of potent and selective small-molecule PAR-2 agonists. J Med Chem. 2008 Sep 25;51(18):5490–3.

378. Al-Ani B, Saifeddine M, Wijesuriya SJ, Hollenberg MD. Modified proteinase-activated receptor-1 and -2 derived peptides inhibit proteinase-activated receptor-2 activation by trypsin. J Pharmacol Exp Ther. 2002 Feb;300(2):702–8.

379. Andoh T, Takayama Y, Yamakoshi T, Lee J-B, Sano A, Shimizu T, et al. Involvement of serine protease and proteinase-activated receptor 2 in dermatophyte-associated itch in mice. J Pharmacol Exp Ther. 2012 Oct;343(1):91–6.

380. Chen Y, Yang C, Wang ZJ. Proteinase-activated receptor 2 sensitizes transient receptor potential vanilloid 1, transient receptor potential vanilloid 4, and transient receptor potential ankyrin 1 in paclitaxel-induced neuropathic pain. Neuroscience. 2011 Oct 13;193:440–51.

381. McLarty JL, Meléndez GC, Brower GL, Janicki JS, Levick SP. Tryptase/Protease-activated receptor 2 interactions induce selective mitogen-activated protein kinase signaling and collagen synthesis by cardiac fibroblasts. Hypertens Dallas Tex 1979. 2011 Aug;58(2):264–70.

382. Davison JS, Pearson GT, Petersen OH. Mouse pancreatic acinar cells: effects of electrical field stimulation on membrane potential and resistance. J Physiol. 1980 Apr;301:295–305.

383. Gallacher DV, Petersen OH. Electrophysiology of mouse parotid acini: effects of electrical field stimulation and ionophoresis of neurotransmitters. J Physiol. 1980 Aug;305:43–57.

384. Gallacher DV, Petersen OH. Substance P increases membrane conductance in parotid acinar cells. Nature. 1980 Jan

24;283(5745):393–5.

385. Caulfield MP, Birdsall NJ. International Union of Pharmacology. XVII. Classification of muscarinic acetylcholine receptors. Pharmacol Rev. 1998 Jun;50(2):279–90.

386. Petersen OH, Gerasimenko OV, Tepikin AV, Gerasimenko JV. Aberrant Ca(2+) signalling through acidic calcium stores in pancreatic acinar cells. Cell Calcium. 2011 Aug;50(2):193–9.

387. Takács T, Rosztóczy A, Maléth J, Rakonczay Z, Hegyi P. Intraductal acidosis in acute biliary pancreatitis. Pancreatol Off J Int Assoc Pancreatol IAP Al. 2013 Aug;13(4):333–5.

388. Kar P, Samanta K, Kramer H, Morris O, Bakowski D, Parekh AB. Dynamic assembly of a membrane signaling complex enables selective activation of NFAT by Orai1. Curr Biol CB. 2014 Jun 16;24(12):1361–8.

389. Gryshchenko O, Gerasimenko JV, Gerasimenko OV, Petersen OH. Ca(2+) signals mediated by bradykinin type 2 receptors in normal pancreatic stellate cells can be inhibited by specific Ca(2+) channel blockade. J Physiol. 2016 Jan 15;594(2):281–93.

390. Gryshchenko O, Gerasimenko JV, Gerasimenko OV, Petersen OH. Calcium signalling in pancreatic stellate cells: Mechanisms and potential roles. Cell Calcium. 2016 Mar;59(2–3):140–4.

391. Gerasimenko JV, Lur G, Ferdek P, Sherwood MW, Ebisui E, Tepikin AV, et al. Calmodulin protects against alcohol-induced pancreatic trypsinogen activation elicited via Ca2+ release through IP3 receptors. Proc Natl Acad Sci U S A. 2011 Apr 5;108(14):5873–8.

392. Spät A, Petersen OH. A Special Issue on the cell-specific roles of mitochondrial Ca^{2+} handling. Pflugers Arch. 2012 Jul;464(1):1–2.

393. Bernardi P. Mitochondrial transport of cations: channels, exchangers, and permeability transition. Physiol Rev. 1999 Oct;79(4):1127–55.

394. Ashby MC, Camello-Almaraz C, Gerasimenko OV, Petersen OH, Tepikin AV. Long distance communication between muscarinic receptors and Ca2+ release channels revealed by carbachol uncaging in cell-attached patch pipette. J Biol Chem. 2003 Jun 6;278(23):20860–4.

395. Maruyama Y, Petersen OH. Cholecystokinin activation of single-channel currents is mediated by internal messenger in pancreatic acinar cells. Nature. 1982 Nov 4;300(5887):61–3.

396. Baker PF, Knight DE. Calcium-dependent exocytosis in bovine adrenal medullary cells with leaky plasma membranes. Nature. 1978 Dec 7;276(5688):620–2.

397. Osipchuk YV, Wakui M, Yule DI, Gallacher DV, Petersen OH. Cytoplasmic Ca2+ oscillations evoked by receptor stimulation, G-protein activation, internal application of inositol trisphosphate or Ca2+: simultaneous microfluorimetry and Ca2+ dependent Cl- current recording in single pancreatic acinar cells. EMBO J. 1990 Mar;9(3):697–704.

398. DiPolo R, Beaugé L. Sodium/calcium exchanger: influence of metabolic regulation on ion carrier interactions. Physiol Rev. 2006 Jan;86(1):155–203.

399. Rizzuto R, Pozzan T. Microdomains of intracellular Ca2+: molecular determinants and functional consequences. Physiol Rev. 2006 Jan;86(1):369–408.

400. Gilabert JA, Parekh AB. Respiring mitochondria determine the pattern of activation and inactivation of the store-operated Ca(2+) current I(CRAC). EMBO J. 2000 Dec 1;19(23):6401–7.

401. Glitsch MD, Bakowski D, Parekh AB. Store-operated Ca2+ entry depends on mitochondrial Ca2+ uptake. EMBO J. 2002 Dec 16;21(24):6744–54.

402. Hoth M, Fanger CM, Lewis RS. Mitochondrial regulation of store-operated calcium signaling in T lymphocytes. J Cell Biol. 1997 May 5;137(3):633–48.

403. Gerasimenko OV, Gerasimenko JV, Tepikin AV, Petersen OH. ATP-dependent accumulation and inositol trisphosphate- or cyclic ADP-ribose-mediated release of Ca2+ from the nuclear envelope. Cell. 1995 Feb 10;80(3):439–44.

404. Gerasimenko OV, Gerasimenko JV, Tepikin AV, Petersen OH. Calcium transport pathways in the nucleus. Pflugers Arch. 1996 May;432(1):1–6.

405. Villalobos C, Nadal A, Núñez L, Quesada I, Chamero P, Alonso MT, et al. Bioluminescence imaging of nuclear calcium oscillations in intact pancreatic islets of Langerhans from the mouse. Cell Calcium. 2005 Aug;38(2):131–9.

406. Carafoli E. Calcium pump of the plasma membrane. Physiol Rev. 1991 Jan;71(1):129–53.

407. Barrow SL, Voronina SG, da Silva Xavier G, Chvanov MA, Longbottom RE, Gerasimenko OV, et al. ATP depletion inhibits Ca2+ release, influx and extrusion in pancreatic acinar cells but not pathological Ca2+ responses induced by bile. Pflugers Arch. 2008 Mar;455(6):1025–39.

408. Bruce JI. Plasma membrane calcium pump regulation by metabolic stress. World J Biol Chem. 2010 Jul 26;1(7):221–8.

409. de Baaij JHF, Hoenderop JGJ, Bindels RJM. Magnesium in man: implications for health and disease. Physiol Rev. 2015 Jan;95(1):1–46.

410. Leyssens A, Nowicky AV, Patterson L, Crompton M, Duchen MR. The relationship between mitochondrial state, ATP hydrolysis, [Mg2+]i and [Ca2+]i studied in isolated rat cardiomyocytes. J Physiol. 1996 Oct 1;496 (Pt 1):111–28.

411. Inoue M, Fujishiro N, Imanaga I, Sakamoto Y. Role of ATP decrease in secretion induced by mitochondrial dysfunction in guinea-pig adrenal chromaffin cells. J Physiol. 2002 Feb 15;539(Pt 1):145–55.

412. Fink MP. Ethyl pyruvate. Curr Opin Anaesthesiol. 2008 Apr;21(2):160–7.

413. Luan Z-G, Ma X-C, Zhang H, Zhang C, Guo R-X. Protective effect of ethyl pyruvate on pancreas injury in rats with severe acute pancreatitis. J Surg Res. 2013 May 1;181(1):76–84.

414. Luan Z-G, Zhang J, Yin X-H, Ma X-C, Guo R-X. Ethyl pyruvate significantly inhibits tumour necrosis factor-α, interleukin-1β and high mobility group box 1 releasing and attenuates sodium taurocholate-induced severe acute pancreatitis associated with acute lung injury. Clin Exp Immunol. 2013 Jun;172(3):417–26.

415. Yang R, Zhu S, Tonnessen TI. Ethyl pyruvate is a novel anti-inflammatory agent to treat multiple inflammatory organ injuries. J Inflamm Lond Engl. 2016;13:37.

416. Jouaville LS, Pinton P, Bastianutto C, Rutter GA, Rizzuto R. Regulation of mitochondrial ATP synthesis by calcium: evidence for a long-term metabolic priming. Proc Natl Acad Sci U S A. 1999 Nov 23;96(24):13807–12.

417. Fonteriz RI, de la Fuente S, Moreno A, Lobatón CD, Montero M, Alvarez J. Monitoring mitochondrial [Ca(2+)] dynamics with rhod-2, ratiometric pericam and aequorin. Cell Calcium. 2010 Jul;48(1):61–9.

418. Rizzuto R, Bernardi P, Pozzan T. Mitochondria as all-round players of the calcium game. J Physiol. 2000 Nov 15;529 Pt 1:37–47.

419. Denton RM, McCormack JG. Ca2+ as a second messenger within mitochondria of the heart and other tissues. Annu Rev Physiol. 1990;52:451–66.

420. Holden HM, Rayment I, Thoden JB. Structure and function of enzymes of the Leloir pathway for galactose metabolism. J Biol Chem. 2003 Nov 7;278(45):43885–8.

421. Bustamante E, Pedersen PL. High aerobic glycolysis of rat hepatoma cells in culture: role of mitochondrial hexokinase. Proc Natl Acad Sci U S A. 1977 Sep;74(9):3735–9.

422. Palty R, Silverman WF, Hershfinkel M, Caporale T, Sensi SL, Parnis J, et al. NCLX is an essential component of mitochondrial Na+/Ca2+ exchange. Proc Natl Acad Sci U S A. 2010 Jan 5;107(1):436–41.

423. Gunter TE, Buntinas L, Sparagna G, Eliseev R, Gunter K. Mitochondrial calcium transport: mechanisms and functions. Cell Calcium. 2000 Dec;28(5–6):285–96.

424. Cox DA, Matlib MA. A role for the mitochondrial Na(+)-Ca2+ exchanger in the regulation of oxidative phosphorylation in isolated heart mitochondria. J Biol Chem. 1993 Jan 15;268(2):938–47.

425. Szabadkai G, Simoni AM, Bianchi K, De Stefani D, Leo S, Wieckowski MR, et al. Mitochondrial dynamics and Ca2+ signaling. Biochim Biophys Acta. 2006 Jun;1763(5–6):442–9.

426. Graier WF, Frieden M, Malli R. Mitochondria and Ca(2+) signaling: old guests, new functions. Pflugers Arch. 2007 Dec;455(3):375–96.

427. Rünzi M, Layer P. Drug-associated pancreatitis: facts and fiction. Pancreas. 1996 Jul;13(1):100–9.

428. Land VJ, Sutow WW, Fernbach DJ, Lane DM, Williams TE. Toxicity of L-asparginase in children with advanced leukemia. Cancer. 1972 Aug;30(2):339–47.

429. Oettgen HF, Stephenson PA, Schwartz MK, Leeper RD, Tallai L, Tan CC, et al. Toxicity of E. coli L-asparaginase in man. Cancer. 1970 Feb;25(2):253–78.

430. Majbar AA, Cusick E, Johnson P, Lynn RM, Hunt LP, Shield JPH. Incidence and Clinical Associations of Childhood Acute Pancreatitis. Pediatrics. 2016 Sep;138(3).

431. Stefanović M, Jazbec J, Lindgren F, Bulajić M, Löhr M. Acute pancreatitis

as a complication of childhood cancer treatment. Cancer Med. 2016;5(5):827–36.

432. Flores-Calderón J, Exiga-Gonzaléz E, Morán-Villota S, Martín-Trejo J, Yamamoto-Nagano A. Acute pancreatitis in children with acute lymphoblastic leukemia treated with L-asparaginase. J Pediatr Hematol Oncol. 2009 Oct;31(10):790–3.

433. Treepongkaruna S, Thongpak N, Pakakasama S, Pienvichit P, Sirachainan N, Hongeng S. Acute pancreatitis in children with acute lymphoblastic leukemia after chemotherapy. J Pediatr Hematol Oncol. 2009 Nov;31(11):812–5.

434. Vrooman LM, Supko JG, Neuberg DS, Asselin BL, Athale UH, Clavell L, et al. Erwinia asparaginase after allergy to E. coli asparaginase in children with acute lymphoblastic leukemia. Pediatr Blood Cancer. 2010 Feb;54(2):199–205.

435. Yeang SH, Chan A, Tan CW, Lim ST, Ng HJ. Incidence and Management of Toxicity Associated with LAsparaginase in the Treatment of ALL and NK/TCell Lymphoma: an Observational Study. Asian Pac J Cancer Prev APJCP. 2016;17(7):3155–60.

436. Liu C, Yang W, Devidas M, Cheng C, Pei D, Smith C, et al. Clinical and Genetic Risk Factors for Acute Pancreatitis in Patients With Acute Lymphoblastic Leukemia. J Clin Oncol Off J Am Soc Clin Oncol. 2016 Jun 20;34(18):2133–40.

437. Phillipson-Weiner L, Mirek ET, Wang Y, McAuliffe WG, Wek RC, Anthony TG. General control nonderepressible 2 deletion predisposes to asparaginase-associated pancreatitis in mice. Am J Physiol Gastrointest Liver Physiol. 2016 Jun 1;310(11):G1061-1070.

438. Ward E, DeSantis C, Robbins A, Kohler B, Jemal A. Childhood and adolescent cancer statistics, 2014. CA Cancer J Clin. 2014 Apr;64(2):83–103.

439. Amylon MD, Shuster J, Pullen J, Berard C, Link MP, Wharam M, et al. Intensive high-dose asparaginase consolidation improves survival for pediatric patients with T cell acute lymphoblastic leukemia and advanced stage lymphoblastic lymphoma: a Pediatric Oncology Group study. Leukemia. 1999 Mar;13(3):335–42.

440. Moghrabi A, Levy DE, Asselin B, Barr R, Clavell L, Hurwitz C, et al. Results of the Dana-Farber Cancer Institute ALL Consortium Protocol 95-01 for children with acute lymphoblastic leukemia. Blood. 2007 Feb

1;109(3):896–904.

441. Barry E, DeAngelo DJ, Neuberg D, Stevenson K, Loh ML, Asselin BL, et al. Favorable outcome for adolescents with acute lymphoblastic leukemia treated on Dana-Farber Cancer Institute Acute Lymphoblastic Leukemia Consortium Protocols. J Clin Oncol Off J Am Soc Clin Oncol. 2007 Mar 1;25(7):813–9.

442. Plattner H, Verkhratsky A. Inseparable tandem: evolution chooses ATP and Ca2+ to control life, death and cellular signalling. Philos Trans R Soc Lond B Biol Sci. 2016 Aug 5;371(1700).

443. Plattner H, Verkhratsky A. The ancient roots of calcium signalling evolutionary tree. Cell Calcium. 2015 Mar;57(3):123–32.

444. Petersen OH, Michalak M, Verkhratsky A. Calcium signalling: past, present and future. Cell Calcium. 2005 Oct;38(3–4):161–9.

445. Eisner DA, Venetucci LA, Trafford AW. Life, sudden death, and intracellular calcium. Circ Res. 2006 Aug 4;99(3):223–4.

446. Lim D, Rodríguez-Arellano JJ, Parpura V, Zorec R, Zeidán-Chuliá F, Genazzani AA, et al. Calcium signalling toolkits in astrocytes and spatio-temporal progression of Alzheimer's disease. Curr Alzheimer Res. 2016;13(4):359–69.

447. Bernardi P, Rasola A, Forte M, Lippe G. The Mitochondrial Permeability Transition Pore: Channel Formation by F-ATP Synthase, Integration in Signal Transduction, and Role in Pathophysiology. Physiol Rev. 2015 Oct;95(4):1111–55.

448. Hegyi P, Pandol S, Venglovecz V, Rakonczay Z. The acinar-ductal tango in the pathogenesis of acute pancreatitis. Gut. 2011 Apr;60(4):544–52.

449. Shore ER, Awais M, Kershaw NM, Gibson RR, Pandalaneni S, Latawiec D, et al. Small Molecule Inhibitors of Cyclophilin D To Protect Mitochondrial Function as a Potential Treatment for Acute Pancreatitis. J Med Chem. 2016 Mar 24;59(6):2596–611.

450. Lur G, Sherwood MW, Ebisui E, Haynes L, Feske S, Sutton R, et al. InsP receptors and Orai channels in pancreatic acinar cells: co-localization and its consequences. Biochem J. 2011 Jun 1;436(2):231–9.

451. Gerasimenko JV, Lur G, Sherwood MW, Ebisui E, Tepikin AV, Mikoshiba K, et al. Pancreatic protease activation by alcohol metabolite depends on Ca2+ release via acid store IP3 receptors. Proc Natl Acad Sci U S A.

2009 Jun 30;106(26):10758–63.

452. Jairaman A, Yamashita M, Schleimer RP, Prakriya M. Store-Operated Ca2+ Release-Activated Ca2+ Channels Regulate PAR2-Activated Ca2+ Signaling and Cytokine Production in Airway Epithelial Cells. J Immunol Baltim Md 1950. 2015 Sep 1;195(5):2122–33.

453. Kim MS, Hong JH, Li Q, Shin DM, Abramowitz J, Birnbaumer L, et al. Deletion of TRPC3 in mice reduces store-operated Ca2+ influx and the severity of acute pancreatitis. Gastroenterology. 2009 Oct;137(4):1509–17.

454. Kim MS, Lee KP, Yang D, Shin DM, Abramowitz J, Kiyonaka S, et al. Genetic and pharmacologic inhibition of the Ca2+ influx channel TRPC3 protects secretory epithelia from Ca2+-dependent toxicity. Gastroenterology. 2011 Jun;140(7):2107–15, 2115.e1-4.

455. Bianchi K, Rimessi A, Prandini A, Szabadkai G, Rizzuto R. Calcium and mitochondria: mechanisms and functions of a troubled relationship. Biochim Biophys Acta. 2004 Dec 6;1742(1–3):119–31.

456. Walsh C, Barrow S, Voronina S, Chvanov M, Petersen OH, Tepikin A. Modulation of calcium signalling by mitochondria. Biochim Biophys Acta. 2009 Nov;1787(11):1374–82.

457. Babcock DF, Herrington J, Goodwin PC, Park YB, Hille B. Mitochondrial participation in the intracellular Ca2+ network. J Cell Biol. 1997 Feb 24;136(4):833–44.

458. Vais H, Mallilankaraman K, Mak D-OD, Hoff H, Payne R, Tanis JE, et al. EMRE Is a Matrix Ca(2+) Sensor that Governs Gatekeeping of the Mitochondrial Ca(2+) Uniporter. Cell Rep. 2016 Jan 26;14(3):403–10.

459. Spät A, Szanda G. Special features of mitochondrial Ca^{2+} signalling in adrenal glomerulosa cells. Pflugers Arch. 2012 Jul;464(1):43–50.

460. Kornberg H. Krebs and his trinity of cycles. Nat Rev Mol Cell Biol. 2000 Dec;1(3):225–8.

461. Bakowski D, Parekh AB. Regulation of store-operated calcium channels by the intermediary metabolite pyruvic acid. Curr Biol CB. 2007 Jun 19;17(12):1076–81.

462. Zima AV, Kockskämper J, Mejia-Alvarez R, Blatter LA. Pyruvate modulates cardiac sarcoplasmic reticulum Ca2+ release in rats via mitochondria-dependent and -independent mechanisms. J Physiol. 2003 Aug 1;550(Pt 3):765–83.

463. Gatenby RA, Gillies RJ. Why do cancers have high aerobic glycolysis? Nat Rev Cancer. 2004 Nov;4(11):891–9.

464. Sharma A, Tao X, Gopal A, Ligon B, Andrade-Gordon P, Steer ML, et al. Protection against acute pancreatitis by activation of protease-activated receptor-2. Am J Physiol Gastrointest Liver Physiol. 2005 Feb;288(2):G388-395.

465. Sharma A, Tao X, Gopal A, Ligon B, Steer ML, Perides G. Calcium dependence of proteinase-activated receptor 2 and cholecystokinin-mediated amylase secretion from pancreatic acini. Am J Physiol Gastrointest Liver Physiol. 2005 Oct;289(4):G686-695.

466. Steinhoff M, Vergnolle N, Young SH, Tognetto M, Amadesi S, Ennes HS, et al. Agonists of proteinase-activated receptor 2 induce inflammation by a neurogenic mechanism. Nat Med. 2000 Feb;6(2):151–8.

467. Hoogerwerf WA, Shenoy M, Winston JH, Xiao S-Y, He Z, Pasricha PJ. Trypsin mediates nociception via the proteinase-activated receptor 2: a potentially novel role in pancreatic pain. Gastroenterology. 2004 Sep;127(3):883–91.

468. Knight DA, Lim S, Scaffidi AK, Roche N, Chung KF, Stewart GA, et al. Protease-activated receptors in human airways: upregulation of PAR-2 in respiratory epithelium from patients with asthma. J Allergy Clin Immunol. 2001 Nov;108(5):797–803.

469. Cocks TM, Fong B, Chow JM, Anderson GP, Frauman AG, Goldie RG, et al. A protective role for protease-activated receptors in the airways. Nature. 1999 Mar 11;398(6723):156–60.

470. Samanta K, Parekh AB. Store-operated Ca2+ channels in airway epithelial cell function and implications for asthma. Philos Trans R Soc Lond B Biol Sci. 2016 Aug 5;371(1700).

471. Parekh AB. Store-operated CRAC channels: function in health and disease. Nat Rev Drug Discov. 2010 May;9(5):399–410.

472. Di Capite JL, Bates GJ, Parekh AB. Mast cell CRAC channel as a novel therapeutic target in allergy. Curr Opin Allergy Clin Immunol. 2011 Feb;11(1):33–8.

473. Ng SW, di Capite J, Singaravelu K, Parekh AB. Sustained activation of the tyrosine kinase Syk by antigen in mast cells requires local Ca2+ influx through Ca2+ release-activated Ca2+ channels. J Biol Chem. 2008 Nov 14;283(46):31348–55.

474. Ashmole I, Duffy SM, Leyland ML, Morrison VS, Begg M, Bradding P. CRACM/Orai ion channel expression and function in human lung mast cells. J Allergy Clin Immunol. 2012 Jun;129(6):1628–1635.e2.

475. van Kruchten R, Braun A, Feijge MAH, Kuijpers MJE, Rivera-Galdos R, Kraft P, et al. Antithrombotic potential of blockers of store-operated calcium channels in platelets. Arterioscler Thromb Vasc Biol. 2012 Jul;32(7):1717–23.

476. Merza M, Hartman H, Rahman M, Hwaiz R, Zhang E, Renström E, et al. Neutrophil Extracellular Traps Induce Trypsin Activation, Inflammation, and Tissue Damage in Mice With Severe Acute Pancreatitis. Gastroenterology. 2015 Dec;149(7):1920–1931.e8.

477. Gukovskaya AS, Vaquero E, Zaninovic V, Gorelick FS, Lusis AJ, Brennan M-L, et al. Neutrophils and NADPH oxidase mediate intrapancreatic trypsin activation in murine experimental acute pancreatitis. Gastroenterology. 2002 Apr;122(4):974–84.

478. Frossard JL, Saluja A, Bhagat L, Lee HS, Bhatia M, Hofbauer B, et al. The role of intercellular adhesion molecule 1 and neutrophils in acute pancreatitis and pancreatitis-associated lung injury. Gastroenterology. 1999 Mar;116(3):694–701.

479. Ferdek PE, Jakubowska MA, Gerasimenko JV, Gerasimenko OV, Petersen OH. Bile acids induce necrosis in pancreatic stellate cells dependent on calcium entry and sodium-driven bile uptake. J Physiol. 2016 Nov 1;594(21):6147–64.

480. Jakubowska MA, Ferdek PE, Gerasimenko OV, Gerasimenko JV, Petersen OH. Nitric oxide signals are interlinked with calcium signals in normal pancreatic stellate cells upon oxidative stress and inflammation. Open Biol. 2016 Aug;6(8).

481. Grote V, Verduci E, Scaglioni S, Vecchi F, Contarini G, Giovannini M, et al. Breast milk composition and infant nutrient intakes during the first 12 months of life. Eur J Clin Nutr. 2016 Feb;70(2):250–6.

482. Letkemann R, Wittkowski H, Antonopoulos A, Podskabi T, Haslam SM, Föll D, et al. Partial correction of neutrophil dysfunction by oral galactose therapy in glycogen storage disease type Ib. Int Immunopharmacol. 2017 Mar;44:216–25.

483. Frustaci A, Chimenti C, Ricci R, Natale L, Russo MA, Pieroni M, et al. Improvement in cardiac function in the cardiac variant of Fabry's disease with galactose-infusion therapy. N Engl J Med. 2001 Jul 5;345(1):25–32.

484. Morelle W, Potelle S, Witters P, Wong S, Climer L, Lupashin V, et al. Galactose Supplementation in Patients With TMEM165-CDG Rescues the Glycosylation Defects. J Clin Endocrinol Metab. 2017 Apr 1;102(4):1375–86.

485. De Smet E, Rioux J-P, Ammann H, Déziel C, Quérin S. FSGS permeability factor-associated nephrotic syndrome: remission after oral galactose therapy. Nephrol Dial Transplant Off Publ Eur Dial Transpl Assoc - Eur Ren Assoc. 2009 Sep;24(9):2938–40.

486. Berry GT, Nissim I, Lin Z, Mazur AT, Gibson JB, Segal S. Endogenous synthesis of galactose in normal men and patients with hereditary galactosaemia. Lancet Lond Engl. 1995 Oct 21;346(8982):1073–4.

487. An F, Yang G, Tian J, Wang S. Antioxidant effects of the orientin and vitexin in Trollius chinensis Bunge in D-galactose-aged mice. Neural Regen Res. 2012 Nov 25;7(33):2565–75.

488. Sclafani A, Ackroff K. Flavor preference conditioning by different sugars in sweet ageusic Trpm5 knockout mice. Physiol Behav. 2015 Mar 1;140:156–63.